



HAL
open science

Robust state estimation for switched systems : application to fault detection

Chaima Zammali

► **To cite this version:**

Chaima Zammali. Robust state estimation for switched systems : application to fault detection. Robotics [cs.RO]. Sorbonne Université, 2020. English. NNT : 2020SORUS124 . tel-03369154

HAL Id: tel-03369154

<https://theses.hal.science/tel-03369154v1>

Submitted on 7 Oct 2021

HAL is a multi-disciplinary open access archive for the deposit and dissemination of scientific research documents, whether they are published or not. The documents may come from teaching and research institutions in France or abroad, or from public or private research centers.

L'archive ouverte pluridisciplinaire **HAL**, est destinée au dépôt et à la diffusion de documents scientifiques de niveau recherche, publiés ou non, émanant des établissements d'enseignement et de recherche français ou étrangers, des laboratoires publics ou privés.

**École doctorale Informatique, Télécommunications et Électronique
Centre d'Études et de Recherche en Informatique et Communications**

THÈSE DE DOCTORAT

présentée par : **Chaima ZAMMALI**
soutenue le : **23 octobre 2020**

pour obtenir le grade de : **Docteur de l'université Sorbonne Université**

Spécialité : **Informatique, Télécommunications et Électronique**

**Robust state estimation for switched systems - application to
fault detection**

THÈSE dirigée par

RAÏSSI Tarek

Professeur des Universités au Cnam

RAPPORTEURS

ALAMO CANTARERO Teodoro
EFIMOV Denis

*Professeur à l'Université de Séville
Chargé de recherche à l'INRIA*

EXAMINATEURS

LAMNABHI-LAGARRIGUE Françoise
RAMDANI Nacim
TRELAT Emmanuel

*Directrice de Recherche émérite au CNRS
Professeur à l'Université d'Orléans
Professeur à Sorbonne Université*

ENCADRANT

VAN GORP Jérémy

Maître de conférences au CNAM

À la mémoire de l'âme de mon cher papa

Ibrahim ZAMMALI

À ma chère maman

Moufida AKACHA

À ma moitié et mes soeurs

À tous, je dédie cette thèse

Remerciements

Les travaux de recherche présentés dans ce mémoire ont été menés au centre d'études et de recherche en informatique et communications (CEDRIC) du Conservatoire National des Arts et Métiers (CNAM).

Je souhaite exprimer d'abord ma reconnaissance à mon directeur de thèse Monsieur Tarek Raïssi, pour la confiance qu'il m'a accordée en acceptant la direction scientifique de mes travaux. Merci de m'avoir soutenue tout au long de ce projet. Je vous remercie également pour votre disponibilité, vos encouragements et vos judicieux conseils, qui ont contribué efficacement à la réalisation de cette thèse.

Je souhaite exprimer ma gratitude envers mon encadrant Monsieur Jérémy Van Gorp. Je vous remercie pour votre pédagogie, votre suivi régulier, votre dévouement et surtout pour votre patience qui ont permis de terminer ces trois années de thèse dans une très bonne ambiance.

J'adresse également mes remerciements aux rapporteurs de thèse Monsieur Denis Efimov et Monsieur Teodoro Alamo Cantarero, pour l'intérêt qu'ils ont porté à ce travail. Je les remercie également pour les différentes remarques très intéressantes qu'ils ont pu apporter. J'associe à ces remerciements Madame Françoise Lamnabhi-Lagarrigue, Monsieur Nacim Ramdani et Monsieur Emmanuel Trelat pour avoir accepté d'examiner cette thèse.

Je tiens ensuite à remercier mes collègues de l'équipe Laetitia dont je fais partie pour leur disponibilité, leur sympathie, et pour l'ambiance amicale sans quoi ma thèse n'aurait pas été pareille.

Enfin, mes remerciements vont à ma famille qui m'a toujours soutenue dans mes études. Merci à toi Chokri pour ton soutien moral et tes conseils. Un grand merci à mes amies Haifa, Naima, Ikhlass et Wafa pour les bons moments partagés avec moi durant cette thèse.

Paris, Octobre 2020
Chaima ZAMMALI

Résumé

Cette thèse s'intéresse à l'estimation d'état et à la détection de défauts de systèmes linéaires à commutations. De nouvelles approches d'estimation par intervalles sont développées pour des systèmes linéaires à commutations à paramètres variants en temps continu et en temps discret en supposant que le signal de commutations est connu. Les conditions de conception sont formulées en termes d'inégalités matricielles linéaires. Une autre approche qui consiste à proposer une nouvelle logique d'estimation du signal de commutations d'un système linéaire à commutations à entrée inconnue est introduite en combinant la technique par modes glissants et l'approche par intervalles. Le problème d'estimation d'état constitue une des étapes fondamentales pour traiter le problème de détection de défauts. Par conséquent, des solutions robustes de détection sont mises en oeuvre en présence des perturbations et du bruit de mesure en utilisant la théorie des ensembles. Tout d'abord, une approche de détection de défaut est proposée en se basant sur des observateurs par intervalles de différentes structures (une structure classique et une structure TNL) avec des performances L_∞ . Ensuite, une nouvelle méthode de détection des défauts est conçue en utilisant des techniques zonotopiques et ellipsoïdales. Ces outils permettent de fournir des seuils dynamiques pour l'évaluation du résidu et d'améliorer la précision des résultats de détection de défauts sans tenir compte de l'hypothèse de coopérativité. Les méthodes développées dans cette thèse sont illustrées par des exemples académiques et les résultats obtenus montrent leur efficacité.

Mots clés : Systèmes à commutations, Observateurs par intervalles, La théorie de Lyapunov, La performance L_∞ , Analyse zonotopique, Analyse ellipsoïdale.

Abstract

This thesis deals with state estimation and fault detection for a class of switched linear systems. New interval observers are investigated for continuous-time and discrete-time linear parameter varying switched systems, with a known switching signal and measured polytopic parameters. The design conditions are formulated in terms of linear matrix inequalities, and include the cases of arbitrary and dwell-time switching. In addition, a new switching signal observer, combining sliding mode and interval techniques, is developed for linear switched systems with unknown input. State estimation remains one of the fundamental steps to deal with fault detection. Hence, robust fault detection solutions are performed for linear switched systems subject to state perturbations and measurement noise using set-membership theory. First, a fault detection approach is proposed based on interval observers of different structures (a conventional one and a TNL structure) with L_∞ performances. Moreover, a new fault detection method is designed using zonotopic and ellipsoidal estimation tools, which can provide a systematic and effective way to improve the accuracy of the residual boundaries without considering the cooperativity assumption. Based on optimization criteria, fault sensitivity and disturbance attenuation conditions are presented. The developed techniques in this thesis are illustrated using academic examples and the results show their effectiveness.

Keywords: Switched systems, Interval observers, Lyapunov theory, L_∞ performance, Zonotopic analysis, Ellipsoidal analysis.

Contents

Remerciements	i
Résumé	iii
Publications of the author	ix
List of Figures	xi
Nomenclature	xv
Notations	xvii
1 Introduction, context and main contributions	1
1.1 Context and motivations	1
1.2 Structure of the Thesis	3
2 State of the art	7
2.1 Introduction	7
2.2 Generality of switched systems	7
2.2.1 Context	7
2.2.2 Modeling	8
2.2.3 Stability analysis	8
2.2.3.1 Classical stability concepts	9
2.2.3.2 Lyapunov stability theory	11
2.2.3.3 Stability analysis under arbitrary switching	11
2.2.3.4 Stability analysis under constrained switching	12
2.3 Observability and observers design tools for switched systems	14
2.3.1 Context	14
2.3.2 Observability for switched systems	15
2.3.3 Observers design for switched systems	16
2.3.4 Interval observer	17
2.3.4.1 Preliminaries	18
2.3.4.2 Interval observers for LTI systems	19
2.3.4.3 Interval observers for LTV systems	20
2.3.4.4 Interval observers for LPV systems	21
2.3.4.5 Interval observers for switched systems	25
2.4 Fault diagnosis for switched systems	25
2.4.1 Diagnosis Process	26
2.4.1.1 Fault detection techniques	27
2.4.1.2 Fault isolation techniques	28
2.4.1.3 Fault identification techniques	28

2.4.2	Classification of faults	29
2.4.2.1	Fault classification based on the faulty component	29
2.4.2.2	Fault classification according to the temporal evolution	29
2.4.2.3	Fault classification according to the impact on system performance	30
2.4.3	Model-based fault diagnosis	31
2.4.3.1	Parity relation approaches	31
2.4.3.2	Parameter estimation approaches	31
2.4.3.3	Observer-based approaches	32
2.4.4	Set-membership fault detection for switched systems	32
2.4.4.1	Interval-based approaches	33
2.4.4.2	Zonotope-based approaches	34
2.4.4.3	Ellipsoid-based approaches	34
2.5	Conclusion	35
3	Interval estimation for synchronous switched systems	37
3.1	Introduction	37
3.2	Interval observer design for continuous-time LPV switched systems	38
3.2.1	Problem statement	38
3.2.2	Interval observer design: cooperativity analysis	39
3.2.3	Interval observer design: Input-to-State Stability	41
3.2.3.1	Common Quadratic Lyapunov Function	41
3.2.3.2	Multiple Quadratic Lyapunov Functions	43
3.2.4	Numerical examples	46
3.2.4.1	Example 1: Common Lyapunov Function	46
3.2.4.2	Example 2: Multiple Lyapunov Functions	49
3.3	Interval observer design for discrete-time LPV switched systems	55
3.3.1	Problem statement	55
3.3.2	Interval observer design	56
3.3.2.1	Positivity of the interval errors	56
3.3.2.2	Interval errors convergence	56
3.3.3	Numerical example	59
3.4	Conclusion	62
4	Interval estimation for asynchronous switched systems	65
4.1	Introduction	65
4.2	System description	66
4.3	Interval observer design for switched systems	67
4.3.1	Interval observer structure	67
4.3.2	Problem formulation	68
4.4	Switching signal estimation	70
4.4.1	Discrete state estimation	70
4.4.2	Switching time instants estimation	73
4.5	Numerical example	77
4.5.1	Simulation settings	77

4.5.2	Simulation results	77
4.6	Conclusion	80
5	Interval observer based-fault detection design for switched systems	83
5.1	Introduction	83
5.2	Problem statement	84
5.3	A common Lyapunov function based-approach	84
5.3.1	Interval observer design for switched systems	84
5.3.2	Interval observer design: TNL structure	89
5.4	Multiple Lyapunov functions based-approach	93
5.4.1	Interval observer scheme for switched systems	93
5.4.2	Interval observer scheme: TNL structure	95
5.5	Residual evaluation	97
5.6	Numerical example	98
5.6.1	Fault detection results based on CQLF	99
5.6.2	Fault detection results based on MQLF	102
5.7	Conclusion	105
6	Set-membership fault detection frameworks for switched systems	107
6.1	Introduction	107
6.2	Zonotope-based fault detection framework	108
6.2.1	Zonotopic set-theory preliminaries	108
6.2.2	Problem formulation	111
6.2.3	Robust fault detection design	111
6.2.3.1	Fault sensitivity condition	112
6.2.3.2	Disturbance attenuation condition	113
6.2.3.3	Fault detection observer design: Luenberger structure	114
6.2.3.4	Zonotope-based residual evaluation	116
6.2.4	Numerical example	117
6.2.4.1	Simulation settings	117
6.2.4.2	Simulation results	118
6.3	Ellipsoid-based fault detection framework	121
6.3.1	Ellipsoidal set-theory preliminaries	121
6.3.2	Problem statement	123
6.3.3	Robust fault detection design: TNL structure	123
6.3.4	Ellipsoid-based residual evaluation	128
6.3.5	Illustrative Example	130
6.3.5.1	Simulation settings	130
6.3.5.2	Simulation results	130
6.4	Conclusion	135
7	Conclusions and Perspectives	137
7.1	Conclusions	137
7.2	Future directions	138
	Appendices	141

A Appendix of chapter 5	143
A.1 Proof of theorem 16	143
A.2 Proof of theorem 18	145
B Résumé des travaux de thèse	147

Publications of the author

Journal papers

1. Chaima Zammali, Jérémy Van Gorp, Zhenhua Wang, and Tarek Raïssi, "Sensor fault detection for switched systems using interval observer with L_∞ performance", European Journal of Control, 2020.
2. Chaima Zammali, Jérémy Van Gorp, and Tarek Raïssi, "Interval estimation for continuous-time LPV switched systems", International Journal of Control, 2020.
3. Chaima Zammali, Jérémy Van Gorp, and Tarek Raïssi, "On interval observer design for continuous-time LPV switched systems", Acta Cybernetica, vol. 24, no. 3, pp. 539-555, 2020.

Conference papers

1. Chaima Zammali, Jérémy Van Gorp, Zhenhua Wang, Xubin Ping, and Tarek Raïssi, "Ellipsoid-based sensor fault detection for discrete-time switched systems", in 59th IEEE Conference on Decision and Control (CDC), 2020.
2. Chaima Zammali, Zhenhua Wang, Jérémy Van Gorp, and Tarek Raïssi, "Fault detection for switched systems based on pole assignment and zonotopic residual evaluation", in 21st IFAC World Congress, 2020.
3. Chaima Zammali, Jérémy Van Gorp, and Tarek Raïssi, "Robust fault detection for switched systems based on interval observers", in 28th Mediterranean Conference on Control and Automation (MED), 2020.
4. Chaima Zammali, Jérémy Van Gorp, and Tarek Raïssi, "Interval observers based fault detection for switched systems with L_∞ performances", in European Control Conference (ECC), 2020.
5. Chaima Zammali, Jérémy Van Gorp, Xubin Ping, and Tarek Raïssi, "Interval estimation for discrete-time LPV switched systems", in 2019 IEEE 58th Conference on Decision and Control (CDC). IEEE, 2019, pp. 2479-2484.

6. Chaima Zammali, Jérémy Van Gorp, Xubin Ping, and Tarek Raïssi, "Switching signal estimation based on interval observer for a class of switched linear systems", in 2019 IEEE 58th Conference on Decision and Control (CDC). IEEE, 2019, pp. 2497-2502.
7. Chaima Zammali, Jérémy Van Gorp, Tarek Raïssi, Interval Estimation for Continuous-time LPV Switched Systems, 11th Summer Workshop on Interval Methods (SWIM), 2018.

List of Figures

2.1	Switching between unstable subsystems.	9
2.2	Switching between stable subsystems.	9
2.3	Multiple Lyapunov functions.	12
2.4	Interval observer.	18
2.5	Diagnosis Process.	26
2.6	Fault detection.	27
2.7	Representation of the most common actuator faults (a) Oscillation, (b) Blocking, (c) Saturation and (d) Loss of Efficiency.	29
2.8	Temporal Evolution of Faults.	30
2.9	Faults Classification: Multiplicative and Additive.	30
2.10	A Zonotope with different reduction orders.	34
3.1	Evolution of the switching signal	48
3.2	Evolutions of the state x and the estimated upper and lower bounds using CQLF.	49
3.3	Evolutions of the state x and the estimated upper and lower bounds (ZOOM) using CQLF.	49
3.4	Evolution of estimation errors using CQLF.	50
3.5	Evolution of the switching signal	52
3.6	Evolutions of the state x and the estimated upper and lower bounds using MQLF.	52
3.7	Evolutions of the state x and the estimated upper and lower bounds (ZOOM) using MQLF.	53
3.8	Evolutions of the estimation errors using MQLF.	53
3.9	Evolutions of the state x and the estimated upper and lower bounds (ZOOM). 54	
3.10	Comparison between the estimated upper and lower bounds of the state x_1 obtained by the proposed polytopic approach and norm bounded approach in [181] (ZOOM).	54
3.11	Comparison between the estimated upper and lower bounds of the state x_2 obtained by the proposed polytopic approach and norm bounded approach in [181] (ZOOM).	55
3.12	Evolution of the switching signal.	61
3.13	Evolutions of the state x and the estimated upper and lower bounds.	61
3.14	Evolutions of the state x and the estimated upper and lower bounds (ZOOM). 62	
3.15	Evolutions of the estimation errors.	62

4.1	A stack of interval observers.	67
4.2	Bloc diagram of the discrete state estimator.	73
4.3	Evolution of the switching signal σ (a), its estimate $\hat{\sigma}$ (b) and the reset instants based on (4.35) (c).	78
4.4	Evolution of the switching signal and its estimate (ZOOM).	79
4.5	Evolution of the continuous state $x(t)$ and its estimated bounds for $i = \hat{\sigma}$	79
4.6	Evolution of the upper error.	80
4.7	Evolution of the upper error.	80
5.1	Evolution of the switching signal	98
5.2	Residual framers using fault detection interval observer	99
5.3	Residual framers using fault detection TNL interval observer	101
5.4	Fault detection performance comparison between the TNL method and the interval approach	101
5.5	Fault detection performance comparison between the TNL method and the interval approach (Small fault)	102
5.6	Residual framers using fault detection interval observer	103
5.7	Fault detection performance comparison between the TNL method and the interval approach (Small fault)	105
6.1	3-zonotope in a two dimension space.	109
6.2	Interval hull of a zonotope	109
6.3	A zonotope \mathbf{Z} and its three dimension reduction zonotopes.	110
6.4	Block diagram of the proposed fault detection approach.	117
6.5	Evolution of the switching signal.	119
6.6	Evolution of the actuator fault.	119
6.7	Comparison between the results of fault detection instant obtained with and without optimisation	120
6.8	Residual and residual zonotope of the proposed FD observer	121
6.9	Residual and residual zonotope of method without optimization	121
6.10	Ellipsoid set	122
6.11	Block diagram of the proposed fault detection approach.	130
6.12	Evolution of the switching signal.	131
6.13	Evolution of the sensor fault.	132
6.14	Comparison between fault detection results obtained with the proposed observer and a Luenberger structure.	132
6.15	Comparison between fault detection results obtained with the proposed observer and a Luenberger structure (small fault).	133
6.16	Residual and residual ellipsoid based on the proposed approach.	134
6.17	Residual and residual ellipsoid using a Luenberger observer.	134
B.1	Observateur par intervalles.	154
B.2	Evolutions de l'état x et les bornes supérieure et inférieure estimées.	157
B.3	Evolution des erreurs d'estimation.	158
B.4	Schéma bloc d'une batterie d'observateurs par intervalles.	159
B.5	Schéma bloc de l'observateur d'état discret.	162

B.6	Evolution du signal de commutation et son estimé (ZOOM).	163
B.7	Comparaison des performances de détection des défauts entre l'approche TNL et la méthode par intervalles classique.	168
B.8	Comparaison des performances de détection des défauts entre l'approche TNL et la méthode par intervalles classique (Défaut de faible amplitude).	169
B.9	Résultats de détection du défaut actionneur : Approche proposée avec opti- misation	171
B.10	Résultats de détection du défaut actionneur : Approche sans optimisation . .	172
B.11	Comparaison entre les résultats de détection de l'observateur proposé et la structure de Luenberger.	174

Nomenclature

Abbreviations and Acronyms

ADT	Average Dwell Time
CQLF	Common Quadratic Lyapunov Function
FD	Fault Detection
HDS	Hybrid Dynamic Systems
ISS	Input to State Stability
LTI	Linear Time-Invariant
LTV	Linear Time-Varying
LMI	Linear Matrix Inequalities
LPV	Linear Parameter Varying
MQLF	Multiple Quadratic Lyapunov Functions
UIO	Unknown Input Observers

Notations

\mathbb{R}	The set of real numbers
\mathbb{Z}	The set of integers
\mathbb{R}_+	The set of positive real numbers
\mathbb{Z}_+	The set of positive integers
\mathbb{R}^n	n dimensional Euclidean space
$\mathbb{R}^{m \times n}$	$m \times n$ dimensional Euclidean space
$ \cdot $	The componentwise absolute value in \mathbb{R}^n
$\ \cdot\ $	The euclidean norm in \mathbb{R}^n
$\ \cdot\ _\infty$	The infinity norm in \mathbb{R}^n
I_n	The identity matrix
$P \succ 0$	P is definite positive
$P = P^T$	P is symmetric
$P \succeq 0$	P semi definite positive
A^+	is defined by $A^+ = \max\{0, A\}$
A^-	is defined by $A^- = A^+ - A$
$ A $	is defined by $ A = A^+ + A^-$
$\leq, \geq, <$ and $>$	should be interpreted elementwise for vectors as well as for matrices

Chapter 1

Introduction, context and main contributions

1.1 Context and motivations

With the continuous growing complexity of industrial systems and rising demand for higher performance and safety, the implementation of optimized fault diagnosis strategies has become a priority for many industrials in order to minimize performance degradation and to avoid severe and irreversible damage to human operator and equipment. Usually, physical systems as mechanical, embedded, power, communication networks, are characterized by hybrid processes which exhibit both discrete and continuous dynamics. Switched systems represent a special class of hybrid systems. They involve a finite number of subsystems and a switching law specifying the active subsystem at each time instant. They can model and control a wide range of engineering systems. Some typical examples of switched systems with greater theoretical challenges and high practical interest can be found, for instance, in power systems, computer disk drives, transmission and stepper motors, robotics and automated highways.

The problem of state estimation for switched systems has received much attention in the control community such as model-predictive control and fault diagnosis. Indeed, in some practical cases, the entire state vector can not be completely measurable or accessible. This is due to economic and technical reasons, such as the high cost of the sensors and their insufficient precision. In order to deal with this problem, state observers have been introduced to estimate the internal variables from the inputs and outputs measurements. In the presence of uncertainties coming either from external disturbances or from the mismatch between the model and the real system, state estimation may not converge to the real state. Therefore, the design of conventional observers such as Luenberger observers or Kalman filter, may not be efficient to solve the estimation problem. Based on a general assumption

that the uncertainties are unknown but bounded, interval observers constitute an interesting alternative by providing the admissible bounds of the state variables using the available information. Actually, most of interval observers for switched systems are designed in a linear time invariant settings. In the context of this thesis, we are interested in interval state estimation for both continuous-time and discrete time LPV switched systems. The main advantage is that a partial linearity of LPV representation provides a systematic and elegant way to deal with state estimation for nonlinear systems.

Usually, interval observer techniques are based on monotone systems theory, which requires the cooperativity of the estimation error. However, this assumption is restrictive. To cope with this difficulty, interval observer design techniques based on coordinate transformations have been achieved to get relaxed design conditions. Meanwhile, when switched systems are affected by time-varying parameters, applying a change of coordinates can constitute an infinite dimensional problem. This thesis is conducted to propose a finite dimensional relaxation for both cooperativity and stability conditions for uncertain LPV switched systems with polytopic time varying parameters.

The problem of state estimation for switched systems becomes more complicated when the switching law is unknown or difficult to obtain. One of the ways to solve this problem is to reconstruct the switching law, which makes the discrete state estimation of the switched system particularly important. To the best of our knowledge, the design of a robust interval discrete state estimation approach for switched linear systems with unknown input has not been fully addressed yet. In this context, a new method, combining sliding modes techniques which provide a finite time convergence and the interval approaches where only the bounds of the unknown input are needed, is proposed to estimate the switching signal.

As well as interval state estimation methods, interval observers have paid a huge attention in fault detection due to their low computational complexity. The major advantage of using interval FD observers consists in providing systematic residual evaluation and avoids the design of threshold generators. In the other side, it is not trivial to design an interval observer by constructing two simultaneously cooperative and stable error systems. Although this restriction can be relaxed based on coordinate transformation, it may lead to additional conservatism and can reduce the FD accuracy. In view of this major drawback, two strategies have been developed in this thesis. The first one is investigated based a new interval observer structure to relax the cooperativity constraint. This method offers more degrees of design freedom by integrating weighted matrices in the structure of the fault detection observer design. The second strategy is introduced based on set-membership theory. Set-membership techniques are considered as powerful tools in giving more accurate FD results without considering the cooperativity constraint. In general, there exist various convex set shapes to represent the uncertainties such as ellipsoids [1], polytopes [2], zonotopes [3], etc. The choice of the shape of convex sets depends on their accuracy and their complexity for solving a given problem. In the context of this thesis, we are mainly interested in fault detection based on zonotopes and ellipsoids methods.

The accuracy of fault detection is highly affected by the modeling uncertainties. Thus, one of the most essential requirements imposed on FD algorithms is the robustness against uncertainties. H_∞ technique, for instance, has been introduced to attenuate the effect of disturbances. Note that the H_∞ norm is a measurement of energy-to-energy gain. Nevertheless, the practical signals are not necessarily energy bounded but have bounded peak

values. Other methods such as disturbances decoupling methods have been proposed with the aim to completely cancel the disturbances effect from the residual signals. However, it may be problematic, in some cases, because the fault impact may also be removed. Hence, appropriate criteria should be designed in order to take into account the effects of both disturbances and faults. To the best of our knowledge, the optimisation of the observer gain in order to achieve robust fault detection is still an open problem for switched systems. In the context of this thesis, robust fault detection is developed for switched systems by introducing set-membership approaches with an L_∞ analysis which describes the peak-to-peak performance index and a novel pole assignment method to maximize the sensitivity of faults on the residual signal. The proposed approaches are designed with the aim to provide better FD accuracy and to detect small faults.

This thesis contributes, on the one hand, to the interval estimation of the continuous state as well as the discrete logic for a class of switched systems subject to unknown but bounded disturbances. On the other hand, it provides robust solutions for fault detection based on set-membership techniques and some optimization tools. The main contributions of this thesis are briefly summarized:

- The first contribution deals with interval state estimation for continuous and discrete-time LPV switched systems with measured polytopic parameter dependence, assuming a known switching signal. The main advantage of the proposed method is to relax cooperativity and stability design conditions thanks to the polytopic form of the time varying parameters. These properties are expressed on the vertices of each polytope and provided in terms of LMIs, adopting common and multiple Lyapunov functions.
- The second contribution considers a new estimation logic of the switching time instants for a switched linear system with unknown input by combining sliding modes techniques and interval approaches.
- The third contribution provides a robust solution for fault detection using classical interval observers as well as interval observers with a new structure (TNL structure). The proposed structure offers more degrees of design freedom. The performance of FD results is improved based on the minimization of an L_∞ criterion.
- The last contribution introduces a robust FD strategy using zonotopic and ellipsoidal approaches. The major advantage of this contribution consists in providing systematic dynamic thresholds for the residual evaluation and improving the accuracy of FD results without taking into account the cooperative assumption.

1.2 Structure of the Thesis

In order to highlight the contributions of this thesis, the following outline is adopted:

- **Chapter 2:** A non-exhaustive overview on hybrid and switched systems is provided with some basic concepts about mathematical definitions and stability analysis. Next, significant results about observability and estimation tools from the literature are introduced within a focus on interval observer theory. Then, some existing results on

diagnosis approaches are presented. In the last section of this chapter, a state of the art on set-membership fault detection for switched systems is reported.

- **Chapter 3:** The primary focus of this chapter is to design an interval observer for both continuous and discrete-time LPV switched systems subject to measured polytopic parameters when the the switching signal is supposed to be known. In a context of unknown but bounded uncertainties, the interval approach consists in providing two suitable conventional observers, designed to compute lower and upper bounds of the state. This approach is based on a closed loop structure where the observer gain is chosen to impose cooperative dynamics for the estimation errors. Nevertheless, the cooperativity condition is restrictive. In the literature, some methods propose a coordinate transformation to relax this constraint. However, when systems are subject to time-varying parameters, applying a change of coordinates can constitute an infinite dimensional problem. This motivates the present chapter which is dedicated to propose a finite dimensional relaxation for the design conditions of the proposed interval observer. Using common and multiple quadratic Lyapunov functions, new conditions of cooperativity and stability are provided in terms of LMIs expressed on the vertices of each polytope. Simulation results, on academic examples, are proposed to illustrate the effectiveness of the proposed approaches.
- **Chapter 4:** In chapter 4, the estimation problem of the switching signal for a class of switched linear systems with unknown input is considered. From a practical point of view, the presence of unknown inputs can not be avoided for the most actual applications which makes the discrete state estimation of switched systems important. In the literature, the reconstruction of the discrete state can be solved using decoupling approaches such that the estimation error dynamics in the transformed state coordinates are not affected by the unknown inputs. Without using decoupling techniques, this chapter discusses a new approach designed by combining a sliding modes observer with an interval observer in order to estimate the discrete mode of the switched system. The combination of both observers is one of the main contributions of this chapter. In fact, sliding modes techniques provide a robust finite-time convergence. Meanwhile, only bounds of the unknown input are needed when the interval approach is used. The feasibility and effectiveness of the proposed approach are illustrated via an academic example.
- **Chapter 5:** This chapter deals with sensor fault detection for a class of discrete-time switched systems subject to bounded disturbances. Two approaches to construct residual framers are considered. First, the classical interval observer is designed based on an L_∞ criterion. The proposed approach is used to improve the performance of FD and to provide a systematic way for residual evaluation based on a belonging test of the zero signal to the residual framers generated by the proposed FD observers. Interval observer design techniques are usually based on the theory of positive systems, which require the nonnegativity of the error dynamics. To relax the aforementioned constraint, a coordinate transformation is proposed in some existing works. However, it is hard to merge the coordinate transformation approach with some additional constraints related to control such as disturbance attenuation performance. In view

of this major drawback, the main purpose of the second approach is to propose a novel interval observer structure (TNL structure) that can give more degrees of design freedom. The basic idea consists of introducing weighted matrices in addition to the gain matrix. First, it offers a solution when a gain matrix cannot be found. Second, better FD performances may be achieved. The design conditions of the observers are given in terms of LMIs using a CQLF, with arbitrary switching signal and MQLF and an ADT switching signal. The efficiency of the present approaches is highlighted through simulation results on academic examples.

- **Chapter 6:** In this chapter, fault detection is studied for discrete-time switched systems using zonotopic and ellipsoidal techniques. The proposed approaches are developed to provide dynamic thresholds for residual evaluation and to improve the accuracy of FD results without considering the cooperative assumption. In the first part, a Luenberger FD observer is designed for switched systems with actuator faults. Pole assignment technique and H_∞ design are used to develop the fault sensitivity and the disturbance attenuation condition of the residual, respectively. The design conditions of the observer are derived in terms of LMIs. In addition, the disturbances and measurement noise are supposed to be unknown but bounded by zonotopes. Thus, a zonotopic method is presented to evaluate the residual. The FD accuracy of the zonotopic techniques can be improved using high dimensional zonotopes. However, the additional dimensional growth may cause heavier computational burden. To handle this problem, the ellipsoidal techniques can be considered as a good trade-off between FD accuracy and computation complexity. In the second part, fault detection is proposed for switched systems with sensor faults, using ellipsoidal analysis. A FD observer with a new structure is investigated based on an L_∞ criterion to attenuate the effects of uncertainties. The design conditions of the proposed observer are given in terms of LMIs using MQLF, with an ADT switching signal. Finally, numerical examples are performed to illustrate the effectiveness of the proposed approaches.
- **Chapter 7:** This chapter gives a summary of the thesis and discusses potential future works arising from this research.

Chapter 2

State of the art

2.1 Introduction

This thesis addresses state estimation and fault diagnosis for a class of switched systems. This class of systems represent a special class of hybrid systems. In this chapter, we intend to provide a non-exhaustive overview on hybrid and switched systems. Some basic concepts about mathematical definitions and stability analysis for switched systems are recalled. Next, significant results about observability and estimation tools from the literature are introduced within a focus on interval observer theory. As the developed work in this thesis concerns mainly model-based fault diagnosis for switched systems, a state of the art on fault diagnosis is reported in the last section of this chapter.

2.2 Generality of switched systems

2.2.1 Context

In recent decades, an outstanding attention has been devoted to Hybrid Dynamic Systems (HDS). This class of systems simultaneously involves continuous and discrete elements represented by differential equations and event dynamic models whether they are deterministic and / or stochastic. They are firstly came out in [4] since the supervision and the control of several processes require continuous data as well as discrete events. Many examples of HDS, with greater theoretical challenges and higher practical interest are encountered in the literature such that opening and closing power switches, biological cells duplication and division, a server switching between buffers in a queueing network, aircraft moving safely and efficiently through the airspace system [5], [6].

Switched systems represent a special class of hybrid systems [7], [8]. They are composed of a finite number of continuous subsystems named generally modes combined with a logical rule that operates switching between these subsystems. For many physical systems, different

modes can be identified. A wide range of physical and engineering systems can be modeled by switched ones: mechanical systems control [9], communication networks [10], embedded control models [11], power systems [12], network control systems [13], automotive supervision [14] and some other areas.

A simple model of switched systems is the temperature regulation system of a room [15]. The behavior of this model is described by discrete and continuous dynamics in interaction. We denote respectively by θ and σ the temperature which is continuous in time and the heater which represents the discrete state of the system. The average temperature of a heated room can be described by these relations:

$$\dot{\theta}(t) = -\rho(\theta(t) - \theta_{ext}) \quad \text{if the heater is off} \quad (2.1)$$

$$\dot{\theta}(t) = -\rho(\theta(t) - \theta_{ext}) + \beta \quad \text{if the heater is on} \quad (2.2)$$

Therefore, the switched system is given by:

$$\dot{\theta}(t) = -\rho(\theta(t) - \theta_{ext}) + \beta\sigma(t) \quad \sigma(t) \in \{0, 1\} \quad (2.3)$$

The state of the heater can be naturally switched either on or off if the temperature exceeds a certain predefined threshold.

In the literature, switched systems can be gathered in different ways. Typically, the switching rule can be state-dependent, time-dependent, autonomous or controlled. An overview of the different switched system classes is given and detailed in [16], [6], [17].

2.2.2 Modeling

Mathematically, a continuous-time switched system can be described as follows:

$$\begin{cases} \dot{x}(t) = A_{\sigma(t)}x(t) + B_{\sigma(t)}u(t) + E_{\sigma(t)}w(t) \\ y(t) = Cx(t) + v(t) \end{cases}, \sigma(t) \in \mathcal{I} \quad (2.4)$$

where $x \in \mathbb{R}^{n_x}$, $u \in \mathbb{R}^{n_u}$, $y \in \mathbb{R}^{n_y}$, $w \in \mathbb{R}^{n_x}$ and $v \in \mathbb{R}^{n_y}$ are respectively the state vector, the input and the output, the disturbance and the measurement noise. The switching signal $\sigma(t) : \mathbb{R}_+ \rightarrow \mathcal{I} = \{1, 2, \dots, N\}$, $N \in \mathbb{Z}_+$, is a piecewise right-continuous function which allows selecting the active subsystem in continuous time among the N possible modes.

Remark 1. *In the sequel, for ease of notation, let $E_{\sigma(t)}w(t) = w_{\sigma(t)}$.*

As likewise, a discrete-time switched system can be represented as follows:

$$\begin{cases} x_{k+1} = A_{\sigma(k)}x_k + B_{\sigma(k)}u_k + w_{\sigma(k)} \\ y_k = Cx_k + v_k \end{cases}, \sigma(k) \in \mathcal{I} \quad (2.5)$$

The switchings between the subsystems are ensured via $\sigma(k) : \mathbb{Z}_+ \rightarrow \mathcal{I} = \{1, 2, \dots, N\}$, $N \in \mathbb{Z}_+$, N is the number of discrete-time subsystems.

2.2.3 Stability analysis

The main purpose of developing stability theory is to analyze dynamic responses of a system to disturbances and uncertainties. It has been and still is the object of great investigations

due to its inherent interest and its relevance to all practical systems in many engineering fields. From a historical perspective, stability analysis has witnessed an impressive progress for different classes of systems [16], [18] especially for switched systems [19], [20]. The stability of switched systems depends on the same property of each subsystem and the switching law. A switched system with unstable modes may be unstable or stabilized by a suitable switching law. These two possibilities can be illustrated on the right of Fig. 2.1 where the two unstable subsystems are shown on the left of Fig. 2.1 (the solid curve and the dotted one).

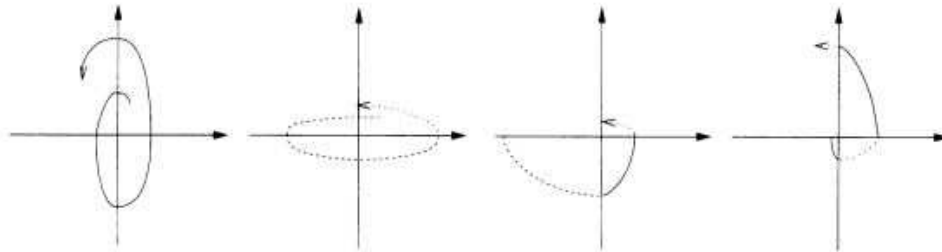


Figure 2.1: Switching between unstable subsystems.

In the other side, the stability of all modes does not imply the same property of the switched system. In Fig. 2.2, a two second-order system is considered where the trajectories of its stable subsystems are shown on the left of Fig. 2.2. The switched system may be either stable or unstable, depending on a particular switching signal (Fig. 2.2 on the right). As a

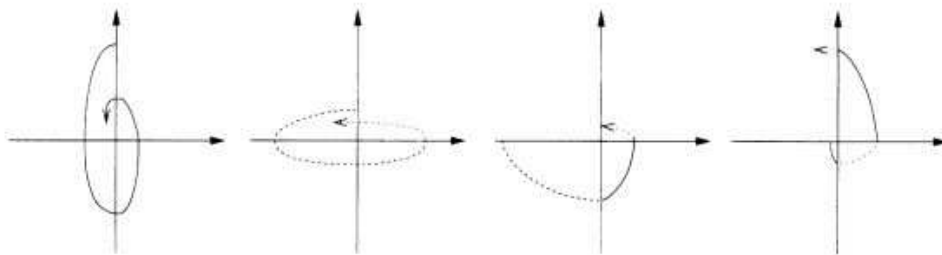


Figure 2.2: Switching between stable subsystems.

result, the study of stability of switched systems is challenging and several existing research activities have been carried out in this field [19], [21], [22], [17], [7]. Some important concepts from the stability theory are first recalled in the following.

2.2.3.1 Classical stability concepts

Instinctively, the stability analysis is the property of a system to return to its equilibrium point after it has been deviated from its initial position.

Let us consider the following invariant system:

$$\dot{x}(t) = f(x(t)) \quad (2.6)$$

$f : \mathbb{R}^n \rightarrow \mathbb{R}^n$ is a locally Lipschitz function. The equilibrium points x^* of the system (2.6) are the solutions of the equation $f(x) = 0$. They can be stable, asymptotically stable, globally asymptotically stable, locally exponentially stable or unstable.

Definition 1. [2] *The equilibrium point of the system (2.6) is*

- *stable if $\forall \varepsilon > 0 \exists \delta > 0$ such that*

$$\|x(0) - x^*\| < \delta \Rightarrow \|x(t) - x^*\| < \varepsilon, \forall t \geq 0$$

- *asymptotically stable if x^* is stable and if there exist $\delta > 0$ such that*

$$\|x(0) - x^*\| < \delta \Rightarrow \lim_{t \rightarrow \infty} x(t) = x^*$$

- *globally asymptotically stable if x^* is stable and $\forall x(0) \in \mathbb{R}^n$*

$$\lim_{t \rightarrow \infty} x(t) = x^*$$

- *locally exponentially stable if there exist three positive real scalars c, K and λ such that*

$$\forall \|x(0) - x^*\| < c, \|x(t) - x^*\| \leq K \|x(0) - x^*\| e^{-\lambda t}$$

Consider the case of autonomous linear switched systems represented by:

$$\dot{x}(t) = A_{\sigma(t)} x(t) \tag{2.7}$$

where the switchings between the subsystems are ensured via the logical rule $\sigma(t)$. The following definitions are needed.

Definition 2. *A function $\zeta : \mathbb{R}_+ \rightarrow \mathbb{R}_+$ is*

- *a \mathcal{K} -function if it is continuous, strictly increasing and $\zeta(0) = 0$*
- *a \mathcal{K}_∞ -function if it is a \mathcal{K} -function and also $\zeta(s) \rightarrow \infty$ as $s \rightarrow \infty$*
- *a \mathcal{KL} -function if for each fixed $t \geq 0$ the function $\zeta(\cdot, t)$ is a \mathcal{K} -function and for each fixed $s \geq 0$ it is decreasing to zero as $t \rightarrow \infty$.*

Definition 3. *The system (2.7) is globally uniformly asymptotically stable if there exists a \mathcal{KL} -function β such that*

$$\|x(t)\| \leq \beta(\|x(0)\|, t), \forall t \geq 0$$

Definition 4. *The system (2.7) is globally uniformly exponentially stable if there exist two real scalars $c, \lambda > 0$ such that*

$$\|x(t)\| \leq c e^{-\lambda t} \|x(0)\|$$

2.2.3.2 Lyapunov stability theory

The Lyapunov theory is one of the most useful paradigm for the stability analysis. Based on this theory, the stability property is ensured as soon as a decreasing energy function, called Lyapunov function, is build.

Definition 5. [2] *Given the system (2.6), if there exist a locally Lipschitz Lyapunov function $V : \mathbb{R}^n \rightarrow \mathbb{R}$ and two \mathcal{K} -functions α and β such that*

$$\alpha(\|x\|) \leq V(x) \leq \beta(\|x\|), \forall x \in \mathbb{R}^n, \quad (2.8)$$

the equilibrium point $x^ = 0$ of the system (2.6) is*

- *stable if*

$$\frac{dV(x)}{dt} \leq 0, \forall x \in \mathbb{R}^n, x \neq 0$$

- *asymptotically stable if x^* is stable and if there exists a \mathcal{K} -function φ such that*

$$\frac{dV(x)}{dt} \leq -\varphi(\|x\|), \forall x \in \mathbb{R}^n, x \neq 0$$

The extensions of these definitions for non-autonomous, discrete and switched systems are detailed in [2], [23] and [24].

2.2.3.3 Stability analysis under arbitrary switching

The Lyapunov theory plays a crucial role in the stability analysis of linear and nonlinear systems. Thus, it is not surprising that it has a similar impact for switched systems under arbitrary switching. A feasible technique consists in looking for a CQLF to guarantee the stability of the switched system. The existence of a CQLF for (2.7) can be expressed in terms of LMIs.

Theorem 1. [25] *Consider system (2.7). If there exists a symmetric positive definite matrix $P \in \mathbb{R}^{n_x \times n_x}$ that satisfies the following inequality:*

$$PA_q + A_q^T P < 0, \forall q \in \mathcal{I} \quad (2.9)$$

then $V(x) = x^T P x$ is a CQLF for the system (2.7).

Remark 2. *For the discrete-time case, the following LMI should be satisfied:*

$$A_q^T P A_q - P < 0, \forall q \in \mathcal{I} \quad (2.10)$$

$P \in \mathbb{R}^{n_x \times n_x}$ is a symmetric positive definite matrix.

In the literature, many authors have used CQLF to consider the stability for switched systems under arbitrary switching signals [19], [26], [18]. The requirement of a CQLF provides a sufficient condition for stability. Nevertheless, the existence of such a function is not always guaranteed and the results may be conservative. Therefore, it is possible to search for MQLF to reduce conservatism. It is worth noting that both Common and Multiple Lyapunov Functions are detailed in chapter 3 and comparative simulation results are provided.

2.2.3.4 Stability analysis under constrained switching

As already mentioned, based on Common Lyapunov Functions, stability criteria of switched systems may be conservative. However, it has been proven in the literature that it is possible to guarantee stability when all the subsystems are stable and the switching between modes is slow enough [19]. In [20], the notion of dwell time is introduced. It is mentioned that the stability can be preserved in the sense of sufficiently large dwell time [27]. In this context, the assumption of minimum dwell time during which no switching occurs is often introduced.

Definition 6. *The minimal dwell time is a constant τ_a such that the class of admissible switching signals satisfies the property that the switching time fulfills the inequality $t_{k+1} - t_k \geq \tau_a$ for all k .*

The stability property under restricted switching signal has been also investigated based on MQLF. MQLF can be defined as non-classical quadratic Lyapunov functions, built by concatenating several quadratic Lyapunov functions. They can be described as follows:

$$V_q = x^T P_q x \quad (2.11)$$

where P_q depends on the active mode q . The following Theorem introduces the asymptotic stability for switched systems based on MQLF.

Theorem 2. [25] *Consider the Lyapunov functions V_σ . For $i < j$, let $t_i < t_j$ be the switching times such that $\sigma(t_i) = \sigma(t_j)$. If there exists a positive scalar $\gamma > 0$ such that*

$$V_{\sigma(t_j)}(x(t_j)) - V_{\sigma(t_i)}(x(t_i)) \leq -\gamma \|x(t_i)\|^2, \forall (t_i, t_j), \sigma(t) \in \mathcal{I} \quad (2.12)$$

then the switched system (2.7) is asymptotically stable.

An example of MQLF for an asymptotically stable system with two switching modes is illustrated in the Fig. 2.3. In this example, when the mode $q = 1$ is active, the value of the

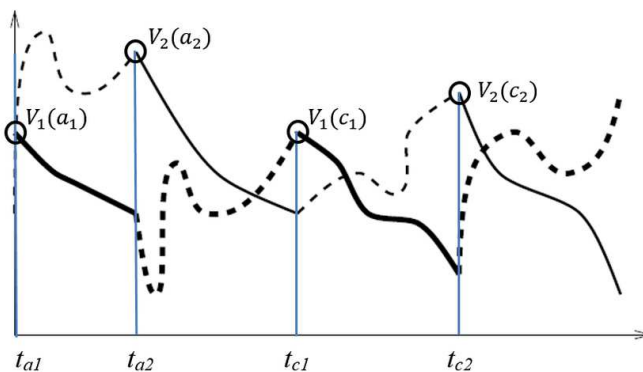


Figure 2.3: Multiple Lyapunov functions.

function V_1 at a given switching time t_{a1} is greater than its value at the next switching time t_{a2} . In the case where $q = 1$ is inactive ($q = 2$ active), between the instants t_{a2} and t_{c1} , the Lyapunov function of the mode $q = 1$ can increase meanwhile, the Lyapunov function of the active mode $q = 2$ is decreasing. In [28], [19], [16], an overview of significant results in the field of stability of switched linear systems based on MQLF is presented.

Under constrained switching, another approach is introduced in the literature when systems are subject to disturbances and noises. It is based on the concept of ISS. The ISS property provides a natural framework about stability with respect to input perturbations [29]. Instinctively, this means that the state should be bounded if bounded inputs are injected, and should converge to equilibrium when inputs tend to zero.

Definition 7. [29] *The system*

$$\dot{x} = f(x, u) \quad (2.13)$$

is said to be Input-to-State Stable if there exist a \mathcal{KL} -function κ and a \mathcal{K} -function φ such that for each input $u \in L_\infty^m$ and each $\ell \in \mathbb{R}^n$, it holds that

$$\|x(t, \ell, u)\| \leq \kappa(\|\ell\|, t) + \varphi(\|u\|_\infty), \forall t \geq 0$$

Definition 8. [29] *A function V is called an ISS-Lyapunov function for system (2.13) if there exist \mathcal{K}_∞ -functions α_1, α_2 and \mathcal{K} -functions α_3 and χ , such that:*

$$\alpha_1(\|x\|) \leq V_q(x) \leq \alpha_2(\|x\|)$$

$$\nabla V(x) \cdot f(x, u) \leq -\alpha_3(\|x\|),$$

for any $x \in \mathbb{R}^{n_x}$ and for any $u \in \mathbb{R}^{n_u}$ such that $\|x\| \geq \chi(\|u\|)$, $\dot{V}(x, u) = \nabla V(x) \cdot f(x, u)$.

The developed work in this thesis is concerned with switched systems subject to unknown but bounded disturbances. Therefore, ISS is considered for the stability analysis. The following definitions and lemmas are needed when ISS is introduced.

Definition 9. [27]. *We denote by $N_\sigma(T, t)$ the number of discontinuities of a switching signal σ on an interval (t, T) . $\sigma(t)$ has an ADT τ_a if there exist two positive numbers N_0 and τ_a such that:*

$$N_\sigma(T, t) \leq N_0 + \frac{(T-t)}{\tau_a}, \forall T \geq t \geq 0. \quad (2.14)$$

Lemma 1. [30] *Given the matrices $A = A^T$, $C = C^T$ and B with appropriate dimensions. The following LMIs are equivalent:*

$$\begin{bmatrix} A & B \\ B^T & C \end{bmatrix} \succ 0$$

$$C \succ 0; \quad A - BC^{-1}B^T \succ 0$$

$$A \succ 0; \quad C - B^T A^{-1}B \succ 0$$

Lemma 2. [31] *Consider the switched system (3.1), and let $\varepsilon > 0$, $\mu > 1$. Suppose that there exist $V_{\sigma(t)} : \mathbb{R}^n \rightarrow \mathbb{R}$, $\sigma(t)$ and two \mathcal{K}_∞ functions α and β such that for each $\sigma(t) = q, q \neq l$, the following conditions hold:*

$$\alpha(\|x(t)\|) \leq V_q(x(t)) \leq \beta(\|x(t)\|), \quad (2.15)$$

$$\dot{V}_q(x(t)) < -\varepsilon V_q(x(t)), \quad (2.16)$$

$$V_q(x(t)) < \mu V_l(x(t)), \quad (2.17)$$

then, the system (3.1) is ISS for any switching signal with an ADT τ_a satisfying

$$\tau_a > \tau_a^* = \frac{\ln(\mu)}{\varepsilon}, \quad (2.18)$$

where τ_a^ is the lower bound of τ_a determined by the parameters ε and μ .*

Conditions (2.15) and (2.16) are common in the literature when an ADT switching signal is considered. The existence of a function $V_q(x)$ satisfying (2.15) and (2.16) is a necessary and sufficient condition for each subsystem to be ISS.

The primary focus of this section is to introduce in more detail the class of switched systems which is considered in this thesis. As it was highlighted, the stability of switched systems has received growing attention. Many works have been proposed to construct a CQLF to satisfy stability under an arbitrary switching law. Since the existence of such a function is not always guaranteed for most practical switched systems and the results may be conservative, more attention has been paid to MQLF which constitute a powerful tool for studying stability under restricted switching signal. Apart from the stability analysis, the problem of estimation for switched systems deserves deep investigation due to its theoretical significance and practical applications. A lot of effort has been addressed to the estimation topic since in most real applications, the measurement of the physical state can be hard or impossible to achieve. Thus, one solution to consider is the reconstruction of the internal state from the inputs and outputs measurement. In the next section observability and observers design tools for switched systems are detailed within a focus on interval observers theory in a context of unknown but bounded uncertainties.

2.3 Observability and observers design tools for switched systems

2.3.1 Context

Several control design methods are based on the assumption that the full state vector is available for measurement. In many systems of practical importance, the entire state vector is not always known. There are almost two reasons: technical difficulties (necessary sensors are not available, insufficient accuracy, ...) and economic considerations (reducing the number of sensors to reduce the costs of diagnosis and maintenance). Thus, the estimation theory constitutes a suitable alternative to estimate unknown variables involved in a system.

The problem of observability and estimation has been widely investigated in the control community such as model-predictive control and fault detection [32], [33], [34]. In the literature, several state estimation design methods have been proposed. One of the most authentic observers is the Luenberger observer which is proposed in a deterministic framework without stochastic modeling on noises [35]. When uncertainties are described by random variables with a Gaussian distribution, the Kalman filter can be used to provide state and noise variance estimation from a series of noisy measurements [36]. Many observers such as unknown input observers [37], high-gain observers [38], functional observers [39], sliding-mode observers [40] have been considered in the state estimation literature. Another approach called set-membership state estimation has been developed to state estimation under unknown but bounded disturbances. In the set-membership context, no statistical information on uncertain variables is required. In general, there exists various set shapes to represent the uncertainties such as intervals [41], ellipsoids [1], polytopes [2], zonotopes [3], etc. The choice of the shape of convex sets depends on their accuracy and their complexity for solving a given problem. In the context of this thesis, we are mainly interested in

fault detection based on intervals, zonotopes and ellipsoids methods. As it was highlighted, the estimation accuracy is affected by state disturbances and measurement noises, robust estimation methods have been also introduced for efficiently handling the uncertainties attenuation problem. Among these methods, the H_∞ observer design which is common in robust estimation approaches [42]. In the aforementioned design method, the uncertainties are supposed to be energy-bounded. However, most uncertainties have bounded peak values. In such a situation, it is more appealing to provide a more practical assumption and to consider that the uncertainties are peak-bounded. Based on this assumption, robust state estimation methods have been developed using the L_∞ analysis which describes the peak-to-peak performance index [43]. Generally, the observability study can be checked by analyzing the rank of the so-called observability matrix. Consider a system defined by the following state representation:

$$\begin{cases} \dot{x} = Ax + Bu \\ y = Cx + Du \end{cases} \quad (2.19)$$

where $x \in \mathbb{R}^{n_x}$, $u \in \mathbb{R}^{n_u}$, $y \in \mathbb{R}^{n_y}$ are respectively the state vector, the input and the output. The system in (2.19) is observable if the following condition is satisfied:

$$\text{rank} \begin{bmatrix} C \\ CA \\ \vdots \\ CA^{n_x-1} \end{bmatrix} = n_x$$

2.3.2 Observability for switched systems

Consider the following switched system:

$$\begin{cases} \dot{x}(t) = A_q x(t) + B_q u(t) \\ y(t) = C_q x(t) \end{cases}, \quad q \in \mathcal{I} = \{1, 2, \dots, N\} \quad (2.20)$$

where $x \in \mathbb{R}^{n_x}$, $u \in \mathbb{R}^{n_u}$ and $y \in \mathbb{R}^{n_y}$ are the states, inputs and outputs, respectively. q denotes the index of the active subsystem. $q \in \mathcal{I} = \{1, 2, \dots, N\}$, $N \in \mathbb{Z}_+$, N is the number of modes. Based on the assumption that the switching signal q is known, the continuous state is observable in the classical sense, if the so-called observability matrix H_q , associated with each mode q is a full rank matrix such that:

$$\text{rank}(H_q) = \text{rank} \begin{bmatrix} C_q \\ C_q A_q \\ \vdots \\ C_q A_q^{n_x-1} \end{bmatrix} = n_x, \quad q \in \mathcal{I} = \{1, 2, \dots, N\}$$

According to [44], the observability which is of fundamental importance in the literature of control can be defined as follows.

Definition 10. *The switched linear system (2.20) is observable, if there exist a time $t_1 > 0$ and a switching path $q : [0, t_1] \rightarrow \mathcal{I}$, such that $x(0)$ can be determined from the knowledge of the output $y(t)$, $t \in [0, t_1]$ and the input $u(t)$, $t \in [0, t_1]$*

Dualistic criteria for observability and determinability are also discussed, the reader can refer to in [44].

In switched systems, the observability can be studied from various perspectives. As mentioned, when the discrete mode is assumed to be known, it requires that each subsystem is observable. However, the problem becomes nontrivial when the switching signal is treated as an unknown discrete state. In this context, several approaches have been developed in order to estimate the discrete state [45], [46], [47]. This problem have been treated using either continuous approaches or discrete ones. Continuous approaches are based on the design of a continuous observer to reconstruct the evolution of the switching signal. In this case, the condition of observability, associated with the discrete state, is often assimilated to the distinguishability concept. Necessary and sufficient distinguishability conditions have been derived for detecting the commutation time in [48], [49] and [50]. However, discrete approaches are based on the discrete event systems theory which consists on designing a discrete observer, modeled by a finite state automaton a petri net, to estimate the active mode. According to this approach, observability conditions have been also reported in [51], [52] and [53].

2.3.3 Observers design for switched systems

The observer design problems for switched systems have been studied using different approaches. In [54], full and reduced order observers are investigated for a class of linear switched systems. The designed observers require the switching signal to be known. In [55], a hybrid observer is introduced for a class of discrete time piecewise-linear systems composed by linear time-invariant subsystems with autonomous switching. The designed method is based on the construction of a discrete observer and a continuous one. Authors in [56] have addressed the state estimation problem for switched linear systems. An exact sliding mode differentiator is designed based on the continuous output information. The proposed approach provides a finite time convergence of the estimates of the entire state (continuous and discrete). In [57], an alternative approach to the state estimation problem is given for switched nonlinear systems with Lipschitz nonlinear subsystems. The aforementioned works did not address the problem of state estimation in presence of uncertainties. To handle this problem, authors in [58] have developed reduced-order unknown input switched observer to estimate the state of switched systems when unknown inputs are considered. For switched systems with both unknown disturbances and noises, simultaneous state and output disturbance estimation are introduced in [59] for a class of switched linear systems using a robust sliding-mode switched observer. In [60], an interval observer is designed for switched systems subject to bounded state disturbances and measurement noises. A coordinate transformation is used to relax the positivity property of the estimation errors. In [61], unknown input estimation is investigated for switched linear systems subject to unknown but bounded uncertainties. Based on a known switching signal, the proposed methodology provides guaranteed upper and lower bounds enclosing the state signal.

In practical cases, the active subsystem cannot always be known. Asynchronous switching between controller/observer and subsystems leads to more complex design problems. In [62], an output feedback controller is designed to ensure the finite-time stability of a switched time-delay system with disturbances and asynchronous switching between con-

troller and subsystems. Two kinds of observers are designed in [63] for switched linear systems with an ADT condition. The first one is based on a synchronous Luenberger observer structure where the state estimation depends of the active mode of the system. The second one considers a more practical case with an asynchronous switching signal. Sufficient conditions for the existence of these observers are proposed. In [64], robust observers are designed for a class of nonlinear uncertain switched linear systems with synchronous and asynchronous switching. The asynchronous switching problem can be considered to design controllers or observers. However, the estimation of the discrete state for switched linear systems is barely considered in the literature. Using a sliding mode approach, a robust estimation of the discrete state for a nonlinear uncertain switched system is proposed in [65] when the continuous state is measured. In [66], based on the output measurement and a high-order sliding mode observer, an estimation technique of the continuous and discrete states is developed for a nonlinear switched systems. In [67], a hybrid sliding mode observer is designed to estimate the continuous and discrete states for a switched linear systems with unknown input. In [68], a parameter identification is proposed to estimate the continuous and discrete states of switched LPV systems.

This thesis proposes two state estimation approaches. The first approach is investigated when the switching signal is assumed to be known and the second one is concerned with a new switching signal observer for a class of switched linear systems with unknown input. The proposed observer combines the sliding mode technique which provides a robust finite-time convergence and an interval approach where only bounds of the unknown input are needed. In the following subsection, more details about interval observer theory are given.

2.3.4 Interval observer

State estimation has been extensively discussed and reported in many engineering fields. From a practical point of view, state estimation may not converge to the real state due to the existence of model uncertainties and the design of classical observers such as Luenberger observers, Kalman filter, can be complicated. For instance, the design of a kalman filter method is based on stochastic theory which requires that the uncertainties have known probability distributions which is not always possible. To overcome this aforementioned drawback, several approaches of state estimation based on set-membership methods provide good results when disturbances and uncertainties are assumed to be unknown but bounded. In the literature, there are mainly two kinds of set-membership estimation methods. The first one is based on the well known prediction/correction mechanism [69], [70] which is similar to the Kalman filter. The prediction stage consists in determining the admissible domain of the state at the time instant t_{j+1} when framers of the state at the time instant t_j are given. In the continuous-time case, this method can be applied by carrying out a guaranteed numerical resolution of an ordinary differential equation [71]. During the correction phase, the predicted set is contracted by removing a set of state vector values inconsistent with the measurements at time t_{j+1} . The second approach is based on a closed loop structure where the gain of the observer is chosen in order to impose a cooperative dynamic for the estimation error [72], [73], [74]. In this case, two suitable conventional observers known by interval observers (Fig. 2.4) are designed to compute lower and upper bounds (\underline{x} and \overline{x}) of the state vector x without no stochastic assumption. In the presence of large uncertainties,

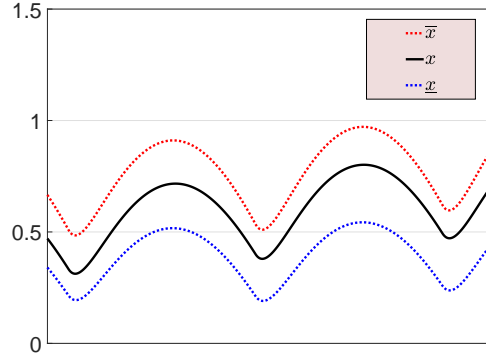


Figure 2.4: Interval observer.

the size of the state frame cannot be controlled by an external parameter using the prediction/correction mechanism which is not the case of interval observers. Several approaches based on interval observers have been developed in many applications to solve in a rigorous way, some engineering problems such as fault diagnosis, and to tackle uncertainty propagation such as [41], [75], [76], [77], [78].

In the following, a detailed study on interval observers is introduced for different classes of systems.

2.3.4.1 Preliminaries

In this subsection lemmas, definitions and basic results are given and dedicated to present some interval theory tools.

Lemma 3. [79] Let $A \in \mathbb{R}^{m \times n}$ be a constant matrix and $x \in \mathbb{R}^n$ be a vector such that $\underline{x} \leq x \leq \bar{x}$, thus

$$A^+ \underline{x} - A^- \bar{x} \leq Ax \leq A^+ \bar{x} - A^- \underline{x}.$$

Definition 11. [80] A matrix $A = \{a_{ij}\} \in \mathbb{R}^{n \times n}$ is called Metzler if its off-diagonal entries are nonnegative, i.e. $a_{ij} \geq 0, \forall i \neq j$.

[81]

Lemma 4. Consider the system described by:

$$\dot{x}(t) = Ax(t) + u(t) \quad (2.21)$$

If A is Metzler, the input u satisfies $u(t) \geq 0$ and the initial condition $x(0)$ is chosen as $x(0) \geq 0$, then the state x remains nonnegative for all $t \geq 0$. The system (2.21) is said to be cooperative or nonnegative.

Definition 12. [82] A matrix $A \in \mathbb{R}^{n \times n}$ is called nonnegative if all its elements are nonnegative.

Lemma 5. [83] Consider a system described by:

$$x(k+1) = Ax(k) + u(k) \quad , \quad u : \mathbb{Z}_+ \rightarrow \mathbb{R}_+^n, \quad k \in \mathbb{Z}_+ \quad (2.22)$$

with $x \in \mathbb{R}^n$. The system (2.22) is cooperative or nonnegative if and only if $u(k) \geq 0$ for all $k \geq 0$, $x(0) \geq 0$ and A is a nonnegative matrix.

In what follows, we provide some preliminary definition and lemmas needed in the following.

2.3.4.2 Interval observers for LTI systems

In the presence of uncertainties coming either from external disturbances or from the mismatch between the model and the real system, conventional observers may not be efficient to solve the estimation problem. Therefore, interval observers are used to compute the set of all admissible values instead of a single point approximation. An interval observer is composed of two classical ones allowing to compute two bounds which enclose in a guaranteed way all the feasible states. In the literature, interval observers have been proven to be suitable in state estimation for LTI systems [84], [85], [86] and [87]. In [84], an interval observer has been developed for LTI systems subject to additive disturbances. Based on time-varying changes of coordinates, cooperativity conditions have been relaxed. The proposed technique can be applied for arbitrary finite dimension LTI systems. However, in [88], interval observers have been introduced only for two-dimensional systems. In [85], an interval observer has been addressed for LTI discrete-time systems. Two approaches have been investigated to ensure the estimation error positivity. The first one is based on a constant transformation of coordinates. The second approach provides a cooperative representation in the same coordinates. Compared with [84] and [85], a discrete-time interval observer to jointly estimate the state and the unknown input is established in [86] for LTI discrete-time systems. Following a change of coordinates, the cooperativity property of the estimation error in the new coordinates is ensured. By integrating robust observer design with reachability analysis, a new interval observer approach is presented for LTI systems in [87].

Consider the following linear time-invariant system

$$\begin{aligned}\dot{x}(t) &= Ax(t) + u(t) \\ y(t) &= Cx(t)\end{aligned}\tag{2.23}$$

Assumption 1. *The upper and lower bounds, $\bar{x}(0)$ and $\underline{x}(0)$, of the initial state are chosen such that $\underline{x}(0) \leq x(0) \leq \bar{x}(0)$.*

Assumption 2. *The pair (A, C) is detectable.*

Assumption 3. *There exists a gain L such that $A - LC$ is Metzler and Hurwitz.*

Theorem 3. *Let Assumptions 1, 2 and 3 be satisfied, then the following system*

$$\begin{aligned}\dot{\bar{x}}(t) &= A\bar{x}(t) + u(t) + L(y(t) - C\bar{x}(t)) \\ \dot{\underline{x}}(t) &= A\underline{x}(t) + u(t) + L(y(t) - C\underline{x}(t))\end{aligned}\tag{2.24}$$

is as interval observer for (2.23) and the inclusion

$$\underline{x}(t) \leq x(t) \leq \bar{x}(t), \forall t \geq 0.$$

is satisfied.

Several interval observers have been proposed in the literature for LTI systems based on monotone systems theory. One of the most restrictive assumptions for the design of interval observers corresponds to the cooperativity of the estimation error dynamics. To relax the design conditions of interval observers, it has been shown that under some mild conditions, a Hurwitz matrix can be transformed into a Hurwitz and Metzler form based on a similarity transformation [89]. This transformation can be time-invariant such as in [41] or time-varying [90], [84].

2.3.4.3 Interval observers for LTV systems

Interval state estimation has been also intensively studied for LTV systems [91], [75] and [92]. In [91], an interval observer design is investigated for LTV systems where static and time-varying similarity transformations have been proposed to represent a time-varying interval matrix in a Metzler form. In [75], interval state estimation is proposed for time-varying discrete-time systems. The proposed technique supposed that the matrix $D(t) = A(t) - L(t)C(t)$, where L is the observer gain, should belong to a thin domain whose size is proportional to the inverse of the system dimension. Then, the bigger the system dimension is, the thinner the domain enclosing $D(t)$ must be. To overcome the aforementioned limitation in [75], authors in [92] propose a new interval method for LTV systems, based on a time-varying change of coordinates, in order to guarantee the cooperativity property. The proposed procedure is inspired from [93].

In this part, we present the method used in [94] for the design of an interval observer. Consider the following LTV system:

$$\begin{aligned} \dot{x} &= A(t, y, u)x + f(t, y, u, \rho) \\ y &= C(t, u)x \end{aligned} \quad (2.25)$$

We denote by $\rho \in \theta$ a vector of unknown signals including uncertain parameters and θ is a known compact set. The following assumptions are needed in this part.

Assumption 4. *The upper and lower bounds of the initial state, $\bar{x}(0)$ and $\underline{x}(0)$ are chosen such that $\underline{x}(0) \leq x(0) \leq \bar{x}(0)$.*

Assumption 5. *The state, the input and the output signal are supposed to be bounded such that $\|x\| \leq X$, $\|u\| \leq U$ and $\|y\| \leq Y$ for given known constants $X \geq 0$, $U \geq 0$ and $Y \geq 0$.*

Assumption 6. *Let $\underline{x} \leq x \leq \bar{x}$, then $\underline{f}(t, \underline{x}, \bar{x}, u) \leq f(t, y, u, \rho) \leq \bar{f}(t, \underline{x}, \bar{x}, u) \forall t \geq 0$ and $\|u\| \leq U$.*

Assumption 7. *There exist matrix functions L and P such that $\forall t \geq 0$, $\|u\| \leq U$, $\|y\| \leq Y$:*

$$\begin{aligned} p_1 I_n &\preceq P(t) \preceq p_2 I_n, p_1, p_2 > 0 \\ \dot{P}(t) + D(t, y, u)^T P(t) + P(t)D(t, y, u) + P^2(t) + Q &\preceq 0 \\ D(t, y, u) &= A(t, y, u) - L(t, y, u)C(t, u), Q = Q^T \succ 0. \end{aligned}$$

According to [94], it is worth to note that when the matrix D is Metzler, then the structure of the interval observer is given by:

$$\begin{cases} \dot{\bar{x}} &= A(t, y, u)\bar{x} + \bar{f}(t, \underline{x}, \bar{x}, u) + L(t, y, u)(y - C(t, u)\bar{x}) \\ \dot{\underline{x}} &= A(t, y, u)\underline{x} + \underline{f}(t, \underline{x}, \bar{x}, u) + L(t, y, u)(y - C(t, u)\underline{x}) \end{cases} \quad (2.26)$$

Theorem 4. For system (2.25), let Assumptions 4, 5, 6 and 7 hold, $D(t, y, u)$ be a Metzler matrix $\forall t \geq 0$, $\|u\| \leq U$, $\|y\| \leq Y$ and one of the following conditions is satisfied:

1. $|\underline{f}(t, \underline{x}, \bar{x}, u)| < +\infty$, $|\bar{f}(t, \underline{x}, \bar{x}, u)| < +\infty$, $\forall t \geq 0$, $\underline{x} \in \mathbb{R}^{n_x}$, $\bar{x} \in \mathbb{R}^{n_x}$.
2. $\forall t \geq 0$, $\|x\| \leq X$, $\|y\| \leq Y$, $\rho \in \theta$ $\underline{x} \in \mathbb{R}^{n_x}$, $\bar{x} \in \mathbb{R}^{n_x}$

$$|f(t, y, u, \rho) - \underline{f}(t, \underline{x}, \bar{x}, u)|^2 + |\bar{f}(t, \underline{x}, \bar{x}, u) - f(t, y, u, \rho)|^2 \leq \beta^2 |x - \underline{x}|^2 + \beta^2 |\bar{x} - x|^2 + \alpha$$

$\forall \alpha \in \mathbb{R}_+$, $\beta \in \mathbb{R}_+$ and

$$\beta I_n - Q + R \preceq 0, \quad R = R^T \succ 0, \quad Q = Q^T \succ 0$$

then $\forall t \geq 0$, $\underline{x}(t)$ and $\bar{x}(t)$ are bounded and the following inclusion holds:

$$\underline{x}(t) \leq x(t) \leq \bar{x}(t)$$

Theorem 4 is based on the Metzler assumption of the matrix D . The boundness of the state and of the input, the existence of upper and lower bounds for the function f , the existence of an estimation gain L with a Lyapunov matrix P are classical in the theory of interval observers. More details and proofs are given in [94].

The Metzler property is one of the most restrictive assumption for the observers design for LTV systems. This assumption has been relaxed by applying a similarity transformation. This transformation is time varying in [75] and [92] while in [95] the transformation matrix is assumed to be constant.

2.3.4.4 Interval observers for LPV systems

In the literature, several interval observers results have been investigated for nonlinear systems [96], [94] and [97]. Generally, state estimation methods for nonlinear systems are based on a system transformation into a canonical form which can lead to an unprecedented level of obstruction in practice [98]. Accordingly, many authors choose to transform nonlinear systems into a LPV forms [99], [100], [101] which provide an elegant way to apply linear systems frameworks to deal with real processes. In this context, many works have been developed to design interval observers for LPV systems [79], [102], [103]. In [79], an interval observer is designed for LPV systems subject to non-detectable or non-strongly-observable parts. The proposed interval method is merged with a High Order Sliding Mode technique in order to improve the estimation accuracy. Moreover, a relaxation of cooperativity constraints usually met in interval estimation theory is proposed based on a transformation coordinate. In [102], the design of interval observers is addressed for discrete-time LPV systems with unmeasurable scheduling parameters. The proposed methodology is used to compute a stabilizing control law guaranteeing an interval estimation of the state and its boundedness with the estimates bounds. Authors in [103] have proposed a new observer framework for passive fault tolerant control for LPV systems subject to unknown but bounded external disturbances. A state-feedback control law is designed ensuring the stability of the system. In addition, the proposed technique consists in using interval observers in order to take into account state disturbances, measurement noises, parameter uncertainties and actuator faults.

Consider the linear parameter varying system in [104]:

$$\begin{aligned} \dot{x}(t) &= A(\rho(t))x(t) + B(\rho(t))u(t) \\ y(t) &= C(\rho(t))x(t) + D(\rho(t))u(t) \end{aligned} \quad (2.27)$$

where $x \in \mathbb{R}^{n_x}$, $u \in \mathbb{R}^{n_u}$ and $y \in \mathbb{R}^{n_y}$ are the states, inputs and outputs, respectively. $\rho(t)$ denotes the vector of scheduling parameters.

An interval observer in [104] is proposed for (2.27) such that:

$$\begin{cases} \dot{\bar{x}}(t) &= \bar{A}\bar{x}(t) + \bar{B}u(t) + \bar{L}(y(t) - \bar{y}(t)) \\ \dot{\underline{x}}(t) &= \underline{A}\underline{x}(t) + \underline{B}u(t) + \underline{L}(y(t) - \underline{y}(t)) \\ \bar{y}(t) &= \bar{C}\bar{x}(t) + \bar{D}u(t) \\ \underline{y}(t) &= \underline{C}\underline{x}(t) + \underline{D}u(t) \end{cases} \quad (2.28)$$

where $\bar{x}(t)$, $\underline{x}(t) \in \mathbb{R}^{n_x}$ are the estimated upper and lower bounds of $x(k)$ respectively. \bar{L} , \underline{L} denote the gain matrices which are chosen according to the bounds of the matrices A , B , C and D . In this context, it is assumed that the measurement noise is bounded by a known scalar $\bar{\epsilon}$ such that the admissible domain of the measurement output is given by:

$$[y(t)] = [y_m(t) - \bar{\epsilon}, y_m(t) + \bar{\epsilon}] \quad (2.29)$$

Based on (2.29), the interval observer structure in (2.28) can be rewritten as follows:

$$\begin{cases} \dot{\bar{x}}(t) &= (\bar{A} - \bar{L}\bar{C})\bar{x}(t) + (\bar{B} - \bar{L}\bar{D})u(t) + \bar{L}(y_m(t) + \bar{\epsilon}) \\ \dot{\underline{x}}(t) &= (\underline{A} - \underline{L}\underline{C})\underline{x}(t) + (\underline{B} - \underline{L}\underline{D})u(t) + \underline{L}(y_m(t) - \bar{\epsilon}) \\ \bar{y}(t) &= \bar{C}\bar{x}(t) + \bar{D}u(t) \\ \underline{y}(t) &= \underline{C}\underline{x}(t) + \underline{D}u(t) \end{cases} \quad (2.30)$$

Let $\bar{e}(t) = \bar{x}(t) - x(t)$ and $\underline{e}(t) = \underline{x}(t) - x(t)$ be the upper and the lower estimation errors. From (2.27) and (2.30), the dynamics of the interval estimation errors are given by:

$$\begin{cases} \dot{\bar{e}}(t) &= (\overline{\Delta A} - \bar{L}\overline{\Delta C})\bar{e}(t) + \bar{\varphi} \\ \dot{\underline{e}}(t) &= (\underline{\Delta A} - \underline{L}\underline{\Delta C})\underline{e}(t) + \underline{\varphi} \end{cases} \quad (2.31)$$

where

$$\begin{cases} \bar{\varphi}(t) &= (\overline{\Delta A} - \bar{L}\overline{\Delta C})x(t) + (\overline{\Delta B} - \bar{D}\overline{\Delta C})u(t) + \bar{L}\bar{\epsilon} \\ A(\rho(t)) &= \bar{A} - \overline{\Delta A} \\ B(\rho(t)) &= \bar{B} - \overline{\Delta B} \\ C(\rho(t)) &= \bar{C} - \overline{\Delta C} \\ D(\rho(t)) &= \bar{D} - \overline{\Delta D} \end{cases} \quad (2.32)$$

and

$$\begin{cases} \underline{\varphi}(t) &= (\underline{\Delta A} - \underline{L}\underline{\Delta C})x(t) + (\underline{\Delta B} - \underline{D}\underline{\Delta C})u(t) - \underline{L}\bar{\epsilon} \\ A(\rho(t)) &= \underline{A} - \underline{\Delta A} \\ B(\rho(t)) &= \underline{B} - \underline{\Delta B} \\ C(\rho(t)) &= \underline{C} - \underline{\Delta C} \\ D(\rho(t)) &= \underline{D} - \underline{\Delta D} \end{cases} \quad (2.33)$$

According to Lemma 2, if the gain matrices \bar{L} , \underline{L} are designed such that the matrices $\overline{\Delta A} - \bar{L}\overline{\Delta C}$ and $\underline{\Delta A} - \underline{L}\underline{\Delta C}$ are Metzler, $\bar{\varphi}(t)$ and $\underline{\varphi}(t)$ are positive. Then, the inclusion

$\underline{x}(t) \leq x(t) \leq \overline{x}(t)$ is satisfied. In addition to the cooperative analysis, the convergence of the interval observer should be characterized. Consider the following error system:

$$\begin{aligned} e(t) &= \overline{e}(t) + \underline{e}(t) \\ &= \overline{x}(t) - \underline{x}(t) \end{aligned} \quad (2.34)$$

According to [104], we denote by $\hat{x}(t)$ and $R_e(t)$ the center and the radius of the estimated interval respectively defined by:

$$\begin{aligned} \hat{x}(t) &= \frac{\overline{x}(t) + \underline{x}(t)}{2} \\ R_e(t) &= \frac{\overline{x}(t) - \underline{x}(t)}{2} = \frac{\overline{e}(t) - \underline{e}(t)}{2} \end{aligned} \quad (2.35)$$

In order to guarantee the stability and the convergence of the interval observer, it is assumed in [104] that the gain matrix $L = \overline{L} = \underline{L}$ should be designed such that the following matrix:

$$A_e = \begin{bmatrix} 2(\text{mid}[A] - L\text{mid}[C]) & (w[A] - Lw[C]) \\ (w[A] - Lw[C]) & 2(\text{mid}[A] - L\text{mid}[C]) \end{bmatrix}$$

is simultaneously stable and Metzler. The width of an interval $[a]$ is defined by $w[a] = \overline{a} - \underline{a}$ and its midpoint by $\text{mid}[a] = (\overline{a} + \underline{a})/2$. Therefore, the error in (2.34) converges asymptotically to a ball with a center \hat{x}_{max} and a radius $R_{e_{max}}$. The ball can be defined as:

$$\begin{bmatrix} \hat{x}_{max} \\ R_{e_{max}} \end{bmatrix} = A_e^{-1} \Lambda_e$$

A_e is a full rank matrix and Λ_e denotes a vector of positive elements bounding the following vector:

$$\begin{bmatrix} \text{mid}[B] - L\text{mid}[D] \\ w[B] - Lw[D] \end{bmatrix} u(t) + \begin{bmatrix} Ly(t) \\ 2L\overline{e} \end{bmatrix}$$

More details are given in [105] and [104].

More recently, in [78], an improved structure of interval observers and stability conditions are proposed for LPV systems in order to compute the bounding solutions as accurate as possible. The proposed methodology is based on an L_1/L_2 optimization of the observer gains.

Consider the LPV in [78] modeled by:

$$\begin{aligned} \dot{x}(t) &= (A_0 + \Delta A(\rho(t)))x(t) + b(t) \\ y(t) &= Cx(t) + v(t) \end{aligned} \quad (2.36)$$

where $x \in \mathbb{R}^{n_x}$, $b \in \mathbb{R}^{n_b}$, $y \in \mathbb{R}^{n_y}$ and $v \in \mathbb{R}^{n_v}$ are the state vector, the input, the output signal and the measurement noise, respectively. $\rho(t) \in \Pi \subset \mathbb{R}^{n_r}$ is the vector of scheduling parameters. The values of the scheduling vector ρ are not available for measurements, and only the set of admissible values Π is known. The matrices A_0 and C are known and given with appropriate dimensions. The matrix function $\Delta A : \Pi \rightarrow \mathbb{R}^{n_x \times n_x}$ is piecewise continuous.

The following notations are used in [78].

Notation 1. The Euclidean norm for a vector $x \in \mathbb{R}^{n_x}$ is denoted by $|x|$. For a measurable and locally essentially bounded input $u : \mathbb{R}^+ \rightarrow \mathbb{R}^+$, $\|u\|$ denotes its L_∞ norm, such that $\|u\| \leq \infty$. I_{n_x} and E_{n_x} denote respectively the identity matrix and the matrix with all

elements equal 1. For a matrix $A = \{a_{ij}\} \in \mathbb{R}^{n_x \times n_x}$, $\|A\|_{\max} = \max_{i,j} |a_{ij}|$, $i = \{1, 2, \dots, n_x\}$, $j = \{1, 2, \dots, n_x\}$ denotes the elementwise maximum norm, $\|A\|_2$ denotes the L_2 matrix norm. This inclusion $\|A\|_{\max} \leq \|A\|_2 \leq n_x \|A\|_{\max}$ is satisfied between these norms.

Lemma 6. [79] Let $A \in \mathbb{R}^{n_y \times n_x}$ be a variable matrix variable such that $\underline{A} \leq A \leq \overline{A}$ and $x \in \mathbb{R}^{n_x}$ be a vector, such that $\underline{x} \leq x \leq \overline{x}$, then

$$\underline{A}^+ \underline{x}^+ - \overline{A}^+ \underline{x}^- - \underline{A}^- \overline{x}^+ + \overline{A}^- \overline{x}^- \leq Ax \leq \overline{A}^+ \overline{x}^+ - \underline{A}^+ \overline{x}^- - \overline{A}^- \underline{x}^+ + \underline{A}^- \underline{x}^-$$

Assumption 8. It is assumed that:

- The state x of the system (2.36) is bounded such that $x \in \mathcal{L}_{\infty}^n$.
- The input b belongs to a known bounded interval such that $\underline{b}(t) \leq b(t) \leq \overline{b}(t)$, \underline{b} and $\overline{b} \in \mathcal{L}_{\infty}^n$.
- The measurement noise $v(t)$ has an upper bound V such that $|v(t)| \leq V$ for all $t \geq 0$ and $V > 0$.
- The matrix $\Delta A(\rho)$ belongs to a known bounded interval such that $\underline{\Delta A} \leq \Delta A(\rho) \leq \overline{\Delta A}$ for all $\rho \in \Pi$, $\underline{\Delta A}$ and $\overline{\Delta A} \in \mathbb{R}^{n_x \times n_x}$.

Under the aforementioned assumptions, the structure of the proposed interval observer in [78] is given by:

$$\begin{cases} \dot{\overline{x}}(t) &= (A_0 - \overline{L}C)\overline{x}(t) + (\overline{\Delta A}^+ \overline{x}^+ - \underline{\Delta A}^+ \overline{x}^- - \overline{\Delta A}^- \underline{x}^+ + \underline{\Delta A}^- \underline{x}^-) \\ &\quad + \overline{L}y(t) - |\overline{L}| VE_{n_y} + \overline{b}(t) \\ \dot{\underline{x}}(t) &= (A_0 - \underline{L}C)\underline{x}(t) + (\underline{\Delta A}^+ \underline{x}^+ - \overline{\Delta A}^+ \underline{x}^- - \underline{\Delta A}^- \overline{x}^+ + \overline{\Delta A}^- \overline{x}^-) \\ &\quad + \underline{L}y(t) - |\underline{L}| VE_{n_y} + \underline{b}(t) \end{cases} \quad (2.37)$$

The conditions ensuring the interval estimation are stated in the following theorem.

Theorem 5. [78] Let Assumption 8 be satisfied and the matrices $A_0 - \underline{L}C$, $A_0 - \overline{L}C$ be Metzler. Then the inclusion $\underline{x}(t) \leq x(t) \leq \overline{x}(t)$ is satisfied provided that $\underline{x}(0) \leq x(0) \leq \overline{x}(0)$. If there exist $P \in \mathbb{R}^{2n_x \times 2n_x}$, $P = P^T \succ 0$ and $\gamma > 0$ such that the following Riccati matrix inequality is verified:

$$G^T P + PG + 2\gamma^{-2} P^2 + \gamma^2 \eta^2 I_{2n_x} + Z^T Z \prec 0 \quad (2.38)$$

where $\eta = 2n_x \|\overline{\Delta A} - \underline{\Delta A}\|_{\max}$, $Z \in \mathbb{R}^{s \times 2n_x}$, $0 \leq s \leq 2n_x$ and

$$G = \begin{bmatrix} A_0 - \underline{L}C + \underline{\Delta A}^+ & -\underline{\Delta A}^- \\ -\overline{\Delta A}^- & A_0 - \overline{L}C + \overline{\Delta A}^+ \end{bmatrix}$$

then \overline{x} and $\underline{x} \in \mathcal{L}_{\infty}^n$ and the operator $\begin{bmatrix} \underline{b} \\ \overline{b} \end{bmatrix} \rightarrow Z \begin{bmatrix} \underline{x} \\ \overline{x} \end{bmatrix}$ has an L_2 gain less than γ .

The main restriction for the interval observer design for LPV systems consists in providing cooperativity of the interval estimation error dynamics by a proper design. Such a complexity has been overcome using a time invariant similarity transformation [98] and a time varying state transformation [106].

2.3.4.5 Interval observers for switched systems

In the recent years, several effective design methods have been investigated for both continuous-time and discrete-time switched systems [107], [60], [108], [109], [110], [14], etc. In [60], the problem of interval state estimation is developed for continuous-time switched system subject to unknown but bounded disturbances. The design conditions are represented based on a change of coordinates in order to ensure the cooperativity of the estimation errors. Authors in [14] investigate the problem of robust state and unknown input interval estimation for uncertain switched linear systems. The stability analysis in [14] is studied by adopting multiple quadratic ISS Lyapunov function and ADT concept, which is not the case in [60]. The stability conditions in [60] are developed based on CQLF. For the case of discrete-time switched systems, the design of interval observers is addressed in [108], [111]. In [108], interval state estimation has been proposed for switched systems subject to unknown inputs. The stability and the non-negativity of the estimation errors are investigated based on ADT assumptions and using a time-varying transformation which consists in finding the proper time-varying transformation matrix to convert the non-negative matrix into its Jordan canonical form. In [111], a new methodology to design interval observers for discrete-time linear switched systems is proposed using a H_∞ formalism. Two design techniques are presented in [111]. The first one requires that the estimation error dynamics are nonnegative while in the second one, a change of coordinates is used to relax the above restrictive requirement.

Interval methods have been also applied for nonlinear switched systems. Generally, interval design techniques for nonlinear systems are based on a system transformation into a canonical form which can lead to an unprecedented level of obstruction in practice [75]. This limitation motivates the development of LPV systems, since a wide class of nonlinear systems can be represented in an LPV form [99], [100], [101]. The main advantage is that a partial linearity of LPV models provides an elegant way to apply several developed frameworks for linear systems to deal with real processes. Based on the above discussion, we are interested in developing interval estimation method for a larger class of switched systems modeled by LPV switched systems subject to bounded disturbances and measurement noise. More details about the proposed estimation approach will be given for continuous-time as well as discrete-time systems.

It is highlighted in this section that various results in estimation design have been generalized to switched systems and widely investigated in the control community such as fault diagnosis techniques. In the following section, basic notions of fault diagnosis terminology, classification of faults and fault diagnosis methods are presented in detail.

2.4 Fault diagnosis for switched systems

With the huge increase in complexity and expense of engineering systems, there is less tolerance for performance degradation, productivity decrease and safety hazards. In the last decades, much attention has been devoted to fault diagnosis which aims to prevent serious system damage by detecting and identifying potential abnormalities and faults as early as possible. Several results have been investigated in the field of fault diagnosis and their applications in many engineering systems such as vehicle dynamics, chemical processes,

manufacturing systems, power networks, electric machines, conversion systems, etc. For a unified terminology, preliminary notions in the field of fault diagnosis are suggested by the IFAC Technical Committee SAFEPROCESS. Some of these definitions are provided in the sequel to introduce the diagnosis field [112].

- **Fault:** An unpermitted deviation of at least one characteristic property or parameter of the system from the acceptable / usual / standard condition.
- **Malfunction:** An intermittent irregularity in the fulfilment of a system's desired function.
- **Fault Diagnosis:** It is the determination of the type, size, location and time of occurrence of a fault; it follows the fault detection and includes the isolation and the identification
- **Residual signal:** A fault indicator, based on a deviation between measurements and model-equation based computations.
- **Threshold:** The limit value of the deviation of a residue with zero, so if it is exceeded, a fault is declared as detected.

2.4.1 Diagnosis Process

According to [113], fault diagnosis includes three tasks (Fig. 2.5).

- **Fault Detection** is the task to check the occurrence of faults in the process.
- **Fault Isolation** is the task to determine the kind, location and time of detection of a fault.
- **Fault Identification** is the task to provide the size and time-variant behaviour of a fault.

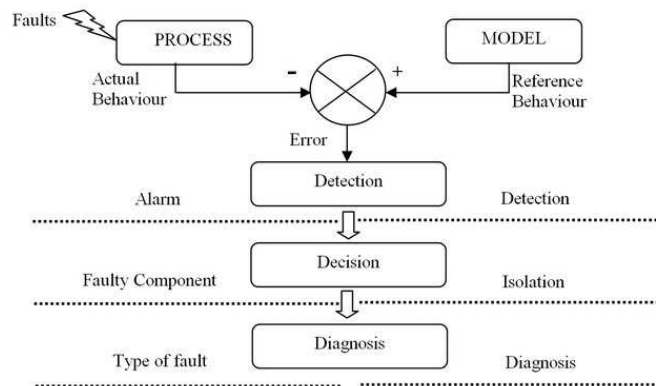


Figure 2.5: Diagnosis Process.

In the following, some results from the literature about fault detection, isolation and identification techniques are given.

2.4.1.1 Fault detection techniques

Fault detection is the first step in diagnosis process. It has a primordial role in safety-critical processes. It consists in determining whether a system is faulty or not and early fault detection can avoid system damage. In the literature, different methods are reported for fault detection [113] [114], [115]. In this thesis, fault detection is considered using model-based methods. The motivation drives from different aspects. In fact, model based methods are well adapted to complex processes since the requirement on additional hardware components, that can increase systematically the cost and the weight of complex systems, is not needed to achieve fault diagnosis. Model based fault detection methods can be investigated for linear systems as well as nonlinear systems. They are based on the concept of analytical redundancy. It involves two stages: residual generation and residual evaluation (Fig. 2.6). The basic idea is to generate and evaluate a residual signal which may be the difference

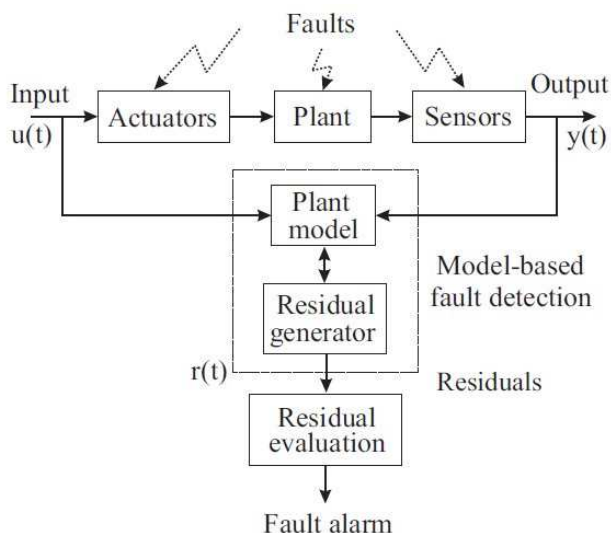


Figure 2.6: Fault detection.

between real measurements and measurements resulting from the model of the considered system. Ideally, in fault-free case, the residual signal is very close to zero while clearly deviates from zero when a system is faulty. However, in the presence of disturbances, model uncertainties and measurement noises, the residual signal can not be zero even in fault-free situations. Therefore, one of the most essential requirements imposed on residual generation algorithms is the robustness against endogenous and exogenous disturbances. Different criteria have been developed in the literature to evaluate the effects of uncertainties on residual signals such as H_∞ and H_2 in [116] and [117]. Other performances have been investigated to measure the sensitivity of residual signals to faults such as H_- and H_∞ in [118]. More recently, fault detection has been formulated as a multiple objective optimization problem by maximizing the effects of faults on the residual signals and minimizing the sensitivity to disturbances using for example H_2/H_2 , H_2/H_∞ , H_∞/H_∞ and H_-/H_∞ such as in [119] and [120]. After residual generation, the next step in fault detection is residual evaluation. This step is based first on generating evaluation functions and thresholds to detect faults. Then a decision on the occurrence of a fault can be made. In the literature, a constant,

an adaptive threshold or a time-varying one could be computed. However, it should be mentioned that the design of an appropriate threshold is still a challenge and an arduous task especially for dynamic systems subject to exogenous disturbances. In fact, if the selected threshold is too high, the residual signal can not exceed the threshold, which can cause missed detection. Also, if the threshold is chosen too low, the rate of appearance of false alarms can increase. In the recent years, several residual evaluation approaches based on set-membership techniques have been introduced for different classes of systems in the presence of unknown but bounded state disturbances and measurement noises such as in [121], [122], [123] and [124]. The merit of set-membership techniques consists in providing systematic dynamic thresholds for residual evaluation. In the next section, set-membership fault detection theory for switched systems will be presented.

2.4.1.2 Fault isolation techniques

Fault isolation is the second step in diagnosis process. Several methods can be used to determine the location of a fault [125], [126] among them:

- A structured residual set designed via a dedicated or a generalized observer scheme [127], [128].
- A directional residual vector designed via a fault detection filter [129], [130].

Structured residual signal methods aims to design a residual signal which is sensitive to the concerned fault, meanwhile robust against other faults, disturbances and modeling errors. In general, a set of residual signals is generated through different and several possible methods including observers, parity space techniques, etc. However, directional residual signal approaches aim to make each residual signal sensitive to all but one fault and robust against modeling errors and disturbances. Several fault isolation works have been investigated for different classes of systems such as LTI systems [131], linear stochastic systems [132], linear systems with unknown inputs [133], LPV descriptor systems [134], uncertain Takagi-Sugeno fuzzy model [135], switched systems [136] and nonlinear systems [137]. Fault isolation techniques have been applied in various application fields such as for aircraft engines [138], robotic manipulators [139], inductor motors [140] and other fields.

2.4.1.3 Fault identification techniques

Fault identification is the final step in diagnosis process. It can also be called fault reconstruction or fault estimation. The fault identification task consists in determining the type, the size, and the shape of a fault. Several achieved results have been proposed for the purpose of fault identification using mainly advanced observer techniques such as proportional and integral (PI) observers [141], proportional multiple-integral (PMI) observers [142], adaptive observers [143], sliding mode observers [40], descriptor observers [144] and interval observers [145]. The basic idea of advanced observers is to design an augmented system by considering the concerned fault as an additional state, then, the original system states and the presented fault can be estimated.

2.4.2 Classification of faults

Generally, for the diagnosis process, it is primordial to seek for a model to characterize a system. Meanwhile, the modeling of faults should be also taken into account when the system is affected by a fault.

2.4.2.1 Fault classification based on the faulty component

Depending on the component [146], faults can affect the sensors, the actuators, and / or the process.

- **Sensor Fault:** sensors are essentially the output interfaces of a system with the external environment. For closed-loop systems, the presence of a sensor fault can cause an inaccurate and inefficient control signal.
- **Actuator Fault:** actuators denote the operative part of a system. This kind of fault can destroy the system input signal. Actuator faults can cause a high consumption of energy and in some cases a total loss of control. The most frequent actuator faults can be seen from Fig. 2.7 where dotted lines represent the desired values of the actuator and the continuous lines denote the actual values.

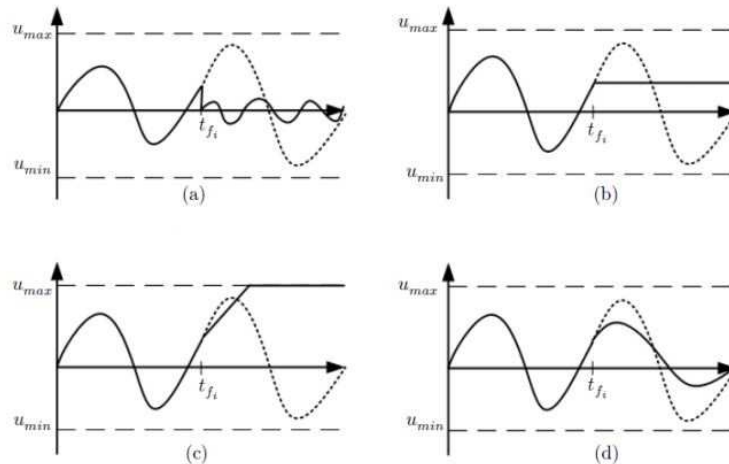


Figure 2.7: Representation of the most common actuator faults (a) Oscillation, (b) Blocking, (c) Saturation and (d) Loss of Efficiency.

- **Process Fault:** this type of fault is called also component fault. It can affect the dynamics of the system. The mathematical representation of the process faults is often difficult to determine and requires extensive experimental tests.

2.4.2.2 Fault classification according to the temporal evolution

Another classification of faults according to their evolution over the time can be considered. In the literature, sudden, incipient and intermittent faults are distinguished [147]. This can be seen from Fig. 2.8:

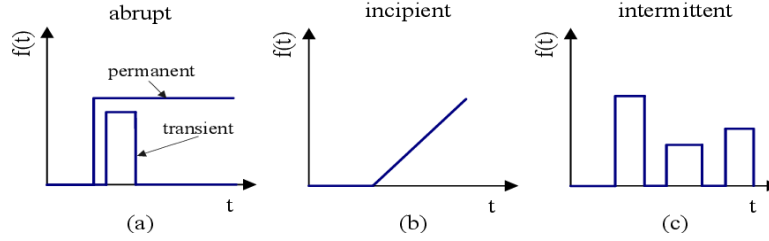


Figure 2.8: Temporal Evolution of Faults.

- Sudden Fault: this type of fault is characterized by a discontinuous temporal behavior. It is relatively easy to be detected. It can cause a sudden failure or a total shutdown. A mathematical representation of this fault can be given by:

$$f(t - t_f) = \begin{cases} \delta & t > t_f \\ 0 & t < t_f \end{cases} \quad (2.39)$$

where $f(t - t_f)$ is the temporal behavior of the sudden fault and δ is a constant threshold.

- Incipient Fault: this type of fault is characterized by a slow temporal evolution as illustrated in Fig. 2.8. It is very difficult to be detected because of its temporal evolution that may be confused with slow parametric change representing the non-stationary process. A mathematical representation of incipient fault can be given by:

$$f(t - t_f) = \begin{cases} \delta(1 - e^{-\alpha(t-t_f)}) & t \geq t_f \\ 0 & t \leq t_f \end{cases} \quad (2.40)$$

δ and α denote two positive constants.

- Intermittent Fault: this type of fault is a special case of sudden faults that appears and disappears quickly.

2.4.2.3 Fault classification according to the impact on system performance

Faults can be also classified into two categories, depending on how they are modeled. They can be additive or multiplicative. This can be seen from Fig. 2.9:

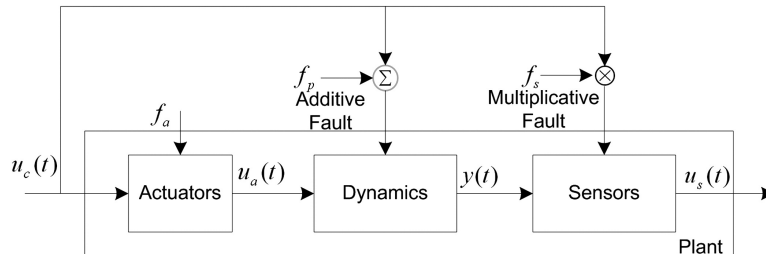


Figure 2.9: Faults Classification: Multiplicative and Additive.

- Additive Fault: this type of fault can affect the input or the output signals of a system. It can be modeled by an additive term as illustrated in Fig. 2.9. Additive faults are usually attributed to sensors and actuator faults.
- Multiplicative Fault: this type of fault is modeled by a multiplicative term. The multiplicative fault can affect the structure of the system by affecting the parameters of the system model.

2.4.3 Model-based fault diagnosis

The development of diagnosis theory has already been active since the early 1970's. Several model-based fault diagnosis methods have been widely investigated and applied to several applications [113], [148], [149] and [150]. These approaches are based on the concept of analytical redundancy [151] which uses signals generated by the mathematical model of the considered system and there is no need of additional hardware components

In the context of this thesis, we are interested in model-based fault diagnosis scheme. In the following, some analytical model-based fault diagnosis approaches such as parity space, parameter estimation and observers are discussed.

2.4.3.1 Parity relation approaches

Parity space approach is one of the earliest used techniques for fault diagnosis. The objective of this approach is to check the consistency of the parity equations which are generated from the system model or transformed version of the state space model. Based on parity relations, the unknown state variables are eliminated from the model equations and the residual signals can be decoupled from the system states. They only depend on the system inputs and outputs. The inconsistency in the parity relations reflect the occurrence of a fault. The parity space methodology has been investigated for different classes of systems such as in [130], [152], [153] and [154]. It has been also extended to hybrid systems [155] in order to estimate the active mode, the switching instants and to detect faults. In [156], the parity space-based approach is investigated for a class of discrete-time switched linear systems under dwell time constraints. Authors in [157] proposed a new scheme for the residual evaluation based on parity space techniques. The designed approach provide high fault detection performance for switched systems. According to [158], [159] and [160], a close relationship between parity space-based and observer-based approach exists.

2.4.3.2 Parameter estimation approaches

The aim of this approach is to detect faults via the estimation of parameters. The estimated parameters can be compared with nominal values obtained in fault free condition. Therefore, any parametric deviation involves the occurrence of a fault. In the literature, several parameter estimation techniques are developed such as in [161], [162] and [163]. Under some mild conditions such as persistency excitation of the signals, an advantage of the parameter estimation approach is that with only one input and one output measurement signal, several parameters can be estimated. Another advantage of this method is that the parameters detection and isolation of faults are straightforward especially when the concerned system is subject to component faults.

2.4.3.3 Observer-based approaches

The observer-based approach is one of the most applied fault diagnosis model-based scheme. In this method, the residual signal is generated by comparing measurements from process with their estimates obtained through estimation process. In the early 70's, the idea of using observers in the aim to achieve the diagnosis task was appeared. To our best of knowledge, the first fault detection filter was introduced by Beard in [129]. Since then, special research efforts have been devoted to observer-based fault detection. In the beginning of 80's, much attention has been carried out for robust fault detection and isolation observers. The first robust observer-based fault detection approach is proposed by Frank in [164] for instrument faults. Later, robust unknown input observers (UIO) have been investigated. The advantage of using UIO is to generate a residual signal decoupled from unknown inputs. However, it has been mentioned in the literature that the existence condition of unknown input observers may be restrictive. An elegant way to solve this problem is to provide a residual signal robust against unknown inputs. Several techniques have been developed in this area based on optimization indices, such as H_2/H_∞ , H_∞/H_∞ and H_-/H_∞ . More recently, in a context of unknown but bounded disturbances, interval observers have been shown to be suitable in fault diagnosis methods as they provide a systematic dynamic thresholds for residual evaluation [165], [166]. In [165], fault estimation is performed for high-speed railway traction motor in the presence of sensor fault and disturbances using interval and unknown input observers. In [166], a robust fault detection and isolation observer technique is proposed. By combining the set-invariance approach with a zonotopic interval observer, the minimum detectable and isolable fault is characterized.

To the best of our knowledge, observer-based fault detection for uncertain switched systems has not been fully investigated in the literature. In the context of this thesis, the aim is to develop observer design methods to detect faults for discrete-time switched systems in the presence of unknown but bounded disturbances. In the following subsection, a state of art about set-membership fault detection observer for switched systems is provided.

2.4.4 Set-membership fault detection for switched systems

Occurrence of faults cannot only make the system unable to reach a number of expected goals but may also lead to severe and irreversible damage to human operator and equipment if they are not detected rapidly. In the past decades, many efforts have been devoted to fault detection techniques for switched systems [167], [76] and [168]. In [167], a fault detection method based on a high-order sliding-modes observer is proposed. Without using decoupling transformations, a high-order sliding mode observer is designed in [76] for the detection of faults that occur in the continuous part of the switched system. In the aforementioned contributions, only actuator faults are considered. In [168], a fault detection scheme is proposed for switched systems in the presence of simultaneous actuator and sensor faults.

From a practical point of view, the presence of state disturbances and measurement noises can affect the performance of fault detection. Accordingly, robust fault detection approaches are essential in order to deal with false alarm issues. The main idea of robust fault detection approach consists in generating a residual signal as a symptom of faults occurrence. It is required that the generated residual signal should be robust against uncertainties meanwhile sensitive to faults. Among several robust fault detection methods, the H_∞ criterion which

is considered in [169] to develop a robust hybrid observer for switched linear systems subject to unknown inputs. The proposed technique allows getting a proper compromise between sensitivity to faults and robustness to the unknown inputs. The work in [170] is concerned with the H_∞ -filtering formulation of fault detection problems for a class of discrete-time switched systems with time-varying state delays. Based on a mixed H_-/H_∞ formulation, authors in [119] investigate the fault detection issue for switched systems to minimize the effect of disturbance and simultaneously maximize the sensitivity of fault on the residual signal. In [77], the fault detection issue is investigated in the finite-frequency domain. The finite frequency L_2 -gain is established for characterizing the disturbance attenuation performance.

When disturbances are assumed to be unknown but bounded, a great interest has been devoted to set-membership techniques. These techniques are based on the computation of the estimated set containing all the possible states consistent with the measurements, the possible perturbations and uncertainties at each time instant. Several sets are used to implement set-membership fault detection methods when uncertainties are bounded in some compact geometrical sets such as intervals, polytopes, zonotopes and ellipsoids [3], [96] and [171].

In the context of this thesis, we are mainly interested in interval, zonotopic and ellipsoidal sets. In the following, more details about the aforementioned compact sets are given.

2.4.4.1 Interval-based approaches

Compared with the above works, interval fault techniques are considered as an attractive way in determining whether the system is faulty or not, since they only rely on the assumption of boundness of uncertainties. The major advantage of using interval-based approaches consists in providing systematic threshold generators for residual evaluation. In [121], an interval observer-based fault detection method is introduced for discrete-time LPV systems. The fault detection decision is based on determining whether the zero signal is excluded from the generated residual interval when the faults occur. The proposed technique avoids the design of residual evaluation functions and threshold generators. More recently, the authors in [124] have proposed an interval fault detection observer for continuous time switched systems subject to bounded disturbances where the fault detection decision can be made directly. Based on the above discussion, a robust set-membership technique based on interval observers is achieved in this thesis to detect faults for discrete-time switched systems. Interval observers have been proven to be effective in fault detection as well as in state estimation.

In the other side, interval observers have additional constraints compared to conventional ones. In fact, the design of interval observers requires not only the stability but also the non-negativity of the estimation errors. Some authors introduce a coordinate transformation to relax the design conditions of interval observers. However, it is still hard to merge the coordinate transformation approach with performance constraints. To overcome the aforementioned drawbacks, zonotopic techniques are investigated to provide systematic dynamic thresholds for residual evaluation as well as improving the accuracy of the residual boundaries without considering the non-negativity assumption.

2.4.4.2 Zonotope-based approaches

Zonotopes are initially introduced by [172]. They are generally used to solve set-membership state estimation, fault detection and diagnosis problems for dynamical systems affected by bounded disturbances and measurement noises [3], [173], [174], [175], [176], [177], [178]. In [3], a guaranteed state estimation is proposed by computing a zonotopic outer approximation of the set of states. Based on volume and segment minimisation approaches, a zonotope-based method is presented in [173] in order to improve the estimation accuracy of the estimates bounds. Moreover, in [179] and [175], the P-radius and F-radius of the zonotopic set were minimised to achieve state estimation. The so-called P-radius and F-radius are introduced as a zonotope size criteria that allow proving that zonotopic state estimation has non-increasing sizes in time for time invariant systems. In the context of set-membership fault detection, zonotopic methods have attracted increasing attention. For instance, in [122], a zonotopic fault detection observer is proposed for discrete-time uncertain system based on the H_- fault sensitivity. In [177], a fault detection approach is developed using the zonotopic set-membership theory in the finite-frequency domain. Using zonotopic techniques, robust fault detection scheme for switched systems has not been fully investigated. In the context of this thesis, a new fault detection technique is proposed for a class of discrete-time switched systems when disturbances can be described by zonotopes.

Zonotopic methods have also some limitations. In fact, the fault detection accuracy of the zonotopic techniques can be improved using higher dimensional zonotopes. This additional dimensional growth may cause heavier computational burden. To handle this problem, a reduction operator can be used to constrain the dimensions of zonotopes [173], however less accurate fault detection results are obtained. This can be seen from Fig. 2.10 where the size of the zonotope with a high-dimensional order ($q = 5$) is tighter than the size of that on with a less-dimensional order ($q = 4$). The example is inspired from [145].

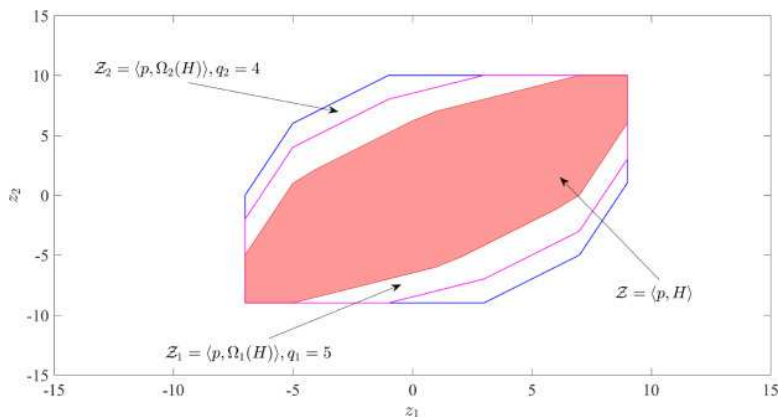


Figure 2.10: A Zonotope with different reduction orders.

2.4.4.3 Ellipsoid-based approaches

Compared with the zonotopic methods, the ellipsoidal techniques can be considered as a good trade-off between fault detection accuracy and computation complexity, the reader can refer to [180] and [181]. It should be mentioned that basic operations for ellipsoids

can be reduced to simple matrix calculations and do not require any reduction operator. In the literature ellipsoidal sets are widely used in several applications, such as identification, estimation and diagnosis since they have an interesting geometry which makes them easy to manipulate and the characteristics of ellipsoidal sets can be used to obtain more simple implementable solutions. In the context of set-membership estimation, the ellipsoidal method has received a great attention. Effectively, it is used by several authors such as [1], [182], [181], [171]. In the context of set-membership fault detection, ellipsoidal analysis for uncertain switched systems has not been fully investigated in the literature. Therefore, a robust fault detection method is achieved, in this thesis, using ellipsoidal techniques for discrete-time switched systems subject to unknown but bounded disturbances and measurement noise. Several definitions and properties of the ellipsoidal sets are further presented.

2.5 Conclusion

In this chapter, a brief literature review is first conducted in order to present the class of switched systems. Different modeling, stability analysis and observability approaches are recalled. Then, some existing results in the literature on diagnosis approaches are presented. The main challenge in this thesis is to develop a model-based diagnosis technique for switched systems subject to unknown but bounded disturbances. Interval observers are considered as a suitable tool to deal with uncertainties. Thus, an overview about intervals is given also in this chapter. As well as interval fault diagnosis, interval state estimation for switched systems has received much attention in recent years. In the next chapter, a new methodology to design interval observers for LPV switched systems subject to disturbances and time-varying parameters is addressed.

Chapter 3

Interval estimation for synchronous switched systems

3.1 Introduction

Interval observers provide two variables evaluating lower and upper bounds of the state values. In the literature, several approaches of state estimation based on interval methods for complex systems provide good results even when the system is affected by disturbances and/or uncertainties which are supposed to be unknown but belong to bounded sets. Their design is often based on the theory of positive systems, which requires the stability and the cooperativity of the estimation error. Among existing works, CQLF and MQLF are used to study the stability of observers. However, the topic of stability becomes much more complex if one considers that the system is subject to uncertainties. Unfortunately, the cooperativity condition is also restrictive. To relax this constraint, some methods propose a coordinate transformation [41], [110]. However, when systems are affected by time-varying parameters, applying a change of coordinates can constitute an infinite dimensional problem. For LPV systems, several techniques have been developed using polytopic tools. However, to the best of our knowledge, interval observers design for LPV switched systems with polytopic time varying parameters has not been fully studied in the literature. This motivates the present chapter, which is devoted to propose a finite dimensional relaxation for the design conditions of the proposed interval observer.

The primary focus of this chapter is to design an interval observer for both continuous and discrete-time LPV switched systems subject to measured polytopic parameters. In particular, the challenge is to develop an interval state estimation method using a new polytopic modeling framework of an interval observer considering the measurement noise and disturbances for a large class of switched systems. In a first part of this chapter, the design of an interval observer for continuous-time LPV switched systems is developed. Using

Common and Multiple Quadratic Lyapunov Functions, new conditions of cooperativity and stability are provided in terms of LMIs expressed on the vertices of each polytope. The second part of this chapter is devoted to the design of an interval observer for discrete-time LPV switched systems. Simulation results for both parts highlight the efficiency of the proposed approaches.

The results presented in this chapter has led to the publication of the communication [183] in the international Conference on Decision and Control and two articles [184], [185] in the international journals International Journal of Control and Acta Cybernetica.

3.2 Interval observer design for continuous-time LPV switched systems

In the continuous-time case, interval observers for switched systems have been widely introduced in the literature. For instance, in [110], an interval observer is developed for continuous-time switched linear systems under the assumption that the disturbances and the measurement noise are bounded. A change of coordinates that transforms the estimation errors into a cooperative form is developed. In [186], a synchronous interval observer is designed for continuous-time switched LPV systems using multiple quadratic ISS-Lyapunov functions. In this part, a new interval observer design method is proposed for a larger class of systems modeled by continuous-time LPV switched systems when disturbances and measurement noise are assumed to be unknown but bounded. The proposed technique provides a finite dimensional relaxation for both cooperativity and ISS conditions.

3.2.1 Problem statement

Consider the following continuous-time LPV switched system

$$\begin{cases} \dot{x}(t) = A_{\sigma(t)}(\eta_q)x(t) + B_{\sigma(t)}(\eta_q)u(t) + w_{\sigma(t)}(t) \\ y(t) = Cx(t) + v(t) \end{cases}, \sigma(t) \in \mathcal{I}, \quad (3.1)$$

where $x \in \mathbb{R}^{n_x}$, $u \in \mathbb{R}^{n_u}$, $y \in \mathbb{R}^{n_y}$, $w_{\sigma} \in \mathbb{R}^{n_x}$ and $v \in \mathbb{R}^{n_y}$ are respectively the state vector, the input, the output, the disturbances and the measurement noise. We denote respectively by $A_{\sigma(t)} \in \mathbb{R}^{n_x \times n_x}$ and $B_{\sigma(t)} \in \mathbb{R}^{n_x \times n_u}$ the state matrices and the input matrices, these matrices are defined with time-varying parameters. The matrix $C \in \mathbb{R}^{n_y \times n_x}$ is the output matrix. The switching between the subsystems is realized via a switching signal $\sigma(t) : \mathbb{R}_+ \rightarrow \mathcal{I}$. In the sequel, the index $q = \sigma(t)$ specifies, at each instant of time, the system currently being followed, $q \in \mathcal{I} = \overline{1, N}$, $N \in \mathbb{N}$, N is the number of linear subsystems. For each subsystem, we denote by $\eta_q = [\eta_{q_1}, \dots, \eta_{q_r}]^T$ the collection of measured time-varying parameters, which are constrained in polytopes E_q ; E_q depends on the active mode. We denote by $\eta_q^{(i)}$, $i = 1, \dots, g$ the vertices of each E_q .

A number of assumptions is considered in the following for the design of the interval observer gains.

Assumption 9. *We assume that the state matrices $A_q(\eta_q)$ and the input $B_q(\eta_q)$ depend*

affinely on η_q such that:

$$\begin{aligned} A_q(\eta_q) &= A_{q_0} + \eta_{q_1} A_{q_1} + \dots + \eta_{q_r} A_{q_r}, \\ B_q(\eta_q) &= B_{q_0} + \eta_{q_1} B_{q_1} + \dots + \eta_{q_r} B_{q_r}, \end{aligned} \quad q \in \mathcal{I}. \quad (3.2)$$

Assumption 10. *The initial state $x(0)$ satisfies $\underline{x}(0) \leq x(0) \leq \bar{x}(0)$ with known $\underline{x}(0), \bar{x}(0) \in \mathbb{R}^{n_x}$.*

Assumption 11. *The measurement noise and the state disturbances are assumed to be unknown but bounded with a priori known bounds such that*

$$\underline{w}_q \leq w_q \leq \bar{w}_q, |v| \leq \bar{v} J_{n_y}, \quad (3.3)$$

where $\underline{w}_q, \bar{w}_q \in \mathbb{R}^{n_x}$ and \bar{v} is a scalar.

Assumption 12. *There exist $L_q(\eta_q^{(i)}) \in \mathbb{R}^{n_x \times n_y}$ such that $A_q(\eta_q^{(i)}) - L_q(\eta_q^{(i)})C$ are Metzler for all $\eta_q^{(i)} \in E_q$, $i = 1, \dots, g$. $A_q(\eta_q^{(i)})$ denote the vertices of the state matrix $A_q(\eta_q)$ of each polytope E_q and $L_q(\eta_q^{(i)})$ the vertices of the observer gain.*

Assumption 13. *For all vertices of E_q and for all $q \in \mathcal{I}$, the pairs $(A_q(\eta_q^{(i)}), C)$ are detectable.*

Based on the representation in Assumption 9 and by assuming that the vectors η_q are measurable, it is worth pointing out that the system matrices are point-valued matrices for the observer implementation but they are overbounded by a convex domain. Assumption 11 is common in the literature of interval observers where the state disturbance and the measurement noise are supposed to be unknown but bounded with known bounds. Assumption 12 is required to ensure the cooperativity condition. Assumption 13 must be satisfied to build the upper and lower bounds of the continuous state. The detectability of the system is a classical assumption in the field of state estimation. In the present chapter, this assumption needs to be satisfied for the vertices of all polytopes in order to design the proposed observer.

The aim of this part is to design an interval observer for continuous-time LPV switched systems subject to unknown but bounded uncertainties and time-varying parameters which belong to polytopes. In the next subsections, the cooperativity design conditions of the proposed interval observer are detailed. Using CQLF and MQLF, stability conditions are also developed.

3.2.2 Interval observer design: cooperativity analysis

Definitions 8-13 and Lemma 2 are essential in the sequel to prove the cooperativity of the estimation errors.

Definition 13. [80] *A matrix $A \in \mathbb{R}^{n \times n}$ is called Metzler if there exists $\epsilon \in \mathbb{R}^+$ such that:*

$$A + \epsilon I_n \geq 0. \quad (3.4)$$

The proposed structure of the interval observer is given in the following theorem.

Theorem 6. *Let Assumptions 10-13 be satisfied then the system*

$$\begin{cases} \dot{\bar{x}} = (A_q(\eta_q) - L_q(\eta_q)C)\bar{x} + B_q(\eta_q)u + \bar{w}_q + L_q(\eta_q)y + |L_q(\eta_q)|\bar{v}J_{n_y} \\ \dot{\underline{x}} = (A_q(\eta_q) - L_q(\eta_q)C)\underline{x} + B_q(\eta_q)u + \underline{w}_q + L_q(\eta_q)y - |L_q(\eta_q)|\bar{v}J_{n_y} \end{cases}, q \in \mathcal{I} \quad (3.5)$$

is a framer for (3.1) such that

$$\underline{x}(t) \leq x(t) \leq \bar{x}(t). \quad (3.6)$$

provided that

$$A_q(\eta_q^{(i)}) - L_q(\eta_q^{(i)})C + \epsilon I_n \geq 0, \forall q \in \mathcal{I}, \epsilon \in \mathbb{R}^+. \quad (3.7)$$

The observer gain $L_q(\eta_q)$ has an affine form given by

$$L_q(\eta_q) = L_{q_0} + \eta_{q_1}L_{q_1} + \dots + \eta_{q_r}L_{q_r}, \quad (3.8)$$

and $L_{q_j} \in \mathbb{R}^{n_x \times n_y}$, $j = 0, 1, \dots, r$, are constant matrices.

In the following proof, we are interested in the positivity of the estimation errors.

Proof. We denote by $T_q(\eta_q) = A_q(\eta_q) - L_q(\eta_q)C$. According to Assumption 9, $A_q(\eta_q)$ and $L_q(\eta_q)$ depend of η_q affinely which involve that $T_q(\eta_q)$ is an affine function of η_q and can be written as a convex combination form [187] such that:

$$\begin{aligned} T_q(\eta_q) &= \lambda_1 T_q(\eta_q^{(1)}) + \dots + \lambda_g T_q(\eta_q^{(g)}) \\ &= \lambda_1 (A_q(\eta_q^{(1)}) - L_q(\eta_q^{(1)})C) + \dots + \lambda_g (A_q(\eta_q^{(g)}) - L_q(\eta_q^{(g)})C) \\ &= \sum_{i=1}^g \lambda_i (A_q(\eta_q^{(i)}) - L_q(\eta_q^{(i)})C), \end{aligned} \quad (3.9)$$

with $\lambda_i \geq 0$ and $\lambda_1 + \dots + \lambda_g = 1$.

Let $\bar{e}(t) = \bar{x} - x$ and $\underline{e}(t) = x - \underline{x}$ be the upper and the lower estimation errors. From (3.1), (3.5) and (3.9), the dynamics of the interval estimation errors are given by:

$$\begin{aligned} \dot{\bar{e}}(t) = \dot{\bar{x}} - \dot{x} &= \sum_{i=1}^g \lambda_i (A_q(\eta_q^{(i)}) - L_q(\eta_q^{(i)})C)\bar{e} + \bar{\chi}_q, \\ \dot{\underline{e}}(t) = \dot{x} - \dot{\underline{x}} &= \sum_{i=1}^g \lambda_i (A_q(\eta_q^{(i)}) - L_q(\eta_q^{(i)})C)\underline{e} + \underline{\chi}_q, \end{aligned} \quad (3.10)$$

where:

$$\begin{aligned} \bar{\chi}_q &= \bar{w}_q - w_q + L_q(\eta_q)v + |L_q(\eta_q)|\bar{v}J_{n_y}, \\ \underline{\chi}_q &= w_q - \underline{w}_q - L_q(\eta_q)v + |L_q(\eta_q)|\bar{v}J_{n_y}. \end{aligned} \quad (3.11)$$

In fact, the upper error dynamics can be written:

$$\begin{aligned} \dot{\bar{e}}(t) &= \dot{\bar{x}} - \dot{x} \\ &= (A_q(\eta_q) - L_q(\eta_q)C)(\bar{x} - x) + \bar{w}_q - w_q + L_q(\eta_q)v + |L_q(\eta_q)|\bar{v}J_{n_y} \\ &= (A_q(\eta_q) - L_q(\eta_q)C)\bar{e} + \bar{w}_q - w_q + L_q(\eta_q)v + |L_q(\eta_q)|\bar{v}J_{n_y} \\ &= \sum_{i=1}^g \lambda_i (A_q(\eta_q^{(i)}) - L_q(\eta_q^{(i)})C)\bar{e} + \bar{w}_q - w_q + L_q(\eta_q)v + |L_q(\eta_q)|\bar{v}J_{n_y}. \end{aligned} \quad (3.12)$$

Similarly, we have:

$$\dot{\underline{e}}(t) = \sum_{i=1}^g \lambda_i (A_q(\eta_q^{(i)}) - L_q(\eta_q^{(i)})C)\underline{e} + w_q - \underline{w}_q - L_q(\eta_q)v + |L_q(\eta_q)|\bar{v}J_{n_y}. \quad (3.13)$$

According to Assumption 11, it follows that $\bar{\chi}_q \geq 0$ and $\underline{\chi}_q \geq 0$. The requirement on the Metzler property of the matrix $(A_q(\eta_q) - L_q(\eta_q)C)$ is relaxed thanks to the polytopic form of the time-varying parameters. Based on (3.9), to show that $(A_q(\eta_q) - L_q(\eta_q)C)$ is Metzler is reduced to show that all matrices $A_q(\eta_q^{(i)}) - L_q(\eta_q^{(i)})C$, for $i = 1, \dots, g$, are Metzler. To that end, based on Definition 13, the Metzler property is satisfied for all $\eta_q^{(i)}$ by solving the following inequality :

$$A_q(\eta_q^{(i)}) - L_q(\eta_q^{(i)})C + \epsilon I_n \geq 0, \forall q \in \mathcal{I}, \epsilon \in \mathbb{R}^+. \quad (3.14)$$

Accordingly, the dynamics of the upper and lower errors are cooperative and thus $\underline{x}(t) \leq x(t) \leq \bar{x}(t)$ provided that $\underline{x}(0) \leq x(0) \leq \bar{x}(0)$.

Remark 3. *It is worth pointing out that the observer gains are variable in time and dependent on polytopic parameters which is very advantageous in practical situations since it is possible to adjust at any moment the observer in function of parameter variations.*

□

3.2.3 Interval observer design: Input-to-State Stability

Apart from the cooperativity analysis, the convergence of the estimation errors should be studied. Both Common and Multiple Lyapunov Functions are investigated in this part.

The following lemma is required in the sequel.

Lemma 7. [27] *Consider two vectors $u, v \in \mathbb{R}^n$, then*

$$2u^T M v \leq \frac{1}{\rho} u^T M u + \rho v^T M v \quad (3.15)$$

holds for any constant $\rho > 0$ and any positive definite matrix M .

3.2.3.1 Common Quadratic Lyapunov Function

In order to check the boundedness of \underline{e} and \bar{e} , a CQLF is considered herein. In the following theorem, ISS conditions are given in terms of LMIs defined on the vertices of each polytope.

Theorem 7. *Consider the continuous-time LPV switched system (3.1), where $A_q(\eta_q)$ and $B_q(\eta_q)$ are affine matrices on η_q and let Assumption 12 hold. If there exist a diagonal $P \succ 0 \in \mathbb{R}^{n_x \times n_x}$, constant matrices Q_{q_0}, \dots, Q_{q_r} and scalars $\rho_q > 0, \forall q \in \mathcal{I}$ such that*

$$A_q(\eta_q^{(i)})^T P + P A_q(\eta_q^{(i)}) - \left(C^T Q_q(\eta_q^{(i)})^T + Q_q(\eta_q^{(i)}) C \right) + \frac{3}{\rho_q} P \prec 0, \forall q \in \mathcal{I}, \quad (3.16)$$

where $Q_q(\eta_q^{(i)})$ are affine matrices of $\eta_q^{(i)}$ given by

$$Q_q(\eta_q^{(i)}) = Q_{q_0} + \eta_{q_1}^{(i)} Q_{q_1} + \dots + \eta_{q_r}^{(i)} Q_{q_r}, \quad (3.17)$$

with $Q_{q_j} \in \mathbb{R}^{n_x \times n_x}, j = 0, 1, \dots, r$ are constant matrices, then the observer gains are obtained such as:

$$L_{q_j} = P^{-1} Q_{q_j}, \quad j = 0, 1, \dots, r, \quad (3.18)$$

and the states \bar{x}, \underline{x} are bounded.

Proof. For the stability analysis, ISS of the interval observer is ensured using a CQLF defined by $V(\bar{e}) = \bar{e}(t)^T P \bar{e}(t)$ and $P = P^T \succ 0$. Based on (3.12), the derivative of V is given by:

$$\begin{aligned} \dot{V}(\bar{e}) &= \dot{\bar{e}}^T P \bar{e} + \bar{e}^T P \dot{\bar{e}} \\ &= \left((A_q(\eta_q) - L_q(\eta_q)C) \bar{e} + \bar{w}_q - w_q + L_q(\eta_q)v + |L_q(\eta_q)| \bar{v} J_{n_y} \right)^T P \bar{e} + \\ &\quad \bar{e}^T P \left((A_q(\eta_q) - L_q(\eta_q)C) \bar{e} + \bar{w}_q - w_q + L_q(\eta_q)v + |L_q(\eta_q)| \bar{v} J_{n_y} \right) \end{aligned} \quad (3.19)$$

$$\begin{aligned} \dot{V}(\bar{e}) &= \bar{e}^T \left((A_q(\eta_q) - L_q(\eta_q)C)^T P + P(A_q(\eta_q) - L_q(\eta_q)C) \right) \bar{e} - 2\bar{e}^T P w_q + \\ &\quad 2\bar{e}^T P \bar{w}_q + 2\bar{e}^T P L_q(\eta_q)v + 2\bar{e}^T P |L_q(\eta_q)| \bar{v} J_{n_y}. \end{aligned}$$

According to Lemma 7, we have

$$\begin{aligned} 2\bar{e}^T P(\bar{w}_q - w_q) &\leq \frac{1}{\varrho_q} \bar{e}^T P \bar{e} + \varrho_q (\bar{w}_q - w_q)^T P (\bar{w}_q - w_q), \\ 2\bar{e}^T P L_q(\eta_q)v &\leq \frac{1}{\varrho_q} \bar{e}^T P \bar{e} + \varrho_q v^T L_q(\eta_q)^T P L_q(\eta_q)v, \\ 2\bar{e}^T P |L_q(\eta_q)| \bar{v} J_{n_y} &\leq \frac{1}{\varrho_q} \bar{e}^T P \bar{e} + \varrho_q J_{n_y}^T \bar{v} |L_q(\eta_q)|^T P |L_q(\eta_q)| \bar{v} J_{n_y}, \end{aligned}$$

then, the derivative of V satisfies

$$\dot{V}(\bar{e}) \leq \bar{e}^T B_1 \bar{e} + C_1, \quad (3.20)$$

where

$$\begin{aligned} B_1 &= (A_q(\eta_q) - L_q(\eta_q)C)^T P + P(A_q(\eta_q) - L_q(\eta_q)C) + \frac{3}{\varrho_q} P \\ &= \sum_{i=1}^g \lambda_i \left(A_q(\eta_q^{(i)})^T P + P A_q(\eta_q^{(i)}) - C^T Q_q(\eta_q^{(i)})^T - Q_q(\eta_q^{(i)})C \right) + \frac{3}{\varrho_q} P, \end{aligned} \quad (3.21)$$

where $Q_q(\eta_q^{(i)}) = P L_q(\eta_q^{(i)})$, and

$$\begin{aligned} C_1 &= \varrho_q (\bar{w}_q - w_q)^T P (\bar{w}_q - w_q) + \varrho_q v^T L_q(\eta_q)^T P L_q(\eta_q)v + \\ &\quad \varrho_q J_{n_y}^T \bar{v} |L_q(\eta_q)|^T P |L_q(\eta_q)| \bar{v} J_{n_y}. \end{aligned} \quad (3.22)$$

Based on similar arguments, the derivative of the CQLF applied for the lower estimation error is given by:

$$\begin{aligned} \dot{V}(\underline{e}) &= \underline{e}^T \left((A_q(\eta_q) - L_q(\eta_q)C)^T P + P(A_q(\eta_q) - L_q(\eta_q)C) \right) \underline{e} + \\ &\quad 2\underline{e}^T P w_q - 2\underline{e}^T P \underline{w}_q - 2\underline{e}^T P L_q(\eta_q)v + 2\underline{e}^T P |L_q(\eta_q)| \underline{v} J_{n_y} \\ &\leq \underline{e}^T B_1 \underline{e} + C_2, \end{aligned} \quad (3.23)$$

where

$$\begin{aligned} C_2 &= \varrho_q (w_q - \underline{w}_q)^T P (w_q - \underline{w}_q) + \varrho_q v^T L_q(\eta_q)^T P L_q(\eta_q)v + \\ &\quad \varrho_q J_{n_y}^T \underline{v} |L_q(\eta_q)|^T P |L_q(\eta_q)| \underline{v} J_{n_y}. \end{aligned} \quad (3.24)$$

From (3.16), we note that $B_1 \prec 0$. Under the Assumption 11, the uncertainties w_q and v are bounded, C_1 and C_2 are also bounded. Therefore, according to Definition 7, the system (3.5) is ISS stable and the upper and lower estimation errors are bounded. \square

Remark 4. *Stability and cooperativity properties have been relaxed thanks to the polytopic shape of the system parameters, the observer has been modeled taking into account the time-varying parameters of the state matrix and not its upper and lower bounds. Also, LMIs and cooperativity conditions are expressed on the vertices of each polytope in order to avoid any infinite dimensional problem due to the time-varying measured parameters. Even if the conditions are relaxed with respect to the work performed in [188], the requirement of a CQLF remains a restrictive condition.*

3.2.3.2 Multiple Quadratic Lyapunov Functions

The results given by Theorem 7 are based on a CQLF approach. Nevertheless, the existence of such a function is not always guaranteed. In this part, based on the construction of MQLF, the conservatism is reduced under an ADT switching signal.

In the following theorem, the aim is to propose a robust interval observer with less restrictive conditions. Indeed, this observer is designed in order to minimize the width of the estimation interval and to reduce the ADT. The designed conditions are detailed hereafter in terms of LMIs.

Theorem 8. *For the continuous-time LPV switched system (3.1), suppose that there exist piecewise Lyapunov functions $V_{\sigma(t)}(\bar{e}(t))$ and $V_{\sigma(t)}(\underline{e}(t))$ where $V_q(\bar{e}(t)) = \bar{e}(t)^T P_q \bar{e}(t)$ and $V_q(\underline{e}(t)) = \underline{e}(t)^T P_q \underline{e}(t)$. If there exist positive definite diagonal matrices P_q, W_l , matrices $Q_q, \beta > \alpha > 0, \gamma > 0$ for a given $\varepsilon \geq 1, \alpha \geq 1, \epsilon > 0$ and $0 \leq \lambda \leq 1$, such that for all $q, l \in \mathcal{I}, q \neq l, \forall \eta_q^{(i)}$ the vertices of $E_q, i = 1, \dots, g$:*

$$\min_{P_q, Q_q, W_q} \lambda \mu + (1 - \lambda) \gamma, \quad (3.25)$$

$$\alpha I_{n_x} \leq P_q \leq \beta I_{n_x}, \quad (3.26)$$

$$\begin{bmatrix} A_q^T(\eta_q^{(i)})P_q + P_q A_q(\eta_q^{(i)}) - C^T Q_q^T(\eta_q^{(i)}) - Q_q(\eta_q^{(i)})C + \varepsilon P_q & P_q \\ P_q & -\gamma^2 I_{n_x} \end{bmatrix} \prec 0, \quad (3.27)$$

$$\begin{bmatrix} W_l & P_q \\ P_q & P_q \end{bmatrix} \succeq 0, \quad (3.28)$$

$$P_q A_q(\eta_q^{(i)}) - Q_q(\eta_q^{(i)})C + \epsilon P_q \geq 0, \quad (3.29)$$

hold, then the solutions of (3.1) and (3.5) satisfy $\underline{x}(t) \leq x(t) \leq \bar{x}(t)$. In addition, if the state x is bounded, then \underline{x} and \bar{x} are also bounded under any switching signal with ADT τ_a satisfying:

$$\tau_a > \tau_a^* = \frac{\ln(\mu)}{\varepsilon}, \quad (3.30)$$

where $\mu = \frac{\beta}{\alpha}$ and $L_q = P^{-1}Q_q$. Moreover, the interval error (3.10) satisfies:

$$\begin{aligned} \lim_{t \rightarrow \infty} \|\bar{e}\| &< \frac{\gamma}{\sqrt{\alpha \varepsilon}} \bar{\chi} \\ \lim_{t \rightarrow \infty} \|\underline{e}\| &< \frac{\gamma}{\sqrt{\alpha \varepsilon}} \underline{\chi}' \end{aligned}$$

where $\bar{\chi}$ and $\underline{\chi}'$ are the upper bounds of $\bar{\chi}_q$ and $\underline{\chi}_q$.

Proof. Now, we are interested in checking ISS of the estimation errors via MQLF $V_q(\bar{\epsilon}(t)) = \bar{\epsilon}^T(t)P_q\bar{\epsilon}(t)$ and $V_q(\underline{\epsilon}(t)) = \underline{\epsilon}^T(t)P_q\underline{\epsilon}(t)$ for the proposed interval observer in (3.5). Based on (3.10), the derivative of $V_q(\bar{\epsilon}(t))$ is given by:

$$\begin{aligned}
\dot{V}_q(\bar{\epsilon}(t)) &= \dot{\bar{\epsilon}}(t)^T P_q \bar{\epsilon}(t) + \bar{\epsilon}(t)^T P_q \dot{\bar{\epsilon}}(t) \\
&= \left((A_q(\eta_q) - L_q(\eta_q)C) \bar{\epsilon}(t) + \bar{\chi}_q(t) \right)^T P_q \bar{\epsilon}(t) + \bar{\epsilon}(t)^T P_q (A_q(\eta_q) - L_q(\eta_q)C) \bar{\epsilon}(t) + \\
&\quad \bar{\epsilon}(t)^T P_q \bar{\chi}_q(t) \\
&= \bar{\epsilon}^T(t) \left((A_q(\eta_q) - L_q(\eta_q)C)^T P_q + P_q (A_q(\eta_q) - L_q(\eta_q)C) \right) \bar{\epsilon}(t) + \bar{\chi}_q^T(t) P_q \bar{\epsilon}(t) + \\
&\quad \bar{\epsilon}^T(t) P_q \bar{\chi}_q(t) \\
&= \bar{\epsilon}^T(t) \sum_{i=1}^g \lambda_i \left((A_q(\eta_q^{(i)}) - L_q(\eta_q^{(i)})C)^T P_q + P_q (A_q(\eta_q^{(i)}) - L_q(\eta_q^{(i)})C) \right) \bar{\epsilon}(t) + \\
&\quad \bar{\chi}_q^T(t) P_q \bar{\epsilon}(t) + \bar{\epsilon}^T(t) P_q \bar{\chi}_q(t).
\end{aligned}$$

By adding and subtracting the following terms $\varepsilon \bar{\epsilon}(t)^T P_q \bar{\epsilon}(t)$ and $-\gamma^2 \bar{\chi}_q(t)^T \bar{\chi}_q(t)$, \dot{V} becomes:

$$\begin{aligned}
\dot{V}_q(\bar{\epsilon}(t)) &= \bar{\epsilon}(t)^T \sum_{i=1}^g \lambda_i \left((A_q(\eta_q^{(i)}) - L_q(\eta_q^{(i)})C)^T P_q + P_q (A_q(\eta_q^{(i)}) - L_q(\eta_q^{(i)})C) \right) \bar{\epsilon}(t) + \\
&\quad \bar{\chi}_q^T(t) P_q \bar{\epsilon}(t) + \bar{\epsilon}(t)^T P_q \bar{\chi}_q(t) + \varepsilon \bar{\epsilon}^T(t) P_q \bar{\epsilon}(t) - \gamma^2 \bar{\chi}_q^T(t) \bar{\chi}_q(t) - \varepsilon \bar{\epsilon}(t)^T P_q \bar{\epsilon}(t) + \\
&\quad \gamma^2 \bar{\chi}_q^T(t) \bar{\chi}_q(t) \\
\dot{V}_q(\bar{\epsilon}(t)) &= \sum_{i=1}^g \lambda_i [\bar{\epsilon}(t)^T \quad \bar{\chi}_q^T(t)] \Theta_q^{(i)} [\bar{\epsilon}(t) \quad \bar{\chi}_q(t)] - \varepsilon \bar{\epsilon}^T(t) P_q \bar{\epsilon}(t) + \gamma^2 \bar{\chi}_q^T(t) \bar{\chi}_q(t) \\
&= \sum_{i=1}^g \lambda_i [\bar{\epsilon}(t)^T \quad \bar{\chi}_q^T(t)] \Theta_q^{(i)} [\bar{\epsilon}(t) \quad \bar{\chi}_q(t)] - \varepsilon V_q(\bar{\epsilon}(t)) + \gamma^2 \bar{\chi}_q^T(t) \bar{\chi}_q(t),
\end{aligned}$$

where

$$\begin{aligned}
\Theta_q^{(i)} &= \begin{bmatrix} \left((A_q(\eta_q^{(i)}) - L_q(\eta_q^{(i)})C \right)^T P_q + P_q (A_q(\eta_q^{(i)}) - L_q(\eta_q^{(i)})C) + \varepsilon P_q & P_q \\ P_q & -\gamma^2 I_{n_x} \end{bmatrix} \\
&= \begin{bmatrix} A_q^T(\eta_q^{(i)}) P_q + P_q A_q(\eta_q^{(i)}) - C^T L_q^T(\eta_q^{(i)}) P_q - P_q L_q(\eta_q^{(i)}) C + \varepsilon P_q & P_q \\ P_q & -\gamma^2 I_{n_x} \end{bmatrix} \\
&= \begin{bmatrix} A_q^T(\eta_q^{(i)}) P_q + P_q A_q(\eta_q^{(i)}) - C^T Q_q^T(\eta_q^{(i)}) - Q_q(\eta_q^{(i)}) C + \varepsilon P_q & P_q \\ P_q & -\gamma^2 I_{n_x} \end{bmatrix}.
\end{aligned}$$

Using the same arguments, the derivative of $V_q(\underline{\epsilon}(t))$ is given by:

$$\begin{aligned}
\dot{V}_q(\underline{\epsilon}(t)) &= \sum_{i=1}^g \lambda_i [\underline{\epsilon}(t)^T \quad \underline{\chi}_q^T(t)] \Theta_q^{(i)} [\underline{\epsilon}(t) \quad \underline{\chi}_q(t)] - \varepsilon \underline{\epsilon}^T(t) P_q \underline{\epsilon}(t) + \gamma^2 \underline{\chi}_q^T(t) \underline{\chi}_q(t) \\
&= \sum_{i=1}^g \lambda_i [\underline{\epsilon}(t)^T \quad \underline{\chi}_q^T(t)] \Theta_q^{(i)} [\underline{\epsilon}(t) \quad \underline{\chi}_q(t)] - \varepsilon V_q(\underline{\epsilon}(t)) + \gamma^2 \underline{\chi}_q^T(t) \underline{\chi}_q(t),
\end{aligned}$$

Notice that if (3.27) holds, then inequality (2.16) is ensured such as:

$$\begin{aligned}
\dot{V}_q(\bar{\epsilon}(t)) &< -\varepsilon V_q(\bar{\epsilon}(t)) + \gamma^2 (\|\bar{\chi}_q(t)\|^2) \\
\dot{V}_q(\underline{\epsilon}(t)) &< -\varepsilon V_q(\underline{\epsilon}(t)) + \gamma^2 (\|\underline{\chi}_q(t)\|^2).
\end{aligned} \tag{3.31}$$

Due to the presence of bounded noise and disturbances, the estimates \underline{x} and \bar{x} cannot converge to the actual state x . However, it is possible to quantify the impact of disturbances and to evaluate the estimation accuracy. Indeed, (3.31) implies:

$$\begin{aligned} V_q(\bar{e}(t)) &< e^{-\varepsilon t} V_q(0) + \gamma^2 \int_0^t e^{-\varepsilon(t-s)} \|\bar{\chi}_q(s)\|^2 ds \\ V_q(\underline{e}(t)) &< e^{-\varepsilon t} V_q(0) + \gamma^2 \int_0^t e^{-\varepsilon(t-s)} \|\underline{\chi}_q(s)\|^2 ds. \end{aligned} \quad (3.32)$$

From (2.15), we have:

$$\begin{aligned} \alpha \bar{e}^T(t) \bar{e}(t) &\leq V_q(\bar{e}(t)) \\ \alpha \underline{e}^T(t) \underline{e}(t) &\leq V_q(\underline{e}(t)). \end{aligned}$$

Combining with (3.32), we deduce that:

$$\begin{aligned} \bar{e}^T(t) \bar{e}(t) &< \frac{1}{\alpha} (e^{-\varepsilon t} V_q(0) + \gamma^2 \int_0^t e^{-\varepsilon(t-s)} ds \|\bar{\chi}_q\|_\infty^2) \\ \underline{e}^T(t) \underline{e}(t) &< \frac{1}{\alpha} (e^{-\varepsilon t} V_q(0) + \gamma^2 \int_0^t e^{-\varepsilon(t-s)} ds \|\underline{\chi}_q\|_\infty^2). \end{aligned}$$

Since w_q and v are bounded, when $t \rightarrow \infty$ then $\bar{\chi}_q$ and $\underline{\chi}_q$ are also bounded, *i.e.* $\|\bar{\chi}_q\|_\infty \leq \bar{\chi}$, $\|\underline{\chi}_q\|_\infty \leq \underline{\chi}'$ and the following inequality holds:

$$\begin{aligned} \lim_{t \rightarrow \infty} \|\bar{e}\| &< \frac{\gamma}{\sqrt{\alpha \varepsilon}} \bar{\chi} \\ \lim_{t \rightarrow \infty} \|\underline{e}\| &< \frac{\gamma}{\sqrt{\alpha \varepsilon}} \underline{\chi}'. \end{aligned}$$

These expressions show that the estimation errors $\bar{e}(t)$ and $\underline{e}(t)$ remain bounded for each mode. It should be highlighted that this bound depends on γ , for a given α and ε . In order to improve the robustness of the observer (3.5), the minimization of γ allows one to reduce the estimation error.

Now let us focus on the interval observer errors stability at the switching instants. The inequality defined in (2.17) becomes:

$$\mu P_l - P_q \succeq 0. \quad (3.33)$$

Then, by using the Schur complement, (3.33) is equivalent to:

$$\begin{bmatrix} \mu P_l & I_{n_x} \\ I_{n_x} & P_q^{-1} \end{bmatrix} \succeq 0. \quad (3.34)$$

We multiply both sides by $\begin{bmatrix} I_{n_x} & O_n \\ O_n & P_q \end{bmatrix}$, thus

$$\begin{bmatrix} W_l & P_q \\ P_q & P_q \end{bmatrix} \succeq 0$$

is obtained, where $W_l = \mu P_l$.

Integrating the inequality (2.16) over the interval $[t, t_q]$ leads to:

$$\begin{aligned} V_q(\bar{e}) &< e^{-\varepsilon(t-t_q)} V_q(\bar{e}(t_q)) \\ V_q(\underline{e}) &< e^{-\varepsilon(t-t_q)} V_q(\underline{e}(t_q)). \end{aligned}$$

For all $q, l \in \mathcal{I} \times \mathcal{I}, q \neq l$

$$\begin{aligned} V_q(\bar{e}) &< e^{-\varepsilon(t-t_q)} V_q(\bar{e}(t_q)) \frac{V_l(\bar{e}(t_l))}{V_l(\bar{e}(t_l))} \\ &< e^{-\varepsilon(t-t_q)} \frac{\bar{e}(t_q)^T P_q \bar{e}(t_q)}{\bar{e}(t_l)^T P_l \bar{e}(t_l)} V_l(\bar{e}(t_l)). \end{aligned}$$

and

$$\begin{aligned} V_q(\underline{e}) &< e^{-\varepsilon(t-t_q)} V_q(\underline{e}(t_q)) \frac{V_l(\underline{e}(t_l))}{V_l(\underline{e}(t_l))} \\ &< e^{-\varepsilon(t-t_q)} \frac{\underline{e}(t_q)^T P_q \underline{e}(t_q)}{\underline{e}(t_l)^T P_l \underline{e}(t_l)} V_l(\underline{e}(t_l)). \end{aligned}$$

Using (3.26), we obtain:

$$\begin{aligned} V_q(\bar{e}(t)) &< \frac{\beta}{\alpha} e^{-\varepsilon(t-t_q)} V_l(\bar{e}(t_l)) \\ V_q(\underline{e}(t)) &< \frac{\beta}{\alpha} e^{-\varepsilon(t-t_q)} V_l(\underline{e}(t_l)), \end{aligned} \quad (3.35)$$

Thus, at the switching instant $t = t_q$, the inequality (3.35) can be written as follows:

$$\begin{aligned} V_q(\bar{e}(t)) &< \frac{\beta}{\alpha} V_l(\bar{e}(t_l)) \\ V_q(\underline{e}(t)) &< \frac{\beta}{\alpha} V_l(\underline{e}(t_l)) \end{aligned}$$

with $\mu = \frac{\beta}{\alpha}$. Under these assumptions, the ISS of the observer (3.5) can be ensured [31]. \square

Remark 5. *Our purpose is to minimize both γ in order to reduce the width of the estimation interval and μ to look for an optimum dwell time from which, the dynamics of estimation errors of the continuous-time LPV switched system is ISS. The resolution of such a problem leads to solve a problem of linear optimization which consists in seeking for a minimisation function. Then, an objective function f , expressed as:*

$$f = \lambda\mu + (1 - \lambda)\gamma$$

can be added to the LMI conditions, where the weight λ is in the range $[0, 1]$.

Remark 6. *One should highlight that using MQLF, the problem formulated with polytopic time varying parameters is less conservative than the ISS conditions given in [186]. Indeed, the infinite dimensional problem due to the time-varying parameters is reduced by expressing LMIs on the vertices of each polytope. A larger class of LPV switched systems can be considered by this approach.*

3.2.4 Numerical examples

In order to illustrate the performance of the proposed interval observer, simulation results are presented in this section.

3.2.4.1 Example 1: Common Lyapunov Function

LPV switched modeling

Let us consider the continuous-time LPV switched system (3.1) with $N = 3$ modes ($q \in \{1, 2, 3\}$) where $\eta_q = [\eta_{q1}, \eta_{q2}]^T$. Based on the representation (3.2), matrices of the system

are chosen as below:

$$\begin{aligned}
A_{10} &= \begin{pmatrix} -3 & 5 \\ -1 & -6 \end{pmatrix} & A_{11} &= \begin{pmatrix} -1.5 & 2.5 \\ -1 & -1 \end{pmatrix} & A_{12} &= \begin{pmatrix} 1 & -1 \\ -1 & -2 \end{pmatrix} \\
B_{10} &= \begin{pmatrix} -1 & 1 \\ 1 & 0 \end{pmatrix} & B_{11} &= \begin{pmatrix} -1 & 2 \\ 2 & 2 \end{pmatrix} & B_{12} &= \begin{pmatrix} 2 & 1 \\ 1 & 4 \end{pmatrix} \\
A_{20} &= \begin{pmatrix} -2 & 5 \\ -1.8 & -1 \end{pmatrix} & A_{21} &= \begin{pmatrix} -1 & -4 \\ 2 & -3 \end{pmatrix} & A_{22} &= \begin{pmatrix} 1 & 2 \\ -1 & -1 \end{pmatrix} \\
B_{20} &= \begin{pmatrix} -1 & 2 \\ 1.5 & 0 \end{pmatrix} & B_{21} &= \begin{pmatrix} -1 & 2 \\ 2 & 1 \end{pmatrix} & B_{22} &= \begin{pmatrix} 1 & 1 \\ 3 & 3 \end{pmatrix} \\
A_{30} &= \begin{pmatrix} -20 & 10 \\ -10 & -1 \end{pmatrix} & A_{31} &= \begin{pmatrix} -3 & 2.5 \\ -2.2 & -1 \end{pmatrix} & A_{32} &= \begin{pmatrix} 1 & -1 \\ -1 & 0 \end{pmatrix} \\
B_{30} &= \begin{pmatrix} -2 & 1.5 \\ 1 & 0 \end{pmatrix} & B_{31} &= \begin{pmatrix} -1 & 3 \\ 1 & 1 \end{pmatrix} & B_{32} &= \begin{pmatrix} 2 & 1 \\ 4 & 3 \end{pmatrix} \\
C &= \begin{pmatrix} 1 & -1 \end{pmatrix}
\end{aligned}$$

For simulation, $x = [x_1, x_2]^T \in \mathbb{R}^2$ is the state, $y \in \mathbb{R}$ is the output and $u = [1, 1]^T \in \mathbb{R}^2$ is the known input. It is assumed in this example that, $w_q(t) \in \mathbb{R}^2$, $q = 1, 2, 3$, the vector of disturbances, is supposed to be bounded. To that end, $w_q(t)$ is chosen as follow:

$$\begin{aligned}
w_1(t) &= [0.005, 0.009]^T \cos(5t), \\
w_2(t) &= [0.001, 0.002]^T \cos(2t), \\
w_3(t) &= [0.004, 0.007]^T \cos(3t).
\end{aligned}$$

$v(t)$ represents the measurement noise which is a uniformly distributed signal bounded by $\bar{v} = 0.005$. The state initial conditions are set as $x(0) = [0, 0]^T$ such that: $\underline{x}(0) \leq x(0) \leq \bar{x}(0)$. η_q is the measured time varying parameters for $q = 1, 2, 3$. $\eta_q \in \mathbb{R}^2$ is given by:

$$\begin{aligned}
\eta_1(t) &= \begin{pmatrix} |\sin(2t)| + 0.5 \\ |\cos(t)| + 0.5 \end{pmatrix} & \eta_2(t) &= \begin{pmatrix} |2\cos(0.2t)| + 0.5 \\ |2\cos(3t)| + 0.5 \end{pmatrix} \\
\eta_3(t) &= \begin{pmatrix} |\cos(0.2t)| + 0.1 \\ |\cos(t)| + 0.1 \end{pmatrix}
\end{aligned}$$

The vertices of the polytope can be easily deduced from these expressions.

Simulation results

The numerical simulation was carried out by using Matlab optimization tools (Yalmip/Sedumi). The following Lyapunov matrix is obtained:

$$P = \begin{pmatrix} 2.11 & 0 \\ 0 & 5.73 \end{pmatrix}$$

The set of observer gains L_{qj} are computed for $q = 1, 2, 3$ and $j = 0, 1$. Thus, we have:

$$\begin{aligned} L_{10} &= \begin{pmatrix} 274 \\ -96 \end{pmatrix}, & L_{11} &= \begin{pmatrix} -124 \\ 47 \end{pmatrix}, & L_{12} &= \begin{pmatrix} 124 \\ -45 \end{pmatrix} \\ L_{20} &= \begin{pmatrix} 268 \\ -98 \end{pmatrix}, & L_{21} &= \begin{pmatrix} -59 \\ 24 \end{pmatrix}, & L_{22} &= \begin{pmatrix} 62 \\ -22 \end{pmatrix} \\ L_{30} &= \begin{pmatrix} 260 \\ -103 \end{pmatrix}, & L_{31} &= \begin{pmatrix} -123 \\ 46 \end{pmatrix}, & L_{32} &= \begin{pmatrix} 124 \\ -47 \end{pmatrix} \end{aligned}$$

Under the switching sequence shown in Fig. 3.1, simulation results of the interval observer are depicted in Fig. 3.2.

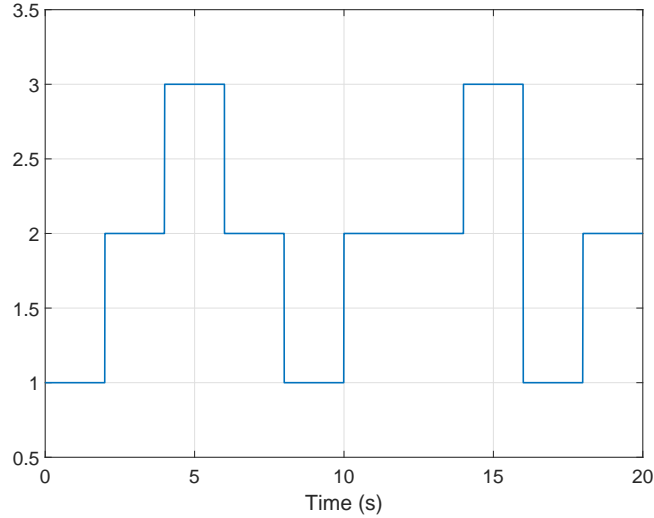


Figure 3.1: Evolution of the switching signal

Figure 3.3 illustrates evolutions of the state x and the estimated upper and lower bounds \bar{x} and \underline{x} (ZOOM). It is worth noting that the state x is between the lower and upper bounds \underline{x} and \bar{x} .

In order to highlight the performance of the proposed interval observer, we notice that the errors \underline{e} and \bar{e} are bounded and positive. The simulation results of the evolutions of the estimation errors are presented in Fig. 3.4.

Remark 7. *This first example shows promising results. However, the existence of a CQLF is not guaranteed especially in the case of large parameter uncertainties. To reduce this conservatism, a MQLF based approach is considered under an ADT switching signal in the following second example.*

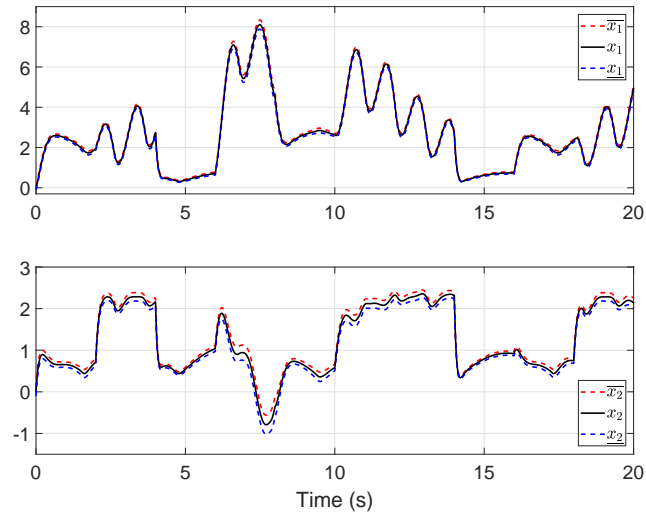


Figure 3.2: Evolutions of the state x and the estimated upper and lower bounds using CQLF.

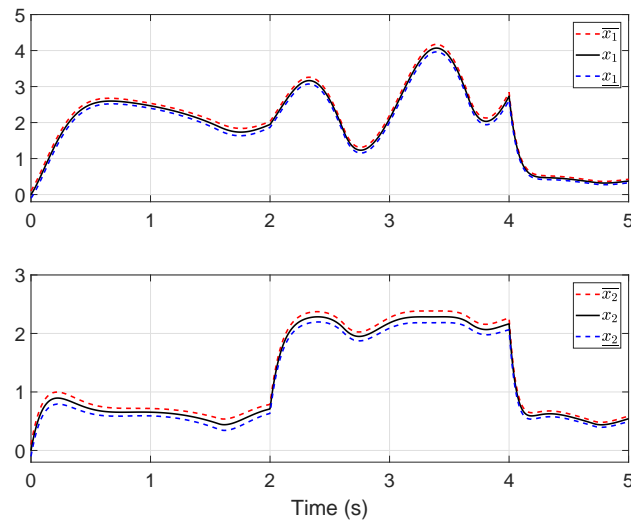


Figure 3.3: Evolutions of the state x and the estimated upper and lower bounds (ZOOM) using CQLF.

3.2.4.2 Example 2: Multiple Lyapunov Functions

LPV switched representation

The second example is based on the construction of MQLF under an ADT switching signal in order to reduce the conservatism. For this purpose, let us consider a continuous-time LPV switched system defined with three subsystems, $N = 3$ and subject to different uncertainties.

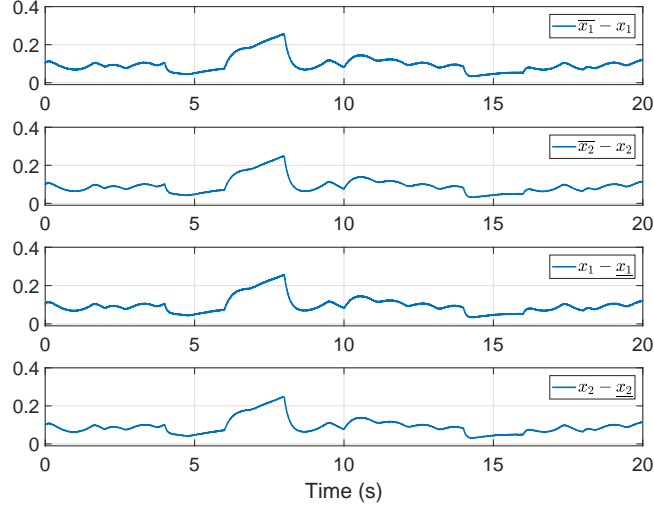


Figure 3.4: Evolution of estimation errors using CQLF.

State matrices, input matrices and the output matrix are chosen as:

$$A_{10} = \begin{pmatrix} -10 & 0.1 \\ -3 & -1 \end{pmatrix} \quad A_{11} = \begin{pmatrix} -0.5 & 1.5 \\ -0.5 & -1 \end{pmatrix} \quad A_{12} = \begin{pmatrix} 2 & -0.5 \\ -0.5 & -1.5 \end{pmatrix}$$

$$B_{10} = \begin{pmatrix} -1 & 1 \\ 1 & 0 \end{pmatrix} \quad B_{11} = \begin{pmatrix} -2 & 2 \\ 1 & 0.5 \end{pmatrix} \quad B_{12} = \begin{pmatrix} 2 & 3 \\ 3 & 2 \end{pmatrix}$$

$$A_{20} = \begin{pmatrix} -15 & 10 \\ -2 & -3 \end{pmatrix} \quad A_{21} = \begin{pmatrix} -0.5 & -2 \\ 1.5 & -2 \end{pmatrix} \quad A_{22} = \begin{pmatrix} 0.5 & 2 \\ -1 & -1.4 \end{pmatrix}$$

$$B_{20} = \begin{pmatrix} -1 & 2 \\ 1.5 & 0 \end{pmatrix} \quad B_{21} = \begin{pmatrix} -1.5 & 1 \\ 1 & 0.5 \end{pmatrix} \quad B_{22} = \begin{pmatrix} 2 & 2 \\ 3 & 1 \end{pmatrix}$$

$$A_{30} = \begin{pmatrix} -3.5 & 5 \\ -10 & -2 \end{pmatrix} \quad A_{31} = \begin{pmatrix} -0.5 & 1.5 \\ -0.5 & -1 \end{pmatrix} \quad A_{32} = \begin{pmatrix} 2 & -0.5 \\ -0.5 & -1.5 \end{pmatrix}$$

$$B_{30} = \begin{pmatrix} -2 & 1.5 \\ 1 & 0 \end{pmatrix} \quad B_{31} = \begin{pmatrix} -1 & 2.5 \\ 1 & 0.75 \end{pmatrix} \quad B_{32} = \begin{pmatrix} 2 & 3 \\ 3 & 2 \end{pmatrix}$$

$$C = \begin{pmatrix} 1 & -1 \end{pmatrix}$$

In this example, $x = [x_1, x_2]^T \in \mathbb{R}^2$ is the state, $y \in \mathbb{R}$ is the output, $u = [1, 1]^T \in \mathbb{R}^2$ is the known input, $w_q(t) \in \mathbb{R}^2$ for $q = 1, 2, 3$ is the vector of disturbances with:

$$w_1(t) = [0.05, 0.02]^T \sin(10t),$$

$$w_2(t) = [0.1, 0.2]^T \sin(5t),$$

$$w_3(t) = [0.03, 0.07]^T \sin(2t).$$

$v(t)$ represents the measurement noise which is a uniformly distributed signal bounded by $\bar{v} = 0.09$. The state initial conditions are set as $x(0) = [0, 0]^T$ such that:

$$\underline{x}(0) \leq x(0) \leq \bar{x}(0)$$

and the measured time varying parameters η_q for $q = 1, 2, 3$ are defined by:

$$\eta_1(t) = \begin{pmatrix} |\sin(t)| + 2 \\ |\cos(2t)| + 2 \end{pmatrix} \quad \eta_2(t) = \begin{pmatrix} |2\cos(0.8t)| + 2 \\ |2\cos(2t)| + 2 \end{pmatrix}$$

$$\eta_3(t) = \begin{pmatrix} |3\sin(3t)| \\ |3\cos(t)| \end{pmatrix}$$

Simulation results

From these expressions, the vertices of the polytope can be easily deduced in order to implement the proposed LMIs. This optimization problem can be solved using the convex optimization software Yalmip/Sedumi in MATLAB. The existence of a solution for the LMIs allows one to minimize the width of the estimation interval and the dwell time in order to guarantee the ISS of the errors $\bar{e} = \bar{x} - x$ and $\underline{e} = x - \underline{x}$. The parameters $\varepsilon = 1000$, $\alpha = 1.2$, $\epsilon = 1$ and $\lambda = 0.1$ are chosen to solve this optimization problem. The following Lyapunov matrices are obtained:

$$P_1 = \begin{pmatrix} 1.287 & 0 \\ 0 & 1.315 \end{pmatrix} \quad P_2 = \begin{pmatrix} 1.288 & 0 \\ 0 & 1.312 \end{pmatrix}$$

$$P_3 = \begin{pmatrix} 1.2 & 0 \\ 0 & 1.66 \end{pmatrix}$$

Then, with assigning $\epsilon = 1$, we obtain $\mu = 1.384$ which leads to an ADT $\tau_a > 0.325s$. The set of observer gains $L_\sigma(\eta)$, are computed and given by:

$$L_{10} = \begin{pmatrix} 30.74 \\ -38.92 \end{pmatrix}, \quad L_{11} = \begin{pmatrix} -18.64 \\ 19.41 \end{pmatrix}, \quad L_{12} = \begin{pmatrix} 20.42 \\ -17.43 \end{pmatrix}$$

$$L_{20} = \begin{pmatrix} 25.17 \\ -36.76 \end{pmatrix}, \quad L_{21} = \begin{pmatrix} -8.96 \\ 10.87 \end{pmatrix}, \quad L_{22} = \begin{pmatrix} 9.62 \\ -8.31 \end{pmatrix}$$

$$L_{30} = \begin{pmatrix} 39.42 \\ -30.68 \end{pmatrix}, \quad L_{31} = \begin{pmatrix} -10 \\ 5.43 \end{pmatrix}, \quad L_{32} = \begin{pmatrix} 7.01 \\ -1.43 \end{pmatrix}$$

The goal is to estimate the lower and upper bounds of the state $x(t)$ in spite of the bounded disturbance $w_q(t)$ and the bounded measurement noise $v(t)$ for the LPV switched system when the time varying parameters are measured and the switching signal is assumed to be known. Figure 3.5 shows the evolution of the switching signal. It indicates the active mode of the LPV switched system. One can notice that the ADT condition is verified. Figures

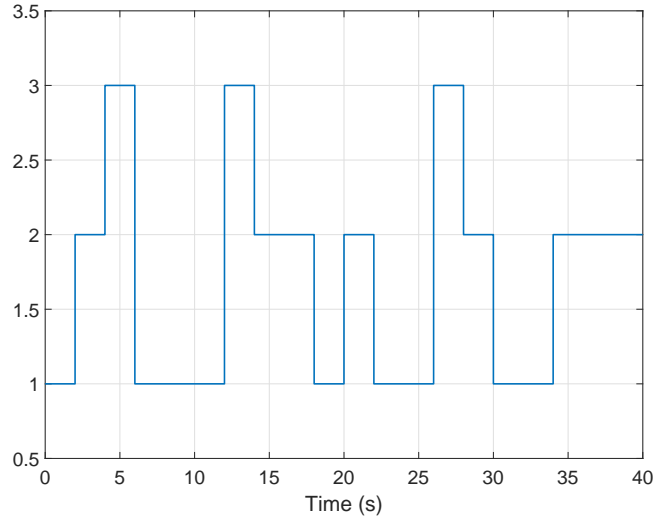


Figure 3.5: Evolution of the switching signal

3.6-3.7 illustrate the evolutions the state x in continuous time. It is worth pointing out that the lower and upper bounds \underline{x} and \bar{x} are estimated. Figure 3.8 highlights the performance of the proposed interval observer. The errors \underline{e} and \bar{e} remain bounded and positive.

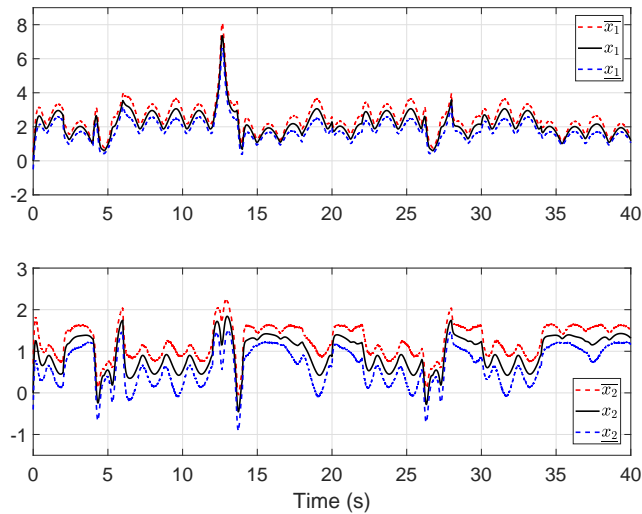


Figure 3.6: Evolutions of the state x and the estimated upper and lower bounds using MQLF.

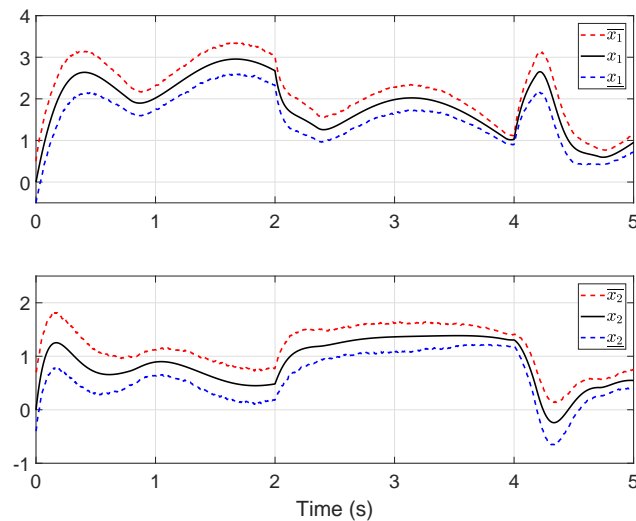


Figure 3.7: Evolutions of the state x and the estimated upper and lower bounds (ZOOM) using MQLF.

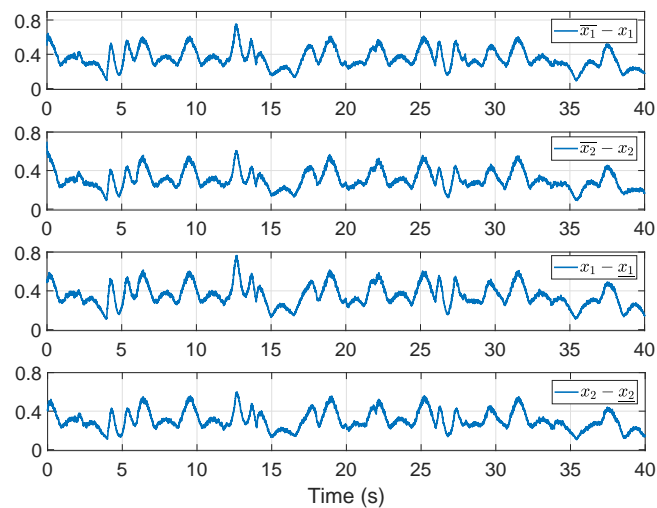


Figure 3.8: Evolutions of the estimation errors using MQLF.

Under similar conditions, the previous numerical example is carried out based on the construction of a CQLF.

The following Lyapunov matrix is obtained:

$$P = \begin{pmatrix} 2.17 & 0 \\ 0 & 5.31 \end{pmatrix}$$

The simulation results in Fig. 3.9 show that the estimated bounds of the states using MQLF, under an ADT switching signal, are more accurate than those obtained by CQLF.

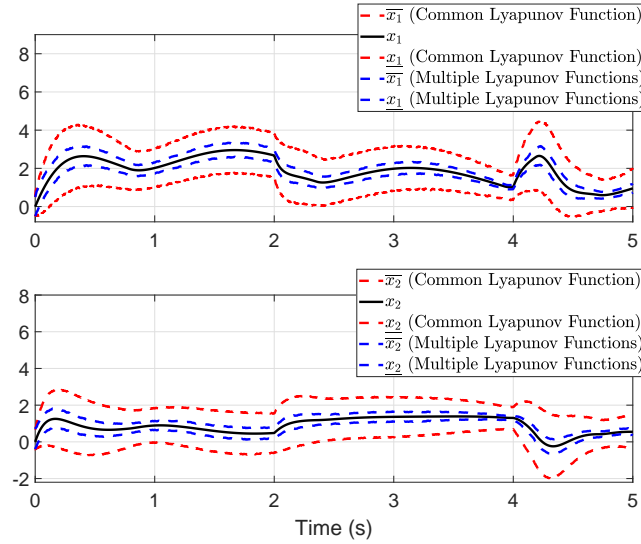


Figure 3.9: Evolutions of the state x and the estimated upper and lower bounds (ZOOM).

This is reasonable since the width of the estimation interval is optimized when using the approach based on the construction of MQLF. However, only conditions of cooperativeness and stability of the upper and lower estimation errors are developed in the case of CQLF.

A comparison has been performed between the LMIs developed in [186], which are expressed as a function of the uniformly bounded state space matrices, and those established in this chapter, expressed on the vertices of each polytope. This comparison was made based on the aforementioned numerical example. The simulation results are depicted in Fig. 3.10 and Fig. 3.11 where solid lines present the state x and the estimated upper and lower bounds obtained in [186] and dashed lines present the state x and the bounds obtained by the proposed approach.

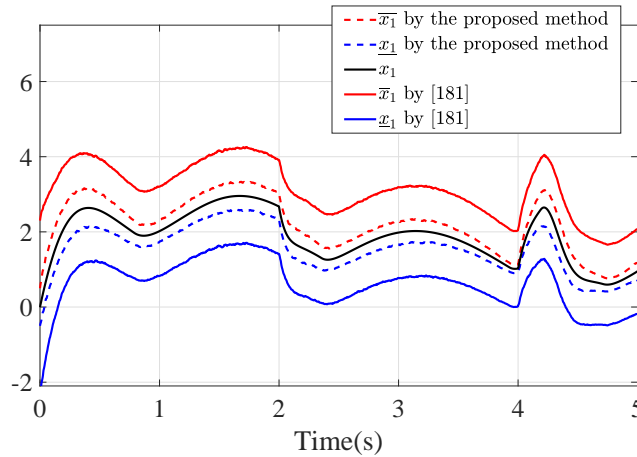


Figure 3.10: Comparison between the estimated upper and lower bounds of the state x_1 obtained by the proposed polytopic approach and norm bounded approach in [181] (ZOOM).

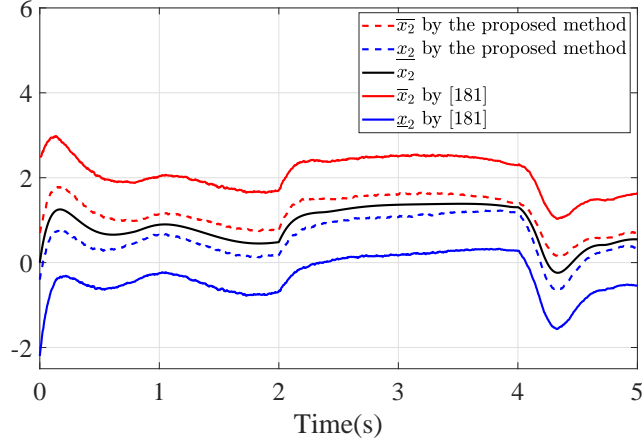


Figure 3.11: Comparison between the estimated upper and lower bounds of the state x_2 obtained by the proposed polytopic approach and norm bounded approach in [181] (ZOOM).

The width of the estimation interval (by using the polytopic approach) is clearly thinner, as well as the ADT time which is 2 times more optimal than that found by applying the LMIs of [186].

3.3 Interval observer design for discrete-time LPV switched systems

In the discrete-time case, interval observers design for switched systems is barely exposed in the literature. For instance, in [108], based on a time-varying transformation, the design of interval observers for discrete-time switched systems is addressed. The stability and the nonnegativity of the estimation errors are studied under ADT conditions. In [109], an interval observer is investigated for switched linear system where new cooperativity conditions are given in discrete time instants. Actually, most of interval observers for discrete-time switched systems are designed in a linear time invariant settings. This motivates the present part of this chapter, which is devoted to propose an interval observer for discrete-time LPV switched systems subject to bounded disturbances and measurement noise. It is worth pointing out that the scheduling vector is described by a convex combination so that the time-varying parameters belong to polytopes.

3.3.1 Problem statement

Consider the following LPV switched system:

$$\begin{cases} x_{k+1} &= A_{\sigma(k)}(\eta_{\sigma(k)})x_k + B_{\sigma(k)}(\eta_{\sigma(k)})u_k + w_{\sigma(k)} \\ y_k &= Cx_k + v_k \end{cases}, \quad \sigma(k) \in \mathcal{I} \quad (3.36)$$

where $x \in \mathbb{R}^{n_x}$, $u \in \mathbb{R}^{n_u}$, $y \in \mathbb{R}^{n_y}$, $w_{\sigma} \in \mathbb{R}^{n_x}$ and $v \in \mathbb{R}^{n_y}$ are respectively the state vector, the input and the output, the disturbances and the measurement noise.

The aim is to design an interval observer for discrete-time LPV switched systems defined by (3.36) using a polytopic representation. In spite of the time-varying parameters, the

state disturbances and the measurement noise, an upper state \bar{x} and a lower one \underline{x} are determined under the assumption that the initial condition x_0 verifies $\underline{x}_0 \leq x_0 \leq \bar{x}_0$ with known $\underline{x}_0, \bar{x}_0 \in \mathbb{R}_x^n$.

3.3.2 Interval observer design

In this part, an interval estimation method is considered. The cooperativity and ISS properties are relaxed thanks to the polytopic representation of the time-varying parameters and based on the construction of MQLF.

The following assumptions are needed in the sequel.

Assumption 14. *The initial state x_0 satisfies $\underline{x}_0 \leq x_0 \leq \bar{x}_0$ with known $\underline{x}_0, \bar{x}_0 \in \mathbb{R}^{n_x}$.*

Assumption 15. *It exists $L_q(\eta_q^{(i)}) \in \mathbb{R}^{n_x \times n_y}$ such that $A_q(\eta_q^{(i)}) - L_q(\eta_q^{(i)})C$ are nonnegative for all $\eta_q^{(i)} \in E_q, i = 1, \dots, g$.*

3.3.2.1 Positivity of the interval errors

Positivity of the interval errors is necessary to satisfy the interval property, i.e, the state trajectories stay within the estimated bounds.

Theorem 9. *Under Assumptions 13-15 and 11, the following proposed system*

$$\begin{cases} \bar{x}_{k+1} = (A_q(\eta_q) - L_q(\eta_q)C) \bar{x}_k + B_q(\eta_q)u_k + \bar{w}_q + L_q(\eta_q)y_k + |L_q(\eta_q)|\bar{v}J_{n_y} \\ \underline{x}_{k+1} = (A_q(\eta_q) - L_q(\eta_q)C) \underline{x}_k + B_q(\eta_q)u_k + \underline{w}_q + L_q(\eta_q)y_k - |L_q(\eta_q)|\bar{v}J_{n_y} \end{cases}, q \in \mathcal{I} \quad (3.37)$$

is a framer for the system (3.36) such that $\underline{x}_k \leq x_k \leq \bar{x}_k$. The observer gain $L_q(\eta_q)$ has an affine form given by:

$$L_q(\eta_q) = L_{q0} + \eta_{q1}L_{q1} + \dots + \eta_{qr}L_{qr}, \quad (3.38)$$

and $L_{qj} \in \mathbb{R}^{n_x \times n_y}, j = 0, 1, \dots, r$, are constant matrices.

Proof. Let $\bar{e}_k = \bar{x}_k - x_k$ and $\underline{e}_k = x_k - \underline{x}_k$ be the upper and the lower estimation errors. From (3.36), (3.37) and (3.9), the dynamics of the estimation errors are given by:

$$\begin{aligned} \bar{e}_{k+1} = \bar{x}_{k+1} - x_{k+1} &= \sum_{i=1}^g \lambda_i \left(A_q(\eta_q^{(i)}) - L_q(\eta_q^{(i)})C \right) \bar{e}_k + \bar{\chi}_q \\ \underline{e}_{k+1} = x_{k+1} - \underline{x}_{k+1} &= \sum_{i=1}^g \lambda_i \left(A_q(\eta_q^{(i)}) - L_q(\eta_q^{(i)})C \right) \underline{e}_k + \underline{\chi}_q. \end{aligned} \quad (3.39)$$

The inputs $\bar{\chi}_q$ and $\underline{\chi}_q$ defined in (3.11) are nonnegative according to Assumption 11. Based on (3.9), the nonnegativity of $(A_q(\eta_q) - L_q(\eta_q)C)$ is equivalent to show that all matrices $A_q(\eta_q^{(i)}) - L_q(\eta_q^{(i)})C$, for $i = 1, \dots, g$, are nonnegative. In addition, from Assumption 15, the dynamics of the upper and lower errors are nonnegative. According to the nonnegativity definition, we have $\underline{x}_k \leq x_k \leq \bar{x}_k$ provided that $\underline{x}_0 \leq x_0 \leq \bar{x}_0$. \square

3.3.2.2 Interval errors convergence

The requirement of a CQLF remains a restrictive condition to introduce ISS conditions. Consequently, for the sake of less conservative conditions, MQLF is adopted for a class of discrete-time LPV switched systems with an ADT switching signal. ISS conditions are developed in Theorem 10 and given in terms of LMIs based on the following Lemma.

Lemma 8. [189] Consider the switched system (3.36), and let $0 < \alpha < 1$, $\mu > 1$. Suppose that there exist $V_{\sigma_k} : \mathbb{R}^n \rightarrow \mathbb{R}$ and two \mathcal{K}_∞ functions α_1 and α_2 such that for each $\sigma_k = q, q \neq l$, the following conditions hold:

$$\alpha_1(\|x_k\|) \leq V_q(x_k) \leq \alpha_2(\|x_k\|), \quad (3.40)$$

$$\Delta V_q(x_k) \leq -\alpha V_q(x_k), \quad (3.41)$$

$$V_q(x_k) \leq \mu V_l(x_k), \quad (3.42)$$

then, the system (3.36) is ISS for any switching signal with an ADT τ_a satisfying

$$\tau_a \geq \tau_a^* = -\frac{\ln(\mu)}{\ln(1-\alpha)}, \quad (3.43)$$

where τ_a^* is the lower bound of τ_a determined by both parameters α and μ .

Theorem 10. Consider the discrete-time LPV switched system (3.36), where $A_q(\eta_q)$ and $B_q(\eta_q)$ are affine matrices on η_q . Suppose that there exist piecewise Lyapunov functions $V_{\sigma_k}(\bar{e}_k)$ and $V_{\sigma_k}(\underline{e}_k)$ where $V_q(\bar{e}_k) = \bar{e}_k^T P_q \bar{e}_k$ and $V_q(\underline{e}_k) = \underline{e}_k^T P_q \underline{e}_k$. Assume that there exist $P_q \in \mathbb{R}^{n_x \times n_x}$, $P_q = P_q^T \succ 0$, constant matrices Q_{q0}, \dots, Q_{qr} , W_l , $\alpha_2 > \alpha_1 > 0$, $\gamma > 0$ for given $0 < \alpha < 1$ and $0 \leq \beta \leq 1$ such that for all $q, l \in \mathcal{I}, q \neq l, \forall \eta_q^{(i)}$ the vertices of E_q , $i = 1, \dots, g$:

$$\min_{P_q, Q_q} \beta\mu + (1-\beta)\gamma, \quad (3.44)$$

$$\alpha_1 I_{n_x} \leq P_q \leq \alpha_2 I_{n_x}, \quad (3.45)$$

$$\begin{bmatrix} -(1-\alpha)P_q & 0 & A_q(\eta_q^{(i)})^T P_q - C^T Q_q(\eta_q^{(i)})^T \\ (*) & -\gamma^2 I_{n_x} & P_q \\ (*) & (*) & -P_q \end{bmatrix} \preceq 0, \quad (3.46)$$

$$\begin{bmatrix} W_l & P_q \\ P_q & P_q \end{bmatrix} \succeq 0, \quad (3.47)$$

hold, where $Q_q(\eta_q^{(i)})$ are affine matrices of $\eta_q^{(i)}$, $i = 1, \dots, g$, given by:

$$Q_q(\eta_q^{(i)}) = Q_{q0} + \eta_{q1}^{(i)} Q_{q1} + \dots + \eta_{qr}^{(i)} Q_{qr}, \quad (3.48)$$

and the observer gains $L_{qj}, j = 0, 1, \dots, r$ are obtained as:

$$L_{qj} = P_q^{-1} Q_{qj}. \quad (3.49)$$

Then, the interval error is input to state stable for any switching signal with an ADT τ_a satisfying:

$$\tau_a \geq \tau_a^* = -\frac{\ln(\mu)}{\ln(1-\alpha)}, \quad (3.50)$$

and

$$\begin{aligned} \lim_{k \rightarrow \infty} \|\bar{e}_k\| &< \frac{\gamma^2}{\alpha_1 \alpha} \bar{\chi}^2 \\ \lim_{k \rightarrow \infty} \|\underline{e}_k\| &< \frac{\gamma^2}{\alpha_1 \alpha} \bar{\chi}'^2, \end{aligned}$$

where $\bar{\chi}$ and $\bar{\chi}'$ are the upper bound of $\bar{\chi}_q$ and $\underline{\chi}$.

Proof. Based on (3.39), the increment of the MQLF yields

$$\begin{aligned}\Delta V_q(\bar{e}_k) &= V_q(\bar{e}_{k+1}) - V_q(\bar{e}_k) \\ &= \bar{e}_k^T \left((A_q(\eta_q) - L_q(\eta_q)C)^T P_q (A_q(\eta_q) - L_q(\eta_q)C) - P_q \right) \bar{e}_k + \\ &\quad \bar{e}_k^T (A_q(\eta_q) - L_q(\eta_q)C)^T P_q \bar{\chi}_q + \bar{\chi}_q^T P_q (A_q(\eta_q) - L_q(\eta_q)C) \bar{e}_k + \bar{\chi}_q^T P_q \bar{\chi}_q.\end{aligned}$$

By adding and subtracting the terms $\alpha \bar{e}_k^T P_q \bar{e}_k$ and $-\gamma^2 \bar{\chi}_q^T \bar{\chi}_q$ we obtain that

$$\begin{aligned}\Delta V_q(\bar{e}_k) &= \bar{e}_k^T \left((A_q(\eta_q) - L_q(\eta_q)C)^T P_q (A_q(\eta_q) - L_q(\eta_q)C) - (1 - \alpha)P_q \right) \bar{e}_k + \\ &\quad \bar{e}_k^T (A_q(\eta_q) - L_q(\eta_q)C)^T P_q \bar{\chi}_q + \bar{\chi}_q^T P_q (A_q(\eta_q) - L_q(\eta_q)C) \bar{e}_k + \bar{\chi}_q^T P_q \bar{\chi}_q - \\ &\quad \alpha \bar{e}_k^T P_q \bar{e}_k - \gamma^2 \bar{\chi}_q^T \bar{\chi}_q + \gamma^2 \bar{\chi}_q^T \bar{\chi}_q \\ \Delta V_q(\bar{e}_k) &= \sum_{i=1}^g \lambda_i [\bar{e}_k^T \quad \bar{\chi}_q^T] \Theta_q^{(i)} [\bar{e}_k \quad \bar{\chi}_q] - \alpha \bar{e}_k^T P_q \bar{e}_k + \gamma^2 \bar{\chi}_q^T(k) \bar{\chi}_q(k)\end{aligned}\tag{3.51}$$

where

$$\Theta_q^{(i)} = \begin{bmatrix} \tilde{A}^T P_q \tilde{A} - (1 - \alpha)P_q & \tilde{A}^T P_q \\ P_q \tilde{A} & P_q - \gamma^2 I_{n_x} \end{bmatrix}\tag{3.52}$$

with $\tilde{A} = (A_q(\eta_q^{(i)} - L_q(\eta_q^{(i)}C))$. Same arguments can be used to prove that:

$$\Delta V_q(\underline{e}_k) = \sum_{i=1}^g \lambda_i [\underline{e}_k^T \quad \underline{\chi}_q^T] \Theta_q^{(i)} [\underline{e}_k \quad \underline{\chi}_q] - \alpha \underline{e}_k^T P_q \underline{e}_k + \gamma^2 \underline{\chi}_q^T(k) \underline{\chi}_q(k)$$

(3.52) can be rewritten as

$$\Theta_q^{(i)} = \begin{bmatrix} -(1 - \alpha)P_q & 0 \\ 0 & -\gamma^2 I_{n_x} \end{bmatrix} + \begin{bmatrix} \tilde{A}^T P_q \\ P_q \end{bmatrix} P_q^{-1} \begin{bmatrix} P_q \tilde{A} & P_q \end{bmatrix}.\tag{3.53}$$

Based on the Schur complement, the following inequality is equivalent to (3.46)

$$\begin{bmatrix} -(1 - \alpha)P_q & 0 & \tilde{A}^T P_q \\ 0 & -\gamma^2 I_{n_x} & P_q \\ P_q \tilde{A} & P_q & -P_q \end{bmatrix} \preceq 0.\tag{3.54}$$

Then, if (3.41) holds, we can get

$$\begin{aligned}\Delta V_q(\bar{e}_k) &< -\alpha \bar{e}_k^T P_q \bar{e}_k + \gamma^2 \|\bar{\chi}_q(k)\|^2 \\ \Delta V_q(\underline{e}_k) &< -\alpha \underline{e}_k^T P_q \underline{e}_k + \gamma^2 \|\underline{\chi}_q(k)\|^2\end{aligned}\tag{3.55}$$

Evaluating (3.55) over the interval $[k_0, k)$, we obtain

$$\begin{aligned}V_q(\bar{e}_k) &\leq (1 - \alpha)^{k-k_0} V_q(\bar{e}_{k_0}) + \gamma^2 \sum_{m=0}^{k-k_0-1} (1 - \alpha)^m \|\bar{\chi}_q(k)\|^2 \\ V_q(\underline{e}_k) &\leq (1 - \alpha)^{k-k_0} V_q(\underline{e}_{k_0}) + \gamma^2 \sum_{m=0}^{k-k_0-1} (1 - \alpha)^m \|\underline{\chi}_q(k)\|^2.\end{aligned}\tag{3.56}$$

Based on (3.40), the following inequalities

$$\begin{aligned}\alpha_1(\|\bar{e}_k\|) &\leq V_q(\bar{e}_k) \\ \alpha_1(\|\underline{e}_k\|) &\leq V_q(\underline{e}_k)\end{aligned}$$

allow one to deduce that

$$\begin{aligned}\|\bar{e}_k\| &\leq \frac{1}{\alpha_1}((1-\alpha)^{k-k_0}V_q(\bar{e}_{k_0}) + \gamma^2 \sum_{m=0}^{k-k_0-1} (1-\alpha)^m \|\bar{\chi}_q\|_\infty^2) \\ \|\underline{e}_k\| &\leq \frac{1}{\alpha_1}((1-\alpha)^{k-k_0}V_q(\underline{e}_{k_0}) + \gamma^2 \sum_{m=0}^{k-k_0-1} (1-\alpha)^m \|\underline{\chi}_q\|_\infty^2)\end{aligned}$$

The state disturbances and measurement noise w_q and v are bounded, then when $k \rightarrow \infty$, $\bar{\chi}_q$ and $\underline{\chi}_q$ are also bounded, *i.e.* $\|\bar{\chi}_q\|_\infty \leq \bar{\chi}$ and $\|\underline{\chi}_q\|_\infty \leq \bar{\chi}'$ which implies that:

$$\begin{aligned}\lim_{k \rightarrow \infty} \|\bar{e}_k\| &< \frac{\gamma^2}{\alpha_1 \alpha} \bar{\chi}^2 \\ \lim_{k \rightarrow \infty} \|\underline{e}_k\| &< \frac{\gamma^2}{\alpha_1 \alpha} \bar{\chi}'^2.\end{aligned}$$

It should be stressed that the interval errors width are upper bounded by $\frac{\gamma^2}{\alpha_1 \alpha} \bar{\chi}^2$ and $\frac{\gamma^2}{\alpha_1 \alpha} \bar{\chi}'^2$ which should be reduced to improve the robustness of the proposed observer. Therefore, the problem of minimizing the upper bound of the interval error is reduced to the minimization of γ for given α_1 and α . In addition, we aim also to minimize μ to look for an optimum dwell time. The optimum solution can be obtained by solving a problem of linear optimization (3.44).

Similar to the continuous-time instants case, the stability at the switching instants, under an arbitrary switching signal, is reduced to the feasibility of the LMI in (3.47). Accordingly, the ISS of the observer (3.37) is ensured [189]. \square

Remark 8. *Similar to the continuous time case, it is noteworthy that in discrete time instants, the time-varying parameters have been incorporated in the proposed interval observer and the nonnegativity and convergence design conditions have been expressed on the vertices of polytopes and based on MQLF in order to reduce the conservatism and provide a tight interval error.*

3.3.3 Numerical example

In this section, a numerical example with simulation results is considered to demonstrate the effectiveness of the proposed state estimation method for the discrete-time LPV switched system (3.36) defined with three subsystems, $N = 3$, with:

$$\begin{aligned}A_{10} &= \begin{pmatrix} 0.015 & 0.035 \\ 0.015 & 0.045 \end{pmatrix} & A_{11} &= \begin{pmatrix} 0.025 & 0.025 \\ 0.015 & 0.06 \end{pmatrix} & A_{12} &= \begin{pmatrix} 0.035 & 0.015 \\ 0.05 & 0.075 \end{pmatrix} \\ B_{10} &= \begin{pmatrix} -1 & 1 \\ 1 & 1 \end{pmatrix} & B_{11} &= \begin{pmatrix} 2 & 2.5 \\ 1.5 & 0.5 \end{pmatrix} & B_{12} &= \begin{pmatrix} 2 & 2 \\ 3 & 2 \end{pmatrix} \\ A_{20} &= \begin{pmatrix} 0.025 & 0.055 \\ 0.005 & 0.045 \end{pmatrix} & A_{21} &= \begin{pmatrix} 0.045 & 0.05 \\ 0.04 & 0.05 \end{pmatrix} & A_{22} &= \begin{pmatrix} 0.03 & 0.04 \\ 0.035 & 0.01 \end{pmatrix}\end{aligned}$$

$$\begin{aligned}
B_{20} &= \begin{pmatrix} -1 & 2 \\ 1.5 & 0 \end{pmatrix} & B_{21} &= \begin{pmatrix} 1.5 & 2 \\ 1.5 & 0.5 \end{pmatrix} & B_{22} &= \begin{pmatrix} 2 & 2 \\ 3 & 1 \end{pmatrix} \\
A_{30} &= \begin{pmatrix} 0.025 & 0.045 \\ 0.005 & 0.065 \end{pmatrix} & A_{31} &= \begin{pmatrix} 0.025 & 0.051 \\ 0.043 & 0.057 \end{pmatrix} & A_{32} &= \begin{pmatrix} 0.032 & 0.008 \\ 0.014 & 0.005 \end{pmatrix} \\
B_{30} &= \begin{pmatrix} -2 & 1.5 \\ 1 & 0 \end{pmatrix} & B_{31} &= \begin{pmatrix} 1 & 2.5 \\ 1.5 & 0.75 \end{pmatrix} & B_{32} &= \begin{pmatrix} 1 & 3 \\ 3 & 1 \end{pmatrix} \\
C &= \begin{pmatrix} 1 & -1 \end{pmatrix}
\end{aligned}$$

For the simulation, the state disturbances w_q are chosen such as:

$$\begin{aligned}
w_1(t) &= [0.005, 0.009]^T \cos(5t), \\
w_2(t) &= [0.001, 0.002]^T \cos(2t), \\
w_3(t) &= [0.004, 0.007]^T \cos(3t).
\end{aligned}$$

The measurement noise v is a uniformly distributed signal bounded by $\bar{v} = 0.5$. The state initial conditions are set as $x(0) = [0, 0]^T$, $\underline{x}_0 = [-2, -2]^T$ and $\bar{x}_0 = [2, 2]^T$. The measured time varying parameters η_q for $q = 1, 2, 3$ are defined by:

$$\begin{aligned}
\eta_1(t) &= \begin{pmatrix} 0.5(|\sin(0.1k)| + 1) \\ 0.5(|\cos(0.1k)| + 1) \end{pmatrix} & \eta_2(t) &= \begin{pmatrix} 1.5|\sin(0.1k)| + 0.5 \\ 1.5|\cos(0.1k)| + 0.5 \end{pmatrix} \\
\eta_3(t) &= \begin{pmatrix} 2.5|\cos(0.1k)| + 0.5 \\ 2.5|\sin(0.1k)| + 0.5 \end{pmatrix}
\end{aligned}$$

The LMIs are solved using the Matlab Yalmip package in combination with the solver Sedumi. The parameters $\alpha = 0.9$ and $\alpha_1 = 2$ are chosen to solve the optimization problem in Theorem 10. The following Lyapunov matrices are obtained:

$$\begin{aligned}
P_1 &= \begin{pmatrix} 2.71 & 0 \\ 0 & 2.43 \end{pmatrix} & P_2 &= \begin{pmatrix} 2 & 0 \\ 0 & 2 \end{pmatrix} \\
P_3 &= \begin{pmatrix} 2.48 & 0 \\ 0 & 2.58 \end{pmatrix}
\end{aligned}$$

Then, $\mu = 2$ is obtained which implies an ADT $\tau_a > 0.301$. Solving the LMIs in Theorem 10 gives an optimal value of γ equal to 2.12 and a set of observer gains defined in (3.49):

$$\begin{aligned}
L_{10} &= \begin{pmatrix} -0.0035 & 0 \end{pmatrix}^T, & L_{11} &= \begin{pmatrix} 0 & 0 \end{pmatrix}^T, & L_{12} &= \begin{pmatrix} 0 & -0.045 \end{pmatrix}^T \\
L_{20} &= \begin{pmatrix} -0.0263 & 0 \end{pmatrix}^T, & L_{21} &= \begin{pmatrix} 0 & 0 \end{pmatrix}^T, & L_{22} &= \begin{pmatrix} 0 & 0.013 \end{pmatrix}^T \\
L_{30} &= \begin{pmatrix} 0.0118 & 0 \end{pmatrix}^T, & L_{31} &= \begin{pmatrix} 0 & 0 \end{pmatrix}^T, & L_{32} &= \begin{pmatrix} 0 & -0.01 \end{pmatrix}^T
\end{aligned}$$

The switching law of the discrete-time LPV switched system is presented in Fig. 3.12.

Figures 3.13-3.14 show the switched interval observer estimation for the states x_1 and x_2 .

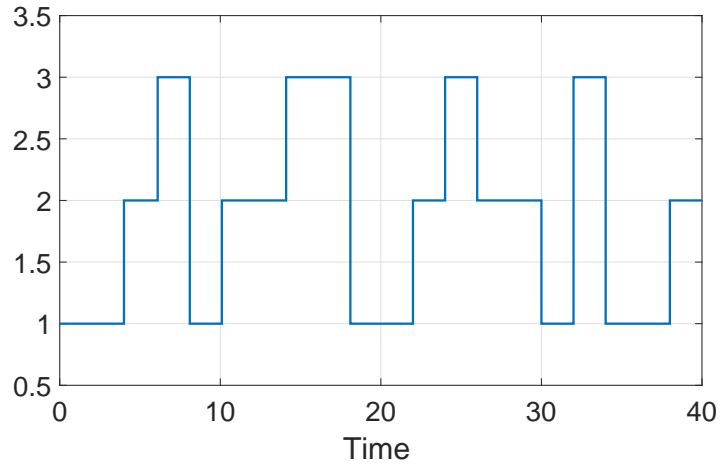


Figure 3.12: Evolution of the switching signal.

The simulation shows the effectiveness of such observer to estimate guaranteed bounds of the state vector and it is pointed out that the state x satisfies the inclusion $\underline{x} \leq x \leq \bar{x}$.

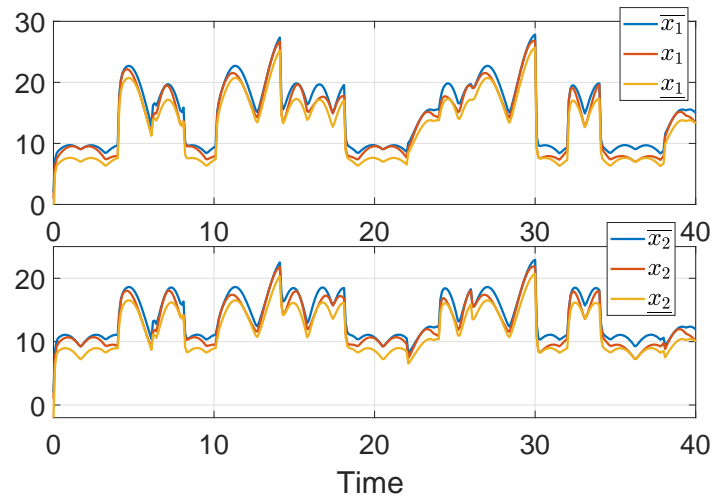


Figure 3.13: Evolutions of the state x and the estimated upper and lower bounds.

The results in Fig. 3.15 show that the errors \underline{e} and \bar{e} stay bounded and positive.

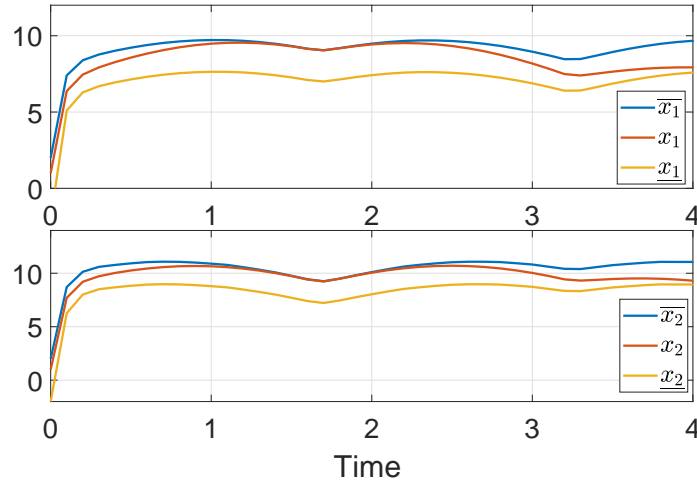


Figure 3.14: Evolutions of the state x and the estimated upper and lower bounds (ZOOM).

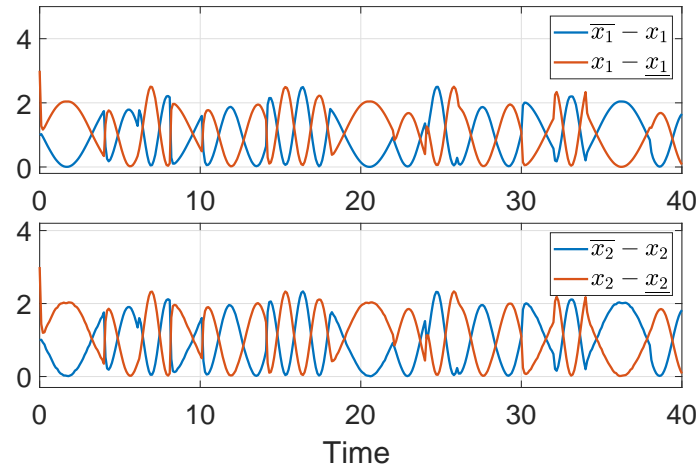


Figure 3.15: Evolutions of the estimation errors.

3.4 Conclusion

In this chapter, an interval state estimation method has been presented for both continuous and discrete-time LPV switched systems subject to measured time-varying parameters. The designed technique is investigated using a polytopic modeling framework to provide a finite dimensional relaxation for the design conditions of the proposed interval observer for a large class of switched systems. In a first part, the design of an interval observer for continuous-time LPV switched systems is developed. New cooperativity and ISS conditions are derived and expressed on the vertices of each polytope based on Common and Multiple Quadratic Lyapunov Functions. In the second part, the discrete case is considered. Simulation results are presented to highlight the effectiveness of the proposed approaches. For both parts, the switching signal is assumed to be known among system modes. However, for most practical systems, the discrete low is usually unknown.

In the next chapter, a more challenging state estimation scenario involving an unknown switching signal is considered for switched linear systems subject to unknown but bounded state disturbances.

Chapter 4

Interval estimation for asynchronous switched systems

4.1 Introduction

The problem of continuous state estimation has been widely investigated when the switching signal is assumed to be known. However, for most actual industrial systems, the switching sequence is often unknown and difficult to obtain. One of the ways to solve this problem is to reconstruct the switching law, which makes the discrete state estimation of the switched system particularly important. This motivates the present chapter which discusses the estimation problem of the switching signal for a class of switched linear systems. In the literature, the estimation of the discrete state for switched systems is barely considered. In [66], based on the output measurement and a high-order sliding modes observer, an estimation technique of the continuous and discrete states is investigated for a nonlinear switched systems. In [68], a parameter identification is proposed to estimate the continuous and discrete states of switched LPV systems. In the above works, the reconstruction of the discrete state is reported by considering the measurements of the output and input. However, the presence of unknown inputs can not be avoided, which can bring a certain difficulty to the active mode estimation. In this work, the discrete state estimation problem is tackled for switched linear systems with unknown input and when the continuous state is assumed to be unknown. Generally, when unknown inputs are presented, the state estimation issue can be solved using the decoupling approach such that the estimation error dynamics in the transformed state coordinates is not affected by the unknown inputs [58], [67]. Without using decoupling techniques, a new approach is proposed in this chapter by combining a sliding modes observer with an interval observer in order to estimate the discrete mode of the switched linear systems, based on distinguishability conditions of the current mode.

The combination of both observers is one of the main contributions of this chapter. In fact, the sliding modes technique provides a robust finite-time convergence. Meanwhile, only bounds of the unknown input are needed when the interval approach is used.

In the first part, the considered class of switched linear systems is introduced under some mild assumptions. The interval observer design is presented in the second part. Then, details about discrete state and switching time instants estimation are given. In this part, based on sliding modes theory, a discrete state observer allowing the estimation of the current mode, in finite time, is proposed. Moreover, based on H_∞ performances and interval observer theory, residuals are defined to quickly detect the discrete state change. The attenuation condition of the disturbance and sensitivity condition of residuals are formulated in terms of LMI conditions. Finally, the feasibility and efficiency of the proposed approach are illustrated by simulations in the last part.

The results presented in this chapter has led to the publication of the communication [190] in the international Conference on Decision and Control.

4.2 System description

Consider a switched linear system described by:

$$\begin{cases} \dot{x}(t) &= A_{\sigma(t)}x(t) + B_{\sigma(t)}u(t) + w(t) \\ y(t) &= Cx(t), \end{cases} \quad (4.1)$$

$x(t) \in \mathbb{R}^{n_x}$ is the continuous state of the system, $y(t) \in \mathbb{R}^{n_y}$ is the output and $w(t) \in \mathbb{R}^{n_x}$ is an unknown input which is assumed to be bounded. The switched linear system is defined by N subsystems. The switching signal $\sigma(t) : \mathbb{R} \rightarrow \mathcal{I} = \{1, 2, \dots, N\}$ allows one to select the active subsystem $q = \sigma(t)$ in continuous time. t_k represents the switching time instants for $k \in \mathbb{Z}_+$. In this approach, the discrete mode q and the continuous state x are assumed to be unknown.

The objective is to design an observer in order to obtain an estimation in finite time of the switching signal $\sigma(t)$ of the system (4.1) in spite of the unknown inputs $w(t)$.

Remark 9. *In this chapter, the measurement noise is not considered since the sliding modes observer provides only a robust finite-time convergence in the presence of state disturbances. Luenberger observers can be used when considering the measurement noise, however, additional optimization performances are required to improve the accuracy of the estimation problem.*

The following assumption is required.

Assumption 16. *It is assumed that:*

- *The pairs (A_q, C) are detectable $\forall q = 1, \dots, N$.*
- *The input u , the continuous state x and the unknown input are assumed to be bounded by known values:*

$$\underline{X} \leq x(t) \leq \overline{X}, \quad |w(t)| \leq \overline{w}. \quad (4.2)$$

- The first time-derivatives of u and w are upper-bounded by known positive constants.
- The system (4.1) satisfies the minimal dwell time condition defined in Chapter 2.

The second and third points in Assumption 16 are not restrictive since in practice, the variables of the system stay bounded and the upper-bounds of time-derivatives can be determined with conservative values. Assumption 16 is needed to design the proposed scheme based on sliding modes observers combined with the interval approach.

4.3 Interval observer design for switched systems

In this section, an interval approach where only bounds of the unknown input are needed is designed to estimate the switching signal $\sigma(t)$ and switching time instants t_k for a class of switched linear systems with unknown input. Based on the evolution of the residual signals, the stability and the positivity conditions of the proposed interval observer, the discrete state change can be detected.

4.3.1 Interval observer structure

The stack of N interval observers, associated to different subsystems, is firstly proposed $\forall i = 1, \dots, N$ in Fig. 4.1:

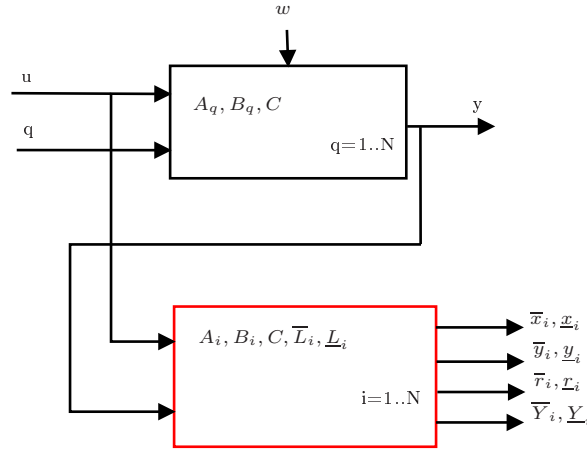


Figure 4.1: A stack of interval observers.

The signals $\bar{x}_i, \underline{x}_i \in \mathbb{R}^{n_x}$ are respectively the upper and the lower bounds of the state x . $\bar{y}_i, \underline{y}_i \in \mathbb{R}^{n_y}$ are the bounds of the output signal y . $\bar{r}_i, \underline{r}_i \in \mathbb{R}^{n_y}$ are the upper and lower residuals. $\bar{Y}_i, \underline{Y}_i \in \mathbb{R}^{n_y}$. $\bar{L}_i, \underline{L}_i \in \mathbb{R}^{n_x \times n_y}$ for $i = 1, \dots, N$ are the observer gains. These signals are given as follows $\forall i = 1, \dots, N$:

$$\left\{ \begin{array}{l} \dot{\bar{x}}_i(t) = (A_i - \bar{L}_i C)\bar{x}_i(t) + B_i u(t) + \bar{L}_i y(t) + \bar{w} \\ \dot{\underline{x}}_i(t) = (A_i - \underline{L}_i C)\underline{x}_i(t) + B_i u(t) + \underline{L}_i y(t) - \bar{w} \\ \bar{y}_i(t) = C^+ \bar{x}_i(t) - C^- \underline{x}_i(t) \\ \underline{y}_i(t) = C^+ \underline{x}_i(t) - C^- \bar{x}_i(t) \\ \bar{r}_i(t) = \bar{y}_i(t) - y(t) \\ \underline{r}_i(t) = \underline{y}_i(t) - y(t) \\ \bar{Y}_i(t) = C \bar{x}_i(t) \\ \underline{Y}_i(t) = C \underline{x}_i(t) \end{array} \right. \quad (4.3)$$

The stack of interval observers provides N possible intervals on the continuous state x . The output signals \underline{Y}_i and \bar{Y}_i are considered to identify the actual discrete mode of the switched linear system (4.1).

Using the proposed interval observer (4.3), the goal is to estimate the discrete mode q of the switched linear system (4.1) and the switching time instants t_k . Based on the evolution of the residuals r_i , the proposed interval observer (4.3) is designed to detect the discrete state change.

For this purpose, let us define the errors $\bar{e}_i = \bar{x}_i - x$ and $\underline{e}_i = x - \underline{x}_i$. The error dynamics are given by:

$$\left\{ \begin{array}{l} \dot{\bar{e}}_i(t) = (A_i - \bar{L}_i C)\bar{e}_i(t) + \chi_i(t) + \bar{w} - w(t) \\ \dot{\underline{e}}_i(t) = (A_i - \underline{L}_i C)\underline{e}_i(t) - \chi_i(t) + \bar{w} + w(t), \end{array} \right. \quad (4.4)$$

where

$$\chi_i(t) = (A_i - A_q)x(t) + (B_i - B_q)u(t). \quad (4.5)$$

In fact, the upper error dynamics can be written:

$$\begin{aligned} \dot{\bar{e}}_i(t) &= \dot{\bar{x}}_i - \dot{x} \\ &= (A_i - \bar{L}_i C)\bar{x}_i + B_i u + \bar{L}_i y + \bar{w} - A_q x - B_q u - w \\ &= (A_i - \bar{L}_i C)\bar{x}_i - A_q x + \bar{L}_i C x + B_i u - B_q u + \bar{w} - w. \end{aligned}$$

By adding and subtracting the following term $A_i x$ previous equation becomes:

$$\begin{aligned} \dot{\bar{e}}_i(t) &= (A_i - \bar{L}_i C)\bar{x}_i - A_i x + \bar{L}_i C x + A_i x - A_q x + B_i u - B_q u + \bar{w} - w \\ &= (A_i - \bar{L}_i C)\bar{e}_i + (A_i - A_q)x + (B_i - B_q)u + \bar{w} - w. \end{aligned}$$

Similarly, we have:

$$\begin{aligned} \dot{\underline{e}}_i(t) &= \dot{x} - \dot{\underline{x}}_i \\ &= A_q x + B_q u + w - (A_i - \underline{L}_i C)\underline{x}_i - B_i u - \underline{L}_i y + \bar{w} \\ &= A_q x - A_i x + A_i x - \underline{L}_i C x - (A_i - \underline{L}_i C)\underline{x}_i + B_q u - B_i u + \bar{w} + w \\ &= (A_i - \underline{L}_i C)\underline{e}_i - (A_i - A_q)x - (B_i - B_q)u + \bar{w} + w. \end{aligned}$$

In the following subsection, a state augmentation approach is proposed to achieve an estimation of the switching time instants.

4.3.2 Problem formulation

In order to estimate the switching signal, the augmented state is defined as:

$$\zeta_i = \begin{pmatrix} \bar{e}_i \\ \underline{e}_i \end{pmatrix}, \quad r_i = \begin{pmatrix} \bar{r}_i \\ \underline{r}_i \end{pmatrix}.$$

The following augmented system can be deduced:

$$\begin{cases} \dot{\zeta}_i(t) &= \mathcal{A}_i \zeta_i(t) + \mathcal{W}(t) + \mathcal{F} \chi_i(t) \\ r_i(t) &= \mathcal{C} \zeta_i(t), \end{cases} \quad (4.6)$$

where

$$\mathcal{A}_i = \begin{pmatrix} (A_i - \bar{L}_i C) & 0 \\ 0 & (A_i - \underline{L}_i C) \end{pmatrix}, \quad \mathcal{W}(t) = \begin{pmatrix} \bar{w} - w(t) \\ \bar{w} + w(t) \end{pmatrix}, \quad \mathcal{F} = \begin{pmatrix} I_n \\ -I_n \end{pmatrix}$$

$$\mathcal{C} = \begin{pmatrix} C^+ & C^- \\ -C^- & -C^+ \end{pmatrix}$$

From representation (4.6), it is clear that $\mathcal{W}(t) \geq 0$ and if $i = q$ the vectors χ_i is null. Based on the idea that the matrices \mathcal{A}_i are stable and Metzler and the bounds \bar{x}_i and \underline{x}_i at each instant t_k can be reset such that $\zeta_i(t_k) \geq 0$, for $k = 0, 1, 2, \dots$, if $i = q$ ($\chi_i = 0$) for $t \in [t_k, t_{k+1})$, one can obtain the following relations:

$$\begin{cases} \zeta_i(t) \geq 0 \\ \underline{x}_i(t) \leq x(t) \leq \bar{x}_i(t) \\ \underline{y}_i(t) \leq y(t) \leq \bar{y}_i(t) \\ 0 \in [\underline{r}_i, \bar{r}_i]. \end{cases}$$

The last relation is deduced from the following inclusion

$$y(t) \in [\underline{y}_i(t), \bar{y}_i(t)]. \quad (4.7)$$

In fact, when $i = q$, the measured output signal $y(t)$ is consistent with the estimation of the proposed interval observer. Thus, based on (4.7), we have

$$\begin{cases} 0 \in [\underline{y}_i(t), \bar{y}_i(t)] - y(t) \\ \Rightarrow 0 \in [\underline{y}_i(t) - y(t), \bar{y}_i(t) - y(t)] \\ \Rightarrow 0 \in [\underline{r}_i, \bar{r}_i]. \end{cases}$$

Based on the evolution of the residuals r_i , the proposed interval observer (4.3) is designed to detect the discrete state change. An estimation of the switching time instants t_k is then provided. For the considered class of switched linear systems, the problem of the switching time instant estimation can be formulated such that:

- (i) \mathcal{A}_i for $i = 1, \dots, N$ are stable and Metzler.
- (ii) The L_2 norm of the operator from \mathcal{W}_i to $r_i(t)$ is less than γ under $\chi_i(t) = 0$

$$\sup_{\mathcal{W}_i \neq 0} \frac{\|r_i(t)\|}{\|\mathcal{W}_i\|} < \gamma^{1/2}. \quad (4.8)$$

- (iii) The L_2 norm of the operator from $\chi_i(t)$ to $r_i(t) - J\chi_i(t)$ is less than β under $\mathcal{W}_i = 0$

$$\sup_{\chi_i \neq 0} \frac{\|r_i(t) - J\chi_i(t)\|}{\|\chi_i(t)\|} < \beta^{1/2}, \quad (4.9)$$

where $J = [J_1^T, J_2^T]^T \in \mathbb{R}^{2n_y \times n_x}$ is a weighting matrix.

Specification (i) ensures the stability and the positivity of the interval observer when $i = q$. The robustness of residuals r_i against the unknown input $w(t)$ is specified in (ii). Specification (iii) allows improving the sensibility of the residuals r_i to χ_i .

Remark 10. *It should be pointed out that the weighting matrix J is considered to maximize the effects of χ_i on r_i . Similar approaches have been investigated in the context of fault detection in order to improve the fault sensitivity specification [191], [121].*

4.4 Switching signal estimation

In this section, based on sliding modes theory, a discrete state observer providing in finite time an estimation \hat{q} of the current mode q of the switched linear system (4.1) is designed. Based on a decision logic on the evolution of the residual $r_{\hat{q}}$, an estimation \hat{t}_k of the switching time instants is developed. Based on H_∞ performance, details on the design of the proposed interval observer are given.

4.4.1 Discrete state estimation

The objective is to design a sliding modes observer in order to estimate in finite time the discrete mode of the switched linear system (4.1) in spite of the unknown input $w(t)$. In the following, an estimation method of the current mode is presented.

A stack of sliding modes observers, each one associated to a different mode of operation is proposed for $i = 1, \dots, N$.

$$\begin{cases} \dot{\bar{z}}_i(t) &= -C\bar{L}_i\bar{z}_i(t) + \bar{v}_i(t) \\ \dot{\underline{z}}_i(t) &= -C\underline{L}_i\underline{z}_i(t) + \underline{v}_i(t) \end{cases} \quad (4.10)$$

where \underline{v}_i and \bar{v}_i are the correction terms that are designed by the following expressions:

$$\begin{aligned} \bar{v}_i &= -k_1|\bar{z}_i - y + \bar{Y}_i|^{\frac{1}{2}}\text{sign}(\bar{z}_i - y + \bar{Y}_i) + \bar{v}_{i,1} \\ \dot{\bar{v}}_{i,1} &= -k_2\text{sign}(\bar{z}_i - y + \bar{Y}_i) \\ \underline{v}_i &= -k_1|\underline{z}_i - y + \underline{Y}_i|^{\frac{1}{2}}\text{sign}(\underline{z}_i - y + \underline{Y}_i) + \underline{v}_{i,1} \\ \dot{\underline{v}}_{i,1} &= -k_2\text{sign}(\underline{z}_i - y + \underline{Y}_i). \end{aligned} \quad (4.11)$$

Remark 11. *The stack of sliding modes observers is designed to provide a robust finite-time convergence of $\bar{Y}_i - y$ and $\underline{Y}_i - y$. \bar{z}_i and \underline{z}_i denote respectively the estimated signals of $\bar{Y}_i - y$ and $\underline{Y}_i - y$. The observer gains $C\bar{L}_i$ and $C\underline{L}_i$ are derived from the dynamics of $\bar{Y}_i - y$ and $\underline{Y}_i - y$.*

Assumption 17. *To guarantee the distinguishability of the current location, it is assumed that there are known positive constants δ_1 and δ_2 such that, for any $t \geq \delta_1$, $\forall i, j = 1, \dots, N$, $i \neq j$:*

$$\int_{t-\delta_1}^t \|\underline{\phi}_{i,j}(s)\| + \|\bar{\phi}_{i,j}(s)\| ds \geq \delta_2 \quad (4.12)$$

and

$$\int_{t-\delta_1}^t \|\underline{\phi}_{i,i}(s)\| + \|\bar{\phi}_{i,i}(s)\| ds < \delta_2 \quad (4.13)$$

where

$$\begin{aligned}\bar{\phi}_{i,j}(t) &= -C\bar{L}_i(\bar{z}_i(t) - y(t) + \bar{Y}_i(t)) + C(B_i - B_j)u(t) - CA_jx(t) + CA_i\bar{x}_i(t) \\ &\quad + C(\bar{w} - w(t)) \\ \underline{\phi}_{i,j}(t) &= -C\underline{L}_i(\underline{z}_i(t) - y(t) + \underline{Y}_i(t)) + C(B_i - B_j)u(t) - CA_jx(t) + CA_i\underline{x}_i(t) \\ &\quad + C(-\bar{w} - w(t)).\end{aligned}$$

The terms $\bar{\phi}_{i,j}(t)$ and $\underline{\phi}_{i,j}(t)$ involve both known and unknown terms. According to [67], δ_1 and δ_2 can be estimated if the unknown terms $\|\bar{\phi}_{i,j}(t)\|$ and $\|\underline{\phi}_{i,j}(t)\|$ are upper and lower bounded by known constants. In order to design an estimation logic of the discrete state, the terms $\bar{\phi}_{i,j}(t)$ and $\underline{\phi}_{i,j}(t)$ can be split into two parts such that:

$$\begin{aligned}a_1(t) &= C\bar{L}_i(\bar{z}_i(t) - y(t) + \bar{Y}_i(t)) + C(B_i - B_j)u(t) + CA_i\bar{x}_i(t) + C\bar{w} \\ b(t) &= CA_jx(t) + Cw(t) \\ a_2(t) &= C\underline{L}_i(\underline{z}_i(t) - y(t) + \underline{Y}_i(t)) + C(B_i - B_j)u(t) + CA_i\underline{x}_i(t) + C\bar{w} \\ b(t) &= CA_jx(t) + Cw(t),\end{aligned}$$

$b(t)$ contains unknown terms. According to Assumption 16, $b(t)$ can be bounded by a known positive constant Π_1 such that:

$$\|b(t)\| \leq \Pi_1. \quad (4.14)$$

In addition, it is assumed also that both $a_1(t)$ and $a_2(t)$ are bounded such that the following inequality holds:

$$\|a_1(t)\| + \|a_2(t)\| \leq \Pi_2. \quad (4.15)$$

Therefore the constants δ_1 and δ_2 can be chosen as follows to satisfy conditions in (4.12) and (4.13):

$$\begin{cases} \delta_1(\Pi_2 - \Pi_1) \geq \delta_2 \\ \delta_1\Pi_1 < \delta_2. \end{cases} \quad (4.16)$$

From Assumption 16, the terms $\underline{\phi}_{i,j}(t)$ and $\bar{\phi}_{i,j}(t)$ are bounded and smooth enough. Indeed, there is a known positive constant Γ such that: $\forall i, j = 1, \dots, N$:

$$\sup(\|\dot{\underline{\phi}}_{i,j}(t)\|, \|\dot{\bar{\phi}}_{i,j}(t)\|) \leq \Gamma, \quad \forall t \neq t_k. \quad (4.17)$$

Theorem 11. *Let us consider the system (4.1) satisfying Assumptions 16-17 and the observer (4.10), (4.11) where the gains satisfy:*

$$\begin{cases} k_1 > 0 \\ k_2 > 3\Gamma + 2\frac{\Gamma^2}{k_1^2} \end{cases} \quad (4.18)$$

The discrete state observer

$$\hat{q}(t) = \arg \min_i \int_{t-\delta_1}^t \|\underline{v}_{i,1}(s)\| + \|\bar{v}_{i,1}(s)\| ds \quad (4.19)$$

provides an estimation of $\sigma(t)$ in each interval $[t_{k-1} + T_1^, t_k)$, i.e.*

$$\hat{q}(t) = \sigma(t), \quad t_{k-1} + T_1^* \leq t < t_k, \quad k = 1, \dots, N \quad (4.20)$$

where $T_1^ < T_\delta$ and T_δ is the minimal dwell time.*

Proof. Based on the designed sliding modes observer, the goal is to provide a robust finite-time convergence of $\bar{Y} - y$ and $\underline{Y} - y$. To that end, let us define the upper output error:

$$\bar{e}_{z,i} = \bar{z}_i - y + \bar{Y}_i. \quad (4.21)$$

The error dynamics can be written as follows:

$$\begin{aligned} \dot{\bar{e}}_{z,i} &= \dot{\bar{z}}_i - \dot{y} + \dot{\bar{Y}}_i \\ &= -C\bar{L}_i\bar{z}_i + \bar{v}_i - CA_q x - CB_q u - Cw + C((A_i - \bar{L}_i C)\bar{x}_i(t) + B_i u(t) + \bar{L}_i y(t) + \bar{w}) \\ &= -C\bar{L}_i\bar{z}_i + \bar{v}_i - CA_q x - CB_q u - Cw + CA_i\bar{x}_i - CB_i u + C\bar{L}_i(y - \bar{Y}_i) + C\bar{w} \\ &= -C\bar{L}_i e_{z,i} - C(B_q + B_i)u - CA_q x + CA_i\bar{x}_i - Cw + C\bar{w} + \bar{v}_i \\ &= \bar{\phi}_{i,q} + \bar{v}_i. \end{aligned}$$

From the stack of sliding modes observers (4.10), the error dynamics can be rewritten as:

$$\dot{\bar{e}}_{z,i} = -k_1 |\bar{e}_{z,i}|^{\frac{1}{2}} \text{sign}(\bar{e}_{z,i}) + \bar{\phi}_{i,j} + \bar{v}_{i,1},$$

where j indicates the actual mode of the system. Let us set $\bar{v}_{i,2} = \bar{v}_{i,1} + \bar{\phi}_{i,j}$. From (4.10), one can deduce $\forall t \in [t_{k-1}, t_k)$

$$\begin{aligned} \dot{\bar{e}}_{z,i} &= -k_1 |\bar{e}_{z,i}|^{\frac{1}{2}} \text{sign}(\bar{e}_{z,i}) + \bar{v}_{i,2} \\ \dot{\bar{v}}_{i,2} &= \dot{\bar{\phi}}_{i,j} - k_2 \text{sign}(\bar{e}_{z,i}). \end{aligned} \quad (4.22)$$

The same development can be given for $\underline{e}_{z,i}$. According to the sliding modes theory, there is $T_1^* > 0$ such that $\forall t \in [t_{k-1} + T_1^*, t_k)$,

$$\|\underline{\mathcal{L}}_{i,2}\| \leq O(\tau), \quad \|\bar{v}_{i,2}\| \leq O(\tau),$$

where τ is the sampling interval. Notice that it is always possible to find observer gains satisfying the condition (4.18) with $T_1^* < T_\delta$. Therefore, one can conclude that:

$$\begin{aligned} \bar{v}_{i,1} &= -\bar{\phi}_{i,j} \\ \underline{\mathcal{L}}_{i,1} &= -\underline{\phi}_{i,j}. \end{aligned} \quad (4.23)$$

From Assumption 17, one gets

$$\begin{aligned} \int_{t-\delta_1}^t \|\underline{\mathcal{L}}_{i,1}(s)\| + \|\bar{v}_{i,1}(s)\| ds &\geq \delta_2 \quad \text{if } i \neq j \\ \int_{t-\delta_1}^t \|\underline{\mathcal{L}}_{i,1}(s)\| + \|\bar{v}_{i,1}(s)\| ds &< \delta_2 \quad \text{if } i = j. \end{aligned} \quad (4.24)$$

Hence, the estimation logic $\arg \min_i \int_{t-\delta_1}^t \|\underline{\mathcal{L}}_{i,1}(s)\| + \|\bar{v}_{i,1}(s)\| ds$ provides an exact estimation of the discrete state after a transient time T_1^* . \square

Remark 12. *The finite time convergence of the sliding modes observer (4.10) is ensured based on (4.18). For more details about the selection of the observer gains in order to satisfy the minimal dwell time the reader can refer to [192].*

The following block diagram is presented to summarize the proposed discrete state observer.

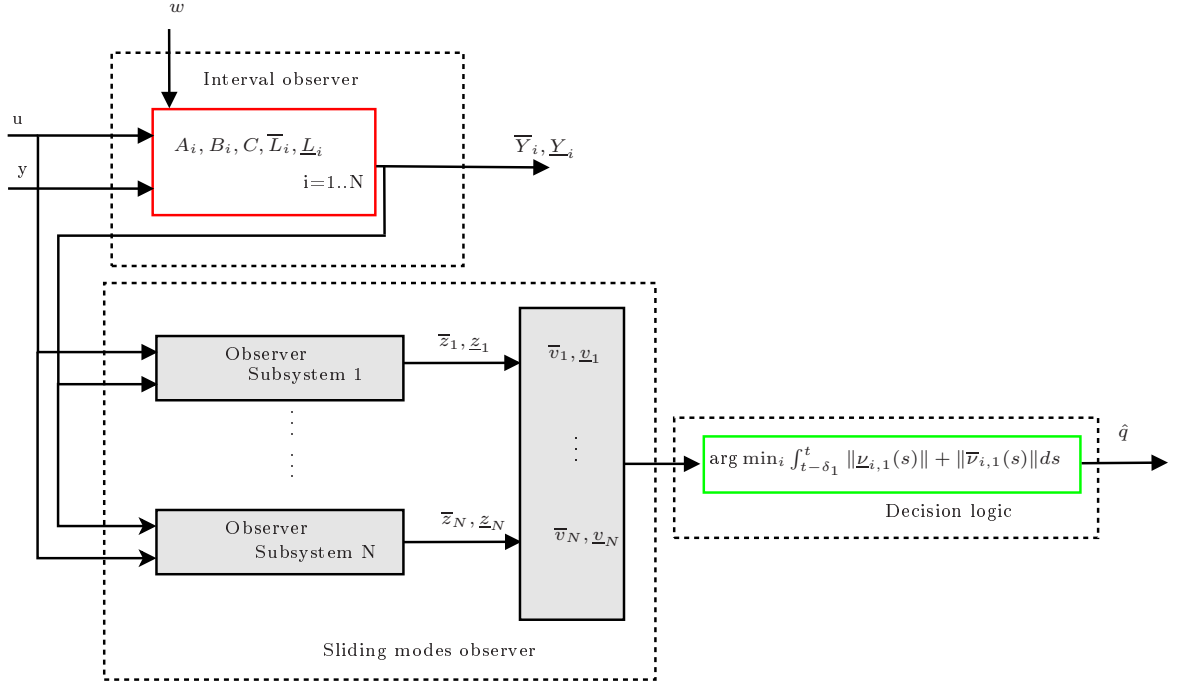


Figure 4.2: Bloc diagram of the discrete state estimator.

Associated with the above decision algorithm, an estimation \hat{q} of the current mode q of the switched linear system (4.1) is achieved based on the stack of the sliding modes observers (4.10). In the following, an estimation \hat{t}_k of the switching time instants is provided based on a decision logic on the evolution of the residual $r_{\hat{q}}$ and H_∞ performances.

4.4.2 Switching time instants estimation

The proposed interval observer (4.3) must be designed in order to detect the discrete state change despite the presence of the unknown input. In this section, conditions are developed such that: (i) the augmented system (4.6) is stable and positive, (ii) the L_2 norm of the operators from \mathcal{W}_i to $r_i(t)$ and from $\chi_i(t)$ to $r_i(t) - J\chi_i(t)$ are minimized. The following theorem provides LMI conditions in order to compute observer gains \bar{L}_i and \underline{L}_i .

Theorem 12. Consider the switched system (4.6), for a given $\epsilon \in \mathbb{R}^+$ and $0 \leq \lambda \leq 1$ if there exist matrices $P = \begin{bmatrix} P_{11} & 0 \\ 0 & P_{22} \end{bmatrix} > 0$, $P \in \mathbb{R}^{2n_x \times 2n_x}$ with diagonal matrices P_{11} and P_{22} , $X_i, Y_i \in \mathbb{R}^{n_x}$ for $i = 1, 2, \dots, N$, $\gamma > 0$ and $\beta > 0$ such that:

$$\min_{P, X_i, Y_i} \lambda\gamma + (1 - \lambda)\beta, \quad (4.25)$$

$$\begin{bmatrix} A_i^T P_{11} - C^T X_i^T + \epsilon P_{11} & 0 \\ 0 & A_i^T P_{22} - C^T Y_i^T + \epsilon P_{22} \end{bmatrix} \geq 0, \quad (4.26)$$

$$\begin{bmatrix} \Theta_{11} & C^{+T}C^- + C^{-T}C^+ & P_{11} & 0 \\ C^{+T}C^- + C^{-T}C^+ & \Theta_{22} & 0 & P_{22} \\ P_{11} & 0 & -\gamma I_n & 0 \\ 0 & P_{22} & 0 & -\gamma I_n \end{bmatrix} \prec 0, \quad (4.27)$$

$$\begin{bmatrix} \Theta_{11} & C^{+T}C^- + C^{-T}C^+ & \Theta_{13} \\ C^{+T}C^- + C^{-T}C^+ & \Theta_{22} & \Theta_{23} \\ \Theta_{31} & \Theta_{32} & \Theta_{33} \end{bmatrix} \prec 0, \quad (4.28)$$

where

$$\begin{cases} \Theta_{11} &= A_i^T P_{11} + P_{11} A_i - C^T X_i^T - X_i C + C^{+T}C^+ + C^{-T}C^-, \\ \Theta_{13} &= P_{11} - C^{+T}J_1 - C^{-T}J_2, \\ \Theta_{22} &= A_i^T P_{22} + P_{22} A_i - C^T Y_i^T - Y_i C + C^{+T}C^+ + C^{-T}C^-, \\ \Theta_{23} &= -P_{22} - C^{-T}J_1 - C^{+T}J_2, \\ \Theta_{31} &= P_{11} - J_1^T C^+ - J_2^T C^-, \\ \Theta_{33} &= J_1^T J_1 + J_2^T J_2 - \beta I_n \end{cases}$$

and $X_i = P_{11} \overline{L}_i$ and $Y_i = P_{22} \underline{L}_i$, then the matrices A_i , for $i = 1, 2, \dots, N$, are Metzler, the augmented system (4.6) is stable and positive and satisfies the H_∞ performance conditions (4.8) and (4.9).

Proof. In this proof, the aim is to prove positivity, unknown attenuation and discrete mode sensitivity conditions.

(i) **Positivity condition**

Considering $X_i = P_{11} \overline{L}_i$ and $Y_i = P_{22} \underline{L}_i$ and from Definition 10 in the chapter 3, it is obvious that if the inequality (4.26) is verified, the matrices \mathcal{A}_i , for $i = 1, 2, \dots, N$, are Metzler. On each time interval $[t_k, t_{k+1})$, this condition is necessary to ensure the positivity of the augmented system (4.6) when $i = q$. From the representation (4.6), it is clear that $\mathcal{W}(t) \geq 0$. If the matrices \mathcal{A}_i are Metzler and, for $i = q$ the states $\overline{x}_i(t_k)$ and $\underline{x}_i(t_k)$ are chosen such that $\underline{x}_i(t_k) \leq x(t_k) \leq \overline{x}_i(t_k)$, then the state $\zeta_i(t)$ stays positive for all $t \in [t_k, t_{k+1})$. In this approach, the switching signal estimation is based on both bounds of the output signal y . The positivity of the augmented state $\zeta_i(t)$ for $t \in [t_k, t_{k+1})$ and $i = q$ must be satisfied.

(ii) **Unknown attenuation condition**

Considering the quadratic Lyapunov function $V(x) = x^T P x$, the system (4.6) with $\chi_i = 0$ satisfies the H_∞ performance condition (4.8) if, for $i = 1, 2, \dots, N$:

$$\frac{dV(\zeta_i)}{dt} + r_i^T r_i - \gamma \mathcal{W}_i^T \mathcal{W}_i < 0. \quad (4.29)$$

Inequality (4.29) implies:

$$\begin{aligned} \zeta_i^T P \dot{\zeta}_i + \zeta_i^T P \dot{\zeta}_i + r_i^T r_i - \gamma \mathcal{W}_i^T \mathcal{W}_i < 0 \\ \zeta_i^T [\mathcal{A}_i^T P + P \mathcal{A}_i + \mathcal{C}^T \mathcal{C}] \zeta_i + \mathcal{W}_i^T P \zeta_i + \zeta_i^T P \mathcal{W}_i - \gamma \mathcal{W}_i^T \mathcal{W}_i < 0. \end{aligned} \quad (4.30)$$

Based on (4.30), the following inequality is equivalent to (4.27)

$$\begin{bmatrix} \zeta_i \\ \mathcal{W}_i \end{bmatrix}^T \begin{bmatrix} \mathcal{A}_i^T P + P \mathcal{A}_i + \mathcal{C}^T \mathcal{C} & P \\ P & -\gamma I_{2n} \end{bmatrix} \begin{bmatrix} \zeta_i \\ \mathcal{W}_i \end{bmatrix} < 0. \quad (4.31)$$

By assigning

$$\left\{ \begin{array}{l} P = \begin{bmatrix} P_{11} & 0 \\ 0 & P_{22} \end{bmatrix} \\ X_i = P_{11} \overline{L}_i \\ Y_i = P_{22} \underline{L}_i \\ \Theta_{11} = A_i^T P_{11} + P_{11} A_i - C^T X_i^T - X_i C + C^{+T} C^+ + C^{-T} C^- \\ \Theta_{22} = A_i^T P_{22} + P_{22} A_i - C^T Y_i^T - Y_i C + C^{+T} C^+ + C^{-T} C^- \end{array} \right.$$

The inequality (4.31) implies (4.8) and the H_∞ is obtained.

(iii) Discrete mode sensitivity condition

Using the quadratic Lyapunov function $V(x) = x^T P x$, the system (4.6) with $\mathcal{W}_i = 0$ is stable and satisfies the H_∞ performance condition (4.9) if, for $i = 1, 2, \dots, N$:

$$\frac{dV(\zeta_i)}{dt} + (r_i - J \chi_i)^T (r_i - J \chi_i) - \beta \chi_i^T \chi_i < 0. \quad (4.32)$$

Inequality (4.32) implies:

$$\zeta_i^T P \dot{\zeta}_i + \zeta_i^T P \dot{\zeta}_i + (r_i - J \chi_i)^T (r_i - J \chi_i) - \beta \chi_i^T \chi_i < 0.$$

Based on (4.6), the following inequality holds:

$$\begin{aligned} \zeta_i^T [\mathcal{A}_i^T P + P \mathcal{A}_i + \mathcal{C}^T \mathcal{C}] \zeta_i + \chi_i^T [\mathcal{F}^T P - J^T \mathcal{C}] \zeta_i + \zeta_i^T [P \mathcal{F} - \mathcal{C}^T J] \chi_i + \\ \chi_i^T [J^T J - \beta I_n] \chi_i < 0. \end{aligned} \quad (4.33)$$

From (4.33), the following inequality is equivalent to (4.28)

$$\begin{bmatrix} \zeta_i \\ \chi_i \end{bmatrix}^T \begin{bmatrix} \mathcal{A}_i^T P + P \mathcal{A}_i + \mathcal{C}^T \mathcal{C} & P \mathcal{F} - \mathcal{C}^T J \\ \mathcal{F}^T P - J^T \mathcal{C} & J^T J - \beta I_n \end{bmatrix} \begin{bmatrix} \zeta_i \\ \chi_i \end{bmatrix} < 0, \quad (4.34)$$

by letting

$$\left\{ \begin{array}{l} P = \begin{bmatrix} P_{11} & 0 \\ 0 & P_{22} \end{bmatrix} \\ X_i = P_{11} \bar{L}_i \\ Y_i = P_{22} \underline{L}_i \\ \Theta_{11} = A_i^T P_{11} + P_{11} A_i - C^T X_i^T - X_i C + C^{+T} C^+ + C^{-T} C^- \\ \Theta_{13} = P_{11} - C^{+T} J_1 - C^{-T} J_2 \\ \Theta_{22} = A_i^T P_{22} + P_{22} A_i - C^T Y_i^T - Y_i C + C^{+T} C^+ + C^{-T} C^- \\ \Theta_{23} = -P_{22} - C^{-T} J_1 - C^{+T} J_2 \\ \Theta_{31} = P_{11} - J_1^T C^+ - J_2^T C^- \\ \Theta_{33} = J_1^T J_1 + J_2^T J_2 - \beta I_n. \end{array} \right.$$

Thus, we can see that (4.34) implies (4.9). □

In order to design the proposed interval observer (4.3), if the LMIs (4.26), (4.27) and (4.28) are verified minimizing $\lambda\gamma + (1-\lambda)\beta$ with the weight $\lambda \in [0, 1]$, the observer gains \bar{L}_i and \underline{L}_i can be computed and the objectives can be fulfilled. From these conditions and the representation of the augmented system (4.6), one can conclude that $i = q$ and $0 \in [\underline{x}_i, \bar{x}_i]$ implies $\underline{x}_i \leq x \leq \bar{x}_i$. However, in contrary case when $i \neq q$ ($\chi_i \neq 0$) the positivity of the system (4.6) cannot be guaranteed. In other words, a discrete state change can be detected from a particular mode i when $0 \notin [\underline{x}_i, \bar{x}_i]$.

Combining this optimal approach with the sliding modes technique, the estimated switching time instant \hat{t}_k , $k = 1, 2, \dots$, can be defined as follows:

$$\hat{t}_k = \min(t \in \mathbb{R}^+ | t \geq \hat{t}_{k-1} + T_1^* \text{ and } \hat{q}(t) \neq \hat{q}(\hat{t}_{k-1} + T_1^*) \vee t \geq \hat{t}_{k-1} + T_1^* \text{ and } 0 \notin [\underline{x}_{\hat{q}(t)}, \bar{x}_{\hat{q}(t)}]). \quad (4.35)$$

Remark 13. Equation (4.35) means that the next estimated time instant \hat{t}_k ($\hat{t}_k > \hat{t}_{k-1} + T_1^*$) is defined as the first time instant when the estimated discrete state changes its value, i.e. $\hat{q}(t) \neq \hat{q}(\hat{t}_{k-1} + T_1^*)$ or when the positivity of the interval observer cannot be guaranteed ($0 \notin [\underline{x}_{\hat{q}(t)}, \bar{x}_{\hat{q}(t)}]$). Its initial value is $\hat{t}_0 = t_0$

From Assumption 16, the state $x(t)$ evolves in a known bounded region. A reset of states $\bar{x}_i(\hat{t}_k)$ and $\underline{x}_i(\hat{t}_k)$ for all $i = 1, \dots, N$ is realized in order to ensure that $\underline{x}_i(\hat{t}_k) \leq x(\hat{t}_k) \leq \bar{x}_i(\hat{t}_k)$ such that:

$$\bar{x}_i(\hat{t}_k) = \bar{X} \quad \underline{x}_i(\hat{t}_k) = \underline{X}. \quad (4.36)$$

Remark 14. Based on the definition of the estimated switching time instant (4.35), the detection of the discrete state change allows highlighting the inconsistencies on the positivity of the observer. Using the proposed reset of the estimated states (4.36) of the interval observer, the positivity of the observer is always ensured.

From (4.19), the estimated switching signal $\hat{\sigma}(t)$ is defined by :

$$\hat{\sigma}(t) = \begin{cases} \hat{q}(t) & t \in [\hat{t}_{k-1} + T_1^*, \hat{t}_k) \\ \hat{q}(\hat{t}_{k-1} + T_1^*) & t \in [\hat{t}_k, \hat{t}_k + T_1^*) \end{cases} \quad (4.37)$$

with $\hat{q}(t) = \sigma(t)$ for $t \in [\hat{t}_{k-1} + T_1^*, t_k)$. Using the proposed approach, the current mode is identified in finite time. The time T_1^* is parametrized by the sliding modes gains k_1 and k_2 . The estimation error $\hat{t}_k - t_k$ can be limited by the robust approach in (4.35). The feasibility and efficiency of the proposed approach are illustrated by simulations in the next section.

4.5 Numerical example

In this section, an illustrative example is given to highlight the designed method.

4.5.1 Simulation settings

Let us consider a system (4.1) with $N = 3$ modes ($q \in \{1, 2, 3\}$). Matrices of the system are chosen as below:

$$A_1 = \begin{pmatrix} -15 & 1 & 0 \\ 0 & -10 & 1 \\ -1 & 0 & -12 \end{pmatrix} \quad A_2 = \begin{pmatrix} -7 & 1 & 1 \\ 0 & -8 & 1 \\ 3 & 0 & -6 \end{pmatrix} \quad A_3 = \begin{pmatrix} -5 & 0 & 1 \\ 1 & -4 & 0 \\ 1 & 1 & -9 \end{pmatrix}$$

$$B_1 = \begin{pmatrix} 0 & 0 & 0 \end{pmatrix} \quad B_2 = \begin{pmatrix} 0 & 0 & -5 \end{pmatrix} \quad B_3 = \begin{pmatrix} 5 & 0 & 0 \end{pmatrix}$$

$$C = \begin{pmatrix} -5 & 0 & 2 \end{pmatrix}$$

In this example, $x(t) = [x_1(t), x_2(t), x_3(t)]^T \in \mathbb{R}^3$ is the state, $y(t) \in \mathbb{R}$ is the output, $u(t) = 5$ is the known input and $w(t) = 0.02 \sin(100\pi t)$ is the unknown input. The initial conditions are chosen such that $x(0) = [0, 0, 0]^T$ and $\sigma(0) = 3$. We assume that the continuous state $x(t)$ is bounded with: $[-1, -0.7, -4.5]^T \leq x(t) \leq [6, 2, 1]^T$. These bounds are used to reset \bar{x}_i and \underline{x}_i , $i = 1, 2, 3$, at each estimated switching time instant \hat{t}_k .

4.5.2 Simulation results

From these modeling, the LMIs (4.26), (4.27) and (4.28) are implemented. The optimization problem in Theorem 12 can be solved using Yalmip/Sedumi in MATLAB. The existence of a solution for LMIs allows one to minimize the operators from \mathcal{W}_i to r_i and from χ_i to $r_i - J\chi_i$. The parameters $\epsilon = 500$, $\lambda = 0.5$ and the weighting matrix

$$J = \begin{pmatrix} 0.5 & 0.5 & 0.5 \\ 0.5 & 0.5 & 0.5 \end{pmatrix}$$

are chosen to solve this optimization problem. The following Lyapunov matrix is obtained:

$$P = \begin{pmatrix} 4.64 & 0 & 0 & 0 & 0 & 0 \\ 0 & 1 & 0 & 0 & 0 & 0 \\ 0 & 0 & 4.4 & 0 & 0 & 0 \\ 0 & 0 & 0 & 1 & 0 & 0 \\ 0 & 0 & 0 & 0 & 1 & 0 \\ 0 & 0 & 0 & 0 & 0 & 4.87 \end{pmatrix}$$

with $\gamma = 0.73$ and $\beta = 2.77$. The obtained observer gains correspond to:

$$\bar{L}_1 = \begin{pmatrix} -10.63 & 0.25 & 6.34 \end{pmatrix}^T, \quad \underline{L}_1 = \begin{pmatrix} -43.3 & 0.25 & 4.2 \end{pmatrix}^T$$

$$\bar{L}_2 = \begin{pmatrix} -98.6 & 0.50 & 40.23 \end{pmatrix}^T, \quad \underline{L}_2 = \begin{pmatrix} -93.50 & 0 & 5.96 \end{pmatrix}^T$$

$$\bar{L}_3 = \begin{pmatrix} -12.36 & -0.1 & 5.04 \end{pmatrix}^T, \quad \underline{L}_3 = \begin{pmatrix} -48.5 & -0.1 & 3.3 \end{pmatrix}^T$$

The parameter values of (4.11) are chosen as: $k_1 = 5000$ and $k_2 = 10000$. The discrete state observer (4.19) is implemented with $\delta_1 = 30ms$ and $\delta_2 = 0.9$. It is tuned such that Assumption 17 is verified.

Using the interval observer (4.3) combined with the sliding modes observer (4.10), the aim is to estimate in finite time the switching signal $\sigma(t)$ despite the unknown input $w(t)$.

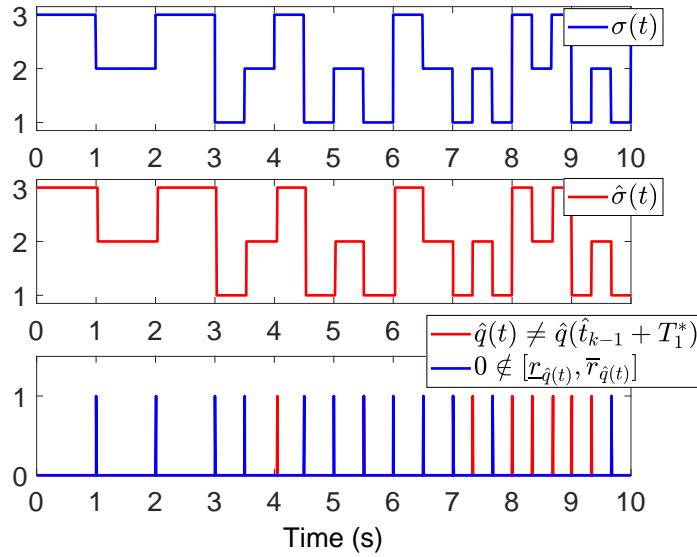


Figure 4.3: Evolution of the switching signal σ (a), its estimate $\hat{\sigma}$ (b) and the reset instants based on (4.35) (c).

Figures 6.6 and 4.4 show the switching signal and its estimate. Figure 6.6 (c) illustrates the reset instants when $t \geq \hat{t}_{k-1} + T_1^*$ and $\hat{q}(t) \neq \hat{q}(\hat{t}_{k-1} + T_1^*)$ or $0 \notin [\underline{r}_{\hat{q}(t)}, \bar{r}_{\hat{q}(t)}]$.

Figure 4.5 shows the evolutions of the continuous state $x(t)$, the upper bound \bar{x}_i and the lower one \underline{x}_i for $i = \hat{\sigma}$. One can see that the state x is always between both bounds.

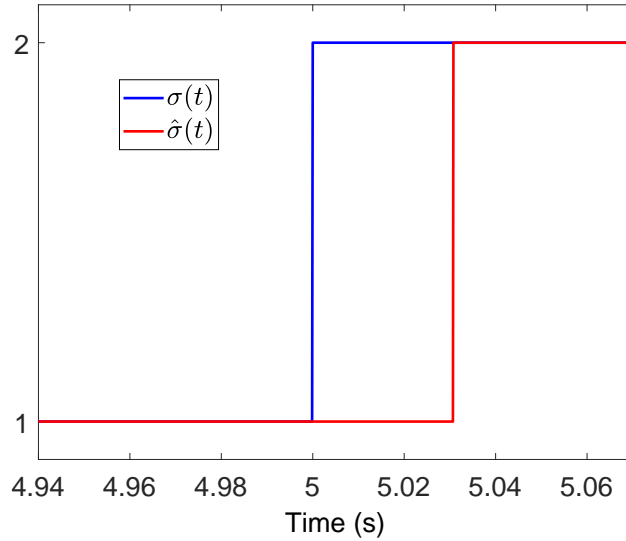


Figure 4.4: Evolution of the switching signal and its estimate (ZOOM).

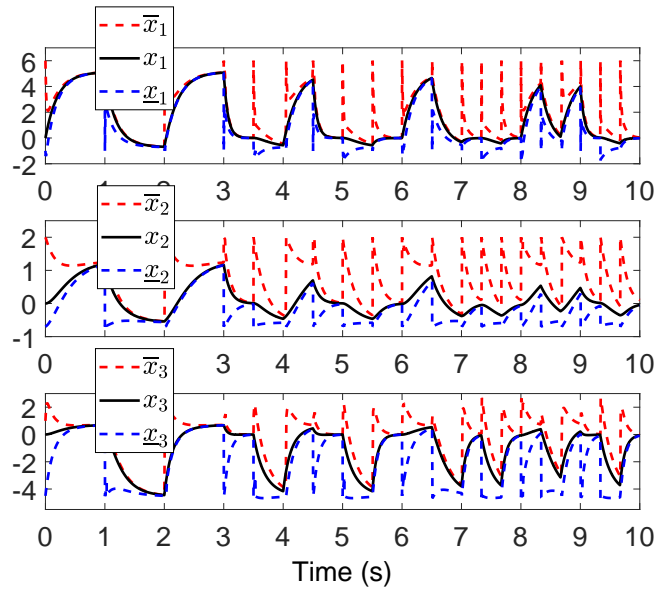


Figure 4.5: Evolution of the continuous state $x(t)$ and its estimated bounds for $i = \hat{\sigma}$.

Figures 4.6 and 4.7 illustrate the performance of the interval observer using the proposed reset (4.36). The estimation errors $\bar{x}_i - x$ and $x - \underline{x}_i$ ($i = \hat{\sigma}$) stay positive.

Using the sliding modes approach, an estimation of the discrete state is obtained in finite time. The proposed interval observer provides a good estimation of the switching time instants t_k with a small error $\hat{t}_k + T_1^* - t_k \leq 50ms$. One can see that the proposed scheme provides no discrete mode identification error except those arising in the transient period $[t_k, \hat{t}_k + T_1^*)$.

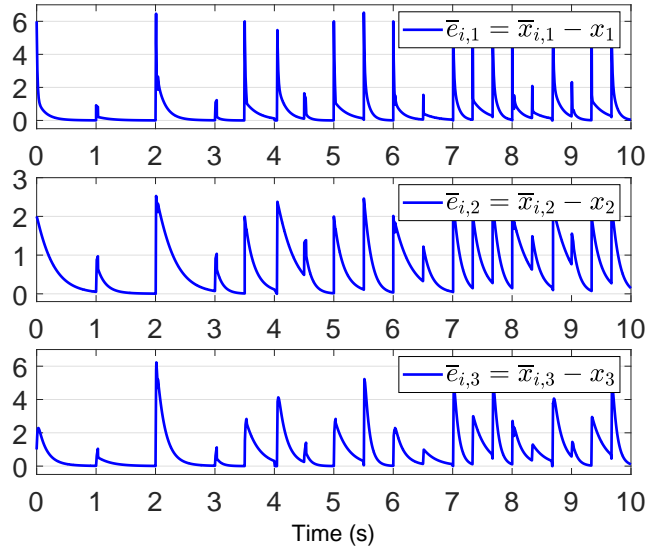


Figure 4.6: Evolution of the upper error.

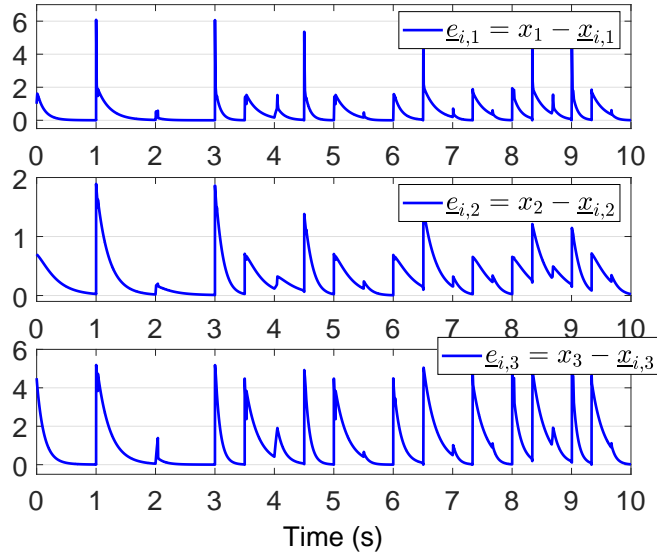


Figure 4.7: Evolution of the upper error.

4.6 Conclusion

In this chapter, based on distinguishability conditions of the current mode, a sliding modes observer combined with an interval observer is designed to estimate the discrete mode of a switched linear system with unknown input. In the proposed approach, two estimation techniques are presented. The first one is based on sliding modes theory where a discrete state observer providing an estimation \hat{q} of the current mode q of the system is investigated. The proposed approach provides a robust finite-time convergence. The second methodology is based on interval observer theory where only bounds of the unknown input are needed

to determine the switching time instants. Using the output estimation errors, residuals are defined to ensure a robust detection of discrete mode change. Using H_∞ performances, an attenuation condition of the disturbance and sensitivity condition of residuals are formulated by LMI conditions in order to design the interval observer.

In this chapter, an original technique merging sliding modes and interval observers has been proposed for the robust estimation of the switching signal. The state estimation problem for switched systems remains one of the fundamental steps to deal with fault detection problems. In the next chapter, the problem of robust fault detection is addressed in discrete-time for a class of switched systems subject to bounded disturbances and based on interval analysis.

Chapter 5

Interval observer based-fault detection design for switched systems

5.1 Introduction

Interval observer design techniques are usually based on the theory of positive systems, which require the nonnegativity of the error dynamics. Unfortunately, this assumption is still restrictive and may lead to more theoretical difficulty and computational complexity in searching for a gain matrix to simultaneously ensure the nonnegativity and stability of the error system. Some methods propose a coordinate transformation to relax the design conditions of interval observers. However, as mentioned in [193], it is hard to merge the coordinate transformation approach with performance constraints such as disturbance attenuation performance. In view of this major drawback, the primary focus of this chapter is to design a new interval observer-based (TNL structure) FD method for a class of discrete-time switched systems subject to unknown but bounded state disturbances and measurement noise. In this chapter, two approaches to construct residual framers are considered. First, a commonly used interval observer is designed based on an L_∞ criterion. By introducing the L_∞ design into interval observers, the proposed method provides a systematic and effective way to improve the accuracy of fault detection. Second, a new interval approach is investigated to reduce the conservatism of gain matrices. Second, a novel interval observer structure (TNL structure) is designed. The proposed technique offers more degrees of design freedom by integrating weighted matrices in the structure of the FD observer design. Using CQLF and MQLF with an ADT control condition, novel solvable conditions are derived in terms of LMIs. Furthermore, the FD decision is based on residual intervals generated by the proposed interval observers. The efficiency of the proposed approaches is highlighted

through simulation results on an academic example.

The work presented in this chapter has led to the publication of a journal paper [194] in "European Journal of Control" and two communications [195] and [196] in "European Control Conference" and "Mediterranean Conference on Control and Automation".

5.2 Problem statement

Consider the following discrete-time switched system:

$$\begin{cases} x_{k+1} = A_q x_k + B_q u_k + D_q w_k \\ y_k = C x_k + D_v v_k + F f_k, \end{cases} \quad (5.1)$$

where $x \in \mathbb{R}^{n_x}$, $u \in \mathbb{R}^{n_u}$, $y \in \mathbb{R}^{n_y}$, $f \in \mathbb{R}^{n_f}$, $w \in \mathbb{R}^{n_w}$ and $v \in \mathbb{R}^{n_v}$ are respectively the state vector, the input, the output, the sensor fault, the state disturbances and the measurement noise. The known matrices A_q , B_q , C , D_q , D_v and F are given with appropriate dimensions. The index q specifies, at each discrete instant k , the subsystem that is currently followed. $q \in \mathcal{I} = \overline{1, N}$, $N \in \mathbb{Z}_+$, N is the number of linear subsystems. The switching signal is assumed to be known.

Assumption 18. *Assume that the state disturbances and the measurement noise are unknown but bounded with a priori known bounds such that*

$$\underline{w} \leq w \leq \overline{w}, \quad \underline{v} \leq v \leq \overline{v},$$

where $\underline{w}, \overline{w} \in \mathbb{R}^{n_w}$ and $\underline{v}, \overline{v} \in \mathbb{R}^{n_v}$.

Assumption 19. *The pairs (A_q, C) are detectable, $\forall q = 1, \dots, N$.*

In the following, the goal is to design residual framers based on robust FD interval observers for discrete-time linear switched systems subject to sensor faults. Two approaches are considered: the first one is based on the design of the commonly used interval observer, while the second is based on a novel TNL structure interval observer. For both approaches, an L_∞ criterion is developed in order to improve the accuracy of FD results. In addition, LMIs conditions are determined using CQLF under an arbitrary switching signal and MQLF with an ADT switching signal.

5.3 A common Lyapunov function based-approach

In this part, the aim is to design a FD approach for discrete-time switched systems defined by (5.1). The proposed method is robust against state disturbances and measurement noise. The stability analysis is analyzed by applying CQLF.

5.3.1 Interval observer design for switched systems

A FD interval observer is proposed for the system (5.1). The following assumptions are needed in this chapter.

Assumption 20. *The upper and lower bounds, \overline{x}_0 and \underline{x}_0 , of the initial state are chosen such that $\underline{x}_0 \leq x_0 \leq \overline{x}_0$.*

Assumption 21. *There exist $\bar{L}_q \in \mathbb{R}^{n_x \times n_y}$ and $\underline{L}_q \in \mathbb{R}^{n_x \times n_y}$ such that $A_q - \bar{L}_q C$ and $A_q - \underline{L}_q C$ are nonnegative $\forall q = 1, \dots, N$.*

Remark 15. *Assumption 20 is common in the literature when interval observers are considered. Assumption 21 is a primordial condition to design interval observers. Since this assumption is still restrictive, it is relaxed in subsection 5.3.2 by integrating new weighted matrices in a TNL observer.*

The FD interval observers is proposed as follows: $\forall q = 1, \dots, N$

$$\begin{cases} \bar{x}_{k+1} = A_q \bar{x}_k + B_q u_k + \bar{L}_q (y_k - C \bar{x}_k) + \bar{\Delta} \\ \underline{x}_{k+1} = A_q \underline{x}_k + B_q u_k + \underline{L}_q (y_k - C \underline{x}_k) + \underline{\Delta} \\ \bar{y}_k = C^+ \bar{x}_k - C^- \underline{x}_k + D_v^+ \bar{v} - D_v^- \underline{v} \\ \underline{y}_k = C^+ \underline{x}_k - C^- \bar{x}_k + D_v^+ \underline{v} - D_v^- \bar{v} \\ \bar{r}_k = \bar{y}_k - y_k \\ \underline{r}_k = \underline{y}_k - y_k \end{cases} \quad (5.2)$$

where $\bar{L}_q, \underline{L}_q \in \mathbb{R}^{n_x \times n_y}$ are the observer gains to be designed. $\bar{\Delta}$ and $\underline{\Delta}$ are given by:

$$\begin{cases} \bar{\Delta} = D_q^+ \bar{w} - D_q^- \underline{w} + (\bar{L}_q D_v)^+ \bar{v} - (\bar{L}_q D_v)^- \underline{v} \\ \underline{\Delta} = D_q^+ \underline{w} - D_q^- \bar{w} + (\underline{L}_q D_v)^+ \underline{v} - (\underline{L}_q D_v)^- \bar{v}. \end{cases}$$

Under the proposed FD interval observer (5.2), the objective is to compute the observer gains \bar{L}_q and \underline{L}_q that stabilize the estimation errors and minimize the L_∞ norm of the transfer function for each mode from state disturbances and measurement noise to the upper and lower bounds of the residual vectors $\bar{r}_k, \underline{r}_k$, respectively.

Let $\bar{e}_k = \bar{x}_k - x_k$ and $\underline{e}_k = x_k - \underline{x}_k$ be the upper and the lower estimation errors, respectively. The error dynamics are given by:

$$\begin{cases} \bar{e}_{k+1} = (A_q - \bar{L}_q C) \bar{e}_k + \bar{\Delta} + \bar{L}_q D_v v_k - D_q w_k + \bar{L}_q F f_k \\ \underline{e}_{k+1} = (A_q - \underline{L}_q C) \underline{e}_k - \underline{\Delta} - \underline{L}_q D_v v_k + D_q w_k - \underline{L}_q F f_k. \end{cases} \quad (5.3)$$

We can define:

$$\bar{d}_k = \begin{bmatrix} \bar{\Delta} - D_q w_k \\ D_v v_k \end{bmatrix}, \quad \underline{d}_k = \begin{bmatrix} -\underline{\Delta} + D_q w_k \\ -D_v v_k \end{bmatrix},$$

$$\bar{H}_q = \begin{bmatrix} I_{n_x} & \bar{L}_q \end{bmatrix}, \quad \underline{H}_q = \begin{bmatrix} I_{n_x} & \underline{L}_q \end{bmatrix}.$$

I_{n_x} represents the identity matrix. Thus, the error dynamics in (5.3) can be rewritten as

$$\begin{cases} \bar{e}_{k+1} = (A_q - \bar{L}_q C) \bar{e}_k + \bar{H}_q \bar{d}_k + \bar{L}_q F f_k \\ \underline{e}_{k+1} = (A_q - \underline{L}_q C) \underline{e}_k + \underline{H}_q \underline{d}_k - \underline{L}_q F f_k. \end{cases} \quad (5.4)$$

On the basis of the error system of (5.4), the nonnegativity, the stability and the robustness of the proposed interval observer are developed in the following parts. The nonnegativity of the estimation errors is ensured in the theorem below.

Theorem 13. *For system (5.1), let Assumptions 18-21 be satisfied. Then, the relation*

$$\underline{x}_k \leq x_k \leq \bar{x}_k \quad (5.5)$$

holds in the fault free case ($f = 0$) for all $k \geq 0$ provided that $\underline{x}_0 \leq x_0 \leq \bar{x}_0$.

Proof. In the fault free case ($f = 0$), according to Assumption 18, we have

$$\begin{aligned}\bar{\Delta} + \bar{L}_q D_v v_k - D_q w_k &\geq 0 \\ -\underline{\Delta} - \underline{L}_q D_v v_k + D_q w_k &\geq 0.\end{aligned}$$

According to Assumption 21, $A_q - \bar{L}_q C$ and $A_q - \underline{L}_q C$ are nonnegative. In addition, from Assumption 20, \underline{x}_0 and \bar{x}_0 are chosen such that $\bar{e}_0 \geq 0$ and $\underline{e}_0 \geq 0$. Then, applying Lemma 3 in chapter 2 to (5.4), one can deduce that the inequality $\underline{x}_k \leq x_k \leq \bar{x}_k$ holds for all $k > 0$. \square

In addition to the cooperativity property in fault free case, it is primordial to ensure the stability of the upper and lower bounds of the residual signal. For this purpose, we denote the augmented state by $e_k = [\bar{e}_k^T \ \underline{e}_k^T]^T$ and $r_k = [\bar{r}_k^T \ \underline{r}_k^T]^T$. The following augmented system can be deduced:

$$\begin{cases} e_{k+1} = \mathcal{A}_q e_k + \mathcal{H}_q d_k + \tilde{\mathcal{F}}_q f_k \\ r_k = \mathcal{C} e_k + \mathcal{V} \tilde{v}_k + \mathcal{F} f_k, \end{cases} \quad (5.6)$$

where

$$\begin{aligned}\mathcal{A}_q &= \begin{bmatrix} A_q - \bar{L}_q C & 0 \\ 0 & A_q - \underline{L}_q C \end{bmatrix}, \quad \mathcal{H}_q = \begin{bmatrix} \bar{H}_q & 0 \\ 0 & \underline{H}_q \end{bmatrix}, \quad \tilde{\mathcal{F}}_q = \begin{bmatrix} \bar{L}_q F \\ -\underline{L}_q F \end{bmatrix}, \quad \mathcal{F} = \begin{bmatrix} -F \\ -F \end{bmatrix}, \\ \mathcal{C} &= \begin{bmatrix} C^+ & C^- \\ -C^- & -C^+ \end{bmatrix}, \quad \mathcal{V} = \begin{bmatrix} -D_v & D_v^+ & -D_v^- \\ -D_v & -D_v^- & D_v^+ \end{bmatrix}, \quad d_k = \begin{bmatrix} \bar{d}_k \\ \underline{d}_k \end{bmatrix}, \quad \tilde{v}_k = \begin{bmatrix} v_k \\ \bar{v} \\ \underline{v} \end{bmatrix},\end{aligned}$$

$d \in \mathbb{R}^{n_d}$, $n_d = 2n_x + 2n_y$.

The error dynamics in (5.6) can be split into two subsystems where (5.7) is decoupled from the effects of $f(k)$ and (5.8) is only affected by the sensor fault.

$$\begin{cases} e_{k+1}^d = \mathcal{A}_q e_k^d + \mathcal{H}_q d_k \\ r_k^d = \mathcal{C} e_k^d + \mathcal{V} \tilde{v}_k, \end{cases} \quad (5.7)$$

$$\begin{cases} e_{k+1}^f = \mathcal{A}_q e_k^f + \tilde{\mathcal{F}}_q f_k \\ r_k^f = \mathcal{C} e_k^f + \mathcal{F} f_k, \end{cases} \quad (5.8)$$

where $e_k = e_k^f + e_k^d$.

For efficient FD, it is required that the impact of state disturbances and measurement noise is attenuated. Many existing works consider the H_∞ performance. It is worth noting that the H_∞ criterion is a measurement of energy-to-energy gain which may not be very efficient for residual evaluation. The reason behind is to assume that the disturbances are energy-bounded signals. Nevertheless, some signals cannot be considered energy-bounded but have bounded peak values. Instead, it is more reasonable to use the L_∞ analysis which introduces the peak-to-peak performance index. Therefore, the proposed observer in (5.2) is designed such that the following conditions hold:

1. The error system in (5.7) is stable.

2. Given scalars $\gamma > 0$, $\gamma_1 > 0$, $\gamma_2 > 0$ and $0 < \lambda < 1$, then r^d should satisfy the following L_∞ performance

$$\|r^d\| < \sqrt{\gamma_1^2 \gamma (\lambda(1-\lambda)^k V_0 + \gamma \theta_d^2) + \gamma_2^2 \theta_v^2}, \quad (5.9)$$

where $V(e_0^d) = e_0^{dT} P e_0^d$ with $P \succ 0 \in \mathbb{R}^{2n_x \times 2n_x}$. θ_d and θ_v are known constants and represent the L_∞ of d and \tilde{v} such that $\theta_d = \|d\|_\infty$ and $\theta_v = \|\tilde{v}\|_\infty$. Sufficient conditions are given in terms of LMIs in the following theorem in order to fulfill both previous conditions.

Theorem 14. *Let Assumptions 19-20 hold. Given scalars $\gamma > 0$, $\gamma_1 > 0$, $\gamma_2 > 0$ and $0 < \lambda < 1$, the error dynamics system in (5.7) are stable and r^d satisfies the L_∞ performance, if there exist a constant $\mu > 0$, a diagonal matrix $P = \begin{bmatrix} P_1 & 0 \\ 0 & P_2 \end{bmatrix} \succ 0$, $P = P^T \succ 0$, $P \in \mathbb{R}^{2n_x \times 2n_x}$ with diagonal matrices P_1, P_2 and constant matrices W_{q1} and $W_{q2} \in \mathbb{R}^{n_x \times n_y}$ for $q = 1, 2, \dots, N$ such that:*

$$\begin{bmatrix} P_1 A_q - W_{q1} C & 0 \\ * & P_2 A_q - W_{q2} C \end{bmatrix} \geq 0, \quad (5.10)$$

$$\begin{bmatrix} \Omega_{11} & 0 & \Omega_{13} \\ * & -\mu I_{n_d} & \Omega_{23} \\ * & * & \Omega_{33} \end{bmatrix} \prec 0, \quad (5.11)$$

$$\begin{bmatrix} \lambda P & 0 & I_{2n_x} \\ * & (\gamma - \mu) I_{n_d} & 0 \\ * & * & \gamma I_{2n_x} \end{bmatrix} \succ 0, \quad (5.12)$$

$$\begin{bmatrix} C^T C - \gamma_1^2 I_{2n_x} & C^T \mathcal{V} \\ * & -\gamma_2^2 I_{2n_x} + \mathcal{V}^T \mathcal{V} \end{bmatrix} \prec 0, \quad (5.13)$$

where

$$\Omega_{11} = \begin{bmatrix} (\lambda - 1) P_1 & 0 \\ * & (\lambda - 1) P_2 \end{bmatrix}, \quad \Omega_{13} = \begin{bmatrix} P_1 A_q - W_{q1} C & 0 \\ * & P_2 A_q - W_{q2} C \end{bmatrix}^T,$$

$$\Omega_{23} = \begin{bmatrix} P_1 & W_{q1} & 0 & 0 \\ 0 & 0 & P_2 & W_{q2} \end{bmatrix}^T, \quad \Omega_{33} = \begin{bmatrix} -P_1 & 0 \\ * & -P_2 \end{bmatrix}$$

are solvable, then the observer gains \bar{L}_q and \underline{L}_q can be chosen such that:

$$\begin{cases} \bar{L}_q = P_1^{-1} W_{q1} \\ \underline{L}_q = P_2^{-1} W_{q2}. \end{cases} \quad (5.14)$$

The stability and the L_∞ performance of the proposed interval observer are satisfied.

Proof. To prove the stability of (5.7) and the L_∞ performance (5.9), sufficient conditions are given in terms of LMIs based on CQLF given by $V(e_k^d) = e_k^{dT} P e_k^d$, $P^T = P \succ 0$, $P \in \mathbb{R}^{2n_x \times 2n_x}$. Note that $P > 0$ since it is a diagonal matrix. Thus, based on Assumption 21,

$P\mathcal{A}_q$ is also nonnegative for all $q = 1, \dots, N$ and the inequality (5.10) is satisfied. The time difference of $V(e_k^d)$ is given by

$$\begin{aligned}\Delta V(e_k^d) &= V(e_k^d + 1) - V(e_k^d) \\ &= e_k^d + 1^T P e_k^d + 1 - e_k^{dT} P e_k^d \\ &= (\mathcal{A}_q e_k^d + \mathcal{H}_q d_k)^T P (\mathcal{A}_q e_k^d + \mathcal{H}_q d_k) - e_k^{dT} P e_k^d \\ &= e_k^{dT} \mathcal{A}_q^T P \mathcal{A}_q e_k^d + e_k^{dT} \mathcal{A}_q^T P \mathcal{H}_q d_k + d_k^T \mathcal{H}_q^T P \mathcal{A}_q e_k^d + d_k^T \mathcal{H}_q^T P \mathcal{H}_q d_k \\ &\quad - e_k^{dT} P e_k^d.\end{aligned}\tag{5.15}$$

From (5.15), $\Delta V(e_k^d)$ can be rewritten as

$$\Delta V(e_k^d) = \begin{bmatrix} e_k^d \\ d_k \end{bmatrix}^T \begin{bmatrix} \mathcal{A}_q^T P \mathcal{A}_q - P & \mathcal{A}_q^T P \mathcal{H}_q \\ * & \mathcal{H}_q^T P \mathcal{H}_q \end{bmatrix} \begin{bmatrix} e_k^d \\ d_k \end{bmatrix}.$$

If inequality (5.11) holds, then it can be rewritten as

$$\begin{bmatrix} (\lambda - 1)P & 0 & (P\mathcal{A}_q)^T \\ * & -\mu I_{n_d} & (P\mathcal{H}_q)^T \\ * & * & -P \end{bmatrix} \prec 0.\tag{5.16}$$

It can also be easily shown by pre- and post- multiplying (5.16) with $\begin{bmatrix} I_{2n_x} & 0 & \mathcal{A}_q^T \\ 0 & I_{n_d} & \mathcal{H}_q^T \end{bmatrix}$

and its transpose, respectively, that (5.17) yields

$$\begin{bmatrix} \mathcal{A}_q^T P \mathcal{A}_q - P & \mathcal{A}_q^T P \mathcal{H}_q \\ * & \mathcal{H}_q^T P \mathcal{H}_q \end{bmatrix} + \begin{bmatrix} \lambda P & 0 \\ * & -\mu I_{n_d} \end{bmatrix} \prec 0.\tag{5.17}$$

In addition, pre- and post-multiplying (5.17) with $[e_k^{dT} \quad d_k^T]$ and its transpose,

$$\begin{bmatrix} e_k^d \\ d_k \end{bmatrix}^T \begin{bmatrix} \mathcal{A}_q^T P \mathcal{A}_q - P & \mathcal{A}_q^T P \mathcal{H}_q \\ * & \mathcal{H}_q^T P \mathcal{H}_q \end{bmatrix} \begin{bmatrix} e_k^d \\ d_k \end{bmatrix} + \begin{bmatrix} e_k^d \\ d_k \end{bmatrix}^T \begin{bmatrix} \lambda P & 0 \\ * & -\mu I_{n_d} \end{bmatrix} \begin{bmatrix} e_k^d \\ d_k \end{bmatrix} \prec 0,$$

it follows that

$$\begin{aligned}\Delta V(e_k^d) + \lambda e_k^{dT} P e_k^d - \mu d_k^T d_k &< 0, \\ \Delta V(e_k^d) &< -\lambda V(e_k^d) + \mu d_k^T d_k.\end{aligned}\tag{5.18}$$

When $w_k = 0$ and $v_k = 0$, it implies that $d_k = 0$ and (5.18) is equivalent to

$$\Delta V(e_k^d) = V(e_k^d + 1) - V(e_k^d) < -\lambda V(e_k^d) < 0.$$

Accordingly, the error system in (5.7) is stable. Furthermore, inequality (5.18) can be rewritten as

$$V(e_k^d + 1) < (1 - \lambda)V(e_k^d) + \mu \theta_d^2.\tag{5.19}$$

From (5.19), one can obtain

$$\begin{aligned} V(e_k^d) &\leq (1-\lambda)^k V(e_0^d) + \mu \sum_{\tau=0}^{k-1} (1-\lambda)^\tau \theta_d^2 \\ &\leq (1-\lambda)^k V(e_0^d) + \mu \frac{(1-\lambda^k)}{\lambda} \theta_d^2 \\ &\leq (1-\lambda)^k V(e_0^d) + \frac{\mu \theta_d^2}{\lambda}. \end{aligned} \quad (5.20)$$

Based on the Schur complement lemma, (5.12) is equivalent to

$$\begin{bmatrix} \lambda P & 0 \\ * & (\gamma - \mu) I_{n_d} \end{bmatrix} - \frac{1}{\gamma} \begin{bmatrix} I_{2n_x} \\ 0 \end{bmatrix} \begin{bmatrix} I_{2n_x} & 0 \end{bmatrix} \succ 0. \quad (5.21)$$

Then, pre-multiplying and post-multiplying (5.21) with $[e_k^{dT} \quad d_k^T]$ and its transpose, one can get

$$e_k^{dT} e_k^d \leq \gamma (\lambda V(e_k^d) + (\gamma - \mu) \theta_d^2). \quad (5.22)$$

Substituting (5.20) into (5.22) gives

$$\begin{aligned} e_k^{dT} e_k^d &\leq \gamma \left(\lambda \left((1-\lambda)^k V(e_0^d) + \frac{\mu \theta_d^2}{\lambda} \right) + (\gamma - \mu) \theta_d^2 \right) \\ &\leq \gamma \left(\lambda (1-\lambda)^k V(e_0^d) + \gamma \theta_d^2 \right). \end{aligned}$$

In addition, the matrix inequality in (5.13) implies that

$$\begin{bmatrix} e_k^d \\ \tilde{v}_k \end{bmatrix}^T \begin{bmatrix} C^T C - \gamma_1^2 I_{2n_x} & C^T \mathcal{V} \\ * & -\gamma_2^2 I_{2n_x} + \mathcal{V}^T \mathcal{V} \end{bmatrix} \begin{bmatrix} e_k^d \\ \tilde{v}_k \end{bmatrix} < 0,$$

which follows

$$\begin{aligned} r_k^{dT} r_k^d &\leq \gamma_1^2 e_k^{dT} e_k^d + \gamma_2^2 \tilde{v}_k^T \tilde{v}_k \\ &\leq \gamma_1^2 \gamma \left(\lambda (1-\lambda)^k V(e_0^d) + \gamma \theta_d^2 \right) + \gamma_2^2 \theta_v^2. \end{aligned}$$

Therefore, the L_∞ criterion (5.9) is satisfied. \square

Even though we have proposed in Theorem 14 a robust FD interval observer to design residual framers, in some cases, it is rarely possible to find gains \bar{L}_q and \underline{L}_q such that the matrices $A_q - \bar{L}_q C$ and $A_q - \underline{L}_q C$ are nonnegative. Inspired by the structure of the observer proposed in [176], a novel FD interval observer is introduced in the sequel. The proposed observer can reduce the conservatism of gain matrices and provide more degree of freedom by introducing weighted matrices \bar{T}_q , \underline{T}_q , \bar{N}_q and \underline{N}_q .

5.3.2 Interval observer design: TNL structure

We propose the following FD interval observer for system (5.1)

$$\left\{ \begin{array}{l} \bar{\xi}_{k+1} = \bar{T}_q A_q \bar{x}_k + \bar{T}_q B_q u_k + \bar{L}_q (y_k - C \bar{x}_k) + \bar{\Delta} \\ \bar{x}_k = \bar{\xi}_k + \bar{N}_q y_k \\ \underline{\xi}_{k+1} = \underline{T}_q A_q \underline{x}_k + \underline{T}_q B_q u_k + \underline{L}_q (y_k - C \underline{x}_k) + \underline{\Delta} \\ \underline{x}_k = \underline{\xi}_k + \underline{N}_q y_k \\ \bar{y}_k = C^+ \bar{x}_k - C^- \underline{x}_k + D_v^+ \bar{v} - D_v^- \underline{v} \\ \underline{y}_k = C^+ \underline{x}_k - C^- \bar{x}_k + D_v^+ \underline{v} - D_v^- \bar{v} \\ \bar{r}_k = \bar{y}_k - y_k \\ \underline{r}_k = \underline{y}_k - y_k \end{array} \right. \quad (5.23)$$

where $\bar{\xi}_k, \underline{\xi}_k \in \mathbb{R}^{n_x}$ are intermediate variables, $\bar{x}_k, \underline{x}_k \in \mathbb{R}^{n_x}$ are the estimated upper and lower bounds of x_k respectively. $\bar{\Delta}$ and $\underline{\Delta}$ are given by:

$$\begin{cases} \bar{\Delta} = (\bar{T}_q D_q)^+ \bar{w} - (\bar{T}_q D_q)^- \underline{w} + (\bar{L}_q D_v)^+ \bar{v} - (\bar{L}_q D_v)^- \underline{v} + (\bar{N}_q D_v)^+ \bar{v} - (\bar{N}_q D_v)^- \underline{v} \\ \underline{\Delta} = (\underline{T}_q D_q)^+ \underline{w} - (\underline{T}_q D_q)^- \bar{w} + (\underline{L}_q D_v)^+ \underline{v} - (\underline{L}_q D_v)^- \bar{v} + (\underline{N}_q D_v)^+ \underline{v} - (\underline{N}_q D_v)^- \bar{v}. \end{cases}$$

In (5.23), $\bar{L}_q \in \mathbb{R}^{n_x \times n_y}$ and $\underline{L}_q \in \mathbb{R}^{n_x \times n_y}$ are the observer gains. $\bar{T}_q \in \mathbb{R}^{n_x \times n_x}$, $\underline{T}_q \in \mathbb{R}^{n_x \times n_x}$, $\bar{N}_q \in \mathbb{R}^{n_x \times n_y}$ and $\underline{N}_q \in \mathbb{R}^{n_x \times n_y}$ are constant matrices that should be designed to satisfy

$$\bar{T}_q + \bar{N}_q C = I_{n_x} \quad (5.24)$$

$$\underline{T}_q + \underline{N}_q C = I_{n_x}. \quad (5.25)$$

Lemma 9. [197] *Given matrices $A \in \mathbb{R}^{a \times b}$, $B \in \mathbb{R}^{b \times c}$ and $C \in \mathbb{R}^{a \times c}$, if $\text{rank}(B) = c$, then the general solution of the following equation $AB = C$ is given by*

$$A = CB^\dagger + S(I - BB^\dagger),$$

where B^\dagger represents the pseudo-inverse of B , defined by $B^\dagger = B^T(BB^T)^{-1}$, and $S \in \mathbb{R}^{a \times b}$ is an arbitrary matrix.

Based on Lemma 9, the general solutions of (5.24) and (5.25) are given by

$$\begin{bmatrix} \bar{T}_q & \bar{N}_q \end{bmatrix} = \begin{bmatrix} I_{n_x} \\ C \end{bmatrix}^\dagger + \bar{S}_q \left(I_{n_x+n_y} - \begin{bmatrix} I_{n_x} \\ C \end{bmatrix} \begin{bmatrix} I_{n_x} \\ C \end{bmatrix}^\dagger \right), \quad (5.26)$$

$$\begin{bmatrix} \underline{T}_q & \underline{N}_q \end{bmatrix} = \begin{bmatrix} I_{n_x} \\ C \end{bmatrix}^\dagger + \underline{S}_q \left(I_{n_x+n_y} - \begin{bmatrix} I_{n_x} \\ C \end{bmatrix} \begin{bmatrix} I_{n_x} \\ C \end{bmatrix}^\dagger \right), \quad (5.27)$$

where $\bar{S}_q, \underline{S}_q \in \mathbb{R}^{n_x \times (n_x+n_y)}$ for $q = 1, \dots, N$ are arbitrary matrices which are designed such that all matrices $\bar{T}_q, \underline{T}_q$ are of full rank.

Under the new structure of the proposed FD interval observer (5.23), the objective is to compute the observer gains \bar{L}_q and \underline{L}_q that minimize the effect of state disturbances and measurement noise on the upper and lower bounds of the residual vectors $\bar{r}_k, \underline{r}_k$, respectively. Let $\bar{e}_k = \bar{x}_k - x_k$ and $\underline{e}_k = x_k - \underline{x}_k$ be the upper and the lower estimation errors. By combining (5.1), (5.24) and (5.25), x_{k+1} can be written in two different ways:

$$\begin{aligned} x_{k+1} &= (\bar{T}_q + \bar{N}_q C)x_{k+1} \\ &= \bar{T}_q x_{k+1} + \bar{N}_q (y_{k+1} - D_v v_{k+1} - F f_{k+1}) \\ &= \bar{T}_q A_q x_k + \bar{T}_q B_q u_k + \bar{T}_q D_q w_k + \bar{N}_q y_{k+1} - \bar{N}_q D_v v_{k+1} - \bar{N}_q F f_{k+1}, \end{aligned} \quad (5.28)$$

$$\begin{aligned} x_{k+1} &= (\underline{T}_q + \underline{N}_q C)x_{k+1} \\ &= \underline{T}_q x_{k+1} + \underline{N}_q (y_{k+1} - D_v v_{k+1} - F f_{k+1}) \\ &= \underline{T}_q A_q x_k + \underline{T}_q B_q u_k + \underline{T}_q D_q w_k + \underline{N}_q y_{k+1} - \underline{N}_q D_v v_{k+1} - \underline{N}_q F f_{k+1}. \end{aligned} \quad (5.29)$$

Then, the dynamics of the upper and lower errors are given by:

$$\begin{cases} \bar{e}_{k+1} = (\bar{T}_q A_q - \bar{L}_q C)\bar{e}_k + \bar{\Delta} + \bar{L}_q D_v v_k + \bar{N}_q D_v v_{k+1} \\ \quad - \bar{T}_q D_q w_k + \bar{L}_q F f_k + \bar{N}_q F f_{k+1} \\ \underline{e}_{k+1} = (\underline{T}_q A_q - \underline{L}_q C)\underline{e}_k - \underline{\Delta} - \underline{L}_q D_v v_k - \underline{N}_q D_v v_{k+1} \\ \quad + \underline{T}_q D_q w_k - \underline{L}_q F f_k - \underline{N}_q F f_{k+1}. \end{cases} \quad (5.30)$$

We introduce

$$\bar{d}_k = \begin{bmatrix} \bar{\Delta} - \bar{T}_q D_q w_k \\ D_v v_k \\ D_v v_{k+1} \end{bmatrix}, \quad \underline{d}_k = \begin{bmatrix} -\underline{\Delta} + \underline{T}_q D_q w_k \\ -D_v v_k \\ -D_v v_{k+1} \end{bmatrix}, \quad \tilde{f}_k = \begin{bmatrix} f_k \\ f_{k+1} \end{bmatrix}.$$

Accordingly, the error dynamics in (5.30) can be rewritten as

$$\begin{cases} \bar{e}_{k+1} = (\bar{T}_q A_q - \bar{L}_q C) \bar{e}_k + \bar{H}_q \bar{d}_k + \bar{F}_q \tilde{f}_k \\ \underline{e}_{k+1} = (\underline{T}_q A_q - \underline{L}_q C) \underline{e}_k + \underline{H}_q \underline{d}_k + \underline{E}_q \tilde{f}_k, \end{cases} \quad (5.31)$$

where

$$\bar{H}_q = \begin{bmatrix} I_n \\ \bar{L}_q^T \\ \bar{N}_q^T \end{bmatrix}^T, \quad \underline{H}_q = \begin{bmatrix} I_n \\ \underline{L}_q^T \\ \underline{N}_q^T \end{bmatrix}^T, \quad \bar{F}_q = \begin{bmatrix} (\bar{L}_q F)^T \\ (\bar{N}_q F)^T \end{bmatrix}^T, \quad \underline{E}_q = \begin{bmatrix} -(\underline{L}_q F)^T \\ -(\underline{N}_q F)^T \end{bmatrix}^T.$$

Based on the error system (5.31), the nonnegativity, the stability and the robustness of the proposed interval observer are studied in the following theorems.

Theorem 15. *For system (5.1), \bar{x}_k and \underline{x}_k in (5.23) satisfy the following inequality*

$$\underline{x}_k \leq x_k \leq \bar{x}_k,$$

in the fault free case, if $\bar{T}_q A_q - \bar{L}_q C$ and $\underline{T}_q A_q - \underline{L}_q C$ are nonnegative for all $k \geq 0$ and $\bar{x}_0, \underline{x}_0$ are chosen such that $\underline{x}_0 \leq x_0 \leq \bar{x}_0$.

Proof. In the fault free case ($f = 0$), according to Assumption 18, we have

$$\begin{aligned} \bar{\Delta} - \bar{T}_q D_q w_k + \bar{L}_q D_v v_k + \bar{N}_q D_v v_{k+1} &\geq 0 \\ -\underline{\Delta} + \underline{T}_q D_q w_k - \underline{L}_q D_v v_k - \underline{N}_q D_v v_{k+1} &\geq 0. \end{aligned}$$

In addition, let Assumption 20 be satisfied. Then, $\bar{e}_0 \geq 0$ and $\underline{e}_0 \geq 0$. Applying Lemma 3 to (5.30), the inequality

$$\underline{x}_0 \leq x_0 \leq \bar{x}_0$$

hold for all $k \geq 0$ if $\bar{T}_q A_q - \bar{L}_q C$ and $\underline{T}_q A_q - \underline{L}_q C$ are nonnegative. \square

In order to study the stability of the proposed residual framers, we propose a new augmented state defined by $\mathcal{E}_k = [\bar{e}_k^T \quad \underline{e}_k^T]^T$ and $\mathcal{R}_k = [\bar{r}_k^T \quad \underline{r}_k^T]^T$. The corresponding augmented system can be deduced:

$$\begin{cases} \mathcal{E}_{k+1} = \mathcal{A}_q \mathcal{E}_k + \mathcal{H}_q d_k + \tilde{\mathcal{F}}_q \tilde{f}_k \\ \mathcal{R}_k = \mathcal{C} \mathcal{E}_k + \mathcal{V} \tilde{v}_k + \mathcal{F} f_k, \end{cases} \quad (5.32)$$

where

$$\mathcal{A}_q = \begin{bmatrix} \bar{T}_q A_q - \bar{L}_q C & 0 \\ 0 & \underline{T}_q A_q - \underline{L}_q C \end{bmatrix}, \quad \mathcal{H}_q = \begin{bmatrix} \bar{H}_q & 0 \\ 0 & \underline{H}_q \end{bmatrix}, \quad \tilde{\mathcal{F}}_q = \begin{bmatrix} \bar{F}_q \\ \underline{E}_q \end{bmatrix}, \quad d_k = \begin{bmatrix} \bar{d}_k \\ \underline{d}_k \end{bmatrix},$$

$$\mathcal{F} = \begin{bmatrix} -F \\ -F \end{bmatrix}, \mathcal{C} = \begin{bmatrix} C^+ & C^- \\ -C^- & -C^+ \end{bmatrix}, \mathcal{V} = \begin{bmatrix} -D_v & D_v^+ & -D_v^- \\ -D_v & -D_v^- & D_v^+ \end{bmatrix}, \tilde{v}_k = \begin{bmatrix} v_k \\ \bar{v} \\ \underline{v} \end{bmatrix}.$$

The error dynamics in (5.32) can be split into two subsystems where (5.33) is decoupled from the effects of $f(k)$ and (5.34) is only affected by the sensor fault.

$$\begin{cases} \mathcal{E}_{k+1}^d = A_q \mathcal{E}_k^d + \mathcal{H}_q d_k \\ \mathcal{R}_k^d = \mathcal{C} \mathcal{E}_k^d + \mathcal{V} \tilde{v}_k, \end{cases} \quad (5.33)$$

$$\begin{cases} \mathcal{E}_{k+1}^f = A_q \mathcal{E}_k^f + \tilde{\mathcal{F}}_q \tilde{f}_k \\ \mathcal{R}_k^f = \mathcal{C} \mathcal{E}_k^f + \mathcal{F} f_k, \end{cases} \quad (5.34)$$

where $\mathcal{E}_k = \mathcal{E}_k^f + \mathcal{E}_k^d$.

The objective in the sequel is to design a FD observer (5.23) such that the error system in (5.33) is stable and the effect of disturbances is minimized and thus the FD accuracy is improved. For this end, we use the well known L_∞ technique such that for given scalars $\gamma > 0$, $\gamma_1 > 0$, $\gamma_2 > 0$ and $0 < \lambda < 1$, the residual signal \mathcal{R}^d should satisfy the following inequality

$$\|\mathcal{R}^d\| < \sqrt{\gamma_1^2(\gamma(\lambda(1-\lambda)^k V_0 + \gamma \theta_d^2)) + \gamma_2^2 \theta_v^2}, \quad (5.35)$$

where $V(\mathcal{E}_0^d) = \mathcal{E}_0^{dT} P \mathcal{E}_0^d$ and $P \succ 0 \in \mathbb{R}^{2n_x \times 2n_x}$.

Theorem 16. *Given scalars $\gamma > 0$, $\gamma_1 > 0$, $\gamma_2 > 0$ and $0 < \lambda < 1$, the error dynamics system in (5.33) are stable and \mathcal{R}^d satisfies the L_∞ performance, if there exist a constant $\mu > 0$, a diagonal matrix $P = \begin{bmatrix} P_1 & 0 \\ 0 & P_2 \end{bmatrix} \succ 0$, $P = P^T \succ 0$, $P \in \mathbb{R}^{2n_x \times 2n_x}$ with diagonal matrices P_1, P_2 and constant matrices $W_{q1}, W_{q2} \in \mathbb{R}^{n_x \times n_y}$ and $Y_{q1}, Y_{q2} \in \mathbb{R}^{n_x \times (n_x + n_y)}$ for $q = 1, 2, \dots, N$ such that:*

$$\begin{bmatrix} P_1 \Theta^\dagger \alpha_1 A_q + Y_{q1} \Psi \alpha_1 A_q - W_{q1} C & 0 \\ * & P_2 \Theta^\dagger \alpha_1 A_q + Y_{q2} \Psi \alpha_1 A_q - W_{q2} C \end{bmatrix} \geq 0, \quad (5.36)$$

$$\begin{bmatrix} \Upsilon_{11} & 0 & \Upsilon_{13} \\ * & -\mu I_{n_d} & \Upsilon_{23} \\ * & * & \Upsilon_{33} \end{bmatrix} \prec 0, \quad (5.37)$$

$$\begin{bmatrix} \lambda P & 0 & I_{2n_x} \\ * & (\gamma - \mu) I_{n_d} & 0 \\ * & * & \gamma I_{2n_x} \end{bmatrix} \succ 0, \quad (5.38)$$

$$\begin{bmatrix} \mathcal{C}^T \mathcal{C} - \gamma_1^2 I_{2n_x} & \mathcal{C}^T \mathcal{V} \\ * & -\gamma_2^2 I_{2n_x} + \mathcal{V}^T \mathcal{V} \end{bmatrix} \prec 0, \quad (5.39)$$

where

$$\Upsilon_{11} = \begin{bmatrix} (\lambda - 1) P_1 & 0 \\ * & (\lambda - 1) P_2 \end{bmatrix}, \Upsilon_{33} = \begin{bmatrix} -P_1 & 0 \\ * & -P_2 \end{bmatrix},$$

$$\Upsilon_{13} = \begin{bmatrix} P_1 \Theta^\dagger \alpha_1 A_q + Y_{q1} \Psi \alpha_1 A_q - W_{q1} C & 0 \\ * & P_2 \Theta^\dagger \alpha_1 A_q + Y_{q2} \Psi \alpha_1 A_q - W_{q2} C \end{bmatrix}^T,$$

$$\Upsilon_{23} = \begin{bmatrix} P_1 & W_{q1} & P_1\Theta^\dagger\alpha_2 + Y_{q1}\Psi\alpha_2 & 0 & 0 & 0 \\ 0 & 0 & 0 & P_2 & W_{q2} & P_2\Theta^\dagger\alpha_2 + Y_{q2}\Psi\alpha_2 \end{bmatrix}^T$$

and

$$\alpha_1 = \begin{bmatrix} I_{n_x} \\ 0 \end{bmatrix}, \alpha_2 = \begin{bmatrix} 0 \\ I_{n_y} \end{bmatrix}, \Theta = \begin{bmatrix} I_{n_x} \\ C \end{bmatrix}, \Psi = I_{n_x+n_y} - \Theta\Theta^\dagger.$$

Moreover, the observer gains $\bar{L}_q, \underline{L}_q, \bar{T}_q, \underline{T}_q, \bar{N}_q$ and \underline{N}_q are given by:

$$\begin{cases} \bar{L}_q = P_1^{-1}W_{q1} \\ \underline{L}_q = P_2^{-1}W_{q2} \\ \bar{T}_q = \Theta^\dagger\alpha_1 + P_1^{-1}Y_{q1}\Psi\alpha_1 \\ \underline{T}_q = \Theta^\dagger\alpha_1 + P_2^{-1}Y_{q2}\Psi\alpha_1 \\ \bar{N}_q = \Theta^\dagger\alpha_2 + P_1^{-1}Y_{q1}\Psi\alpha_2 \\ \underline{N}_q = \Theta^\dagger\alpha_2 + P_2^{-1}Y_{q2}\Psi\alpha_2. \end{cases} \quad (5.40)$$

Proof. The proof is available in Appendix A. \square

Remark 16. It has been shown in the literature that it is rarely possible to find gains \bar{L}_q and \underline{L}_q such that the matrices $A_q - \bar{L}_q C$ and $A_q - \underline{L}_q C$ are nonnegative. However, the interval observer given by equation (5.23) can reduce the conservatism of gain matrices and brings more degree of freedom. The designed LMIs conditions are relaxed by introducing weighted matrices $\bar{T}_q, \underline{T}_q, \bar{N}_q$ and \underline{N}_q using CQLF under an arbitrary switching signal. However, the existence of such a function is not always guaranteed. Therefore, MQLF with an ADT switching signal are introduced in the following to reduce the conservatism.

5.4 Multiple Lyapunov functions based-approach

In this part, the stability analysis is analysed by applying MQLF with an ADT switching signal. Two subsections are introduced in the sequel. The first one deals with the stability analysis of the traditional interval observer, while the second concerns the novel structure (TNL) of the FD interval observer.

5.4.1 Interval observer scheme for switched systems

The results given by Theorem 14 can be extended to achieve the interval FD of sensor faults using MQLF. New LMIs conditions are developed hereafter in the following theorem.

Theorem 17. Let Assumption 20 hold and suppose that there exists a piecewise Lyapunov function $V_q(e_k^d)$ where $V_q(e_k^d) = e_k^{dT} P_q e_k^d$. Given scalars $\gamma > 0, \gamma_1 > 0, \gamma_2 > 0, 0 < \lambda < 1$ and $0 < \beta < 1$, the error dynamics system in (5.7) are stable and r^d satisfies the L_∞ performance, if there exist a constant $\mu > 0, a_2 > a_1 > 0$, diagonal matrices $P_q \in \mathbb{R}^{2n_x \times 2n_x}$ such that $P_q = \begin{bmatrix} P_{q1} & 0 \\ 0 & P_{q2} \end{bmatrix} > 0, P_q = P_q^T > 0$ with diagonal matrices P_{q1}, P_{q2} and constant matrices $M_l \in \mathbb{R}^{2n_x \times 2n_x}, W_{q1}, W_{q2} \in \mathbb{R}^{n_x \times n_y}$ for $q = 1, 2, \dots, N$ such that:

$$\min_{P_q, q \in \mathcal{I}} \beta\rho + (1 - \beta)\mu, \quad (5.41)$$

$$a_1 I_{2n_x} \leq P_q \leq a_2 I_{2n_x}, \quad (5.42)$$

$$\begin{bmatrix} P_{q1}A_q - W_{q1}C & 0 \\ * & P_{q2}A_q - W_{q2}C \end{bmatrix} \geq 0, \quad (5.43)$$

$$\begin{bmatrix} \Omega_{q11} & 0 & \Omega_{q13} \\ * & -\mu I_{n_d} & \Omega_{q23} \\ * & * & \Omega_{q33} \end{bmatrix} \prec 0, \quad (5.44)$$

$$\begin{bmatrix} \lambda P_q & 0 & I_{2n_x} \\ * & (\gamma - \mu)I_{n_d} & 0 \\ * & * & \gamma I_{2n_x} \end{bmatrix} \succ 0, \quad (5.45)$$

$$\begin{bmatrix} \mathcal{C}^T \mathcal{C} - \gamma_1^2 I_{2n_x} & \mathcal{C}^T \mathcal{V} \\ * & -\gamma_2^2 I_{2n_x} + \mathcal{V}^T \mathcal{V} \end{bmatrix} \prec 0, \quad (5.46)$$

$$\begin{bmatrix} M_l & P_q \\ P_q & P_q \end{bmatrix} \succeq 0, \quad (5.47)$$

hold for all $q, l \in \mathcal{I}, q \neq l$. In addition, the estimation errors are stable under a switching signal with an ADT τ_a satisfying:

$$\tau_a > \tau_a^* = -\frac{\ln(\rho)}{\ln(1 - \lambda)}, \quad (5.48)$$

where $\rho = \frac{a_2}{a_1}$ and the observer gains $\bar{L}_q, \underline{L}_q$ are given by:

$$\begin{cases} \bar{L}_q = P_{q1}^{-1} W_{q1} \\ \underline{L}_q = P_{q2}^{-1} W_{q2}. \end{cases} \quad (5.49)$$

Moreover, the interval error (5.7) satisfies:

$$\lim_{k \rightarrow \infty} \|e_0^d\| < \frac{\mu}{a_1 \lambda} \theta_d^2,$$

where $\theta_d = \|d\|_\infty$ and

$$\begin{aligned} \Omega_{q11} &= \begin{bmatrix} (\lambda - 1)P_{q1} & 0 \\ * & (\lambda - 1)P_{q2} \end{bmatrix}, \quad \Omega_{q13} = \begin{bmatrix} P_{q1}A_q - W_{q1}C & 0 \\ * & P_{q2}A_q - W_{q2}C \end{bmatrix}^T, \\ \Omega_{q23} &= \begin{bmatrix} P_{q1} & W_{q1} & 0 & 0 \\ 0 & 0 & P_{q2} & W_{q2} \end{bmatrix}^T, \quad \Omega_{q33} = \begin{bmatrix} -P_{q1} & 0 \\ * & -P_{q2} \end{bmatrix}. \end{aligned}$$

Proof. First of all, the requirement on the nonnegativity property of the matrices $A_q - \bar{L}_q C$ and $A_q - \underline{L}_q C$ is achieved via the inequality (5.43). We are interested in checking the stability of the estimation errors via MQLF for the proposed interval observer in (5.2). According to (5.20), we have

$$V_q(e_k^d) \leq (1 - \lambda)^k V_q(e_0^d) + \frac{\mu \theta_d^2}{\lambda}.$$

Based on Lemma 3, the following inequality

$$a_1 \|e_k^d\| \leq V_q(e_k^d),$$

allows one to deduce that

$$\|e_k^d\| \leq \frac{1}{a_1}((1-\lambda)^k V_q(e_0^d) + \frac{\mu \theta_d^2}{\lambda}).$$

When $k \rightarrow \infty$, one can deduce that:

$$\lim_{k \rightarrow \infty} \|e_k^d\| < \frac{\mu}{a_1 \lambda} \theta_d^2.$$

Therefore, it has been shown that the interval error width is asymptotically upper bounded by $\frac{\mu}{a_1 \lambda} \theta_d^2$ which should be made as small as possible to improve the accuracy of FD. One highlights that this bound depends on μ , for a given a_1 and λ . Consequently, the minimization of μ allows one reducing the interval width of the estimation error and thus the interval width of the residual signal. We aim also to minimize ρ to look for optimum dwell time. The resolution of such a problem leads to solving a problem of linear optimization which consists of seeking a minimization function. Then, the objective function can be added to the LMIs conditions and expressed as:

$$\beta \rho + (1 - \beta) \mu,$$

where the weight β is in the range $[0, 1]$.

Let us now focus on the stabilization of subsystems at the switching instants. The inequality defined in (3.46) in chapter 3 becomes:

$$\rho P_l - P_q \succeq 0, \quad (5.50)$$

where $q, l \in \mathcal{I}, q \neq l$, q is the current mode. Then applying the Schur complement lemma, (5.50) implies:

$$\begin{bmatrix} \rho P_l & I_{2n_x} \\ I_{2n_x} & P_q^{-1} \end{bmatrix} \succeq 0. \quad (5.51)$$

The multiplication of both side of (5.51) by $\begin{bmatrix} I_{2n_x} & O_{2n_x} \\ O_{2n_x} & P_q \end{bmatrix}$ yields $\begin{bmatrix} M_l & P_q \\ P_q & P_q \end{bmatrix} \succeq 0$ where $M_l = \rho P_l$. Therefore, (5.47) is verified. LMIs conditions in (5.44), (5.45) and (5.46) have been proven in Theorem 14. \square

Remark 17. *The requirement of CQLF remains a restrictive condition to introduce stability conditions. Accordingly, for the sake of less conservative conditions, MQLF are adopted with an ADT switching signal. LMIs conditions are developed in the previous theorem based on FD interval observers. However, as mentioned before in this work, it is rarely possible to find gains \bar{L}_q and \underline{L}_q such that the matrices $A_q - \bar{L}_q C$ and $A_q - \underline{L}_q C$ are nonnegative even though we have used MQLF. In the sequel, the conservatism of gain matrices is reduced and more degree of freedom is provided by integrating at the same time weighted matrices \bar{T}_q , \underline{T}_q , \bar{N}_q and \underline{N}_q and based on the construction of MQLF.*

5.4.2 Interval observer scheme: TNL structure

The results given by Theorem 16 are extended and new LMIs conditions are developed hereafter in the following theorem based on MQLF with an ADT switching signal.

Theorem 18. *Let Assumption 20 hold and suppose that there exists a piecewise Lyapunov function $V_q(\mathcal{E}_k^d)$ where $V_q(\mathcal{E}_k^d) = \mathcal{E}_k^{dT} P_q \mathcal{E}_k^d$. Given scalars $\gamma > 0$, $\gamma_1 > 0$, $\gamma_2 > 0$, $0 < \lambda < 1$ and $0 < \beta < 1$, the error dynamics system in (5.33) are stable and \mathcal{R}^d satisfies the L_∞ performance, if there exist a constant $\mu > 0$, $a_2 > a_1 > 0$, diagonal matrices $P_q \in \mathbb{R}^{2n_x \times 2n_x}$ such that $P_q = \begin{bmatrix} P_{q1} & 0 \\ 0 & P_{q2} \end{bmatrix} > 0$, $P_q = P_q^T > 0$ with diagonal matrices P_{q1} , P_{q1} and constant matrices $M_l \in \mathbb{R}^{2n_x \times 2n_x}$, $W_{q1}, W_{q2} \in \mathbb{R}^{n_x \times n_y}$, $Y_{q1}, Y_{q2} \in \mathbb{R}^{n_x \times (n_x + n_y)}$, for $q = 1, 2, \dots, N$ such that:*

$$\min_{P_q, q \in \mathcal{I}} \beta \rho + (1 - \beta) \mu, \quad (5.52)$$

$$a_1 I_{2n_x} \leq P_q \leq a_2 I_{2n_x}, \quad (5.53)$$

$$\begin{bmatrix} P_{q1} \Theta^\dagger \alpha_1 A_q + Y_{q1} \Psi \alpha_1 A_q - W_{q1} C & 0 \\ * & P_{q2} \Theta^\dagger \alpha_1 A_q + Y_{q2} \Psi \alpha_1 A_q - W_{q2} C \end{bmatrix} \geq 0, \quad (5.54)$$

$$\begin{bmatrix} \Upsilon_{q11} & 0 & \Upsilon_{q13} \\ * & -\mu I_{n_d} & \Upsilon_{q23} \\ * & * & \Upsilon_{q33} \end{bmatrix} < 0, \quad (5.55)$$

$$\begin{bmatrix} \lambda P_q & 0 & I_{2n_x} \\ * & (\gamma - \mu) I_{n_d} & 0 \\ * & * & \gamma I_{2n_x} \end{bmatrix} \succ 0, \quad (5.56)$$

$$\begin{bmatrix} \mathcal{C}^T \mathcal{C} - \gamma_1^2 I_{2n_x} & \mathcal{C}^T \mathcal{V} \\ * & -\gamma_2^2 I_{2n_x} + \mathcal{V}^T \mathcal{V} \end{bmatrix} < 0, \quad (5.57)$$

$$\begin{bmatrix} M_l & P_q \\ P_q & P_q \end{bmatrix} \succeq 0, \quad (5.58)$$

hold for all $q, l \in \mathcal{I}, q \neq l$ where

$$\Upsilon_{q11} = \begin{bmatrix} (\lambda - 1) P_{q1} & 0 \\ * & (\lambda - 1) P_{q2} \end{bmatrix}, \quad \Upsilon_{q33} = \begin{bmatrix} -P_{q1} & 0 \\ * & -P_{q2} \end{bmatrix},$$

$$\Upsilon_{q13} = \begin{bmatrix} P_{q1} \Theta^\dagger \alpha_1 A_q + Y_{q1} \Psi \alpha_1 A_q - W_{q1} C & 0 \\ * & P_{q2} \Theta^\dagger \alpha_1 A_q + Y_{q2} \Psi \alpha_1 A_q - W_{q2} C \end{bmatrix}^T,$$

$$\Upsilon_{q23} = \begin{bmatrix} P_{q1} & W_{q1} & P_{q1} \Theta^\dagger \alpha_2 + Y_{q1} \Psi \alpha_2 & 0 & 0 & 0 \\ 0 & 0 & 0 & P_{q2} & W_{q2} & P_{q2} \Theta^\dagger \alpha_2 + Y_{q2} \Psi \alpha_2 \end{bmatrix}^T$$

and

$$\alpha_1 = \begin{bmatrix} I_{n_x} \\ 0 \end{bmatrix}, \quad \alpha_2 = \begin{bmatrix} 0 \\ I_{n_y} \end{bmatrix}, \quad \Theta = \begin{bmatrix} I_{n_x} \\ C \end{bmatrix}, \quad \Psi = I_{n_x + n_y} - \Theta \Theta^\dagger.$$

In addition, the estimation errors are stable under a switching signal with an ADT τ_a satisfying:

$$\tau_a > \tau_a^* = -\frac{\ln(\rho)}{\ln(1 - \lambda)}, \quad (5.59)$$

where $\rho = \frac{a_2}{a_1}$ and the observer gains \bar{L}_q , \underline{L}_q , \bar{T}_q , \underline{T}_q , \bar{N}_q and \underline{N}_q are given by:

$$\begin{cases} \bar{L}_q = P_{q1}^{-1}W_{q1} \\ \underline{L}_q = P_{q2}^{-1}W_{q2} \\ \bar{T}_q = \Theta^\dagger\alpha_1 + P_{q1}^{-1}Y_{q1}\Psi\alpha_1 \\ \underline{T}_q = \Theta^\dagger\alpha_1 + P_{q2}^{-1}Y_{q2}\Psi\alpha_1 \\ \bar{N}_q = \Theta^\dagger\alpha_2 + P_{q1}^{-1}Y_{q1}\Psi\alpha_2 \\ \underline{N}_q = \Theta^\dagger\alpha_2 + P_{q2}^{-1}Y_{q2}\Psi\alpha_2. \end{cases} \quad (5.60)$$

Moreover, the interval error (5.33) satisfies:

$$\lim_{k \rightarrow \infty} \|\mathcal{E}_k^d\| < \frac{\mu}{a_1\lambda}\theta_d^2.$$

Proof. The proof is available in Appendix A. □

5.5 Residual evaluation

Compared with the traditional methods of designing constant or time-varying thresholds, the present method provides a systematic way for residual evaluation based on a belonging test of the zero signal to the residual framers generated by the proposed FD observers. The corresponding FD decision scheme is based on determining whether the zero signal is excluded from the residual intervals or not such that:

$$\begin{cases} 0 \in [\underline{r}_k \ \bar{r}_k] & \text{Fault-free} \\ 0 \notin [\underline{r}_k \ \bar{r}_k] & \text{Faulty.} \end{cases} \quad (5.61)$$

The FD evaluation in (5.61) is deduced from the following relation

$$y_k \notin [\underline{y}_k \ \bar{y}_k]. \quad (5.62)$$

In fact, in the fault free case, the output signal is consistent with the estimation of the proposed interval observer, i.e. $y \in [\underline{y} \ \bar{y}]$. In contrary case, an inconsistency on the output signal is detected and it indicates the existence of a fault. Based on (5.62), the consistency test can be written as follow

$$0 \notin [\underline{y}_k \ \bar{y}_k] - y_k \Rightarrow 0 \notin [\underline{y}_k - y_k \ \bar{y}_k - y_k]. \quad (5.63)$$

If zero is contained in the estimated framers, the system is assumed fault free. Otherwise an alarm is triggered.

In the next section, an illustrative example is introduced to show the efficiency of the developed results using both CQLF and MQLF.

5.6 Numerical example

The numerical example is considered for a discrete-time switched system (5.1) defined with three subsystems, $N = 3$, with:

$$\begin{aligned}
 A_1 &= \begin{pmatrix} 0.6 & 0.5 & 1 \\ 0.2 & 0 & 1 \\ 0 & 0.2 & 0 \end{pmatrix} & A_2 &= \begin{pmatrix} 0.9 & -0.8 & 0 \\ 0.1 & 0 & 1 \\ 0 & 0.5 & 0.1 \end{pmatrix} & A_3 &= \begin{pmatrix} 0.5 & 0.5 & 0.1 \\ 0.4 & 0 & 0.5 \\ 0.1 & 0.2 & 0 \end{pmatrix} \\
 B_1 &= \begin{pmatrix} 1 \\ 0.1 \\ 1.3 \end{pmatrix} & B_2 &= \begin{pmatrix} 0.1 \\ 1 \\ 1 \end{pmatrix} & B_3 &= \begin{pmatrix} 1.2 \\ 1 \\ 0.5 \end{pmatrix} & D_1 &= \begin{pmatrix} 0.05 \\ 0.1 \\ 0 \end{pmatrix} & D_2 &= \begin{pmatrix} 0.05 \\ 0.1 \\ 0 \end{pmatrix} \\
 D_3 &= \begin{pmatrix} 0 \\ 0.1 \\ 0.1 \end{pmatrix} & D_v &= \begin{pmatrix} 0.1 & 0 \\ 0 & 0.1 \end{pmatrix} & F &= \begin{pmatrix} 0.5 \\ -0.5 \end{pmatrix} & C &= \begin{pmatrix} 1.2 & 0.01 & 0 \\ 0.1 & 1.1 & 0.1 \end{pmatrix}
 \end{aligned}$$

Remark 18. *It is pointed out that the matrices C and F are considered to be constant and common for all modes. However, there is no theoretical difficulty with allowing them to be switched.*

In this example, $w_k \in \mathbb{R}$ and $v_k \in \mathbb{R}^2$ are uniformly distributed bounded signals such that $|w_k| \leq 1$ and $|v_k| \leq [0.1 \ 0.1]$. The state initial conditions are set as $x_0 = [0 \ 0 \ 0]^T$, $\underline{x}_0 = [-0.1 \ -0.1 \ -0.1]^T$ and $\bar{x}_0 = [0.1 \ 0.1 \ 0.1]^T$ such that $\underline{x}_0 \leq x_0 \leq \bar{x}_0$. Figure 5.1 shows the evolution of the switching signal. It indicates the active mode of the discrete-time switched system. FD results are given in the sequel adopting firstly CQLF and then MQLF

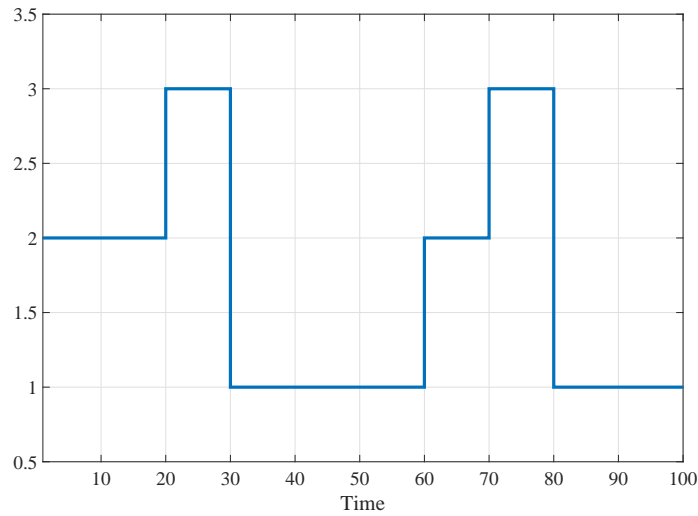


Figure 5.1: Evolution of the switching signal

with an ADT switching signal. The numerical simulation was carried out by using Matlab optimization tools (Yalmip/Sedumi).

5.6.1 Fault detection results based on CQLF

Case 1: Fault detection Interval observer

Based on Theorem 14, a common Lyapunov matrix can be obtained as follows:

$$P_1 = \begin{pmatrix} 1.21 & 0 & 0 \\ 0 & 1.37 & 0 \\ 0 & 0 & 4.16 \end{pmatrix}, \quad P_2 = \begin{pmatrix} 1.5 & 0 & 0 \\ 0 & 1.5 & 0 \\ 0 & 0 & 4.74 \end{pmatrix}.$$

The gain matrices are obtained as:

$$\bar{L}_1 = \begin{pmatrix} 0.38 & 0.39 \\ 0.09 & -0.04 \\ -0.04 & -0.03 \end{pmatrix}, \quad \underline{L}_1 = \begin{pmatrix} 0.42 & 0.44 \\ 0.12 & 0 \\ -0.04 & -0.01 \end{pmatrix}, \quad \bar{L}_2 = \begin{pmatrix} 0.57 & -0.96 \\ -0.05 & -0.15 \\ -0.09 & 0.34 \end{pmatrix},$$

$$\underline{L}_2 = \begin{pmatrix} 0.46 & -0.89 \\ -0.03 & -0.14 \\ -0.05 & 0.34 \end{pmatrix}, \quad \bar{L}_3 = \begin{pmatrix} 0.16 & 0.26 \\ 0.13 & -0.13 \\ 0.04 & -0.02 \end{pmatrix}, \quad \underline{L}_3 = \begin{pmatrix} 0.16 & 0.35 \\ 0.12 & -0.08 \\ 0.05 & 0 \end{pmatrix}.$$

In the simulation, an abrupt sensor fault f_k is carried out and represented as follows:

$$f_k = \begin{cases} 1 & 35 \leq k \leq 55 \\ 0 & \text{otherwise} \end{cases}$$

Under the switching sequence shown in Fig. 5.1, simulation results of the FD interval observer are depicted in Fig. 5.2 which illustrates the evolution of the residual signals. Under the proposed interval observer (5.2), the zero signal is excluded from the residual interval. Thus, the fault $f(k)$ can be detected.

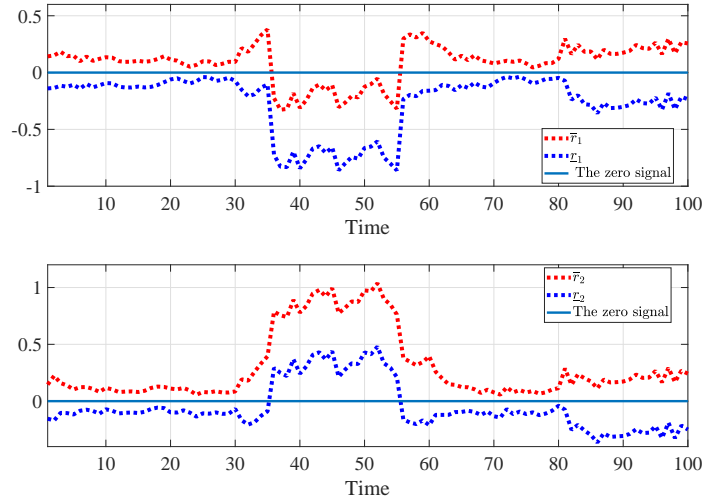


Figure 5.2: Residual framers using fault detection interval observer

Case 2: Fault detection Interval observer: TNL structure

Based on the TNL structure used in (5.23), the following Lyapunov matrix is given by:

$$P_1 = \begin{pmatrix} 1.28 & 0 & 0 \\ 0 & 1.23 & 0 \\ 0 & 0 & 1.67 \end{pmatrix}, \quad P_2 = \begin{pmatrix} 1.5 & 0 & 0 \\ 0 & 1.5 & 0 \\ 0 & 0 & 1.92 \end{pmatrix}.$$

By solving LMIs in Theorem 16, the matrices $\bar{L}_q, \underline{L}_q, \bar{N}_q, \underline{N}_q, \bar{T}_q$ and \underline{T}_q can be obtained as follows:

$$\begin{aligned} \bar{L}_1 &= \begin{pmatrix} 0.1 & 0.12 \\ -0.14 & -0.25 \\ -0.05 & 0.09 \end{pmatrix}, \quad \underline{L}_1 = \begin{pmatrix} 0.16 & 0.21 \\ -0.08 & -0.17 \\ -0.06 & 0.03 \end{pmatrix}, \quad \bar{L}_2 = \begin{pmatrix} 0.19 & -0.38 \\ -0.13 & -0.08 \\ 0.01 & 0.17 \end{pmatrix}, \\ \underline{L}_2 &= \begin{pmatrix} 0.17 & -0.35 \\ -0.05 & 0 \\ 0.05 & 0.18 \end{pmatrix}, \quad \bar{L}_3 = \begin{pmatrix} 0.2 & 0.18 \\ 0.02 & -0.16 \\ 0.02 & 0.05 \end{pmatrix}, \quad \underline{L}_3 = \begin{pmatrix} 0.19 & 0.2 \\ 0.05 & -0.13 \\ 0.027 & 0.06 \end{pmatrix}, \\ \bar{N}_1 &= \begin{pmatrix} 0.36 & 0.26 \\ 0.22 & 0.41 \\ -0.06 & -0.09 \end{pmatrix}, \quad \underline{N}_1 = \begin{pmatrix} 0.40 & 0.25 \\ 0.26 & 0.40 \\ -0.05 & -0.05 \end{pmatrix}, \quad \bar{N}_2 = \begin{pmatrix} 0.51 & -0.12 \\ 0 & 0.63 \\ -0.14 & -0.08 \end{pmatrix}, \\ \underline{N}_2 &= \begin{pmatrix} 0.47 & -0.08 \\ 0.01 & 0.60 \\ -0.11 & -0.06 \end{pmatrix}, \quad \bar{N}_3 = \begin{pmatrix} 0.17 & -0.13 \\ -0.02 & 0.39 \\ 0.01 & -0.18 \end{pmatrix}, \quad \underline{N}_3 = \begin{pmatrix} 0.18 & -0.08 \\ 0 & 0.38 \\ 0.02 & -0.14 \end{pmatrix}, \\ \bar{T}_1 &= \begin{pmatrix} 0.53 & -0.29 & -0.02 \\ -0.31 & 0.53 & -0.04 \\ 0.08 & 0.10 & 1 \end{pmatrix}, \quad \underline{T}_1 = \begin{pmatrix} 0.48 & -0.28 & -0.02 \\ -0.36 & 0.55 & -0.04 \\ 0.07 & 0.06 & 1 \end{pmatrix}, \\ \bar{T}_2 &= \begin{pmatrix} 0.39 & 0.13 & 0.01 \\ -0.06 & 0.30 & -0.06 \\ 0.18 & 0.09 & 1 \end{pmatrix}, \quad \underline{T}_2 = \begin{pmatrix} 0.43 & 0.08 & 0 \\ -0.07 & 0.33 & -0.06 \\ 0.14 & 0.073 & 1 \end{pmatrix}, \\ \bar{T}_3 &= \begin{pmatrix} 0.80 & 0.14 & 0.01 \\ 0 & 0.56 & -0.03 \\ 0 & 0.20 & 1.01 \end{pmatrix}, \quad \underline{T}_3 = \begin{pmatrix} 0.78 & 0.09 & 0 \\ -0.03 & 0.58 & -0.03 \\ -0.02 & 0.15 & 1.01 \end{pmatrix}. \end{aligned}$$

Note that $\bar{N}_q, \underline{N}_q, \bar{T}_q$ and \underline{T}_q are designed to satisfy (5.24) and (5.25). The same fault f_k vector is assumed to occur. In the fault free case, the cooperativity property is ensured and one can remark from Fig. 5.3 that $0 \in [\underline{r}_k \quad \bar{r}_k]$. When a fault occurs ($k = 35$), the additive sensor fault is detected at the time instant $k = 36$ under the proposed FD TNL approach and $0 \notin [\underline{r}_k \quad \bar{r}_k]$.

In the simulation study, the proposed TNL method is compared with the traditional interval approach using CQLF. The simulation results are shown in Fig. 5.4. The two proposed methods show their effectiveness for the detection of the sensor fault after its occurrence. Meanwhile, the results show that the FD obtained by the TNL method is more accurate than by the commonly used interval observer.

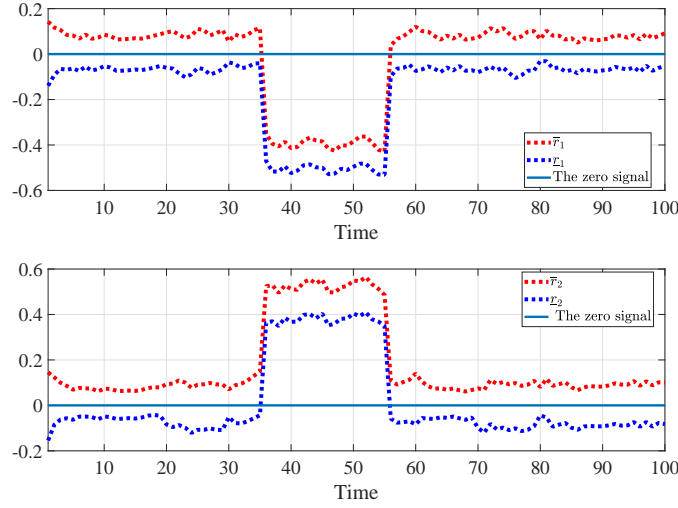


Figure 5.3: Residual framers using fault detection TNL interval observer

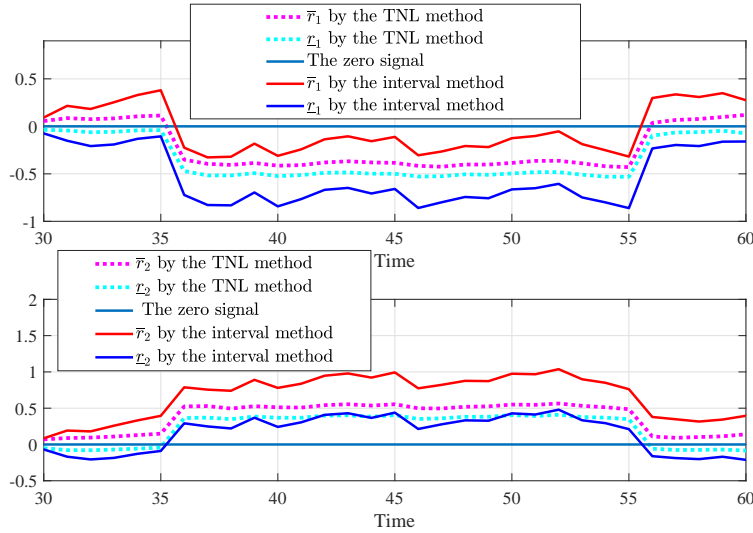


Figure 5.4: Fault detection performance comparison between the TNL method and the interval approach

The case of a small abrupt sensor fault is also considered and simulation results in Fig. 5.5 show that the sensor fault can be detected based on the TNL technique. However, based on the traditional interval technique, the cooperativity property is still guaranteed even after the occurrence of the fault and some missed alarms can be generated.

Remark 19. *The proposed new observer structure reduces the conservatism regarding uncertainties in fault detection. Compared to traditional interval observers, the TNL observer combined with the L_∞ criterion provides a better estimation of residuals. The proposed method can detect small faults while the rate of missing alarms is reduced.*

The first example shows promising results based on CQLF. However, in some cases, the

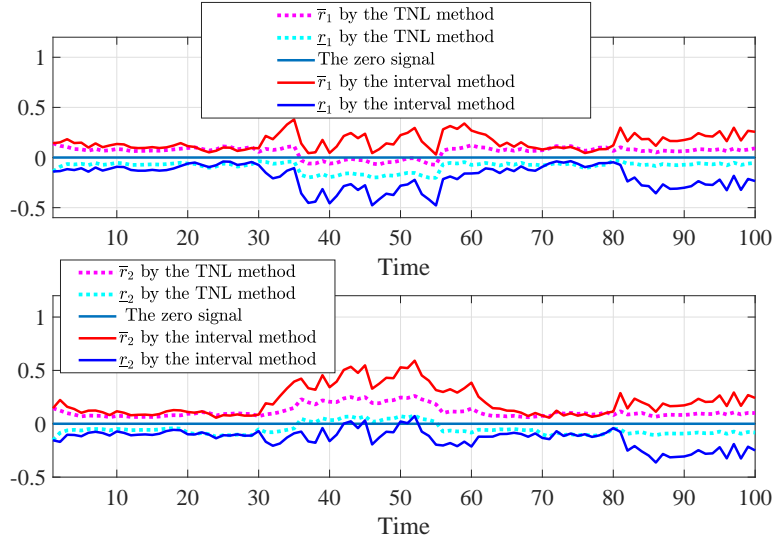


Figure 5.5: Fault detection performance comparison between the TNL method and the interval approach (Small fault)

existence of such a function is not always guaranteed. The second example is based on the construction of MQLF with an ADT switching signal in order to reduce the conservatism.

5.6.2 Fault detection results based on MQLF

Case 1: Fault detection Interval observer

For the same switched system used in the first example, the optimization problem in (5.41) is solved using the software Yalmip/Sedumi in MATLAB. The existence of a solution for the LMIs in Theorem 17 allows minimizing the interval width of the residual signal and optimum dwell time. The parameters $\lambda = 0.5$ and $\alpha = 1$ are chosen to solve the proposed LMIs. The following Lyapunov matrices are obtained:

$$P_{11} = \begin{pmatrix} 1.11 & 0 & 0 \\ 0 & 1.4 & 0 \\ 0 & 0 & 6.25 \end{pmatrix}, \quad P_{12} = \begin{pmatrix} 1.49 & 0 & 0 \\ 0 & 1.49 & 0 \\ 0 & 0 & 6.95 \end{pmatrix}, \quad P_{21} = \begin{pmatrix} 3.91 & 0 & 0 \\ 0 & 1.86 & 0 \\ 0 & 0 & 6.37 \end{pmatrix},$$

$$P_{22} = \begin{pmatrix} 3.9 & 0 & 0 \\ 0 & 1.96 & 0 \\ 0 & 0 & 6.46 \end{pmatrix}, \quad P_{31} = \begin{pmatrix} 5.67 & 0 & 0 \\ 0 & 4.24 & 0 \\ 0 & 0 & 5.94 \end{pmatrix}, \quad P_{32} = \begin{pmatrix} 5.69 & 0 & 0 \\ 0 & 4.27 & 0 \\ 0 & 0 & 5.96 \end{pmatrix}.$$

Then, we obtain $\mu = 6.95$ which leads to an ADT $\tau_a > 2.79$. The set of observer gains L_q are computed using (5.49) and given by:

$$\bar{L}_1 = \begin{pmatrix} 0.4 & 0.42 \\ 0.12 & -0.02 \\ -0.01 & 0 \end{pmatrix}, \quad \underline{L}_1 = \begin{pmatrix} 0.44 & 0.45 \\ 0.15 & 0 \\ 0 & 0 \end{pmatrix}, \quad \bar{L}_2 = \begin{pmatrix} 0.67 & -0.79 \\ -0.03 & -0.07 \\ -0.12 & 0.36 \end{pmatrix},$$

$$\underline{L}_2 = \begin{pmatrix} 0.67 & -0.79 \\ -0.02 & -0.06 \\ -0.12 & 0.36 \end{pmatrix}, \quad \bar{L}_3 = \begin{pmatrix} 0.26 & 0.36 \\ 0.22 & -0.06 \\ -0.01 & -0.06 \end{pmatrix}, \quad \underline{L}_3 = \begin{pmatrix} 0.26 & 0.37 \\ 0.23 & -0.06 \\ -0.01 & -0.06 \end{pmatrix}.$$

A comparison has been performed between FD performances based on CQLF and MQLF. The results of the simulation are depicted in Fig. 5.6 where solid lines present the residual signals obtained by CQLF and dashed lines present the residual framers obtained by MQLF. The simulation results show that the interval width obtained by the construction of MQLF is tighter than that given by CQLF. With the same initial conditions introduced before, the fault f_k can be detected more quickly using MQLF.

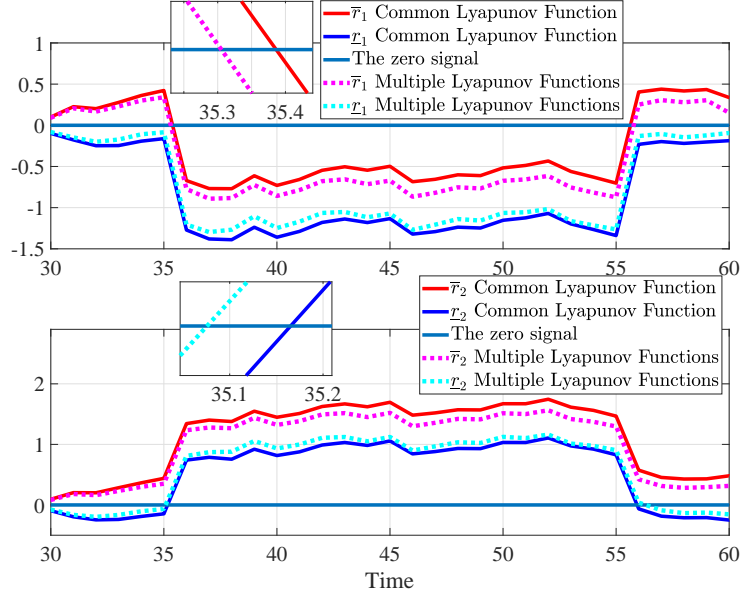


Figure 5.6: Residual framers using fault detection interval observer

Case 2: Fault detection Interval observer: TNL structure

The conservatism of gain matrices is reduced by integrating weighted matrices \bar{T}_q , \underline{T}_q , \bar{N}_q and \underline{N}_q and based on the construction of MQLF. The existence of a solution for LMIs in Theorem 18 allows one to improve the accuracy of FD and to obtain an optimum dwell time. The resolution of the optimization problem in (5.52) can be then solved and the Lyapunov matrices are obtained:

$$P_{11} = \begin{pmatrix} 1.29 & 0 & 0 \\ 0 & 1.26 & 0 \\ 0 & 0 & 1.67 \end{pmatrix}, \quad P_{12} = \begin{pmatrix} 1.5 & 0 & 0 \\ 0 & 1.5 & 0 \\ 0 & 0 & 1.92 \end{pmatrix}, \quad P_{21} = \begin{pmatrix} 1.35 & 0 & 0 \\ 0 & 1.23 & 0 \\ 0 & 0 & 1.63 \end{pmatrix},$$

$$P_{22} = \begin{pmatrix} 1.5 & 0 & 0 \\ 0 & 1.49 & 0 \\ 0 & 0 & 1.84 \end{pmatrix}, \quad P_{31} = \begin{pmatrix} 1.5 & 0 & 0 \\ 0 & 1.39 & 0 \\ 0 & 0 & 1.62 \end{pmatrix}, \quad P_{32} = \begin{pmatrix} 1.49 & 0 & 0 \\ 0 & 1.58 & 0 \\ 0 & 0 & 1.77 \end{pmatrix}.$$

In the simulation study, $\mu = 2$ which leads to an ADT $\tau_a > 1$. It is worth noting that the ADT is improved using an interval observer based on the TNL structure.

The set of observer gains $\bar{L}_q, \underline{L}_q$ and the weighted matrices $\bar{N}_q, \underline{N}_q, \bar{T}_q$ and \underline{T}_q are computed according to (5.60):

$$\bar{L}_1 = \begin{pmatrix} 0.10 & 0.13 \\ -0.15 & -0.24 \\ -0.05 & 0.11 \end{pmatrix}, \quad \underline{L}_1 = \begin{pmatrix} 0.13 & 0.18 \\ -0.11 & -0.20 \\ -0.04 & 0.11 \end{pmatrix}, \quad \bar{L}_2 = \begin{pmatrix} 0.21 & -0.35 \\ -0.11 & -0.05 \\ 0.03 & 0.20 \end{pmatrix},$$

$$\underline{L}_2 = \begin{pmatrix} 0.18 & -0.36 \\ -0.05 & 0.01 \\ 0.08 & 0.25 \end{pmatrix}, \quad \bar{L}_3 = \begin{pmatrix} 0.21 & 0.23 \\ 0.02 & -0.12 \\ 0.03 & 0.06 \end{pmatrix}, \quad \underline{L}_3 = \begin{pmatrix} 0.22 & 0.23 \\ 0.05 & -0.10 \\ 0.04 & 0.07 \end{pmatrix},$$

$$\bar{N}_1 = \begin{pmatrix} 0.39 & 0.29 \\ 0.26 & 0.45 \\ -0.04 & -0.08 \end{pmatrix}, \quad \underline{N}_1 = \begin{pmatrix} 0.42 & 0.29 \\ 0.29 & 0.45 \\ -0.03 & -0.08 \end{pmatrix}, \quad \bar{N}_2 = \begin{pmatrix} 0.51 & -0.09 \\ 0 & 0.73 \\ -0.15 & -0.05 \end{pmatrix},$$

$$\underline{N}_2 = \begin{pmatrix} 0.48 & -0.06 \\ 0 & 0.71 \\ -0.14 & -0.08 \end{pmatrix}, \quad \bar{N}_3 = \begin{pmatrix} 0.21 & -0.08 \\ 0 & 0.51 \\ 0.02 & -0.18 \end{pmatrix}, \quad \underline{N}_3 = \begin{pmatrix} 0.21 & -0.08 \\ 0.02 & 0.5 \\ 0.03 & -0.16 \end{pmatrix},$$

$$\bar{T}_1 = \begin{pmatrix} 0.49 & -0.32 & -0.02 \\ -0.36 & 0.49 & -0.04 \\ 0.06 & 0.08 & 1 \end{pmatrix}, \quad \underline{T}_1 = \begin{pmatrix} 0.45 & -0.32 & -0.02 \\ -0.39 & 0.49 & -0.04 \\ 0.054 & 0.09 & 1 \end{pmatrix},$$

$$\bar{T}_2 = \begin{pmatrix} 0.38 & 0.09 & 0 \\ -0.07 & 0.19 & -0.07 \\ 0.19 & 0.06 & 1 \end{pmatrix}, \quad \underline{T}_2 = \begin{pmatrix} 0.42 & 0.06 & 0 \\ -0.07 & 0.21 & -0.07 \\ 0.18 & 0.09 & 1 \end{pmatrix},$$

$$\bar{T}_3 = \begin{pmatrix} 0.75 & 0.08 & 0 \\ -0.06 & 0.42 & -0.05 \\ -0.01 & 0.20 & 1.01 \end{pmatrix}, \quad \underline{T}_3 = \begin{pmatrix} 0.75 & 0.09 & 0 \\ -0.08 & 0.44 & -0.05 \\ -0.01 & 0.18 & 1.01 \end{pmatrix}.$$

As shown before FD performances based on MQLF are better than those obtained by CQLF. Same findings in the case of interval FD observer based on the TNL structure are obtained.

The case of a small abrupt sensor fault is also considered and simulation results in Fig. 5.7 show that the small fault can be detected based on the TNL technique which is not the case when using the interval approach.

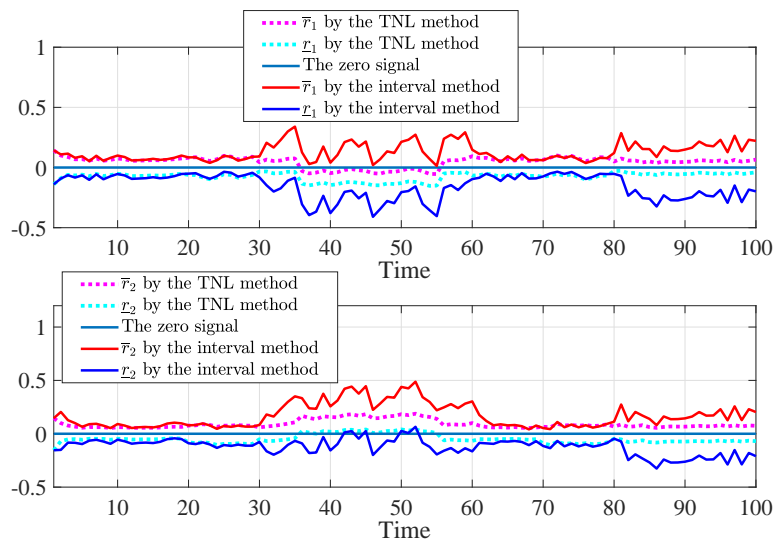


Figure 5.7: Fault detection performance comparison between the TNL method and the interval approach (Small fault)

5.7 Conclusion

In this chapter, a new LMIs formulation has been presented to design a robust observer-based FD scheme for discrete-time switched systems with sensor faults. Two approaches to construct residual framers have been considered. The first one is based on the commonly used interval observer. The second approach is based on a new interval observer structure to relax the cooperativity constraints. The proposed technique offers more degrees of design freedom by integrating weighted matrices in the structure of the FD observer design. For both approaches, an L_∞ performance is introduced to improve the accuracy of fault detection. Cooperativity and stability conditions are expressed in terms of LMIs based on CQLF and MQLF with an ADT control condition. Finally, the fault detection decision is based on determining whether the zero signal is excluded from the generated residual intervals when the faults occur. The proposed techniques avoid the design of residual evaluation functions and threshold generators.

Recently, as another effective approach to detect faults in the presence of bounded noise and perturbations, the method of set-membership fault detection has been developed. There are several used geometrical forms, such as ellipsoid, polytope, parallelotope and zonotope. In the next chapter, we are interested in robust fault detection techniques for a class of discrete-time switched systems using zonotopic and ellipsoidal techniques.

Chapter 6

Set-membership fault detection frameworks for switched systems

6.1 Introduction

Much attention has been devoted to the set-based fault detection area under the assumption that the uncertainties are unknown but bounded. Roughly speaking, they can be further divided into: interval methods and set-membership fault detection approaches. Interval methods require the nonnegativity condition, which may be too restrictive for many practical systems. Compared with intervals, set-membership fault detection techniques are introduced to improve the accuracy of the residual boundaries without considering the nonnegativity assumption. They aim to construct tight estimation of the admissible residual sets based on the representation of different shapes of convex sets such as polytopes, ellipsoids, zonotopes [198], [3], [171]. The polytope-based methods can be used to achieve accurate set-membership fault detection results. However, the computation complexity may be high [199]. Zonotopes, known as a particular class of convex polytopes, can provide a good tradeoff between fault detection accuracy and computation complexity. In addition, the ellipsoid-based methods have attracted much attention especially in set-membership estimation, due to their interesting characteristics and the simplicity of their computation. Note that the basic operations for ellipsoids can be reduced to simple matrix calculations and do not require reduction operator. To the best of our knowledge, FD using zonotopic and ellipsoidal analysis for uncertain switched systems has not been fully investigated in the literature. The first part in this chapter is devoted to design a robust fault detection scheme for switched systems with actuator fault using zonotopic set-membership approach. In this part, notations, preliminaries about zonotopes and the problem formulation are presented. Then, the proposed method is developed by combining the benefits of a novel pole assignment approach to maximize the sensitivity of faults on the residual signal, the H_∞ criterion

to minimize the effect of disturbances, and a zonotope-based residual evaluation. The main challenge, in the second part, is to achieve a robust fault detection using ellipsoidal analysis in the case of sensor faults. First, preliminaries about ellipsoidal set-theory, the system description and problem statement are provided. Then, the designed approach is based on a new fault detection observer structure with an L_∞ performance. It is worth noting that the H_∞ criterion is a measurement of energy-to-energy gain which may not be very efficient for residual evaluation. Therefore, L_∞ performance is used since some signals cannot be considered energy-bounded but have bounded peak values. The design conditions of the proposed observer are given in terms of LMIs using MQLF, with an ADT switching signal. The residual evaluation is based on ellipsoid-based methods. The efficiency of the proposed approaches is highlighted through simulation results on academic examples. The work presented in this chapter has led to the publication of two international conference papers [200] and [201] in "IFAC World Congress" and "Conference on Decision and Control".

6.2 Zonotope-based fault detection framework

6.2.1 Zonotopic set-theory preliminaries

The following definitions are essential in this chapter.

Definition 14. [202] An s -order zonotope \mathbf{Z} represents the affine image of a hypercube $\mathbb{B}^s = [-1, 1]^s$ as follows:

$$\mathbf{Z} = \langle p, H \rangle = p + H\mathbb{B}^s = \{p + Hz, z \in \mathbb{B}^s\},$$

$p \in \mathbb{R}^n$ denotes the center of \mathbf{Z} and $H \in \mathbb{R}^{n \times s}$ its generation matrix, which represents the shape of \mathbf{Z} .

Example 1. Figure 6.1 shows a third order zonotope $\mathbf{Z} = \langle p, H \rangle$ with

$$p = \begin{bmatrix} 1 \\ 0 \end{bmatrix}, H = \begin{bmatrix} 1 & 2 & 3 \\ 3 & 2 & 1 \end{bmatrix}.$$

This zonotope can be constructed as the affine image of a hypercube in \mathbb{R}^3 under the projection of H in \mathbb{R}^2 .

Definition 15. A set \mathbf{X} is included in a set \mathbf{Y} , i.e. $\mathbf{X} \subseteq \mathbf{Y}$, if and only if $x \in \mathbf{Y}, \forall x \in \mathbf{X}$.

Definition 16. Consider two sets \mathbf{X} and \mathbf{Y} . The Minkowski sum of \mathbf{X} and \mathbf{Y} is defined as:

$$\mathbf{X} \oplus \mathbf{Y} = \{x + y, x \in \mathbf{X}, y \in \mathbf{Y}\}$$

Definition 17. The linear product of a matrix $K \in \mathbb{R}^{m \times n}$ and a set $\mathbf{X} \in \mathbb{R}^n$ is denoted as \odot and defined as:

$$K \odot \mathbf{X} = \{Kx, x \in \mathbf{X}\}$$

Definition 18. The interval hull of the zonotope $\mathbf{Z} = \langle p, H \rangle \subset \mathbb{R}^n$ is the smallest box that contains \mathbf{Z} denoted by $\mathbf{Z} \subseteq \text{Box}(\mathbf{Z}) = \langle p, rs(H) \rangle$ where $rs(H) \in \mathbb{R}^{n \times n}$ is a diagonal matrix given by:

$$rs(H) = \text{diag} \left(\left[\sum_{j=1}^s |H_{1,j}| \quad \cdots \quad \sum_{j=1}^s |H_{n,j}| \right] \right).$$

$\text{diag}(\cdot)$ is a diagonal matrix whose diagonal terms are the arguments of diag .

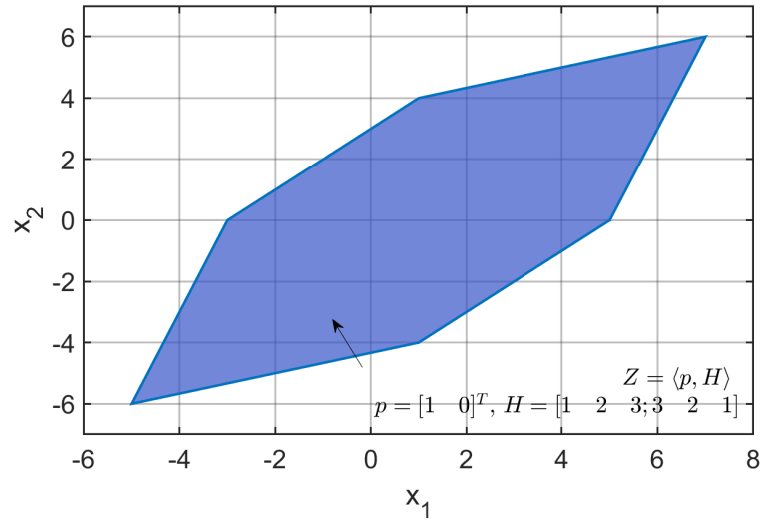


Figure 6.1: 3-zonotope in a two dimension space.

Example 2. Consider a zonotope $Z = \langle p, H \rangle$ with

$$p = \begin{bmatrix} 1 \\ 0 \end{bmatrix}, H = \begin{bmatrix} 1 & 2 & 3 \\ 3 & 2 & 1 \end{bmatrix}.$$

Applying the interval hull approximation leads to a box in Fig. 6.2 containing the original zonotope.

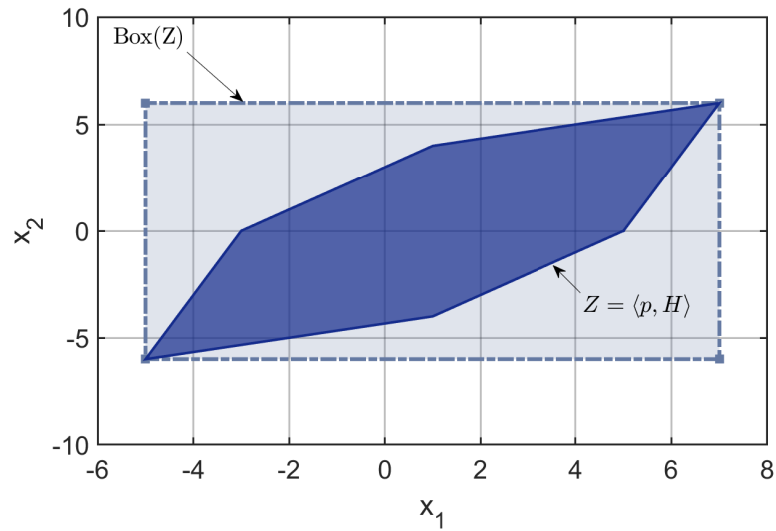


Figure 6.2: Interval hull of a zonotope

Definition 19. A lower zonotope can bound a high-dimensional zonotope using a reduction operation [3]. The reduction operator for a zonotope can be described by

$\mathbf{Z} = \langle p, H \rangle \subseteq \langle p, \downarrow_l(H) \rangle$ where $\downarrow_l(H)$ represents the complexity reduction operator with $n \leq l \leq s$ denotes the maximum number of columns of the generator matrix H .

The detailed reduction procedure is summarized in the following algorithm:

Algorithm 1 Zonotopic reduction algorithm

Input: H

Output: $\downarrow_l(H)$

- 1: Reorder the columns of $H \in \mathbb{R}^{n \times s}$ in decreasing euclidean vector norm $\|\cdot\|$

$$H = [h_1, h_2, \dots, h_s], \quad \|h_j\|^2 \geq \|h_{j+1}\|^2, j = 1, 2, \dots, s - 1.$$

- 2: Replace the last $s - l + n$ columns of H with a diagonal matrix $rs(H)_<$ such that the zonotope generated by these columns are enclosed by a box called interval hull.

- 3: **If** $s \leq l$ **then** $\downarrow_q(H) = H$

- 4: **Else** $\downarrow_l(H) = [H_> \ rs(H)_<] \in \mathbb{R}^{n \times l}$, where $H_> = [h_1, \dots, h_{l-n}]$, and $H_< = [h_{l-n+1}, \dots, h_s]$.
-

Example 3. Consider a zonotope $\mathbf{Z} = p + HB^8 \subset \mathbb{R}^2$ with:

$$p = \begin{bmatrix} 1 \\ 0 \end{bmatrix}, H = \begin{bmatrix} 0.9 & 0.8 & 0.35 & 0.1 & 0.2 & 0.6 & 0.19 & 0.7 \\ 0.4 & 0.05 & 0.81 & 0.13 & 0.19 & 0.27 & 0.01 & 0.44 \end{bmatrix}.$$

Figure 6.3 gives three dimension reduction zonotopes \mathbf{Z}_1 , \mathbf{Z}_2 and \mathbf{Z}_3 of \mathbf{Z} with $l_1 = 7$, $l_2 = 5$ and $l_3 = 3$ specify the maximum numbers of column of segment matrix H after reduction. \mathbf{Z}_1 , \mathbf{Z}_2 and \mathbf{Z}_3 can include \mathbf{Z} , and higher dimensional zonotopes can bring more accurate results.

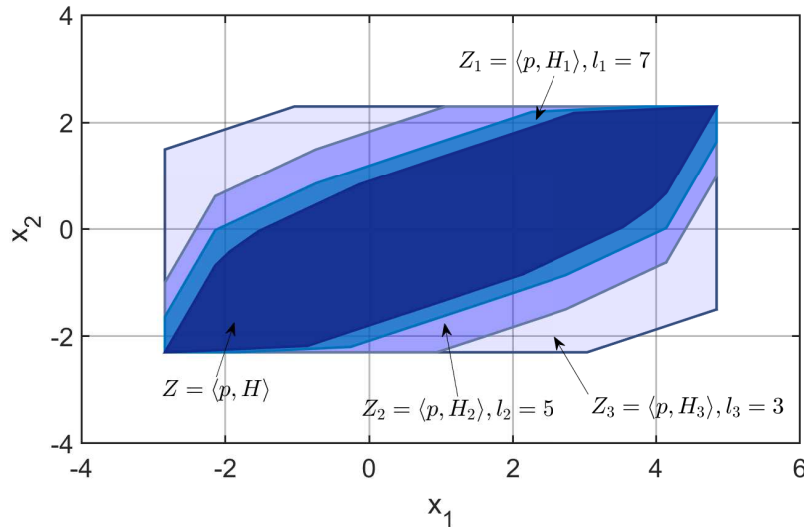


Figure 6.3: A zonotope \mathbf{Z} and its three dimension reduction zonotopes.

6.2.2 Problem formulation

Consider the following discrete-time switched system:

$$\begin{cases} x_{k+1} &= A_q x_k + B_q u_k + D w_k + F_q f_k \\ y_k &= C x_k + D_v v_k \end{cases} \quad (6.1)$$

where $x \in \mathbb{R}^{n_x}$, $y \in \mathbb{R}^{n_y}$, $u \in \mathbb{R}^{n_u}$, $f \in \mathbb{R}^{n_f}$, $w \in \mathbb{R}^{n_w}$ and $v \in \mathbb{R}^{n_v}$ are respectively the state vector, the input, the output, the actuator fault, the state disturbances and the measurement noise. The known matrices A_q , B_q , C , D , D_v and F_q are given with appropriate dimensions. The index q defines the active subsystem. $q \in \mathcal{I} = \overline{1, N}$, $N \in \mathbb{Z}_+$, N denotes the number of linear subsystems (modes). The switching signal is assumed to be known.

The following assumption is introduced.

Assumption 22. *The initial state x_0 , the measurement noise v_k and the state disturbances w_k are supposed to be unknown but bounded such that:*

$$x_0 \in \langle p_0, H_0 \rangle, \quad w_k \in \langle 0, H_w \rangle, \quad v_k \in \langle 0, H_v \rangle \quad (6.2)$$

where $H_0 = \text{diag}(\bar{x})$, $H_w = \text{diag}(\bar{w})$ and $H_v = \text{diag}(\bar{v})$.

Remark 20. *The disturbances and noise, in standard model-based fault detection techniques, are supposed to have a known probability distribution, such as Gaussian distribution. However, in practice, it is not trivial to obtain a priori information of probability distribution. In this part, the proposed method provides a more realistic assumption by assuming that the state disturbances and measurement noise are unknown but bounded by zonotopes.*

It is worth noting that the existing results on set-membership fault detection methods only consider the disturbances robustness, without considering the fault sensitivity. In the following, the aim is to design a robust FD approach for the discrete-time switched systems defined by (6.1) where fault sensitivity is investigated with a novel pole placement technique. The observer gains should be designed with two main objectives: (i) sensitivity to faults to detect faults with low magnitudes; (ii) robustness against uncertainties including system disturbances and measurement noise to allow distinguishing uncertainties and faults. Based on the designed observer, the occurred faults in the uncertain system (6.1) can be detected using a zonotopic analysis.

6.2.3 Robust fault detection design

In this section, we propose a Fault Detection Observer (FDO) for the system (6.1) described by:

$$\begin{cases} \hat{x}_{k+1} &= A_q \hat{x}_k + B_q u_k + L_q (y_k - C \hat{x}_k) \\ r_k &= y_k - C \hat{x}_k \end{cases} \quad (6.3)$$

where \hat{x}_k is the estimation of x_k and $L_q \in \mathbb{R}^{n_x \times n_y}$, $q \in \{1, \dots, N\}$, are the observer gains to be designed. The goal is to compute the FDO gains L_q that improve the sensitivity to fault and minimize the H_∞ performance of the transfer function for each mode from disturbances to the residual vector r_k . The estimation error and the residual signal at the time instant k

are defined respectively as $e_k = x_k - \hat{x}_k$ and $r_k = y_k - \hat{y}_k$.

Then, the error dynamics are given by:

$$\begin{cases} e_{k+1} &= (A_q - L_q C)e_k + F_q f_k + Dw_k - L_q D_v v_k \\ r_k &= C e_k + D_v v_k \end{cases} \quad (6.4)$$

The error dynamics (6.4) can be split into two subsystems where the subsystem (6.5) is decoupled from the effects of f_k and the subsystem (6.6) is only affected by the actuator fault.

$$\begin{cases} e_{k+1}^d &= (A_q - L_q C)e_k^d + Dw_k - L_q D_v v_k \\ r_k^d &= C e_k^d + D_v v_k \end{cases} \quad (6.5)$$

$$\begin{cases} e_{k+1}^f &= (A_q - L_q C)e_k^f + F_q f_k \\ r_k^f &= C e_k^f \end{cases} \quad (6.6)$$

where $e_k = e_k^f + e_k^d$, $e_0^f = 0$ and $e_0^d = 0$.

The reason behind splitting the error dynamics given in (6.4) is to handle the nonzero condition in fault sensitivity analysis. In the sequel, the fault sensitivity condition is achieved based a novel pole placement technique.

6.2.3.1 Fault sensitivity condition

For efficient FD, it is required that the sensitivity to fault on the residual vector should be improved. Herein, since the error dynamics (6.4) can be split and only the subsystem (6.6) is affected by the additive fault, a pole placement technique is considered for (6.6). The designed FDO gains L_q are introduced to improve fault sensitivity on residual signal.

In the FD scheme, the observer gain matrices L_q is designed such that:

$$(A_q - L_q C)F_q = \lambda F_q \quad (6.7)$$

where λ is a scalar satisfying $0 < \lambda < 1$.

In fact, if the condition (6.7) holds, it can be easily shown that:

$$e_k^f = \lambda^{k-1} F_q f_0 + \dots + \lambda F_q f_{k-2} + F_q f_{k-1} \quad (6.8)$$

Based on (6.6) and (6.7), we have:

$$\begin{aligned} e_k^f &= (A_q - L_q C)e_{k-1}^f + F_q f_{k-1} \\ &= \lambda e_{k-1}^f + F_q f_{k-1} \\ &= \lambda((A_q - L_q C)e_{k-2}^f + F_q f_{k-2}) + F_q f_{k-1} \\ &= \lambda((A_q - L_q C)((A_q - L_q C)e_{k-3}^f + F_q f_{k-3}) + \lambda F_q f_{k-2}) + F_q f_{k-1} \\ &= \lambda(\lambda^2 e_{k-3}^f + \lambda F_q f_{k-3}) + \lambda F_q f_{k-2} + F_q f_{k-1} \\ &= \lambda^3 e_{k-3}^f + \lambda^2 F_q f_{k-3} + \lambda F_q f_{k-2} + F_q f_{k-1} \\ &= \vdots \\ &= \lambda^{k-1} e_1^f + \dots + \lambda F_q f_{k-2} + F_q f_{k-1} \\ &= \lambda^{k-1}((A_q - L_q C)e_0^f + F_q f_0) + \dots + \lambda F_q f_{k-2} + F_q f_{k-1} \end{aligned} \quad (6.9)$$

Since $e_0^f = 0$, (6.9) implies (6.8). It follows from $r_k^f = C e_k^f$ that:

$$r_k^f = \lambda^{k-1} C F_q f_0 + \dots + \lambda C F_q f_{k-2} + C F_q f_{k-1} \quad (6.10)$$

From (6.10), it is worth noting that r_k depends on a weighting scalar λ . Thus, in order to improve fault sensitivity, it is required to increase the value of λ as much as possible and to let it closer to 1. To that end, a pole assignment method is considered.

Based on Lemma 9 in chapter 5, the FDO gains L_q can be obtained by solving (6.7). They are given by:

$$L_q = (A_q F_q - \lambda F_q)(C F_q)^\dagger + S(I - C F_q(C F_q)^\dagger) \quad (6.11)$$

where $S \in \mathbb{R}^{n_x \times n_y}$ is a matrix to be designed.

6.2.3.2 Disturbance attenuation condition

In order to attenuate the effects of uncertainties and thus to increase the fault detection accuracy, an H_∞ criterion is used to design the observer gains L_q . Based on the bounded real lemma [30], the performance

$$\|r^d\| < \gamma \sqrt{(\|w\|^2 + \|v\|^2)} \quad (6.12)$$

is considered. $\|w\|$ and $\|v\|$ represent the L_2 -norm of w and v . The design conditions are expressed in terms of LMIs in the following theorem.

Theorem 19. *For a given scalar $\gamma > 0$, the error system (6.5) is stable and satisfies the H_∞ performance (6.12), if there exist a positive definite matrix $P \in \mathbb{R}^{n_x \times n_x}$ and $Q_q \in \mathbb{R}^{n_x \times n_y}$ such that:*

$$\begin{bmatrix} -P + C^T C & * & * & * \\ 0 & -\gamma^2 I_n & 0 & * \\ D_v^T C & 0 & D_v^T D_v - \gamma^2 I_n & * \\ P A_q - Q_q C & P D & -Q_q D_v & -P \end{bmatrix} < 0. \quad (6.13)$$

Moreover, the FDO gains L_q are given by:

$$L_q = P^{-1} Q_q. \quad (6.14)$$

Proof. To prove the stability of (6.5) and the H_∞ performance (6.12), sufficient conditions are given in terms of LMIs using the bounded real lemma and based on a CQLF given by $V(e_k^d) = e_k^{d^T} P e_k^d$, $P^T = P \succ 0$, such that:

$$\Delta V(e_k^d) + r_k^{d^T} r_k^d - \gamma^2 w_k^T w_k - \gamma^2 v_k^T v_k < 0. \quad (6.15)$$

One can obtain from (6.15)

$$\begin{aligned} V(e_{k+1}^d) - V(e_k^d) + r_k^{d^T} r_k^d - \gamma^2 w_k^T w_k - \gamma^2 v_k^T v_k &< 0 \\ e_{k+1}^{d^T} P e_{k+1}^d - e_k^{d^T} P e_k^d + r_k^{d^T} r_k^d - \gamma^2 w_k^T w_k - \gamma^2 v_k^T v_k &< 0. \end{aligned} \quad (6.16)$$

Based on (6.5), (6.16) implies:

$$\begin{aligned} ((A_q - L_q C) e_k^d + D w_k - L_q D_v v_k)^T P ((A_q - L_q C) e_k^d + D w_k - L_q D_v v_k) - e_k^{d^T} P e_k^d + \\ (C e_k^d + D_v v_k)^T (C e_k^d + D_v v_k) - \gamma^2 w_k^T w_k - \gamma^2 v_k^T v_k < 0. \end{aligned}$$

Then, the following inequality can be obtained:

$$[e_k^{dT} \quad w_k^T \quad v_k^T]^T \Sigma_q [e_k^{dT} \quad w_k^T \quad v_k^T] < 0 \quad (6.17)$$

where

$$\Sigma_q = \begin{bmatrix} \Theta_{11} & * & * \\ \Theta_{21} & \Theta_{22} & * \\ \Theta_{31} & \Theta_{32} & \Theta_{33} \end{bmatrix},$$

and

$$\begin{aligned} \Theta_{11} &= (A_q - L_q C)^T P (A_q - L_q C) + C^T C - P \\ \Theta_{21} &= D^T P (A_q - L_q C) \\ \Theta_{22} &= D^T P D - \gamma^2 I_n \\ \Theta_{31} &= -(L_q D_v)^T P (A_q - L_q C) + D_v^T C \\ \Theta_{32} &= -(L_q D_v)^T P D \\ \Theta_{33} &= (L_q D_v)^T P (L_q D_v) + D_v^T D_v - \gamma^2 I_n. \end{aligned}$$

The inequality (6.17) can be rewritten as:

$$\begin{bmatrix} -P + C^T C & * & * \\ 0 & -\gamma^2 I_n & * \\ D_v^T C & 0 & D_v^T D_v - \gamma^2 I_n \end{bmatrix} - \Omega^T P \Omega \prec 0, \quad (6.18)$$

with $\Omega = [(A_q - L_q C) \quad D \quad (L_q D_v)]$.

From (6.18) and based on the Schur complement, it is easy to show that (6.13) implies (6.17). Therefore, the observer gains are deduced with $Q_q = P L_q$. The stability and the H_∞ are satisfied. \square

Considering the above two aspects, sensitivity to faults and robustness against uncertainties including system disturbances and measurement noise, the optimal FDO gains L_q can be designed by solving an optimization problem. In the following, both sensitivity and robustness conditions are developed.

6.2.3.3 Fault detection observer design: Luenberger structure

In this part, convenient LMI conditions are derived and given in the following theorem by means of the H_∞ performance criterion and the pole placement method.

Theorem 20. *For a given value of λ with $0 < \lambda < 1$, if there exist a symmetric positive definite matrix $P \in \mathbb{R}^{n_x \times n_x}$ and $Y \in \mathbb{R}^{n_x \times n_y}$ such that:*

$$\begin{bmatrix} \Psi_{11} & * & * & * \\ 0 & \Psi_{22} & * & * \\ \Psi_{31} & 0 & \Psi_{33} & * \\ \Psi_{41} & \Psi_{42} & \Psi_{43} & \Psi_{44} \end{bmatrix} \prec 0, \quad (6.19)$$

where

$$\begin{aligned}
\Psi_{11} &= -P + C^T C \\
\Psi_{22} &= -\gamma^2 I_n \\
\Psi_{31} &= D_v^T C \\
\Psi_{33} &= D_v^T D_v - \gamma^2 I_n \\
\Psi_{41} &= P A_q - P(A_q F_q - \lambda F_q)(C F_q)^\dagger C - Y(C F_q)^\perp C \\
\Psi_{42} &= P D \\
\Psi_{43} &= -(P(A_q F_q - \lambda F_q)(C F_q)^\dagger C - Y(C F_q)^\perp) D_v \\
\Psi_{44} &= -P.
\end{aligned}$$

$Y = PS$, $(C F_q)^\perp = (I - C F_q (C F_q)^\dagger)$, $L_q = (A_q F_q - \lambda F_q)(C F_q)^\dagger + S(C F_q)^\perp$ and $S \in \mathbb{R}^{n_x \times n_y}$ is an arbitrary matrix, the following statements hold:

1. The stability of the observer (6.3) and the H_∞ performance (6.12) are satisfied.
2. The sensitivity of the residual r_k to the fault is improved.

Moreover, if (6.19) is solvable, the optimal FDO gain matrices can be determined by:

$$L_q = (A_q F_q - \lambda F_q)(C F_q)^\dagger + S(C F_q)^\perp \quad (6.20)$$

and computed by solving the following minimization problem:

$$\begin{aligned}
&\min_{L_q} \gamma^2, \quad q = 1, \dots, N \\
&\text{s.t.} \quad (6.19)
\end{aligned} \quad (6.21)$$

Proof. The proof is divided into the following two parts.

(i) **H_∞ disturbance attenuation condition**

A common Lyapunov function is chosen such that

$$V(e_k^d) = e_k^{dT} P e_k^d, P^T = P \succ 0.$$

Given a positive scalar γ , the Lyapunov function $V(e^d)$ satisfies the following relation

$$\|r^d\| < \gamma \sqrt{(\|w\|^2 + \|v\|^2)}.$$

The above relation implies (6.13).

(ii) **Fault sensitivity condition**

Based on the pole assignment technique, the FDO L_q is given by:

$$L_q = (A_q F_q - \lambda F_q)(C F_q)^\dagger + S(C F_q)^\perp$$

where λ is chosen such that $0 < \lambda < 1$ and it is required to increase the value of λ to improve fault sensitivity. By substituting the expression of L_q in (6.13), one can obtain (6.19).

Then, robustness against disturbances and sensitivity to faults are achieved.

Remark 21. By minimizing the H_∞ index γ , the proposed method attenuates the effect of disturbances as much as possible by minimizing the cost function (6.21).

□

6.2.3.4 Zonotope-based residual evaluation

$$\begin{cases} r_k \in \mathbf{R}_k & \text{Fault-free} \\ r_k \notin \mathbf{R}_k & \text{Faulty} \end{cases} \quad (6.22)$$

The fault detection decision can be checked by solving the following constraint problem:

$$R_k z_i = r_k \quad (6.23)$$

$$s.t. \quad -1 \leq z_i \leq 1 \quad \forall i = 1, \dots, l$$

where R_k denotes the generation matrix of the residual zonotope \mathbf{R}_k and z_i denotes the i th element of uncertain vector z bounded by hypercube \mathbb{B}^l (the residual zonotope \mathbf{R}_k is reduced to dimension l).

The overall procedure of the zonotopic fault detection decision can be summarized in the following Algorithm.

Algorithm 2 Zonotopic residual evaluation

Input: u_k, y_k

Output: r_k

1: **Initialization:**

$$x_0 \in \langle p_0, H_0 \rangle; \hat{x}_0 = p_0$$

$$w \in \mathbf{W} = \langle 0, H_w \rangle; v \in \mathbf{V} = \langle 0, H_v \rangle$$

2: **for** $k = 1$ to N **do**

3: $\hat{x}_{k+1} = (A_q - L_q C)\hat{x}_k + B_q u_k + L_q(y_k - C\hat{x}_k)$

4: $r_k = y_k - C\hat{x}_k$

5: $H_{k+1} = [(A_q - L_q C) \downarrow_l(H_k) \quad DH_w \quad -L_q D_v H_v]$

6: $R_k = [CH_k \quad D_v H_v]$

7: Define $\mathbf{R}_k = \langle 0, R_k \rangle$

8: Determine the FD alarm (index = 0: no fault detected; index = 1: fault detected)

by checking :

$$index = \begin{cases} 0 & \text{if } r_k \in \mathbf{R}_k \\ 1 & \text{if } r_k \notin \mathbf{R}_k \end{cases}$$

9: **end for**

Proof. Based on Assumption 22, $x_0 \in \langle p_0, H_0 \rangle$. We assume that $\hat{x}_0 = p_0$ then according to Definition 16, $e_0^d \in \langle 0, H_0 \rangle$. From (6.5) and based on Definition 17, the error zonotope can be obtained iteratively such that:

$$\begin{cases} e_k^d & \in \langle 0, H_0 \rangle \\ H_{k+1} & = [(A_q - L_q C)(H_k) \quad DH_w \quad -L_q D_v H_v] \end{cases} \quad (6.24)$$

Note that the order of the zonotope \mathbf{R}_k increase at each integration step. Thus, to reduce the computational load, a high-dimensional zonotope \mathbf{R}_k can be bounded by a lower dimensional

one using the reduction operator [3] such that $H_k \subset \downarrow_l(H_k)$. It follows from system (6.3) and (6.24) that $r_k \in \langle 0, R_k \rangle$ such that:

$$\begin{cases} R_k &= [CH_k \quad D_v H_v] \\ H_{k+1} &= [(A_q - L_q C) \downarrow_l(H_k) \quad DH_w \quad -L_q D_v H_v]. \end{cases} \quad (6.25)$$

Then, the residual signal r_k , defined in (6.4), is bounded by the zonotope $\mathbf{R}_k = \langle 0, R_k \rangle$ and R_k satisfies (6.25). \square

Remark 22. *The overall block diagram for the proposed robust fault detection approach is depicted in Fig. 6.4. It is worth noting that the designed residual zonotope can be directly used to achieve residual evaluation. Thus, compared with the conventional fault detection methods [203], [204], [205], the proposed approach avoids the design of residual evaluation functions or threshold generator and provides a systematic way to improve fault detection accuracy by combining robust observer design and zonotopic techniques.*

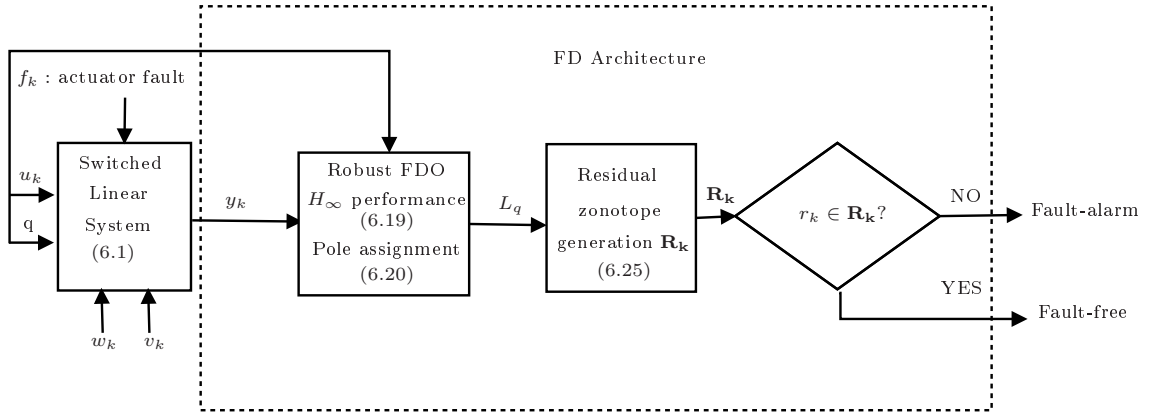


Figure 6.4: Block diagram of the proposed fault detection approach.

6.2.4 Numerical example

6.2.4.1 Simulation settings

To show the effectiveness and the advantages of the proposed FD method, a numerical example is considered for a discrete-time switched system defined with three subsystems, $N = 3$, with:

$$A_1 = \begin{pmatrix} 0.78 & 0 & 0.05 \\ 0 & 0.45 & -0.015 \\ 0.06 & 0.012 & 0.01 \end{pmatrix} \quad A_2 = \begin{pmatrix} -0.02 & -0.2 & 0.4 \\ 0.08 & 1 & -0.2 \\ 0.09 & 0.8 & -0.1 \end{pmatrix} \quad B_1 = \begin{pmatrix} 0 \\ 0.17 \\ -0.12 \end{pmatrix}$$

$$A_3 = \begin{pmatrix} 0.55 & 0 & 0.25 \\ 0 & 0.45 & 0 \\ 0 & 0.075 & -0.03 \end{pmatrix} \quad B_2 = \begin{pmatrix} 0.2 \\ 0 \\ 0.1 \end{pmatrix} \quad B_3 = \begin{pmatrix} 0.1 \\ -0.1 \\ 0 \end{pmatrix} \quad F_1 = \begin{pmatrix} -1 \\ 1 \\ -1 \end{pmatrix}$$

$$F_2 = \begin{pmatrix} -2 \\ 2 \\ -2 \end{pmatrix} \quad F_3 = \begin{pmatrix} 1 \\ 2 \\ -1 \end{pmatrix} \quad D = \begin{pmatrix} 0.005 & -0.01 & -0.002 \\ 0.01 & 0 & 0.005 \\ 0.001 & 0.001 & 0.008 \end{pmatrix}$$

$$D_v = \begin{pmatrix} 0.01 & -0.002 & 0.01 \\ 0.001 & 0.001 & 0.01 \end{pmatrix} \quad C = \begin{pmatrix} 1 & -0.5 & 1 \\ -1 & 1 & 0 \end{pmatrix}$$

In the simulation study, the initial state x_0 is bounded by the zonotope $\mathbf{X}_0 = \langle p_0, H_0 \rangle$ with:

$$p_0 = \begin{pmatrix} 0 \\ 0 \\ 0 \end{pmatrix} \quad H_0 = \begin{pmatrix} 0.1 & 0 & 0 \\ 0 & 0.1 & 0 \\ 0 & 0 & 0.1 \end{pmatrix}$$

The disturbances w_k and measurement noise v_k are considered with the random signals that are bounded by $[-0.1, 0.1]$. In order to reduce the column number of the zonotope generator matrix, the reduction order of the matrix $\downarrow_l(H)$ is chosen as $l = 5$.

6.2.4.2 Simulation results

By setting $\lambda = 0.7$ and solving the LMIs in (6.19), the H_∞ index value $\gamma = 6.56$ is obtained and the following gain matrices L_1 , L_2 and L_3 are given by:

$$L_1 = \begin{pmatrix} -0.038 & -0.112 \\ -0.219 & -0.391 \\ -0.304 & -0.059 \end{pmatrix} \quad L_2 = \begin{pmatrix} -0.099 & -0.064 \\ -0.378 & -0.264 \\ -0.340 & -0.030 \end{pmatrix}$$

$$L_3 = \begin{pmatrix} 0.136 & -0.236 \\ 0.143 & -0.356 \\ -0.821 & 0.058 \end{pmatrix}$$

In the simulation study, the following Lyapunov matrix is deduced:

$$P = \begin{pmatrix} 17.92 & 2.16 & -3.88 \\ 2.16 & 15.9 & -2.69 \\ -3.88 & -2.69 & 13.7 \end{pmatrix}$$

and S is obtained as follows:

$$S = \begin{pmatrix} 0.349 & -0.423 \\ 1.767 & -1.980 \\ 2.306 & 1.542 \end{pmatrix}$$

Under the switching sequence exposed in Fig. 6.5, simulation results are provided.

Figure 6.5 indicates the active mode of the discrete-time switched system. To show the effectiveness of the designed fault detection approach, a comparison has been made with the fault detection approach without considering sensitivity and robustness analysis. We call in the sequel, method without optimization, a method where only the observer's stability is considered using a CQLF. An abrupt actuator fault f_k is carried out and represented as follows:

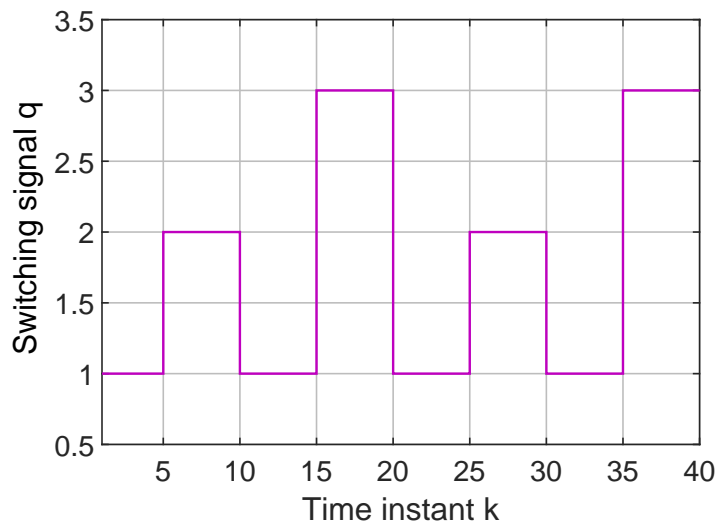


Figure 6.5: Evolution of the switching signal.

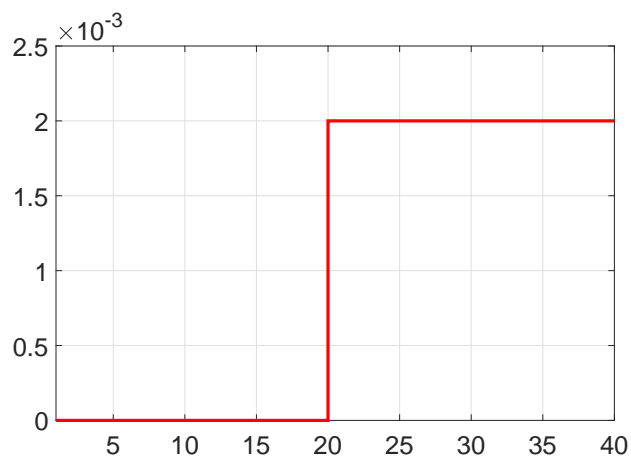
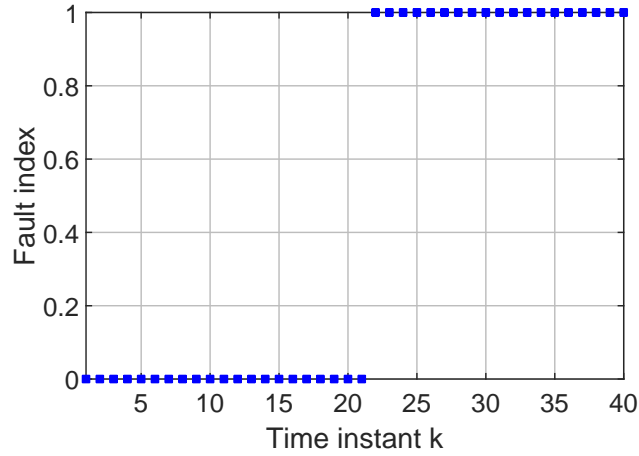


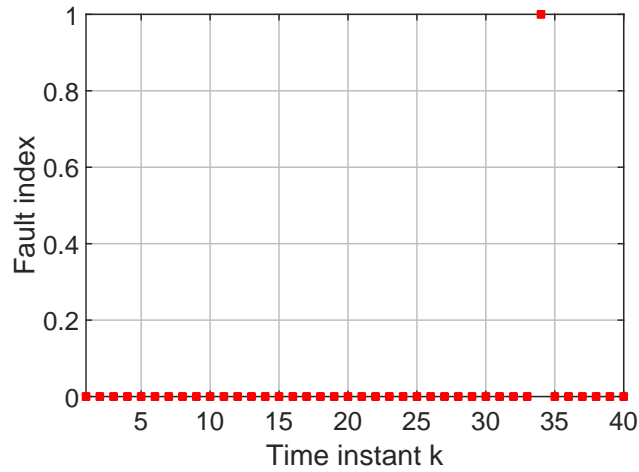
Figure 6.6: Evolution of the actuator fault.

The comparison results of the detection moments are depicted in Fig. 6.7. The fault f_k can be detected at the time instant $k = 22$ using the designed approach where both sensitivity to faults and robustness against uncertainties are considered, however the same fault f_k can hardly be detected using method without optimization. Thus, it should be pointed out that the designed approach is able to ensure better fault detection performances.

The fault detection logic is developed based on residual zonotopes. The comparison results are shown in Fig. 6.8 and Fig. 6.9. These figures highlight the residuals and the residual zonotopes of the FD technique designed without considering fault sensitivity and robustness performances and with the optimized method. In the fault free case, one can remark from Fig. 6.8 and Fig. 6.9 that $r(k) \in R(k)$ at the time instant $k = 19$. When a fault occurs ($k = 20$), the additive actuator fault is detected at the time instant $k = 22$ under the proposed FD approach $r(k) \notin R(k)$. However, under the approach without optimization, it



(a) Fault detection with optimisation



(b) Fault detection without optimisation

Figure 6.7: Comparison between the results of fault detection instant obtained with and without optimisation

cannot be detected at this instant of time ($k = 22$) and the zonotope $\mathbf{R}(k)$ still contains the residual signal $r(k)$. This is reasonable since the proposed approach has larger fault sensitivity performances and the impact of uncertainties is attenuated using H_∞ performances.

Therefore, these results press the effectiveness of the designed approach in actuator fault detection.

In this part, a new LMIs formulation has been introduced to design a robust observer-based fault detection scheme for a discrete-time switched system. The fault detection decision is achieved based on zonotopic techniques. The dimensions of zonotope can grow linearly, which increases the computational burden. To handle this problem, a reduction operator has been used to constrain the dimensions of zonotope. However, the zonotope based approach requires higher dimensional zonotopes if we want to obtain more accurate

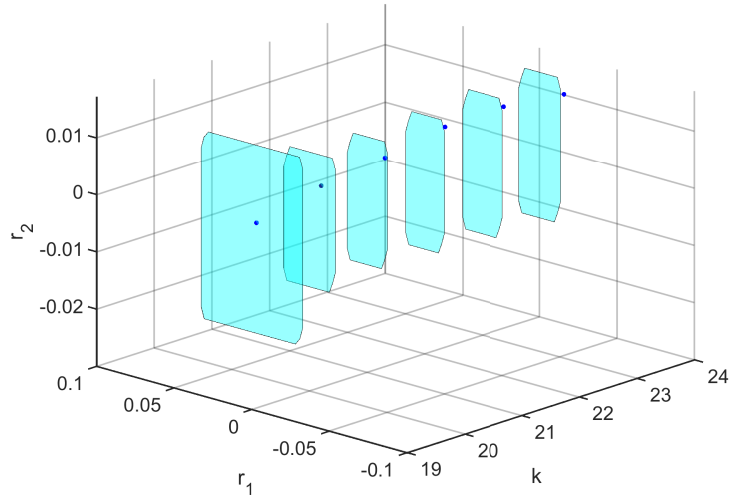


Figure 6.8: Residual and residual zonotope of the proposed FD observer

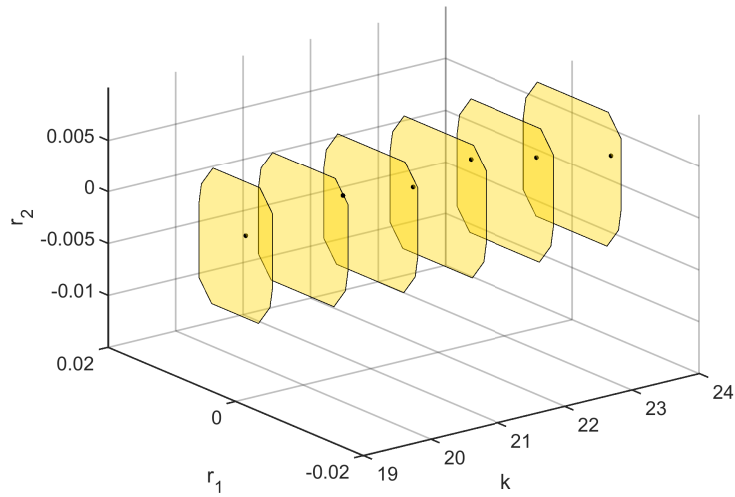


Figure 6.9: Residual and residual zonotope of method without optimization

fault detection results. Note that the basic operations for ellipsoids can reduce to simple matrix calculations and do not require a reduction operator, which provides a good trade-off between fault detection accuracy and computation complexity. In the next part, robust fault detection is investigated for switched systems based on ellipsoidal analysis.

6.3 Ellipsoid-based fault detection framework

6.3.1 Ellipsoidal set-theory preliminaries

The following definitions are essential in this part.

Definition 20. [206] An ellipsoid set $\mathcal{E}(c, X) \subset \mathbb{R}^n$ is given by:

$$\mathcal{E}(c, X) = \{x \in \mathbb{R}^n : (x - c)^T X^{-1}(x - c) \leq 1\}. \quad (6.26)$$

The center of $\mathcal{E}(c, X)$ is denoted by $c \in \mathbb{R}^n$. $X \in \mathbb{R}^{n \times n}$ is a symmetric positive definite matrix and represents the shape and size of the ellipsoid $\mathcal{E}(c, X)$.

Example 4. Figure 6.10 presents an example of an ellipsoid set $\mathcal{E}(c, X)$ in a two-dimension space with:

$$C = \begin{bmatrix} 0 \\ 0 \end{bmatrix}, X = \begin{bmatrix} 2 & 0 \\ 0 & 2 \end{bmatrix}.$$

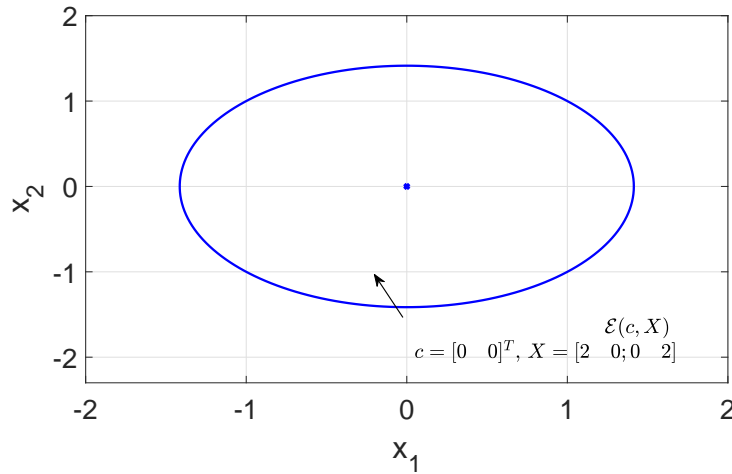


Figure 6.10: Ellipsoid set

Definition 21. [207] Let $x \in \mathcal{E}(c, X)$, the affine transformation $y = Kx + b$ gives the ellipsoid:

$$K\mathcal{E}(c, X) + b = \mathcal{E}(Kc + b, KXK^T). \quad (6.27)$$

Definition 22. [207] Let $\mathcal{E}(c_1, X_1)$ and $\mathcal{E}(c_2, X_2)$ be two ellipsoids, the inclusion

$$\mathcal{E}(c_1, X_1) \oplus \mathcal{E}(c_2, X_2) \subseteq \mathcal{E}(c_1 + c_2, X(p)) \quad (6.28)$$

holds for every matrix

$$X(p) = (1 + \frac{1}{p})X_1 + (1 + p)X_2, \quad (6.29)$$

where $p > 0$ and $\mathcal{E}(c_1 + c_2, X(p))$ represents an outer approximation of the Minkowski sum of $\mathcal{E}(c_1, X_1)$ and $\mathcal{E}(c_2, X_2)$.

Remark 23. The minimum volume ellipsoid enclosing $\mathcal{E}(c_1 + c_2, X(p))$ is denoted by $\mathcal{E}(c_1 + c_2, X(p^*))$ where p^* is the optimal parameter given by:

$$p^* = \sqrt{\frac{\text{trace}(X_1)}{\text{trace}(X_2)}} \quad (6.30)$$

where $\text{trace}()$ represents the trace operator.

6.3.2 Problem statement

In this part, the aim is to develop a FD decision via ellipsoidal techniques for discrete-time switched systems with sensor faults.

Consider the following discrete-time switched system:

$$\begin{cases} x_{k+1} = A_q x_k + B_q u_k + D_q w_k \\ y_k = C x_k + D_v v(k) + F f_k, \end{cases} \quad (6.31)$$

where $x \in \mathbb{R}^{n_x}$, $u \in \mathbb{R}^{n_u}$, $y \in \mathbb{R}^{n_y}$, $f \in \mathbb{R}^{n_f}$, $w \in \mathbb{R}^{n_w}$ and $v \in \mathbb{R}^{n_v}$ are the state vector, the input, the output, the sensor fault, the state disturbances and the measurement noise, respectively. A_q , B_q , C , D_q , D_v and F are known matrices with appropriate dimensions. q denotes the index of the active subsystem. $q \in \mathcal{S} = \overline{1, N}$, $N \in \mathbb{Z}_+$, N is the number of modes. The switching signal is supposed to be known.

The following assumption is used in the sequel.

Assumption 23. *Assume that the initial state x_0 , the state disturbances w_k and the measurement noise v_k are unknown but bounded such that:*

$$x_0 \in \mathcal{E}(c_0, X_0), \quad w_k \in \mathcal{E}(0, W), \quad v_k \in \mathcal{E}(0, V), \quad (6.32)$$

where $c_0 \in \mathbb{R}^{n_x}$ is a known vector, $X_0 = \tilde{x}_0^2 I_{n_x}$, $W = \|w\|_\infty^2 I_{n_w}$ and $V = \|v\|_\infty^2 I_{n_v}$. $\|w\|_\infty$ and $\|v\|_\infty$, assumed to be known, are the L_∞ norm of w and v , respectively. The known constant \tilde{x}_0 is given such that $\|x_0 - c_0\| \leq \tilde{x}_0$.

6.3.3 Robust fault detection design: TNL structure

The structure of the observer for (6.31) is given by:

$$\begin{cases} \hat{x}_{k+1} = T_q A_q \hat{x}_k + T_q B_q u_k + N_q y_{k+1} + L_q (y_k - C \hat{x}_k) \\ r_k = y_k - C \hat{x}_k \end{cases} \quad (6.33)$$

where $\hat{x} \in \mathbb{R}^{n_x}$ denotes the estimation of x , r_k denotes the residual signal and $L_q \in \mathbb{R}^{n_x \times n_y}$ are the observer gains. $T_q \in \mathbb{R}^{n_x \times n_x}$ and $N_q \in \mathbb{R}^{n_x \times n_y}$ are constant matrices that should be designed to satisfy

$$T_q + N_q C = I_{n_x} \quad (6.34)$$

Based on Lemma 9 in chapter 5, the general solution of (6.34) is given by

$$\begin{bmatrix} T_q & N_q \end{bmatrix} = \begin{bmatrix} I_{n_x} \\ C \end{bmatrix}^\dagger + S_q \left(I_{n_x+n_y} - \begin{bmatrix} I_{n_x} \\ C \end{bmatrix} \begin{bmatrix} I_{n_x} \\ C \end{bmatrix}^\dagger \right) \quad (6.35)$$

where $S_q \in \mathbb{R}^{n_x \times (n_x+n_y)}$ are matrices to be designed.

Remark 24. *It should be pointed out that if T_q and N_q are chosen such that $T_q = I_{n_x}$ and $N_q = 0$, the proposed observer (6.33) is reduced to the commonly used Luenberger form. The proposed structure can provide more design degrees of freedom by introducing matrices T_q and N_q .*

Define the estimation error as $e_k = x_k - \hat{x}_k$. According to (6.31) and (6.34), x_{k+1} can be written as:

$$\begin{cases} x_{k+1} = (T_q + N_q C)x_{k+1} \\ \quad = T_q x_{k+1} + N_q C x_{k+1} \\ \quad = T_q(A_q x_k + B_q u_k + D_q w_k) + N_q(y_{k+1} - D_v v(k+1) - F f_{k+1}) \\ \quad = T_q A_q x_k + T_q B_q u_k + T_q D_q w_k + N_q y_{k+1} - N_q D_v v_{k+1} - N_q F f_{k+1}. \end{cases} \quad (6.36)$$

Then, the error dynamics can be obtained:

$$\begin{cases} e_{k+1} = T_q A_q x_k + T_q B_q u_k + T_q D_q w_k + N_q y_{k+1} - N_q D_v v_{k+1} - N_q F f_{k+1} - \\ \quad T_q A_q \hat{x}_k - T_q B_q u_k - N_q y_{k+1} - L_q(y_k - C \hat{x}_k) \\ \quad = T_q A_q x_k + T_q D_q w_k - N_q D_v v_{k+1} - N_q F f_{k+1} - T_q A_q \hat{x}_k - \\ \quad L_q(C x_k + D v(k) + F f_k - C \hat{x}_k) \\ \quad = T_q A_q x_k - T_q A_q \hat{x}_k - L_q C x_k + L_q C \hat{x}_k + T_q D_q w_k - L_q D_v v(k) - \\ \quad N_q D_v v(k+1) - L_q F f_k - N_q F f_{k+1} \\ r_k = C x_k - C \hat{x}_k + D_v v(k) + F f_k \end{cases}$$

which can be rewritten as

$$\begin{cases} e_{k+1} = \mathcal{A}_q e_k + \mathcal{D}_{w_q} w_k + \mathcal{D}_{v_q} d_{v_{k+1}} + \mathcal{F}_q d_{f_{k+1}} \\ r_k = C e_k + D_v v_k + F f_k \end{cases} \quad (6.37)$$

where

$$\begin{cases} \mathcal{A}_q = T_q A_q - L_q C & \mathcal{D}_{w_q} = T_q D_q & \mathcal{D}_{v_q} = [-L_q D_v \quad -N_q D_v] \\ \mathcal{F}_q = [-L_q F \quad -N_q F] & d_v = [v(k)^T \quad v(k+1)^T]^T & d_f = [f(k)^T \quad f(k+1)^T]^T. \end{cases}$$

In order to obtain accurate FD results, it is required that state disturbances and measurement noise are attenuated. Hence, the error dynamics in (6.37) can be split into two subsystems where the subsystem (6.38) is decoupled from the effects of $f(k)$ and the subsystem (6.39) is only affected by the sensor fault.

$$\begin{cases} e_{k+1}^d = \mathcal{A}_q e_k^d + \mathcal{D}_{w_q} w_k + \mathcal{D}_{v_q} d_{v_{k+1}} \\ r_k^d = C e_k^d + D_v v_k \end{cases} \quad (6.38)$$

$$\begin{cases} e_{k+1}^f = \mathcal{A}_q e_k^f + \mathcal{F}_q d_{f_{k+1}} \\ r_k^f = C e_k^f + F f_k \end{cases} \quad (6.39)$$

where $e_k = e_k^f + e_k^d$.

The requirement of a CQLF provides a sufficient condition for stability. Nevertheless, the existence of such a function is not always guaranteed and the results may be conservative. Consequently, the stability analysis of the proposed observer is addressed using MQLF with an ADT switching signal.

Based on Lemma 8 in chapter 3, sufficient stability conditions are derived in terms of LMIs in Theorem 21 such that the error system in (6.38) is stable and for given scalars $\gamma_w > 0$, $\gamma_v > 0$, $\gamma_1 > 0$, $\gamma_2 > 0$ and $0 < \lambda < 1$, the residual signal r^d satisfies the L_∞ performance given by:

$$\|r_k^d\| < \sqrt{\gamma_1^2 \theta + \gamma_2^2} \|v\|_\infty^2 \quad (6.40)$$

where $\theta = (\gamma_w + \gamma_v)(\lambda(1 - \lambda)^k V_{q0} + \gamma_w \|w\|_\infty^2 + \gamma_v \|d_v\|_\infty^2)$, the constant $\|d_v\|_\infty$ is the L_∞ norm of d_v , $V_{q0} = e_0^{dT} P_q e_0^d$ and $P_q \succ 0 \in \mathbb{R}^{n_x \times n_x}$.

Theorem 21. Consider the switched system (6.31) and let $V_q(e_k^d)$ be the MQLF defined by $V_q(e_k^d) = e_k^{dT} P_q e_k^d$. If there exist positive definite matrices $P_q \succ 0 \in \mathbb{R}^{n_x \times n_x}$, constant matrices $M_l \in \mathbb{R}^{n_x \times n_x}$, $Q_q \in \mathbb{R}^{n_x \times n_y}$ and $Y_q \in \mathbb{R}^{n_x \times (n_x + n_y)}$, $a_2 > a_1 > 0$, $\mu > 0$ for given scalars $\gamma_w > 0$, $\gamma_v > 0$, $\gamma_1 > 0$, $\gamma_2 > 0$, $0 < \lambda < 1$ and $0 < \beta < 1$ such that the following conditions hold for all $q, l \in \mathcal{I}, q \neq l$

$$\min_{P_q, M_l} \beta \rho + (1 - \beta) \mu, \quad (6.41)$$

$$a_1 I_{n_x} \leq P_q \leq a_2 I_{n_x}, \quad (6.42)$$

$$\begin{bmatrix} (\lambda - 1)P_q & 0 & 0 & \Omega_{q14} \\ * & -\mu I_{n_w} & 0 & \Omega_{q24} \\ * & * & -\mu I_{n_{d_v}} & \Omega_{q34} \\ * & * & * & -P_q \end{bmatrix} \prec 0, \quad (6.43)$$

$$\begin{bmatrix} \lambda P_q & 0 & 0 & I_{n_x} \\ * & (\gamma_w - \mu) I_{n_w} & 0 & 0 \\ * & * & (\gamma_v - \mu) I_{n_{d_v}} & 0 \\ * & * & * & (\gamma_v + \gamma_w) I_{n_x} \end{bmatrix} \succ 0, \quad (6.44)$$

$$\begin{bmatrix} C^T C - \gamma_1^2 I_{n_x} & C^T D_v \\ * & -\gamma_2^2 I_{n_x} + D_v^T D_v \end{bmatrix} \prec 0, \quad (6.45)$$

$$\begin{bmatrix} M_l & P_q \\ P_q & P_q \end{bmatrix} \succeq 0, \quad (6.46)$$

then, the error dynamics system in (6.38) are stable and the L_∞ performance (6.40) is satisfied. Moreover, the state x is bounded with an ADT τ_a satisfying:

$$\tau_a > \tau_a^* = -\frac{\ln(\rho)}{\ln(1 - \lambda)}, \quad (6.47)$$

where $\rho = \frac{a_2}{a_1}$ and the observer gains L_q , T_q and N_q are given by:

$$\begin{cases} L_q = P_q^{-1} Q_q, \\ T_q = \Theta^\dagger \alpha_1 + P_q^{-1} Y_q \Psi \alpha_1, \\ N_q = \Theta^\dagger \alpha_2 + P_q^{-1} Y_q \Psi \alpha_2. \end{cases} \quad (6.48)$$

In addition, the error (6.38) implies:

$$\lim_{k \rightarrow \infty} \|e_k^d\| < \frac{\mu}{\alpha_1 \lambda} (\|w\|_\infty^2 + \|d_v\|_\infty^2) \quad (6.49)$$

and

$$\begin{cases} \Omega_{q14} = (P_q \Theta^\dagger \alpha_1 A_q + Y_q \Psi \alpha_1 A_q - Q_q C)^T, \\ \Omega_{q24} = (P_q \Theta^\dagger \alpha_1 A_q + Y_q \Psi \alpha_1 A_q) D_q^T, \\ \Omega_{q34} = [-W_q D_v \quad (-P \Theta^\dagger \alpha_2 - Y_q \Psi \alpha_2) D_v]^T, \end{cases} \quad (6.50)$$

$$\alpha_1 = \begin{bmatrix} I_{n_x} \\ 0 \end{bmatrix}, \quad \alpha_2 = \begin{bmatrix} 0 \\ I_{n_y} \end{bmatrix}, \quad \Theta = \begin{bmatrix} I_{n_x} \\ C \end{bmatrix}, \quad \Psi = I_{n_x + n_y} - \Theta \Theta^\dagger.$$

Proof. The asymptotic stability of the designed observer and the L_∞ performances are ensured using a MQLF defined by $V_q(e_k^d) = e_k^{dT} P_q e_k^d$, $P_q \succ 0$, $P_q \in \mathbb{R}^{n_x \times n_x}$. The increment of $V_q(e_k^d)$ is given by:

$$\Delta V_q(e_k^d) = \begin{bmatrix} e_k^{dT} & w_k^T & d_{vk}^T \end{bmatrix}^T \Gamma_q \begin{bmatrix} e_k^d & w_k & d_{vk} \end{bmatrix},$$

where

$$\Gamma_q = \begin{bmatrix} \mathcal{A}_q^T P_q \mathcal{A}_q - P_q & \mathcal{A}_q^T P_q \mathcal{D}_{w_q} & \mathcal{A}_q^T P_q \mathcal{D}_{v_q} \\ * & \mathcal{D}_{w_q}^T P_q \mathcal{D}_{w_q} & \mathcal{D}_{w_q}^T P_q \mathcal{D}_{v_q} \\ * & * & \mathcal{D}_{v_q}^T P_q \mathcal{D}_{v_q} \end{bmatrix}.$$

The inequality (6.43) can be rewritten as

$$\begin{bmatrix} (\lambda - 1)P_q & 0 & 0 & (P_q \mathcal{A}_q)^T \\ * & -\mu I_{n_w} & 0 & (P_q \mathcal{D}_{w_q})^T \\ * & * & -\mu I_{n_{d_v}} & (P_q \mathcal{D}_{v_q})^T \\ * & * & * & -P_q \end{bmatrix} \prec 0. \quad (6.51)$$

Pre- and post-multiplying (6.51) with

$$\begin{bmatrix} I_{n_x} & 0 & 0 & \mathcal{A}_q^T \\ 0 & I_{n_w} & 0 & \mathcal{D}_{w_q}^T \\ 0 & 0 & I_{n_{d_v}} & \mathcal{D}_{v_q}^T \end{bmatrix}$$

and its transpose, respectively, we can get:

$$\Gamma_q + \begin{bmatrix} \lambda P_q & 0 & 0 \\ * & -\mu I_{n_w} & 0 \\ * & * & -\mu I_{n_{d_v}} \end{bmatrix} \prec 0. \quad (6.52)$$

In addition, by pre-multiplying and post-multiplying (6.52) with $\begin{bmatrix} e_k^{dT} & w_k^T & d_{vk}^T \end{bmatrix}$ and its transpose, it follows that:

$$\Delta V_q(e_k^d) < -\lambda V_q(e_k^d) + \mu w_k^T w_k + \mu d_{vk}^T d_{vk}. \quad (6.53)$$

When $w_k = 0$ and $d_{vk} = 0$, (6.53) is equivalent to

$$\Delta V_q(e_k^d) = V_q(e_k^d + 1) - V_q(e_k^d) < -\lambda V_q(e_k^d) < 0. \quad (6.54)$$

Consequently, the error system in (6.38) is stable.

Based on the Schur complement, (6.44) is equivalent to

$$\nabla_q - \frac{1}{\gamma_w + \gamma_v} \begin{bmatrix} I_{n_x} \\ 0 \\ 0 \end{bmatrix} \begin{bmatrix} I_{n_x} & 0 & 0 \end{bmatrix} \succ 0 \quad (6.55)$$

where

$$\nabla_q = \begin{bmatrix} \lambda P_q & 0 & 0 \\ * & (\gamma_w - \mu) I_{n_w} & 0 \\ * & * & (\gamma_v - \mu) I_{n_{d_v}} \end{bmatrix}.$$

Pre-multiplying and post-multiplying (6.55) with $[e_k^{dT} \quad w_k^T \quad d_{v_k}^T]$ and its transpose, we obtain:

$$e_k^{dT} e_k^d \leq (\gamma_w + \gamma_v)(\lambda V_q(e_k^d) + (\gamma_w - \mu)\|w\|_\infty^2 + (\gamma_v - \mu)\|d_v\|_\infty^2). \quad (6.56)$$

Furthermore, inequality (6.53) can be bounded by:

$$V_q(e_k^d + 1) < (1 - \lambda)V_q(e_k^d) + \mu(\|w\|_\infty^2 + \|d_v\|_\infty^2). \quad (6.57)$$

According to (6.57), we can obtain:

$$\begin{aligned} V_q(e_k^d) &< (1 - \lambda)^k V_q(e_0^d) + \mu \sum_{\tau=0}^{k-1} (1 - \lambda)^\tau (\|w\|_\infty^2 + \|d_v\|_\infty^2) \\ &\leq (1 - \lambda)^k V_q(e_0^d) + \frac{\mu \|w\|_\infty^2}{\lambda} + \frac{\mu \|d_v\|_\infty^2}{\lambda}. \end{aligned} \quad (6.58)$$

According to inequalities in (6.58) and (A.10), we have:

$$e_k^{dT} e_k^d \leq (\gamma_w + \gamma_v)(\lambda(1 - \lambda)^k V_q(e_0^d) + \gamma_w \|w\|_\infty^2 + \gamma_v \|d_v\|_\infty^2).$$

In addition, the matrix inequality in (6.45) implies that

$$\begin{bmatrix} e_k^d \\ v_k \end{bmatrix}^T \begin{bmatrix} C^T C - \gamma_1^2 I_{n_x} & C^T D_v \\ * & -\gamma_2^2 I_{n_x} + D_v^T D_v \end{bmatrix} \begin{bmatrix} e_k^d \\ v_k \end{bmatrix} < 0, \quad (6.59)$$

which follows

$$\begin{aligned} r_k^{dT} r_k^d &\leq \gamma_1^2 e_k^{dT} e_k^d + \gamma_2^2 v_k^T v_k \\ &\leq \gamma_1^2 ((\gamma_w + \gamma_v)(\lambda(1 - \lambda)^k V_q(e_0^d) + \gamma_w \|w\|_\infty^2 + \gamma_v \|d_v\|_\infty^2)) + \gamma_2^2 \|v\|_\infty^2. \end{aligned} \quad (6.60)$$

Therefore, the L_∞ criterion is satisfied. Moreover, based on the first condition in Lemma 8 and (6.58), the following inequality

$$\|e_k^d\| \leq \frac{1}{\alpha_1} ((1 - \lambda)^k V_q(e_0^d) + \frac{\mu \|w\|_\infty^2}{\lambda} + \frac{\mu \|d_v\|_\infty^2}{\lambda})$$

holds. Then, when $k \rightarrow \infty$, (6.49) is deduced.

The error width is asymptotically bounded by $\frac{\mu}{\alpha_1 \lambda} (\|w\|_\infty^2 + \|d_v\|_\infty^2)$ which should be as small as possible by minimizing μ to enhance the accuracy of FD results. In addition, to look for an optimum dwell time, ρ should be minimized. The resolution of such a problem leads to solve the following objective function:

$$\beta \rho + (1 - \beta) \mu$$

The weight β should be in the range $[0, 1]$. Based on the third condition in Lemma 8, the observer errors stability at the switching instants is studied. The inequality defined in (3.46) becomes:

$$\rho P_l - P_q \succeq 0, \quad (6.61)$$

where $q, l \in \mathcal{I}, q \neq l, q$ is the current mode. Then based on the Schur complement Lemma, (6.61) implies:

$$\begin{bmatrix} \rho P_l & I_{n_x} \\ I_{n_x} & P_q^{-1} \end{bmatrix} \succeq 0. \quad (6.62)$$

The multiplication both side of (6.62) by $\begin{bmatrix} I_{n_x} & O_{n_x} \\ O_{n_x} & P_q \end{bmatrix}$ yields to $\begin{bmatrix} M_l & P_q \\ P_q & P_q \end{bmatrix} \succeq 0$ where $M_l = \rho P_l$. Then, (6.46) is satisfied. \square

6.3.4 Ellipsoid-based residual evaluation

The residual evaluation is based on determining whether the residual signal r_k defined in (6.38) is excluded from the residual ellipsoid $\mathcal{E}(0, R_k)$ or not. The corresponding FD decision scheme is made as follows:

$$\begin{cases} r(k) \in \mathcal{E}(0, R_k) & \text{Fault-free} \\ r(k) \notin \mathcal{E}(0, R_k) & \text{Faulty} \end{cases} \quad (6.63)$$

The residual ellipsoid $\mathcal{E}(0, R_k)$ is obtained based on the following theorem.

Theorem 22. *Consider the system (6.31) and the designed observer (6.33), let $x_0 \in \mathcal{E}(c_0, X_0)$ and $\hat{x}_0 = c_0$, then r_k can be bounded by the ellipsoid $\mathcal{E}(0, R_k)$ and R_k satisfies the following iteration equations:*

$$p_v^* = \sqrt{\frac{\text{trace}((L_q D_v) V (L_q D_v)^T)}{\text{trace}((N_q D_v) V (N_q D_v)^T)}} \quad (6.64)$$

$$H_v = (1 + \frac{1}{p_v^*}) (L_q D_v) V (L_q D_v)^T + (1 + p_v^*) (N_q D_v) V (N_q D_v)^T \quad (6.65)$$

$$p_d^* = \sqrt{\frac{\text{trace}(\mathcal{D}_{w_q} W \mathcal{D}_{w_q}^T)}{\text{trace}(H_v)}} \quad (6.66)$$

$$H_d = (1 + \frac{1}{p_d^*}) \mathcal{D}_{w_q} W \mathcal{D}_{w_q}^T + (1 + p_d^*) H_v \quad (6.67)$$

$$p_{x_k}^* = \sqrt{\frac{\text{trace}(\mathcal{A}_q X_k \mathcal{A}_q^T)}{\text{trace}(H_d)}} \quad (6.68)$$

$$X_{k+1} = (1 + \frac{1}{p_{x_k}^*}) \mathcal{A}_q X_k \mathcal{A}_q^T + (1 + p_{x_k}^*) H_d \quad (6.69)$$

$$p_{r_k}^* = \sqrt{\frac{\text{trace}(C X_k C^T)}{\text{trace}(D_v V D_v^T)}} \quad (6.70)$$

$$R_k = (1 + \frac{1}{p_{r_k}^*}) C X_k C^T + (1 + p_{r_k}^*) D_v V D_v^T \quad (6.71)$$

Proof. The aim is to determine the residual ellipsoid $\mathcal{E}(0, R_k)$. By assumption, we have $x_0 \in \mathcal{E}(c_0, X_0)$. Accordingly the following equation holds:

$$e_0 = x_0 - \hat{x}_0 \in \mathcal{E}(c_0, X_0) \oplus (-\hat{x}_0) = \mathcal{E}(0, X_0). \quad (6.72)$$

Based on Assumption 23, the state disturbances w_k and the measurement noise v_k are unknown but bounded such that $w_k \in \mathcal{E}(0, W)$, $v_k \in \mathcal{E}(0, V)$ and we have from (6.72), $e_0 \in \mathcal{E}(0, X_0)$. Consequently, we can deduce that $e_k \in \mathcal{E}(0, X_k)$.

The ellipsoid $\mathcal{E}(0, X_k)$ is determined in the following. We have from (6.38):

$$\begin{aligned} e_{k+1}^d &= \mathcal{A}_q e_k^d + \mathcal{D}_{w_q} w_k - L_q D_v v_k - N_q D_v v_{k+1} \\ &\in \mathcal{A}_q \mathcal{E}(0, X_k) \oplus (\mathcal{D}_{w_q} \mathcal{E}(0, W) \oplus (L_q D_v \mathcal{E}(0, V) \oplus N_q D_v \mathcal{E}(0, V))) \in \mathcal{E}(0, X_{k+1}). \end{aligned}$$

According to Definition 21,

$$\begin{cases} \mathcal{A}_q \mathcal{E}(0, X_k) = \mathcal{E}(0, \mathcal{A}_q X_k \mathcal{A}_q^T) \\ \mathcal{D}_{w_q} \mathcal{E}(0, W) = \mathcal{E}(0, \mathcal{D}_{w_q} W \mathcal{D}_{w_q}^T) \\ L_q D_v \mathcal{E}(0, V) = \mathcal{E}(0, (L_q D_v) V (L_q D_v)^T) \\ N_q D_v \mathcal{E}(0, V) = \mathcal{E}(0, (N_q D_v) V (N_q D_v)^T) \end{cases}$$

and to Definition 22,

$$\begin{cases} L_q D_v \mathcal{E}(0, V) \oplus N_q D_v \mathcal{E}(0, V) \in \mathcal{E}(0, H_v) \\ \mathcal{E}(0, \mathcal{D}_{w_q} W \mathcal{D}_{w_q}^T) \oplus \mathcal{E}(0, H_v) \in \mathcal{E}(0, H_d) \\ \mathcal{E}(0, \mathcal{A}_q X_k \mathcal{A}_q^T) \oplus \mathcal{E}(0, H_d) \in \mathcal{E}(0, X_{k+1}) \end{cases}$$

where

$$\begin{cases} H_v = (1 + \frac{1}{p_v^*}) (L_q D_v) V (L_q D_v)^T + (1 + p_v^*) (N_q D_v) V (N_q D_v)^T \\ H_d = (1 + \frac{1}{p_d^*}) \mathcal{D}_{w_q} W \mathcal{D}_{w_q}^T + (1 + p_d^*) H_v \\ X_{k+1} = (1 + \frac{1}{p_{x_k}^*}) \mathcal{A}_q X_k \mathcal{A}_q^T + (1 + p_{x_k}^*) H_d. \end{cases}$$

Based on Remark 23, p_v^* , p_d^* and $p_{x_k}^*$ are given by:

$$p_v^* = \sqrt{\frac{\text{trace}((L_q D_v) V (L_q D_v)^T)}{\text{trace}((N_q D_v) V (N_q D_v)^T)}} \quad p_d^* = \sqrt{\frac{\text{trace}(\mathcal{D}_{w_q} W \mathcal{D}_{w_q}^T)}{\text{trace}(H_v)}} \quad (6.73)$$

$$p_{x_k}^* = \sqrt{\frac{\text{trace}(\mathcal{A}_q X_k \mathcal{A}_q^T)}{\text{trace}(H_d)}} \quad (6.74)$$

In addition, we can obtain from (6.38):

$$\begin{aligned} r_k &= C e_k + D_v v_k \in C \mathcal{E}(0, X_k) \oplus D \mathcal{E}(0, V) \\ &\in \mathcal{E}(0, C X_k C^T) \oplus \mathcal{E}(0, D_v V D_v^T) \in \mathcal{E}(0, R_k). \end{aligned}$$

According to Definition 21, R_k is given by:

$$R_k = (1 + \frac{1}{p_{r_k}^*}) C X_k C^T + (1 + p_{r_k}^*) D_v V D_v^T$$

and $p_{r_k}^*$ is given as follows using Remark 23:

$$p_{r_k}^* = \sqrt{\frac{\text{trace}(C X_k C^T)}{\text{trace}(D_v V D_v^T)}}. \quad (6.75)$$

□

Remark 25. *The overall block diagram for the proposed robust fault detection approach is depicted in Fig. 6.11. It is pointed out that the proposed approach can be directly used to achieve residual evaluation and to improve fault detection accuracy by combining L_∞ performances and ellipsoidal techniques.*

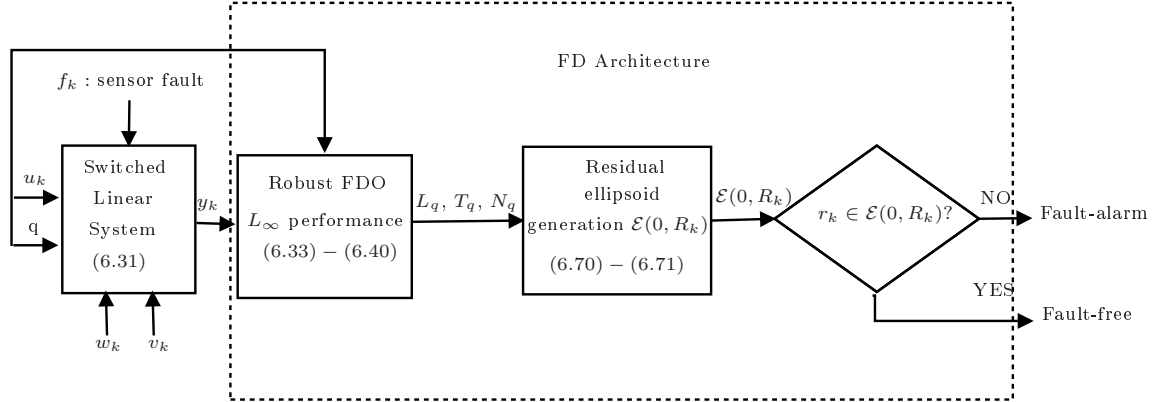


Figure 6.11: Block diagram of the proposed fault detection approach.

6.3.5 Illustrative Example

6.3.5.1 Simulation settings

The numerical example is considered for a discrete-time switched system defined with three subsystems, $N = 3$, with:

$$\begin{aligned}
 A_1 &= \begin{pmatrix} 0.6 & 2 & 1 \\ 0.2 & 0.5 & 0.2 \\ -0.9 & 0.2 & 0.8 \end{pmatrix} & A_2 &= \begin{pmatrix} 0.1 & 1.5 & 1 \\ 0.5 & 0.7 & 0.5 \\ -0.8 & 0 & 0.5 \end{pmatrix} & B_1 &= \begin{pmatrix} 1 \\ 0.5 \\ 0 \end{pmatrix} \\
 A_3 &= \begin{pmatrix} 0.5 & 0.3 & 1 \\ 0.1 & 0 & 1 \\ 0 & 0.1 & 0.1 \end{pmatrix} & B_2 &= \begin{pmatrix} 0.1 \\ 0.1 \\ 0.5 \end{pmatrix} & B_3 &= \begin{pmatrix} 1.2 \\ 1 \\ 0.5 \end{pmatrix} & D_1 &= \begin{pmatrix} 0.2 \\ 0.1 \\ 0.1 \end{pmatrix} \\
 D_2 &= \begin{pmatrix} 0.3 \\ 0.1 \\ 0.2 \end{pmatrix} & D_3 &= \begin{pmatrix} 0 \\ 0.1 \\ 0.1 \end{pmatrix} & D_v &= \begin{pmatrix} 0.1 & 0 \\ 0 & 0.1 \end{pmatrix} \\
 F &= \begin{pmatrix} 0.5 \\ -0.5 \end{pmatrix} & C &= \begin{pmatrix} 1 & 0.1 & 0 \\ 1 & 1 & 0.1 \end{pmatrix}
 \end{aligned}$$

In the simulation study, $w_k \in \mathbb{R}$ and $v_k \in \mathbb{R}^2$ denote distributed bounded signals such that:

$$|w_k| \leq 0.1, \quad |v_k| \leq [0.1 \quad 0.1].$$

The initial conditions are chosen such that:

$$x_0 = [1 \quad 1 \quad 1]^T, \quad \hat{x}_0 = [1 \quad 1 \quad 1]^T, \quad c_0 = [0 \quad 0 \quad 0]^T \quad \text{and} \quad X_0 = I_3.$$

6.3.5.2 Simulation results

The switching signal between the three subsystems is plotted in Fig. 6.12.

Based on Theorem 21, MQLF are obtained:

$$P_1 = \begin{pmatrix} 2.71 & 0.05 & 0.24 \\ 0.05 & 1.85 & 1.10 \\ 0.24 & 1.10 & 1.64 \end{pmatrix} \quad P_2 = \begin{pmatrix} 2.65 & 0.16 & 0.17 \\ 0.16 & 2.61 & 0.23 \\ 0.17 & 0.23 & 2.59 \end{pmatrix}$$

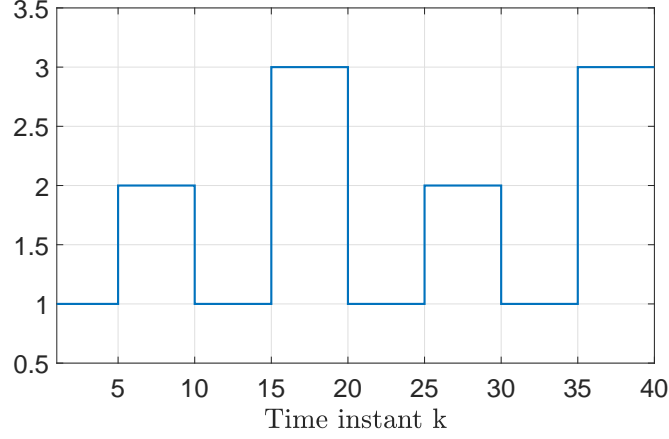


Figure 6.12: Evolution of the switching signal.

$$P_3 = \begin{pmatrix} 2.43 & 0.23 & 0.32 \\ 0.23 & 2.64 & 0.12 \\ 0.32 & 0.12 & 2.54 \end{pmatrix}$$

The scalar μ is given by $\mu = 7.61$ which leads to an ADT $\tau_a > 0.9$. By solving LMIs in Theorem 21, the matrices L_q , N_q and T_q can be obtained as follows:

$$L_1 = \begin{pmatrix} -0.04 & 0.10 \\ 0.03 & 0.02 \\ -0.23 & -1.03 \end{pmatrix} \quad L_2 = \begin{pmatrix} -0.12 & -0.01 \\ 0.19 & 0.13 \\ -0.20 & -0.70 \end{pmatrix} \quad L_3 = \begin{pmatrix} 0.04 & 0.09 \\ -0.06 & -0.13 \\ -0.05 & 0.07 \end{pmatrix}$$

$$N_1 = \begin{pmatrix} 0.39 & 0.41 \\ 0.01 & 0.20 \\ 0.25 & 0.24 \end{pmatrix} \quad N_2 = \begin{pmatrix} 0.36 & 0.41 \\ 0.04 & 0.22 \\ 0.22 & 0.23 \end{pmatrix} \quad N_3 = \begin{pmatrix} 0.34 & 0.27 \\ 0.01 & 0.49 \\ -0.2 & 0.21 \end{pmatrix}$$

$$T_1 = \begin{pmatrix} 0.19 & -0.45 & -0.04 \\ -0.21 & 0.79 & -0.02 \\ 0.50 & -0.27 & 0.97 \end{pmatrix} \quad T_2 = \begin{pmatrix} 0.21 & -0.45 & -0.04 \\ -0.27 & 0.77 & -0.02 \\ -0.44 & -0.24 & 1 \end{pmatrix}$$

$$T_3 = \begin{pmatrix} 0.38 & -0.30 & -0.02 \\ -0.50 & 0.50 & -0.05 \\ 0.03 & -0.18 & 1 \end{pmatrix}$$

Two fault scenarios are considered in the sequel.

Case 1: A sensor fault with the amplitude of 0.25 is supposed to occur after the time instant $k = 14$. This fault is presented in Fig. 6.13.

In order to demonstrate the effectiveness of the proposed fault detection method, a comparison has been made with the fault detection approach using a Luenberger observer and a robustness analysis. The comparison results are shown in Fig. 6.14.

The fault f_k can be detected at the time instant $k = 14$ using both methods since the effect of uncertainties is minimized based on an L_∞ performance.

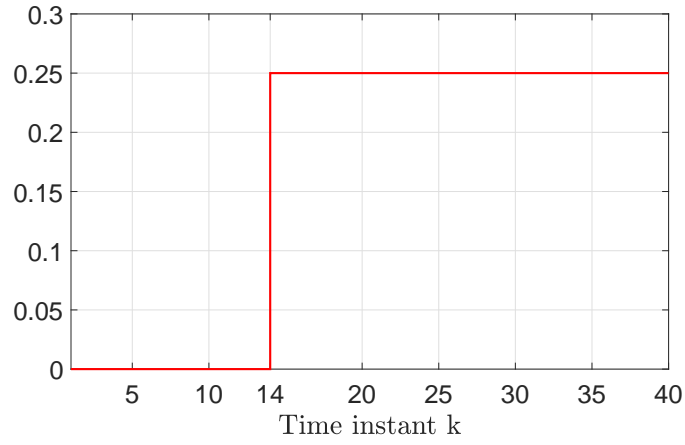
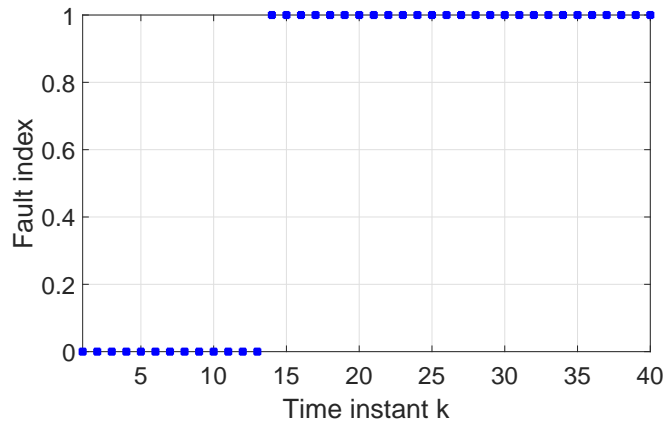
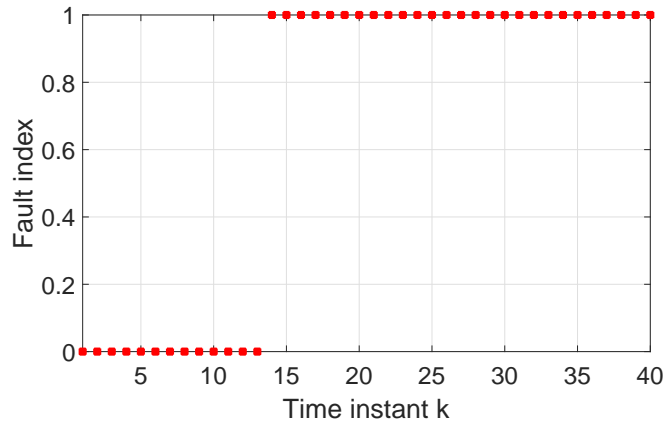


Figure 6.13: Evolution of the sensor fault.



(a) Fault detection using the TNL observer and L_∞ performance



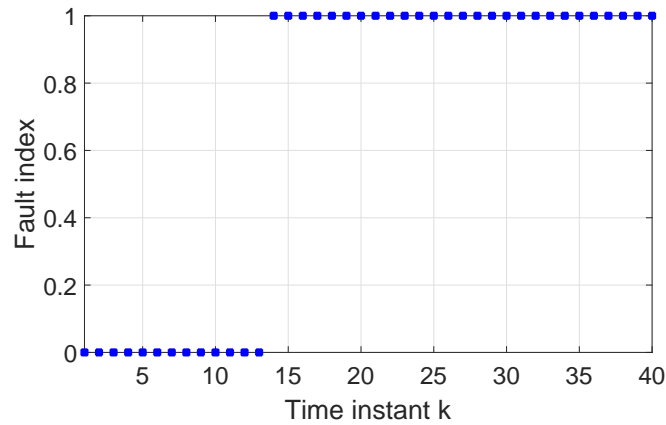
(b) Fault detection using the Luenberger observer and L_∞ performance

Figure 6.14: Comparison between fault detection results obtained with the proposed observer and a Luenberger structure.

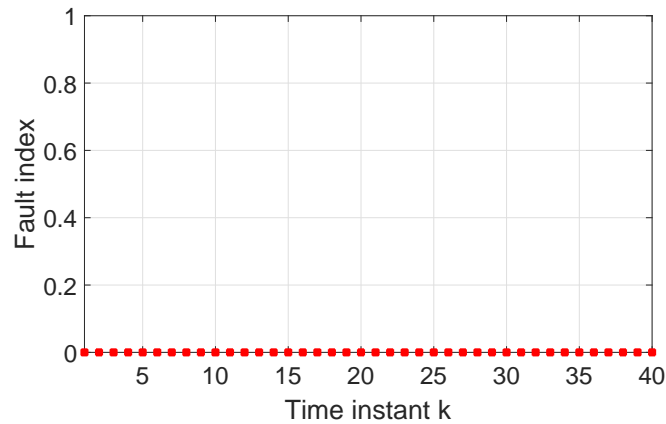
Case 2: In the second fault scenario, a fault with a smaller amplitude $f = 0.08$ is considered to happen after the same time instant $k = 14$. The sensor fault can be described as follows:

$$f_k = \begin{cases} 0.08 & k \geq 14 \\ 0 & \text{otherwise} \end{cases} \quad (6.76)$$

The simulation results of the detection moments are depicted in Fig. 6.15. The fault f_k can be detected at the time instant $k = 14$ using the designed technique where both robustness against uncertainties and ellipsoid analysis are considered, however the same fault f_k can not be detected using a Luenberger observer. Therefore, the results show the feasibility and effectiveness of the designed method in fault detection.



(a) Fault detection using the TNL observer and L_∞ performance



(b) Fault detection using the Luenberger observer and L_∞ performance

Figure 6.15: Comparison between fault detection results obtained with the proposed observer and a Luenberger structure (small fault).

The FD results are obtained via the ellipsoidal analysis. The comparison results are shown in Fig. 6.16 and Fig. 6.17.

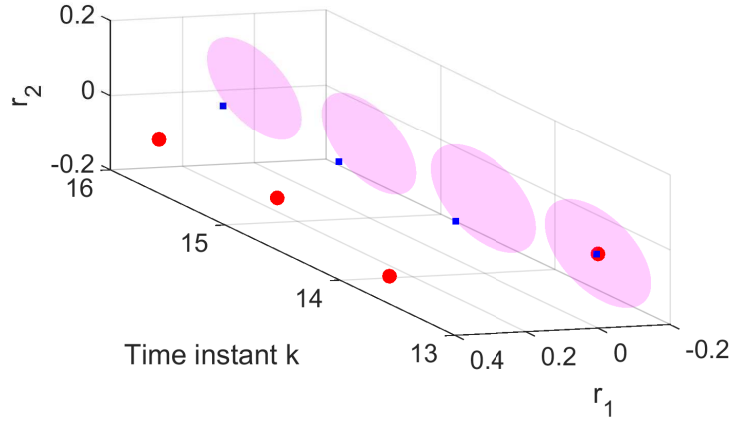


Figure 6.16: Residual and residual ellipsoid based on the proposed approach.

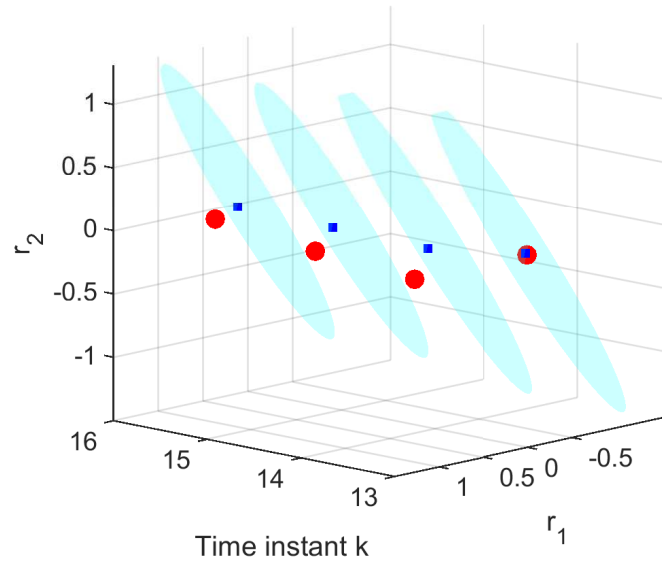


Figure 6.17: Residual and residual ellipsoid using a Luenberger observer.

These figures present the residuals and the residual ellipsoids based on the proposed method and Luenberger observers. Herein, the red points and the blue ones represent the residual signals when considering $f = 0.25$ and $f = 0.08$, respectively. In the fault free case, from Fig. 6.16 and Fig. 6.17, one can remark that $r(k) \in \mathcal{E}(0, R_k)$ until the time instant $k = 13$. When a fault occurs ($k = 14$), it is immediately detected under the proposed FD approach and $r(k) \notin \mathcal{E}(0, R_k)$, in both cases. However, based on Luenberger observers, the fault cannot be detected and the ellipsoid $\mathcal{E}(0, R_k)$ still includes the residual signal $r(k)$ when a small fault $f = 0.08$ is occurred.

6.4 Conclusion

In this chapter, set-membership FD frameworks have been developed for switched systems using zonotopic and ellipsoidal analysis. These methods are investigated to provide systematic dynamic thresholds for residual evaluation as well as improving the accuracy of the residual boundaries without considering the nonnegativity assumption. In the first part, a new LMIs formulation is presented to design a robust observer-based FD scheme for a discrete-time switched system. The proposed technique takes into account the robustness of the FDO against disturbances and sensitivity to fault. H_∞ performance is investigated to minimize the effect of disturbances and the impact of fault on the residual signal is maximised by a novel pole placement method. Then, the FD decision is evaluated based on zonotopic techniques. The FD accuracy of the zonotopic algorithm can be improved using higher dimensional zonotopes. However, the additional dimensional growth may cause heavier computational burden. Compared with the zonotopic methods, the ellipsoidal techniques can be considered as a good trade-off between FD accuracy and computation complexity. The second part of this chapter is concerned with robust FD scheme based on ellipsoidal analysis. A FD observer with a new structure is investigated based on an L_∞ criterion to attenuate the effects of uncertainties. The design conditions are given in terms of LMIs using MQLF, with an ADT switching signal. Finally, numerical examples are performed to illustrate the effectiveness of both set-membership FD frameworks.

Chapter 7

Conclusions and Perspectives

7.1 Conclusions

This thesis has mainly considered the study of state estimation and fault detection for a class of switched linear systems. Most of the developed approaches are introduced in the presence of unknown but bounded state disturbances and measurement noise. In order to deal with these uncertainties, set-membership techniques are investigated to achieve robust state estimation and to improve FD accuracy results.

After reviewing the state of the art, presented in chapter 2, about switched systems, interval observer theory, model-based diagnosis approaches and set-membership fault detection, an interval estimation approach is conducted in chapter 3 for both continuous and discrete-time LPV switched systems subject to measured polytopic parameters. In this chapter, the switching signal is supposed to be known, the measurement noise and the state disturbances are assumed to be unknown but bounded with known bounds. The designed techniques are investigated using a new polytopic modeling framework to provide a finite dimensional relaxation for the design conditions of the proposed interval observers. Based on common Lyapunov functions, the cooperativity and stability conditions have been relaxed and expressed on the vertices of each polytope. In some cases, the existence of a CQLF is not always guaranteed. In this chapter, based on the construction of MQLF with an ADT switching signal, the conservatism is further reduced.

In chapter 4, the switching signal is supposed to be unknown. Therefore, a new approach combining a sliding modes observer with an interval observer is designed in order to estimate the discrete mode of the switched system subject to an unknown input. Based on distinguishability conditions of the current mode, the sliding modes theory provides a robust finite-time convergence. While, only bounds of the unknown input are needed to determine the switching time instants using interval observer theory. Based on the output estimation errors and H_∞ performances, an attenuation condition of the disturbance and sensitivity condition of residuals are designed and are formulated in terms of LMIs to ensure

a robust detection of discrete mode change.

In chapter 5, robust fault detection frameworks for uncertain switched systems were proposed. In this context, set-membership methods based on interval analysis were used. Two different case studies were considered. In the first approach, the traditional interval observer was designed based on the L_∞ criterion in order to enhance the FD performance results. It is worth noting that the interval analysis avoids the design of residual evaluation functions or threshold generator and provides a systematic way for residual evaluation. The FD decision is based on a belonging test of the zero signal to the residual boundaries given by the proposed classical interval observer. In the second study, a novel interval observer structure (TNL structure) was investigated. It has been shown that the new structure reduces the conservatism regarding uncertainties in fault detection. Compared to classical interval observers, the TNL observer provides a better estimation of residuals. In addition, it can detect small faults while the rate of missing alarms is reduced. The stability analysis is first achieved by applying CQLF. However, the requirement of CQLF remains a restrictive condition to introduce stability settings. Accordingly, for the sake of less conservative conditions, MQLF are adopted with an ADT switching signal.

Interval methods require the nonnegativity condition. Compared with intervals, set-membership fault detection techniques are considered in chapter 6 to improve the accuracy of the residual framers without considering the nonnegativity assumption. Two robust FD strategies are introduced for discrete-time switched systems based on zonotopic and ellipsoidal analysis.

- In the first part, the case of actuator faults is considered. Based on a Luenberger structure, the observer gains are designed with two main objectives: (i) sensitivity to detect faults with low magnitudes; (ii) robustness against uncertainties including system disturbances and measurement noise to allow distinguishing uncertainties and faults. The design conditions of the observer are derived in terms of (LMIs) using a new pole assignment technique and H_∞ performance. In addition, the disturbances and measurement noise are supposed to be unknown but bounded by zonotopes. Thus, the FD decision is based on zonotopic residual evaluation methods and performed by deciding whether the residual signal is excluded from the residual zonotope when a fault occurs.
- The second part of this chapter is concerned with robust FD scheme based on ellipsoidal analysis. The case of sensor faults is considered. The proposed FD method has integrated a new observer structure providing accurate FD results. Based on an L_∞ performance, LMIs conditions are derived using MQLF with an ADT switching signal. In this part, the FD results are obtained via an ellipsoidal analysis. Compared with the zonotopic methods, the ellipsoidal techniques can be considered as a good trade-off between FD accuracy and computation complexity.

7.2 Future directions

This thesis has addressed the issue of state estimation and fault detection for switched linear systems. A number of interesting topics, based on the research issues studied in this thesis,

could also be addressed. Some perspectives and possible extensions to the work that have not been addressed in the thesis could be provided and studied as future works:

- The design conditions of the interval observer in chapter 3 are formulated in order to check the boundedness and the positivity of the estimation errors \underline{e} and \bar{e} . From a practical point of view, the uncertainties signals can not be always energy-bounded but have bounded peak values. Therefore, an optimization with respect to L_∞ performance, which describes the peak-to-peak performance index, could be introduced to enhance the robustness of the estimation error intervals. The work carried out in [208] can be considered as a starting point.
- In chapter 3, the time varying parameters are considered measured. Therefore, extensions of the developed results with unmeasured scheduling vector and the relaxation of Assumption 12 by finding a change of coordinates could be expected.
- The proposed fault detection methods are investigated for linear switched systems assuming a measured switching signal. It would be interesting to extend the proposed results for LPV switched systems when the switching logic is assumed to be unknown.
- The goal of fault detection is to indicate faults occurrence while the fault estimation is achieved to estimate the magnitude of faults. In this thesis, the fault estimation problem has not been addressed. A new design technique of fixed-time observers is investigated in [209] in order to achieve some transient performance such as guaranteeing the fixed-time convergence of the estimation error. Based on past values of the input and the output signals, the proposed technique provides a dead bit estimation of the state without the need of the initial states bounds or nonnegative conditions. Hence, one can expect the extension of the proposed state estimation technique in [209] to achieve fault estimation for discrete-time nonlinear switched systems.
- The presence of a time delay can affect the stability, the performance of dynamical systems and also make the fault diagnosis design problem more complicated. Time delay systems can be classified into two types: delay-independent methods and delay-dependent methods. The delay-independent methods do not consider the size of the delay which is not the case of the delay-dependent methods. It is worth noting that, the developed results in this thesis concern switched systems without time delay. In the literature, few works deal with robust fault detection for switched systems with a time-varying delay assumption. Thus, in future works, a time delay could be introduced to consider fault diagnosis problems for switched systems using zonotopic and ellipsoidal analysis.
- A practical application of the proposed approaches on real processes such as robotic and electrical systems will be considered in future works.

Appendices

Appendix A

Appendix of chapter 5

A.1 Proof of theorem 16

Based on the error system in (5.33), the aim is to design an observer (5.23) satisfying the following conditions:

- (i) The error system in (5.33) is stable.
- (ii) The L_∞ performance (5.35) is satisfied.

Choose the following CQLF

$$V(\mathcal{E}_k^d) = \mathcal{E}_k^{dT} P \mathcal{E}_k^d, P^T = P \succ 0, P \in \mathbb{R}^{2n_x \times 2n_x}.$$

It is worth noting that $P > 0$ since it is a diagonal matrix. Consequently, $\mathcal{A}_q \geq 0$ holds if

$$P \begin{bmatrix} \overline{T}_q A_q - \overline{L}_q C & 0 \\ 0 & \underline{T}_q A_q - \underline{L}_q C \end{bmatrix} \geq 0. \quad (\text{A.1})$$

Substituting (5.40) into (A.1) gives

$$\begin{bmatrix} P_1 \Theta^\dagger \alpha_1 A_q + Y_{q1} \Psi \alpha_1 A_q - W_{q1} C & 0 \\ * & P_2 \Theta^\dagger \alpha_1 A_q + Y_{q2} \Psi \alpha_1 A_q - W_{q2} C \end{bmatrix} \geq 0. \quad (\text{A.2})$$

Therefore, inequality (A.2) is a sufficient condition of $\mathcal{A}_q \geq 0$.

The time difference of $V(\mathcal{E}_k^d)$ is given by

$$\begin{aligned} \Delta V(\mathcal{E}_k^d) &= V(\mathcal{E}_k^d + 1) - V(\mathcal{E}_k^d) \\ &= \mathcal{E}_{k+1}^{dT} P \mathcal{E}_{k+1}^d - \mathcal{E}_k^{dT} P \mathcal{E}_k^d \\ &= (\mathcal{A}_q \mathcal{E}_k^d + \mathcal{H}_q d_k)^T P (\mathcal{A}_q \mathcal{E}_k^d + \mathcal{H}_q d_k) - \mathcal{E}_k^{dT} P \mathcal{E}_k^d \\ &= \mathcal{E}_k^{dT} \mathcal{A}_q^T P \mathcal{A}_q \mathcal{E}_k^d + \mathcal{E}_k^{dT} \mathcal{A}_q^T P \mathcal{H}_q d_k + d_k^T \mathcal{H}_q^T P \mathcal{A}_q \mathcal{E}_k^d + d_k^T \mathcal{H}_q^T P \mathcal{H}_q d_k \\ &\quad - \mathcal{E}_k^{dT} P \mathcal{E}_k^d. \end{aligned} \quad (\text{A.3})$$

Based on (A.3), the following equation can be obtained

$$\Delta V(\mathcal{E}_k^d) = \begin{bmatrix} \mathcal{E}_k^d \\ d_k \end{bmatrix}^T \begin{bmatrix} \mathcal{A}_q^T P \mathcal{A}_q - P & \mathcal{A}_q^T P \mathcal{H}_q \\ * & \mathcal{H}_q^T P \mathcal{H}_q \end{bmatrix} \begin{bmatrix} \mathcal{E}_k^d \\ d_k \end{bmatrix}.$$

If inequality (5.37) holds, then it can be rewritten as

$$\begin{bmatrix} (\lambda - 1)P & 0 & (P \mathcal{A}_q)^T \\ * & -\mu I_{n_d} & (P \mathcal{H}_q)^T \\ * & * & -P \end{bmatrix} \prec 0. \quad (\text{A.4})$$

By pre- and post- multiplying (A.4) with $\begin{bmatrix} I_{2n_x} & 0 & \mathcal{A}_q^T \\ 0 & I_{n_d} & \mathcal{H}_q^T \end{bmatrix}$ and its transpose, respectively, the relation in (A.5) yields

$$\begin{bmatrix} \mathcal{A}_q^T P \mathcal{A}_q - P & \mathcal{A}_q^T P \mathcal{H}_q \\ * & \mathcal{H}_q^T P \mathcal{H}_q \end{bmatrix} + \begin{bmatrix} \lambda P & 0 \\ * & -\mu I_{n_d} \end{bmatrix} \prec 0. \quad (\text{A.5})$$

Pre- and post-multiplying (A.5) with $[\mathcal{E}_k^{dT} \quad d_k^T]$ and its transpose

$$\begin{bmatrix} \mathcal{E}_k^d \\ d_k \end{bmatrix}^T \begin{bmatrix} \mathcal{A}_q^T P \mathcal{A}_q - P & \mathcal{A}_q^T P \mathcal{H}_q \\ * & \mathcal{H}_q^T P \mathcal{H}_q \end{bmatrix} \begin{bmatrix} \mathcal{E}_k^d \\ d_k \end{bmatrix} + \begin{bmatrix} \mathcal{E}_k^d \\ d_k \end{bmatrix}^T \begin{bmatrix} \lambda P & 0 \\ * & -\mu I_{n_d} \end{bmatrix} \begin{bmatrix} \mathcal{E}_k^d \\ d_k \end{bmatrix} \prec 0,$$

it follows that

$$\begin{aligned} \Delta V(\mathcal{E}_k^d) + \lambda \mathcal{E}_k^{dT} P \mathcal{E}_k^d - \mu d_k^T d_k &< 0 \\ \Delta V(\mathcal{E}_k^d) &< -\lambda V(\mathcal{E}_k^d) + \mu d_k^T d_k. \end{aligned} \quad (\text{A.6})$$

When process disturbance w_k and measurement noise v_k are zero, $d_k = 0$ and the increment of Lyapunov function $V(\mathcal{E}_k^d)$ becomes

$$\Delta V(\mathcal{E}_k^d) = V(\mathcal{E}_k^d + 1) - V(\mathcal{E}_k^d) < -\lambda V(\mathcal{E}_k^d) < 0.$$

Hence, the error system in (5.33) is stable.

Note that the following inequality can be derived from (A.6)

$$V(\mathcal{E}_k^d + 1) < (1 - \lambda)V(\mathcal{E}_k^d) + \mu \theta_d^2, \quad (\text{A.7})$$

where θ_d is a known constant and represents the L_∞ of d . From (A.7), one can obtain

$$\begin{aligned} V(\mathcal{E}_k^d) &\leq (1 - \lambda)^k V(\mathcal{E}_0^d) + \mu \sum_{\tau=0}^{k-1} (1 - \lambda)^\tau \theta_d^2 \\ &\leq (1 - \lambda)^k V(\mathcal{E}_0^d) + \mu \frac{(1 - \lambda^k)}{\lambda} \theta_d^2 \\ &\leq (1 - \lambda)^k V(\mathcal{E}_0^d) + \frac{\mu \theta_d^2}{\lambda}. \end{aligned} \quad (\text{A.8})$$

On the other hand, by using the Schur complement lemma, (5.38) is equivalent to

$$\begin{bmatrix} \lambda P & 0 \\ * & (\gamma - \mu) I_{n_d} \end{bmatrix} - \frac{1}{\gamma} \begin{bmatrix} I_{2n_x} \\ 0 \end{bmatrix} \begin{bmatrix} I_{2n_x} & 0 \end{bmatrix} \succ 0. \quad (\text{A.9})$$

Then, pre-multiplying and post-multiplying (A.9) with $[\mathcal{E}_k^{dT} \quad d_k^T]$ and its transpose, one can obtain

$$\mathcal{E}_k^{dT} \mathcal{E}_k^d \leq \gamma (\lambda V(\mathcal{E}_k^d) + (\gamma - \mu) \theta_d^2). \quad (\text{A.10})$$

Substituting (A.8) into (A.10) gives

$$\begin{aligned} \mathcal{E}_k^{dT} \mathcal{E}_k^d &\leq \gamma \left(\lambda \left((1 - \lambda)^k V(\mathcal{E}_0^d) + \frac{\mu \theta_d^2}{\lambda} \right) + (\gamma - \mu) \theta_d^2 \right) \\ &\leq \gamma \left(\lambda (1 - \lambda)^k V(\mathcal{E}_0^d) + \gamma \theta_d^2 \right). \end{aligned}$$

In addition, the matrix inequality in (5.39) implies that

$$\begin{bmatrix} \mathcal{E}_k^d \\ \tilde{v}_k \end{bmatrix}^T \begin{bmatrix} \mathcal{C}^T \mathcal{C} - \gamma_1^2 I_{2n_x} & \mathcal{C}^T \mathcal{V} \\ * & -\gamma_2^2 I_{2n_x} + \mathcal{V}^T \mathcal{V} \end{bmatrix} \begin{bmatrix} \mathcal{E}_k^d \\ \tilde{v}_k \end{bmatrix} < 0,$$

which follows

$$\begin{aligned} \mathcal{R}_k^{dT} \mathcal{R}_k^d &\leq \gamma_1^2 \mathcal{E}_k^{dT} \mathcal{E}_k^d + \gamma_2^2 \tilde{v}_k^T \tilde{v}_k \\ &\leq \gamma_1^2 \gamma (\lambda (1 - \lambda)^k V(\mathcal{E}_0^d) + \gamma \theta_d^2) + \gamma_2^2 \theta_v^2. \end{aligned}$$

Therefore, the L_∞ criterion (5.35) is satisfied.

A.2 Proof of theorem 18

The requirement on the nonnegativity property of the matrices $\overline{T}_q A_q - \overline{T}_q C$ and $\underline{T}_q A_q - \underline{T}_q C$ is achieved via the inequality (5.54). We are interested in checking the stability of the estimation errors (5.33) via MQLF for the proposed observer in (5.23).

Based on Lemma 8 in chapter 3, the following inequality

$$a_1 \|\mathcal{E}_k^d\| \leq V_q(\mathcal{E}_k^d), \quad (\text{A.11})$$

holds. From (A.8), we have

$$V_q(\mathcal{E}_k^d) \leq (1 - \lambda)^k V_q(\mathcal{E}_0^d) + \frac{\mu \theta_d^2}{\lambda}. \quad (\text{A.12})$$

Thus, according to (A.11) and (A.12), it is easy to derive that

$$\|\mathcal{E}_k^d\| \leq \frac{1}{a_1} \left((1 - \lambda)^k V_q(\mathcal{E}_0^d) + \frac{\mu \theta_d^2}{\lambda} \right).$$

Hence, when $k \rightarrow \infty$, $(1 - \lambda)^k$ converge to zero, implies that:

$$\lim_{k \rightarrow \infty} \|\mathcal{E}_k^d\| < \frac{\mu}{a_1 \lambda} \theta_d^2.$$

Note that with the proposed interval observer with the TNL structure, the boundedness of the resulting interval error is guaranteed. In addition, the design of a robust interval observer with a tight interval may be achieved optimally, if the bound $\frac{\mu}{a_1 \lambda} \theta_d^2$ is minimized. Consequently, the problem of minimizing the interval width of the estimation error and thus the interval width of the residual signal is reduced to the minimization of the scalar μ for a given a_1 and λ . The second purpose consists in minimizing ρ to look for optimum dwell time. The resolution of such a problem leads to solving a problem of linear optimization

which consists of seeking a minimization function. Then, the objective function can be added to the LMIs conditions and given by:

$$\beta\rho + (1 - \beta)\mu,$$

where the weight β is in the range $[0, 1]$.

Let us now focus on the stabilization of subsystems at the switching instants. It is straightforward to show that the inequality defined in (3.46) becomes:

$$\rho P_l - P_q \succeq 0, \quad (\text{A.13})$$

where $q, l \in \mathcal{I}, q \neq l$, q is the current mode. Then applying the Schur complement lemma, we obtain the following expression:

$$\begin{bmatrix} \rho P_l & I_{2n_x} \\ I_{2n_x} & P_q^{-1} \end{bmatrix} \succeq 0. \quad (\text{A.14})$$

Multiplying the left and right by $\begin{bmatrix} I_{2n_x} & O_{2n_x} \\ O_{2n_x} & P_q \end{bmatrix}$ and defining $M_l = \rho P_l$, then (6.62) becomes:

$$\begin{bmatrix} M_l & P_q \\ P_q & P_q \end{bmatrix} \succeq 0.$$

Therefore, (5.47) is verified. LMIs conditions in (5.44), (5.45) and (5.46) have been proven in Theorem 14.

Appendix B

Résumé des travaux de thèse

Introduction

Ces dernières années, en raison de la complexité croissante des technologies industrielles, l'un des enjeux les plus importants concerne le diagnostic des systèmes complexes [210], [211], [212], [123]. Ainsi, les industriels accordent au diagnostic et à la maintenance un intérêt croissant et cherchent à mettre en place des procédures pour améliorer la sécurité des personnels lors de l'apparition de défauts, réduire les risques encourus et assurer la fiabilité des machines et des installations. D'une manière générale, la tâche de diagnostic permet de détecter, isoler et identifier les défauts affectant un système. L'objectif de la détection est de déterminer si un système se comporte normalement ou non. La localisation et l'identification d'un défaut correspondent respectivement à la connaissance de l'instant de son apparition, sa nature et son évolution dans le temps. Plusieurs approches du diagnostic existent selon qu'un modèle du système est disponible ou non [213], [77], [214]. En l'absence de modèle, le diagnostic est basé sur les données fournies par les outils statistiques, les techniques issues du traitement du signal ou par la reconnaissance de formes [215]. Quant aux méthodes à base de modèles [216], elles s'appuient uniquement sur la vérification de la consistance entre le comportement réellement observé du système et celui estimé.

Les travaux de cette thèse se situent dans le cadre du diagnostic à base de modèles. Parmi ces méthodes, on trouve celles utilisant les techniques d'estimation paramétriques [162], l'espace de parité [77] et les méthodes utilisant des observateurs d'états [217]. Le principe de l'approche paramétrique repose sur l'estimation des paramètres du système. Ainsi tout écart notable entre les paramètres estimés et les paramètres nominaux, à savoir les paramètres en fonctionnement normal, est révélateur d'un défaut. Concernant l'approche utilisant l'espace de parité, elle a pour objectif de vérifier la cohérence des informations issues du procédé et les mesures issues des capteurs. Récemment, cette méthode a été proposée pour le diagnostic des modèles complexes tels que les systèmes non linéaires flous [218] et appliquée à

divers systèmes industriels tels que [219] et [220]. L'idée générale de l'approche par observateur consiste à estimer les sorties du système et les comparer aux mesures réelles. Pour un modèle déterministe, on utilise par exemple les observateurs de Luenberger [35] et pour un modèle stochastique on se base sur l'utilisation des filtres de Kalman [36].

En raison des inconvénients liés au coût impliqué par l'approche espace de parité et de la difficulté de mise en oeuvre de l'identification paramétrique surtout pour les systèmes complexes, l'approche par observateur est celle qui a été retenue pour le développement de cette thèse. Dans la littérature, de nombreux travaux ont montré l'intérêt que porte les chercheurs au problème du diagnostic à base d'observateurs en utilisant notamment les observateurs par modes glissants [177], [76], les observateurs adaptatifs [221], [143], les observateurs de type proportionnel intégral [144], [141] et les observateurs par intervalles [104], [121]. Les méthodes de diagnostic à base d'observateurs ont été introduites et appliquées pour différentes classes de systèmes telles que les systèmes non linéaires [222], les systèmes linéaires [77], les systèmes linéaire à paramètres variants (LPV) [121], les systèmes Takagi-Sugeno (T-S) [223], les systèmes à commutations [76], etc. Dans cette thèse, on s'intéresse à la détection des défauts des systèmes à commutations. Cet intérêt est justifié non seulement par la dynamique combinée, continue et discrète, des systèmes à commutations mais aussi en raison de leurs applications étendues dans plusieurs domaines de l'ingénierie, telles que le contrôle des systèmes mécaniques [9], l'automobile [14], les réseaux de communications [10], les systèmes embarqués [11], et par leur capacité à reproduire la nature de la plupart des systèmes industriels complexes. Dans [224], un observateur robuste dédié pour la détection des défauts est fourni pour les systèmes linéaires à commutations. L'approche proposée est établie sans considérer le bruit de mesure. Une procédure de détection de défaut a été discutée dans [225] pour une classe de systèmes à commutations en temps discret. Dans [77], le problème de détection des défauts a été traité dans le domaine des fréquences finies. L'approche introduite dans [77] est basée sur la minimisation du gain de fréquence finie L_2 permettant de réduire l'impact des perturbations sur le système. Dans [76], le problème de détection de défaut a été considéré en utilisant une approche basée sur les observateurs par mode glissants d'ordre réduit, pour une classe de systèmes linéaires à commutations. Les défauts considérés n'affectent que la partie continue du système.

D'un point de vue pratique, les systèmes complexes sont sujets à des incertitudes liées à l'existence inévitable de bruits de mesure et à la méconnaissance de certaines perturbations. Dans certains cas, le bruit de mesure ou les perturbations sur l'état sont difficilement modélisables par des distributions stochastiques. Une alternative intéressante consiste à considérer des perturbations bornées. Ainsi, les méthodes ensemblistes se révèlent pertinentes lorsque les incertitudes sont inconnues mais bornées. Dans la littérature, plusieurs recherches ont été développées pour la détection des défauts des systèmes dynamiques complexes où les perturbations et le bruit de mesure sont approximés par des formes géométriques simples telles que les intervalles [41], les polytopes [2], les zonotopes [3], les ellipsoïdes [1], etc. L'avantage majeur des approches ensemblistes consiste à fournir un moyen systématique d'évaluation de résidus. Dans le cadre de cette thèse, la détection des défauts des systèmes à commutations est envisagée en se basant sur les techniques ensemblistes en considérant notamment les intervalles, les zonotopes et les ellipsoïdes.

Dans le domaine du diagnostic, il est primordial de connaître l'état du système. Dans de nombreux cas, l'état n'est pas complètement mesurable ou accessible. Ceci est lié à des raisons économiques, à savoir le coût élevé des capteurs et aussi à des raisons techniques telles que la précision insuffisante d'un certain nombre de capteurs ou encore leur non-disponibilité. Les observateurs d'état ont été introduits dans la littérature pour remédier à ce problème en considérant notamment l'observateur de Luenberger [35] dans un cadre déterministe et le filtre de Kalman [36] dans un cadre stochastique. Dans le cas non linéaire, les méthodes d'estimation d'état reposent généralement sur une linéarisation approximative du système, ce qui peut être contraignant dans la pratique [75]. En conséquence, une large classe de systèmes non linéaires est présentée sous une forme LPV [100], [226]. L'intérêt des systèmes LPV a augmenté en raison de la possibilité d'appliquer des méthodologies établies pour les systèmes linéaires pour traiter les systèmes non linéaires. Ainsi, de nombreuses recherches ont été menées sur les systèmes LPV [101], [68]. Dans un contexte à incertitudes bornées, plusieurs travaux se sont focalisés sur l'exploitation des observateurs par intervalles. Dans [84], [86], [176], les observateurs par intervalles ont été considérés pour des systèmes linéaires invariants dans le temps (LTI). Dans [75], [82], la synthèse d'observateurs a été développée pour des systèmes linéaires variants dans le temps (LTV) où une nouvelle approche basée sur un changement de coordonnées est fournie afin de garantir la coopérativité de l'erreur d'observation. Dans [78], une estimation par intervalles de l'état est proposée pour les systèmes LPV en temps continu en supposant que le vecteur de paramètres n'est pas disponible. La construction des observateurs intervalles est abordée également pour la classe de systèmes non linéaires dans [41], [227], [107]. L'estimation par intervalles a fait l'objet d'intenses recherches dans la littérature pour la classe de systèmes linéaires à commutations [107], [186], [60], [110], etc. Bien que les théories d'estimation à base d'observateurs par intervalles aient atteint une certaine maturité, plusieurs points méritent d'être approfondis pour traiter une plus large gamme de systèmes dans des conditions peu restrictives. Inspiré par les discussions ci-dessus, l'estimation par intervalles de l'état pour une classe de systèmes LPV à commutations sujets à des perturbations supposées inconnues mais bornées et à des paramètres polytopiques variants dans le temps, n'a pas été suffisamment abordée. Les travaux de cette thèse apportent une solution et une relaxation dimensionnelle finie pour les conditions de coopérativité et de stabilité au sens entrée-état des erreurs d'estimation.

Souvent, l'évolution du signal de commutation est supposée connue ou mesurée. Dans la pratique, le mode actif ne peut pas toujours être connu. Dans la littérature, l'estimation de l'état discret pour une classe de systèmes à commutations est rarement étudiée. En utilisant l'approche par modes glissants, une estimation robuste de l'état discret pour un système à commutations incertain et non linéaire est proposée dans [65] lorsque l'état continu est mesuré. Dans [67], un observateur par modes glissants hybride est conçu pour estimer les états continu et discret d'un système linéaire à commutations à entrée inconnue. Dans [68], une identification de paramètres est proposée pour estimer les états continu et discret des systèmes LPV à commutations. A notre connaissance, la synthèse d'une procédure robuste de détection du mode actif par l'approche par intervalles pour un système linéaire à commutations à entrée inconnue n'a pas encore été abordée. Dans cette thèse, une nouvelle méthode, combinant la technique du mode glissant qui fournit une convergence robuste dans

un temps fini et l'approche par intervalles où seulement les bornes de l'entrée inconnue sont nécessaires, est proposée pour l'estimation du signal de commutation.

Contributions de la thèse

Ce mémoire contribue, d'une part, à l'estimation par intervalles de l'état continu ainsi que l'état discret pour une classe des systèmes à commutations soumis à des perturbations supposées inconnues mais bornées. D'autre part, il apporte des solutions robustes à la détection de défauts à bases des techniques ensemblistes et des critères d'optimisation. Les contributions de cette thèse peuvent être divisées en quatre parties.

- La première contribution consiste à proposer une estimation par intervalles de l'état pour une classe des systèmes LPV à commutations en temps continu ainsi qu'en temps discret. Le principal avantage de l'approche proposée est que les conditions de coopérativité et de stabilité sont relaxées grâce à la forme polytopique des paramètres variants dans le temps. Ces propriétés sont introduites en fonction des sommets de chaque polytope et exprimées en termes d'Inégalités Matricielles Linéaires (LMI), en adoptant des fonctions de Lyapunov communes et multiples.
- La deuxième contribution apporte une nouvelle logique d'estimation du signal de commutation pour un système linéaire à commutations à entrée inconnue en combinant la technique des modes glissants et l'approche par intervalles.
- La troisième contribution apporte une solution robuste à la détection de défauts en utilisant les observateurs classiques par intervalles ainsi que des observateurs par intervalles avec une structure TNL. Cette dernière structure permet d'offrir plus de degrés de liberté de conception. Les performances de détection de défauts sont améliorées en se basant sur la minimisation d'un critère L_∞ .
- La dernière contribution propose une stratégie robuste de détection de défauts en utilisant des approches zonotopiques et ellipsoïdales. L'avantage majeur de cette contribution consiste à fournir des seuils dynamiques systématiques pour l'évaluation du résidu et d'améliorer la précision des résultats de détection des défauts sans tenir compte de l'hypothèse de coopérativité liée aux observateurs par intervalles.

Organisation du mémoire

Ce manuscrit est organisé en cinq chapitres principaux, une introduction et une conclusion générale.

Chapitre 2

Le Chapitre 2 fournit une étude bibliographique et permet de définir le contexte général dans lequel s'inscrit cette thèse. Des notions de base sur la modélisation, l'analyse de stabilité, l'observabilité et l'observation des systèmes à commutations sont introduites. Ensuite, un état de l'art sur les techniques d'estimation par intervalles est développé pour différentes classes de systèmes y compris la classe des systèmes à commutations. La dernière partie

présente les différentes approches existantes dans la littérature dans le domaine du diagnostic et fournit un état de l'art sur la détection des défauts en utilisant les approches ensemblistes.

Chapitre 3

Le Chapitre 3 considère le problème d'estimation par intervalles pour les systèmes linéaires à paramètres variants (LPV) à commutations. On considère dans cette étude que le signal de commutations est connu. Dans un contexte à erreur inconnue mais bornée, l'approche par intervalles utilise deux observateurs ponctuels basés sur une structure de Luenberger et permet de fournir des bornes inférieure et supérieure pour le vecteur d'état. Elle est basée sur une structure en boucle fermée où le gain de l'observateur est conçu afin d'imposer une dynamique coopérative pour l'erreur d'estimation. Néanmoins, cette condition est très restrictive. Dans la littérature, un changement de coordonnées a été utilisé pour relaxer cette contrainte. Lorsque les systèmes sont sujets à des paramètres variant dans le temps, l'application d'un changement de coordonnées peut constituer un problème de dimension infinie. Cela motive le présent chapitre qui fournit une relaxation de dimension finie pour les conditions de conception de l'observateur par intervalles proposé pour des systèmes LPV à commutations soumis à des paramètres polytopiques mesurés, des perturbations et au bruit de mesure. Dans un premier temps, le problème d'estimation est abordé pour des systèmes LPV à commutations en temps continu. En utilisant les fonctions de Lyapunov quadratiques communes et multiples, des nouvelles conditions de coopérativité et de stabilité sont fournies en termes d'inégalités matricielles linéaires exprimées en fonction des sommets de chaque polytope. Dans un second temps, la conception de l'observateur par intervalles est proposée en temps discret. Des résultats de simulation, sur des exemples académiques, sont proposés pour valider les différentes approches proposées.

Chapitre 4

Le Chapitre 4 s'intéresse à l'estimation du signal de commutations pour une classe de systèmes linéaires à commutations avec entrée inconnue. D'un point de vue pratique, la présence d'entrées inconnues ne peut être évitée, ce qui peut apporter une certaine difficulté à l'estimation du mode actif. Dans la littérature, plusieurs travaux ont été développés pour la reconstruction de l'état discret en utilisant la technique de découplage de sorte que la dynamique d'erreur d'estimation ne soit pas affectée par les entrées inconnues. Sans avoir recours à des techniques de découplage, une nouvelle approche est proposée dans ce chapitre en combinant un observateur par intervalles avec un observateur par modes glissants. La combinaison des deux observateurs est l'une des principales contributions de ce chapitre pour identifier le mode actif en temps fini et de détecter de manière robuste les instants de commutations. D'une part, l'observateur par intervalles offre la possibilité de créer un seuil adaptatif robuste par rapport aux perturbations en considérant les bornes de l'entrée inconnue. En se basant sur des conditions de positivité, de robustesse et de sensibilité aux modes de fonctionnement, une logique de décision est développée pour la détection d'un changement de mode. D'autre part, l'observateur par modes glissants est un observateur robuste qui permet de définir des nouvelles conditions pour identifier le mode actif en temps fini. Cette identification se fait à partir de l'estimation des bornes de l'état continu calculées

par l'observateur par intervalles. La faisabilité et l'efficacité de l'approche proposée sont illustrées via un exemple académique.

Chapitre 5

Le Chapitre 5 traite le problème de détection des défauts des systèmes linéaires à commutations en présence des perturbations et de bruits de mesure. Deux approches pour construire deux vecteurs de résidu supérieur et inférieur sont considérées. La première est basée sur la conception des observateurs par intervalles classiques et la minimisation d'un critère L_∞ , permettant d'atténuer l'effet des bruits et des perturbations, sur les bornes du résidu générées. Cette approche ensembliste permet d'améliorer les performances de détection de défauts. Elle fournit également un moyen systématique d'évaluation de résidus basée sur un test d'appartenance du signal zéro à l'intervalle délimité par les bornes supérieure et inférieure du résidu. L'enjeu principal pour la synthèse d'un observateur par intervalles classique réside généralement dans sa capacité à satisfaire simultanément les conditions de coopérativité et un certain niveau de performance souhaité. Certaines méthodes proposent une transformation de coordonnées pour relaxer les conditions de conception des observateurs par intervalles. Cependant, il est difficile de fusionner la technique de transformation de coordonnées avec des contraintes de performance. Compte tenu de cet inconvénient majeur, l'objectif de la deuxième partie de ce chapitre est de concevoir une nouvelle méthode de détection de défauts basée sur les observateurs par intervalles avec une structure TNL pour une classe de systèmes linéaires à commutations. La technique proposée offre plus de degrés de liberté de conception en introduisant des matrices de pondération dans la structure de l'observateur par intervalles. Les conditions de conception de l'observateur sont données en termes d'inégalités matricielles linéaires en utilisant les fonctions de Lyapunov commune et multiples. L'efficacité des approches proposées est mise en évidence par des résultats de simulation sur un exemple académique.

Chapitre 6

Le Chapitre 6 propose une stratégie robuste de détection de défauts pour une classe des systèmes linéaires à commutations en présence des perturbations et de bruits de mesure en utilisant des approches zonotopiques et ellipsoïdales. Ces approches sont développées pour fournir des seuils dynamiques pour l'évaluation du résidu ainsi que pour améliorer la précision des résultats de détection des défauts sans tenir compte de l'hypothèse de coopérativité. Dans la première partie, une méthode basée sur la conception d'un observateur de Luenberger est proposée. Cette méthode permet de générer des résidus à la fois sensibles aux défauts et robustes aux perturbations et au bruit de mesure. Le problème est formulé en exploitant une nouvelle méthode de placement des pôles pour augmenter l'impact des défauts sur le vecteur résidu et une approche d'optimisation H_∞ pour minimiser l'effet des perturbations. L'ensemble de ces conditions est exprimé en termes d'inégalités matricielles linéaires. Ensuite, la prise décision est évaluée en utilisant l'approche zonotopique. La précision des résultats de détection via la technique zonotopique peut être améliorée en utilisant des zonotopes de dimensions supérieures. Cependant, l'utilisation des zonotopes de grandes tailles peut entraîner une complexité de calcul élevée. Pour remédier à ce problème, les techniques ellipsoïdales peuvent être considérées comme un bon compromis entre

la précision de détection et la complexité de calcul. La deuxième partie de ce chapitre est consacrée à la détection des défauts basée sur l'approche ellipsoïdale. Une nouvelle structure d'observateur est proposée en se basant sur le critère de performance L_∞ pour atténuer les effets des incertitudes. Enfin, des exemples numériques sont mis en évidence pour illustrer l'efficacité des deux méthodes ensemblistes proposées.

Systèmes à commutations

Ces dernières années, de nombreux travaux allant de la modélisation au diagnostic se sont focalisés sur l'étude des systèmes dynamiques hybrides. Cette classe de systèmes est représentée à la fois par des variables continues et discrètes. La classe des systèmes à commutations présente une catégorie importante des systèmes dynamiques hybrides [7], [8] en raison de sa capacité de modéliser une large classe de systèmes physiques. Les systèmes à commutations sont constitués d'une famille de sous-systèmes, qui sont appelés souvent modes, et une loi de commutation qui spécifie le mode de fonctionnement actif à chaque instant.

Formellement, en temps continu, un système à commutations est défini par :

$$\begin{cases} \dot{x}(t) = A_{\sigma(t)}x(t) + B_{\sigma(t)}u(t) + w_{\sigma(t)} \\ y(t) = Cx(t) + v(t) \end{cases}, \sigma(t) \in \mathcal{I}, \quad (\text{B.1})$$

où $x \in \mathbb{R}^{n_x}$, $u \in \mathbb{R}^{n_u}$, $y \in \mathbb{R}^{n_y}$, $w_\sigma \in \mathbb{R}^{n_x}$ et $v \in \mathbb{R}^{n_y}$ sont respectivement le vecteur d'état, l'entrée, la sortie, les perturbations et le bruit de mesure. La commutation entre les sous-systèmes est assurée par un signal de commutation, une fonction constante par morceau, $\sigma(t) : \mathbb{R}_+ \rightarrow \mathcal{I} = \{1, 2, \dots, N\}$, $N \in \mathbb{Z}_+$.

En temps discret, un système à commutations peut être représenté comme suit :

$$\begin{cases} x_{k+1} = A_{\sigma(k)}x_k + B_{\sigma(k)}u_k + w_{\sigma(k)} \\ y_k = Cx_k + v_k \end{cases}, \sigma(k) \in \mathcal{I}. \quad (\text{B.2})$$

Cette thèse s'intéresse principalement au diagnostic des systèmes linéaires à commutations. La procédure de diagnostic nécessite à un certain moment l'estimation d'état du système en question. Néanmoins, les processus réels sont souvent soumis à des perturbations. Dans un contexte à erreurs bornées, les observateurs par intervalles se révèlent pertinents pour résoudre le problème d'estimation d'état.

Observateurs par intervalles

L'estimation de l'état a été largement discutée dans la littérature. D'un point de vue pratique, l'estimation d'état peut ne pas converger vers l'état réel en raison de l'existence d'incertitudes de modèle. C'est pourquoi, la conception des observateurs classiques tels que les observateurs de Luenberger et le filtre de Kalman, peut être compliquée. Pour remédier à ce problème, plusieurs approches d'estimation d'état basées sur les techniques ensemblistes fournissent de bons résultats en présence de perturbations inconnues mais bornées. Dans ce cadre, on distingue principalement deux méthodes pour l'estimation d'état. La première est basée sur le mécanisme de prédiction/correction [69], [70], similaire au filtre de Kalman. La prédiction consiste à déterminer le domaine admissible de l'état à l'instant

t_{j+1} ayant un encadrement à t_j . En temps continu, cette méthode peut être appliquée en réalisant une résolution numérique garantie d'une équation différentielle ordinaire [71]. Lors de la phase de correction, l'ensemble prédit est contracté en supprimant un ensemble de valeurs du vecteur d'état incompatibles avec les mesures prises à l'instant t_{j+1} . La seconde approche est basée sur une structure en boucle fermée où le gain de l'observateur est choisi afin d'imposer une dynamique coopérative pour l'erreur d'estimation [72], [73], [74]. Dans ce cas, deux observateurs ponctuels basés sur une structure de Luenberger sont conçus et permettent d'estimer des bornes inférieures et supérieures du vecteur d'état (Fig. B.1). Ces

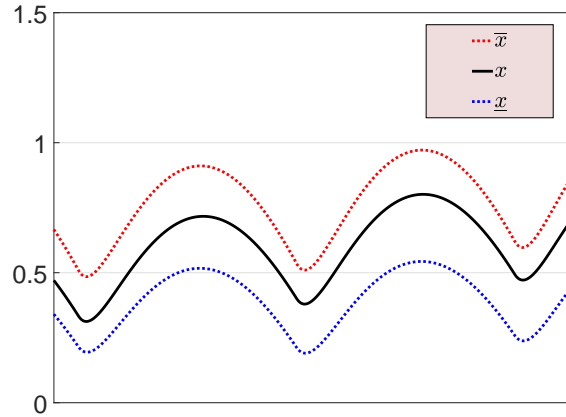


Figure B.1: Observateur par intervalles.

dernières années, les méthodes à base d'observateurs par intervalles ont significativement progressé pour de nombreuses applications pour résoudre de manière rigoureuse certains problèmes d'ingénierie tels que le diagnostic de défauts [41], [75], [76], [77], [78].

Dans cette thèse, les observateurs par intervalles sont adoptés pour résoudre le problème d'estimation d'état.

Synthèse d'un observateur par intervalles pour les systèmes LPV à commutations

Les techniques de conception des observateurs par intervalles reposent généralement sur la théorie des systèmes positifs. Ceux-ci exigent que les conditions de coopérativité des erreurs d'estimation $\bar{x} - x$ et $x - \underline{x}$ soient vérifiées. Néanmoins, cette condition est très restrictive et difficile à satisfaire tout en assurant la stabilité de l'observateur. Pour relaxer ces contraintes, un changement de coordonnées peut être utilisé. En présence des paramètres variant dans le temps, l'application d'un changement de coordonnées peut constituer un problème de dimension infinie. Dans le cadre de cette thèse, une approche d'estimation d'état à base d'observateurs par intervalles est proposée. Celle-ci permet une relaxation des conditions de conception de l'observateur pour une classe des systèmes LPV à commutations soumis à des paramètres polytopiques variant dans le temps. On considère le système LPV à

commutations en temps continu suivant :

$$\begin{cases} \dot{x}(t) = A_q(\eta_q)x(t) + B_q(\eta_q)u(t) + w_q(t) \\ y(t) = Cx(t) + v(t) \end{cases}, q \in \mathcal{I}, \quad (\text{B.3})$$

où $x \in \mathbb{R}^{n_x}$, $u \in \mathbb{R}^{n_u}$, $y \in \mathbb{R}^{n_y}$, $w_\sigma \in \mathbb{R}^{n_x}$ et $v \in \mathbb{R}^{n_y}$ sont respectivement le vecteur d'état, l'entrée, la sortie, les perturbations et le bruit de mesure. $A_{\sigma(t)} \in \mathbb{R}^{n_x \times n_x}$, $B_{\sigma(t)} \in \mathbb{R}^{n_x \times n_u}$ et $C \in \mathbb{R}^{n_y \times n_x}$ sont respectivement les matrices d'état, d'entrée et de sortie. La commutation entre les sous-systèmes est assurée par un signal de commutation $\sigma(t) : \mathbb{R}_+ \rightarrow \mathcal{I}$, supposé connu. Dans la suite, l'indice $q = \sigma(t)$ définit, à chaque instant, le mode actif, $q \in \mathcal{I} = \overline{1, N}$, $N \in \mathbb{N}$, N est le nombre de sous-systèmes. Pour chaque sous-système, on note par $\eta_q = [\eta_{q_1}, \dots, \eta_{q_r}]^T$ la collection de paramètres variants dans le temps supposés mesurés et contraints dans des polytopes E_q , E_q dépend du mode actif. On note par $\eta_q^{(i)}$, $i = 1, \dots, g$ les sommets de chaque polytope E_q .

Les hypothèses et les définitions suivantes sont nécessaires pour la construction d'un observateur associé au système (B.3).

Hypothèse 1. $A_q(\eta_q)$, $B_q(\eta_q)$ dépendent affinement de η_q :

$$\begin{aligned} A_q(\eta_q) &= A_{q_0} + \eta_{q_1}A_{q_1} + \dots + \eta_{q_r}A_{q_r} \\ B_q(\eta_q) &= B_{q_0} + \eta_{q_1}B_{q_1} + \dots + \eta_{q_r}B_{q_r} \end{aligned}, q \in \mathcal{I}. \quad (\text{B.4})$$

Hypothèse 2. L'état initial $x(0)$ satisfait $\underline{x}(0) \leq x(0) \leq \overline{x}(0)$ avec $\underline{x}(0), \overline{x}(0) \in \mathbb{R}^{n_x}$.

Hypothèse 3. Les perturbations et le bruit de mesure sont inconnus mais bornés tel que :

$$\underline{w}_q \leq w_q \leq \overline{w}_q, |v| \leq \overline{v}J_{n_y}, \quad (\text{B.5})$$

avec $\underline{w}_q, \overline{w}_q \in \mathbb{R}^{n_x}$ et \overline{v} est un scalaire.

Definition 23. Une matrice $A = a_{ij} \in \mathbb{R}^{n \times n}$ est dite Metzler si tous ses éléments hors diagonale sont positifs ou nuls, i.e. $a_{ij} \geq 0, \forall i \neq j$.

Definition 24. Une matrice $A \in \mathbb{R}^{n \times n}$ est dite Metzler s'il existe $\epsilon \in \mathbb{R}^+$ tel que :

$$A + \epsilon I_n \geq 0. \quad (\text{B.6})$$

Definition 25. On considère le système suivant :

$$\dot{x}(t) = Ax(t) + u(t). \quad (\text{B.7})$$

Si A est Metzler, l'entrée u satisfait $u(t) \geq 0$ et l'état initial $x(0)$ est choisi tel que $x(0) \geq 0$, alors l'état x reste non négatif pour tout $t \geq 0$. Le système (B.7) est dit coopératif ou nonnégatif.

Hypothèse 4. Il existe des gains $L_q(\eta_q^{(i)}) \in \mathbb{R}^{n_x \times n_y}$ tel que les matrices $A_q(\eta_q^{(i)}) - L_q(\eta_q^{(i)})C$ sont Metzler pour tout $\eta_q^{(i)} \in E_q$, $i = 1, \dots, g$. $A_q(\eta_q^{(i)})$ représentent les sommets des matrices d'état $A_q(\eta_q)$ de chaque polytope E_q et $L_q(\eta_q^{(i)})$ sont les sommets des gains d'observateurs.

Hypothèse 5. Pour tous les sommets de E_q et pour tous $q \in \mathcal{I}$, les paires $(A_q(\eta_q^{(i)}), C)$ sont détectables.

Definition 26. Etant donné un système hybride, il existe une constante $T_\delta > 0$ tel que la classe admissible des signaux de commutations satisfait l'inégalité $t_{k+1} - t_k \geq T_\delta$ pour tous $k \geq 0$.

Structure de l'observateur par intervalles

La structure proposée de l'observateur par intervalles est donnée par :

$$\begin{cases} \dot{\bar{x}} = (A_q(\eta_q) - L_q(\eta_q)C) \bar{x} + B_q(\eta_q)u + \bar{w}_q + L_q(\eta_q)y + |L_q(\eta_q)|\bar{v}J_{n_y} \\ \dot{\underline{x}} = (A_q(\eta_q) - L_q(\eta_q)C) \underline{x} + B_q(\eta_q)u + \underline{w}_q + L_q(\eta_q)y - |L_q(\eta_q)|\bar{v}J_{n_y} \end{cases}, q \in \mathcal{I}. \quad (\text{B.8})$$

Les gains de l'observateur $L_q(\eta_q)$ ont une forme affine :

$$L_q(\eta_q) = L_{q_0} + \eta_{q_1}L_{q_1} + \dots + \eta_{q_r}L_{q_r}, \quad (\text{B.9})$$

avec $L_{qj} \in \mathbb{R}^{n_x \times n_y}$, $j = 0, 1, \dots, r$, sont des matrices constantes.

Coopérativité et Stabilité des erreurs d'estimation

En présence des perturbations de l'état et du bruit de mesure, l'objectif est de trouver un gain $L_q(\eta_q)$ qui assure à la fois la coopérativité et la stabilité des erreurs d'estimation supérieure $\bar{e}(t) = \bar{x} - x$ et inférieure $\underline{e}(t) = x - \underline{x}$.

Les dynamiques de ces erreurs sont données par :

$$\begin{aligned} \dot{\bar{e}}(t) = \dot{\bar{x}} - \dot{x} &= \sum_{i=1}^g \lambda_i \left(A_q(\eta_q^{(i)}) - L_q(\eta_q^{(i)})C \right) \bar{e} + \bar{\chi}_q, \\ \dot{\underline{e}}(t) = \dot{x} - \dot{\underline{x}} &= \sum_{i=1}^g \lambda_i \left(A_q(\eta_q^{(i)}) - L_q(\eta_q^{(i)})C \right) \underline{e} + \underline{\chi}_q, \end{aligned}$$

avec :

$$\begin{aligned} \bar{\chi}_q &= \bar{w}_q - w_q + L_q(\eta_q)v + |L_q(\eta_q)|\bar{v}J_{n_y}, \\ \underline{\chi}_q &= w_q - \underline{w}_q - L_q(\eta_q)v + |L_q(\eta_q)|\bar{v}J_{n_y}. \end{aligned}$$

Les matrices $A_q(\eta_q) - L_q(\eta_q)C$ dépendent affinement de η_q , elles peuvent être écrites sous forme d'une combinaison convexe [22] :

$$\begin{aligned} A_q(\eta_q) - L_q(\eta_q)C &= \lambda_1 (A_q(\eta_q^{(1)}) - L_q(\eta_q^{(1)})C) + \dots + \lambda_g (A_q(\eta_q^{(g)}) - L_q(\eta_q^{(g)})C) \\ &= \sum_{i=1}^g \lambda_i \left(A_q(\eta_q^{(i)}) - L_q(\eta_q^{(i)})C \right), \end{aligned}$$

avec $\lambda_i \geq 0$ et $\lambda_1 + \dots + \lambda_g = 1$. La coopérativité des erreurs d'estimation est prouvée si les matrices $A_q(\eta_q) - L_q(\eta_q)C$ sont Metzler et $\bar{\chi}_q$ et $\underline{\chi}_q$ sont nonnegatives (Définition 25). Les conditions $\bar{\chi}_q(t) \geq 0$ et $\underline{\chi}_q(t) \geq 0$, sont justifiées par le fait que les perturbations et le bruit de mesure sont inconnus mais bornés (Hypothèse 3).

En se basant sur la Définition 24, la condition Metzler est montrée via la résolution de cette relation

$$PA_q(\eta_q^{(i)}) + Q_q(\eta_q^{(i)})C + \epsilon P \geq 0 \quad , \quad \epsilon \in \mathbb{R}^+ \quad , \quad \forall q \in \mathcal{I}.$$

La stabilité des erreurs d'estimation peut être assurée en utilisant la fonction de Lyapunov commune $V(e) = e(t)^T P e(t)$.

Ainsi, l'analyse de la stabilité est réduite à la faisabilité des inégalités matricielles linéaires suivantes :

$$A_q(\eta_q^{(i)})^T P + P A_q(\eta_q^{(i)}) - \left(C^T Q_q(\eta_q^{(i)})^T + Q_q(\eta_q^{(i)}) C \right) + \frac{3}{\varrho_q} P \prec 0, \forall q \in \mathcal{I}.$$

$Q_q(\eta_q^{(i)})$ dépendent affinement de $\eta_q^{(i)}$:

$$Q_q(\eta_q^{(i)}) = Q_{q_0} + \eta_{q_1}^{(i)} Q_{q_1} + \dots + \eta_{q_r}^{(i)} Q_{q_r}, \quad (\text{B.10})$$

avec $Q_{q_j} \in \mathbb{R}^{n_x \times n_y}$, $j = 0, 1, \dots, r$ sont des matrices constantes. Ces conditions LMIs sont à vérifier pour tous les sommets $\eta_q^{(i)}$ de E_q , $i = 1, \dots, g$.

Dans le cadre de l'approche proposée, les conditions LMIs relatives à la coopérativité et à la stabilité des erreurs d'estimation établies sont relaxées grâce à la forme polytopique des paramètres du système. Elles sont exprimées en fonction des sommets de chaque polytope afin d'éviter tout problème dimensionnel infini dû aux paramètres variants dans le temps. L'existence de la fonction de Lyapunov commune n'est pas toujours garantie. De ce fait, il est possible de chercher des fonctions de Lyapunov multiples $V_q(e) = e^T(t) P_q e(t)$ assurant la stabilité de l'observateur proposé et la minimisation à la fois de la largeur de l'intervalle d'estimation et le temps minimal de séjour.

Des résultats de simulations illustrés par la figure B.2 montre qu'en présence des incertitudes, l'état est encadré par deux trajectoires supérieure et inférieure. La positivité et la stabilité de l'observateur par intervalles sont assurées (Fig. B.3).

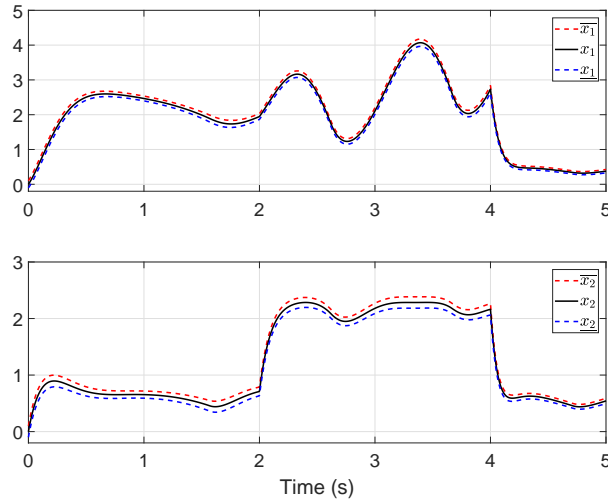


Figure B.2: Evolutions de l'état x et les bornes supérieure et inférieure estimées.

Actuellement, la plupart des observateurs par intervalles sont suggérés pour des systèmes à commutations en temps discret lorsque les paramètres sont invariants dans le temps. Une estimation par intervalles, similaire à celle en temps continu, est proposée pour une classe des systèmes LPV à commutations en temps discret. En admettant les mêmes hypothèses, des nouvelles conditions de nonnégalité et de stabilité sont données en termes de LMIs. Le principal avantage de cette approche est la réduction du conservatisme grâce à la forme polytopique des incertitudes paramétriques et aux fonctions de Lyapunov multiples.

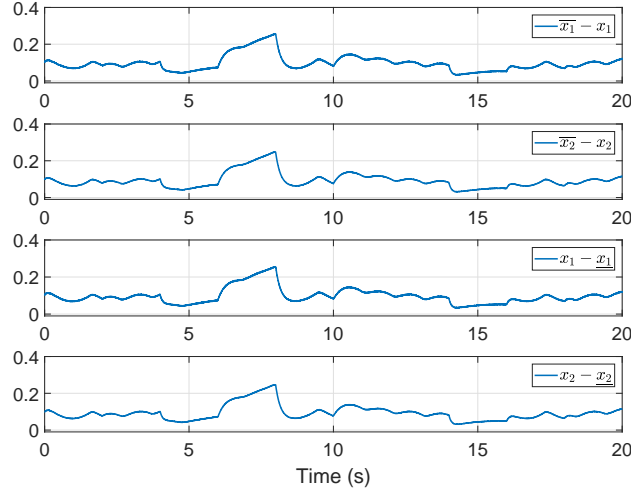


Figure B.3: Evolution des erreurs d'estimation.

Les résultats ont fait l'objet d'une communication [183] dans la conférence internationale "Conference on Decision and Control" et deux articles [184] et [185] dans les revues internationales "International Journal of Control" et "Acta Cybernetica".

Observateur par intervalles pour l'estimation de l'état discret

Dans la littérature, l'estimation de l'état discret pour une classe de systèmes à commutations est rarement étudiée. Dans ce mémoire, un nouvel observateur pour l'estimation du signal de commutation est développé pour une classe de systèmes linéaires à commutations à entrée inconnue.

On considère le système linéaire à commutations à entrée inconnue suivant :

$$\begin{cases} \dot{x}(t) &= A_{\sigma(t)}x(t) + B_{\sigma(t)}u(t) + w(t) \\ y(t) &= Cx(t), \end{cases} \quad (\text{B.11})$$

avec $w(t) \in \mathbb{R}^{n_x}$ est l'entrée inconnue qui est supposée inconnue mais bornée.

Hypothèse 6. *On assume que :*

- Les paires (A_q, C) sont détectables $\forall q = 1, \dots, N$.
- L'état x évolue dans une région bornée.
- u et w et leurs dérivées premières sont bornées par des constantes positives connues.
- Le système (B.11) satisfait la condition de temps de séjour minimal.
- L'état continu et l'entrée inconnue sont supposés bornés par des valeurs connues :

$$\underline{X} \leq x(t) \leq \overline{X}, \quad |w(t)| \leq \bar{w}. \quad (\text{B.12})$$

Approches par intervalles

Une batterie de N observateurs par intervalles, associée aux différents modes de fonctionnement, est présentée dans la figure B.4.

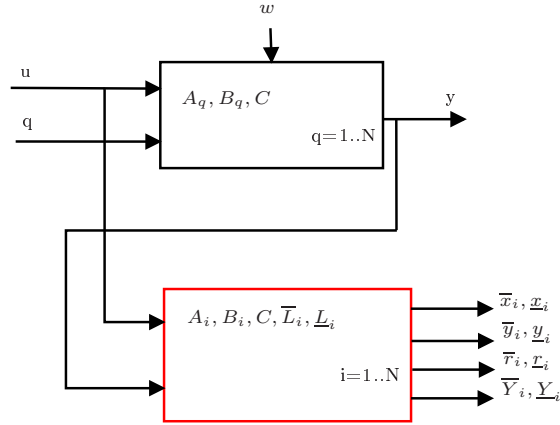


Figure B.4: Schéma bloc d'une batterie d'observateurs par intervalles.

Les signaux $\bar{x}_i, \underline{x}_i \in \mathbb{R}^{n_x}$, $\bar{y}_i, \underline{y}_i \in \mathbb{R}^{n_y}$, $\bar{r}_i, \underline{r}_i \in \mathbb{R}^{n_y}$ sont respectivement les bornes supérieure et inférieure de l'état x , de la sortie y et du vecteur résidu. Les signaux de sortie \underline{Y}_i et \bar{Y}_i sont utilisés pour identifier le mode actif du système linéaire à commutations. $\bar{L}_i, \underline{L}_i \in \mathbb{R}^{n_x \times n_y}$ pour $i = 1, \dots, N$ représentent les gains d'observateur.

Les erreurs d'estimation sont définies par $\bar{e}_i = \bar{x}_i - x$ et $\underline{e}_i = x - \underline{x}_i$. La dynamique de ces erreurs est donnée par :

$$\begin{aligned}\dot{\bar{e}}_i(t) &= (A_i - \bar{L}_i C) \bar{e}_i(t) + \chi_i(t) + \bar{w} - w(t) \\ \dot{\underline{e}}_i(t) &= (A_i - \underline{L}_i C) \underline{e}_i(t) - \chi_i(t) + \bar{w} + w(t),\end{aligned}$$

avec

$$\chi_i(t) = (A_i - A_q)x(t) + (B_i - B_q)u(t). \quad (\text{B.13})$$

Afin d'estimer le signal de commutation, un état augmenté est proposé comme suit :

$$\zeta_i = \begin{pmatrix} \bar{e}_i \\ \underline{e}_i \end{pmatrix}, \quad r_i = \begin{pmatrix} \bar{r}_i \\ \underline{r}_i \end{pmatrix}.$$

Le système augmenté peut être alors déduit :

$$\begin{cases} \dot{\zeta}_i(t) = \mathcal{A}_i \zeta_i(t) + \mathcal{W}(t) + \mathcal{F} \chi_i(t) \\ r_i(t) = \mathcal{C} \zeta_i(t), \end{cases} \quad (\text{B.14})$$

avec

$$\begin{aligned} \mathcal{A}_i &= \begin{pmatrix} (A_i - \bar{L}_i C) & 0 \\ 0 & (A_i - \underline{L}_i C) \end{pmatrix}, \quad \mathcal{W}(t) = \begin{pmatrix} \bar{w} - w(t) \\ \bar{w} + w(t) \end{pmatrix}, \quad \mathcal{F} = \begin{pmatrix} I_n \\ -I_n \end{pmatrix}, \\ \mathcal{C} &= \begin{pmatrix} C^+ & C^- \\ -C^- & -C^+ \end{pmatrix}. \end{aligned}$$

A partir de cette dernière représentation, il est clair que $\mathcal{W}(t) \geq 0$ et si $i = q$, χ_i est nul. Basé sur l'idée que les matrices \mathcal{A}_i sont stables et Metzler et les bornes \bar{x}_i et \underline{x}_i peuvent être réinitialisés à chaque instant t_k tel que $\zeta_i(t_k) \geq 0$, pour $k = 0, 1, 2, \dots$, si $i = q$ ($\chi_i = 0$) pour $t \in [t_k, t_{k+1})$, les relations suivantes sont déduites :

$$\begin{cases} \zeta_i(t) \geq 0 \\ \underline{x}_i(t) \leq x(t) \leq \bar{x}_i(t) \\ \underline{y}_i(t) \leq y(t) \leq \bar{y}_i(t) \\ 0 \in [\underline{r}_i, \bar{r}_i]. \end{cases}$$

En fonction de l'évolution des résidus r_i , l'observateur par intervalles proposé est conçu pour détecter le changement d'état discret à partir d'un mode particulier i lorsque $0 \notin [\underline{r}_i, \bar{r}_i]$. Une estimation des instants de commutation t_k est alors fournie. Le problème d'estimation des instants de commutation peut être formulé de telle sorte que :

- (i) \mathcal{A}_i soient stable et Metzler pour $i = 1, \dots, N$.
- (ii) La norme L_2 de $r_i(t)$ par rapport à \mathcal{W}_i soit inférieure à $\gamma^{1/2}$ quand $\chi_i(t) = 0$

$$\sup_{\mathcal{W}_i \neq 0} \frac{\|r_i(t)\|}{\|\mathcal{W}_i\|} < \gamma^{1/2}.$$

- (iii) La norme L_2 de $r_i(t) - J\chi_i(t)$ par rapport à $\chi_i(t)$ soit inférieure à $\beta^{1/2}$ quand $\mathcal{W}_i = 0$

$$\sup_{\chi_i \neq 0} \frac{\|r_i(t) - J\chi_i(t)\|}{\|\chi_i(t)\|} < \beta^{1/2},$$

avec $J = [J_1^T, J_2^T]^T \in \mathbb{R}^{2m \times n}$ est une matrice de pondération.

La spécification (i) assure la stabilité et la positivité de l'observateur par intervalles lorsque $i = q$. La robustesse des résidus r_i par rapport à l'entrée inconnue $w(t)$ est spécifiée dans (ii). La spécification (iii) permet d'améliorer la sensibilité des résidus r_i par rapport à χ_i (terme qui met en évidence le changement du mode). L'ensemble des spécifications est exprimé en terme de LMIs.

Approche par modes glissants

En se basant sur la théorie des modes glissants, un observateur fournissant une estimation \hat{q} du mode actuel q du système linéaire à commutations est proposé. Une batterie d'observateurs par modes glissants est conçue pour $i = 1, \dots, N$.

$$\begin{cases} \dot{\bar{z}}_i(t) &= -C\bar{L}_i\bar{z}_i(t) + \bar{v}_i(t) \\ \dot{\underline{z}}_i(t) &= -C\underline{L}_i\underline{z}_i(t) + \underline{v}_i(t), \end{cases}$$

avec \underline{v}_i et \bar{v}_i sont les termes de correction donnés par les expressions suivantes :

$$\begin{aligned} \bar{v}_i &= -k_1|\bar{z}_i - y + \bar{Y}_i|^{\frac{1}{2}} \text{sign}(\bar{z}_i - y + \bar{Y}_i) + \bar{v}_{i,1} \\ \dot{\bar{v}}_{i,1} &= -k_2 \text{sign}(\bar{z}_i - y + \bar{Y}_i) \\ \underline{v}_i &= -k_1|\underline{z}_i - y + \underline{Y}_i|^{\frac{1}{2}} \text{sign}(\underline{z}_i - y + \underline{Y}_i) + \underline{v}_{i,1} \\ \dot{\underline{v}}_{i,1} &= -k_2 \text{sign}(\underline{z}_i - y + \underline{Y}_i). \end{aligned}$$

La batterie d'observateurs par modes glissants est conçue pour fournir une convergence en temps fini de $\bar{Y}_i - y$ et $\underline{Y}_i - y$. \bar{z}_i et \underline{z}_i désignent respectivement les signaux estimés de $\bar{Y} - y$ et $\underline{Y} - y$.

Hypothèse 7. Afin de garantir la distinguabilité du mode actif, il est supposé qu'il existe des constantes positives connues δ_1 et δ_2 telles que, pour tout $t \geq \delta_1$, $\forall i, j = 1, \dots, N$, $i \neq j$

$$\int_{t-\delta_1}^t \|\underline{\phi}_{i,j}(s)\| + \|\bar{\phi}_{i,j}(s)\| ds \geq \delta_2 \quad (\text{B.15})$$

et

$$\int_{t-\delta_1}^t \|\underline{\phi}_{i,i}(s)\| + \|\bar{\phi}_{i,i}(s)\| ds < \delta_2, \quad (\text{B.16})$$

avec

$$\begin{aligned} \bar{\phi}_{i,j}(t) &= -C\bar{L}_i(\bar{z}_i(t) - y(t) + \bar{Y}_i(t)) + C(B_i - B_j)u(t) - CA_jx(t) + CA_i\bar{x}_i(t) \\ &\quad + C(\bar{w} - w(t)) \end{aligned}$$

$$\begin{aligned} \underline{\phi}_{i,j}(t) &= -C\underline{L}_i(\underline{z}_i(t) - y(t) + \underline{Y}_i(t)) + C(B_i - B_j)u(t) - CA_jx(t) + CA_i\underline{x}_i(t) \\ &\quad + C(-\bar{w} - w(t)). \end{aligned}$$

Une approximation de cette hypothèse est définie dans [67] afin de concevoir une logique d'estimation de l'état discret.

Admettant les hypothèses 6-7, si les gains d'observateur sont conçus tel que :

$$\begin{cases} k_1 > 0 \\ k_2 > 3\Gamma + 2\frac{\Gamma^2}{k_1^2}, \end{cases} \quad (\text{B.17})$$

alors, l'observateur d'état discret

$$\hat{q}(t) = \arg \min_i \int_{t-\delta_1}^t \|\underline{\mathcal{L}}_{i,1}(s)\| + \|\bar{\mathcal{V}}_{i,1}(s)\| ds \quad (\text{B.18})$$

fournit une estimation de $\sigma(t)$ dans chaque intervalle $[t_{k-1} + T_1^*, t_k)$, i.e.

$$\hat{q}(t) = \sigma(t), \quad t_{k-1} + T_1^* \leq t < t_k, \quad k = 1, \dots, N \quad (\text{B.19})$$

avec $T_1^* < T_\delta$ et T_δ est le temps de séjour minimal.

Logique de décision

En combinant les deux approches, l'instant estimé de commutation \hat{t}_k , $k = 1, 2, \dots$, peut être défini comme suit :

$$\begin{aligned} \hat{t}_k &= \min(t \in \mathbb{R}^+ | t \geq \hat{t}_{k-1} + T_1^* \text{ and } \hat{q}(t) \neq \hat{q}(\hat{t}_{k-1} + T_1^*)) \vee \\ &\quad t \geq \hat{t}_{k-1} + T_1^* \text{ and } 0 \notin [\underline{\mathcal{L}}_{\hat{q}(t)}, \bar{\mathcal{R}}_{\hat{q}(t)}]. \end{aligned}$$

Le signal de commutation estimé $\hat{\sigma}(t)$ est alors défini par :

$$\hat{\sigma}(t) = \begin{cases} \hat{q}(t) & t \in [\hat{t}_{k-1} + T_1^*, \hat{t}_k) \\ \hat{q}(\hat{t}_{k-1} + T_1^*) & t \in [\hat{t}_k, \hat{t}_k + T_1^*) \end{cases}$$

avec $\hat{q}(t) = \sigma(t)$ pour $t \in [\hat{t}_{k-1} + T_1^*, t_k)$.

En utilisant l'approche proposée, le mode actuel est identifié en temps fini. T_1^* est paramétré par les gains des modes glissants.

L'état $x(t)$ évolue dans une région bornée connue $\underline{X} \leq x \leq \overline{X}$ (Hypothèse 6). Une réinitialisation des états $\bar{x}_i(\hat{t}_k)$ et $\underline{x}_i(\hat{t}_k)$ pour tout $i = 1, \dots, N$ est réalisé afin de s'assurer

$$\underline{x}_i(\hat{t}_k) \leq x(\hat{t}_k) \leq \bar{x}_i(\hat{t}_k)$$

tel que :

$$\bar{x}_i(\hat{t}_k) = \overline{X} \quad \underline{x}_i(\hat{t}_k) = \underline{X}.$$

La figure B.5 présente la synthèse de l'observateur proposé.

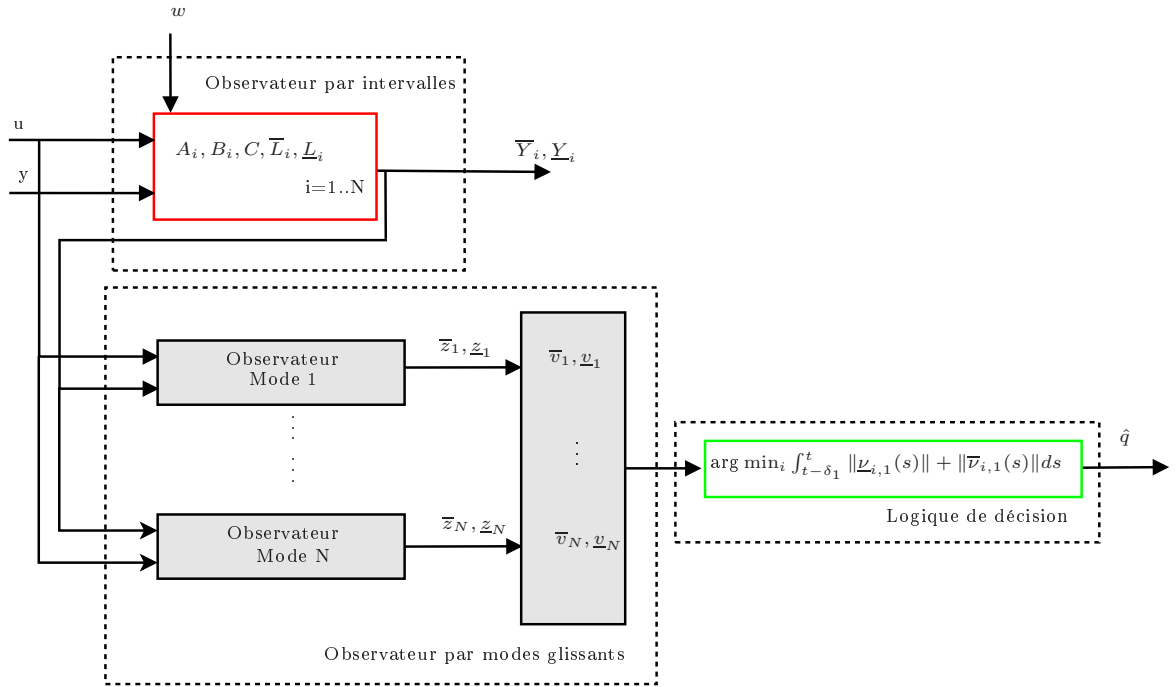


Figure B.5: Schéma bloc de l'observateur d'état discret.

Des résultats de simulations proposés dans la figure B.6 montre le signal de commutation et son estimation. L'approche proposé fournit une bonne estimation des instants de temps de commutation t_k avec une petite erreur $\hat{t}_k + T_1^* - t_k \leq 50ms$.

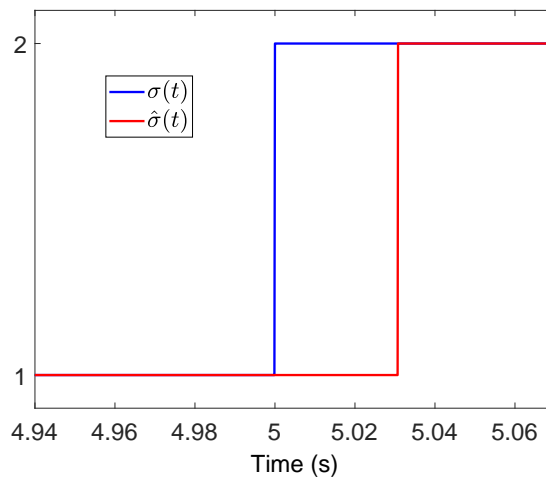


Figure B.6: Evolution du signal de commutation et son estimé (ZOOM).

Les résultats établis ont fait l'objet d'une communication [190] dans la conférence internationale "Conference on Decision and Control".

Généralités sur le diagnostic

Le diagnostic de défaillance d'un système est primordial afin de maintenir la sécurité non seulement de son environnement mais également pour les opérateurs humains. Plusieurs travaux ont été rapportés sur les méthodes de diagnostic telles que [213] et [114] et leurs applications dans divers processus industriels. Le principe de base du diagnostic des défauts repose sur la notion de redondance qui permet de fournir au système plusieurs informations différentes sur une même variable. On peut distinguer deux approches. La première est dite redondance matérielle ou physique. Elle consiste à ajouter des capteurs pour obtenir des informations supplémentaires sur l'état du système, ce qui entraîne un coût important en instrumentation. Ce type de diagnostic se limite à la surveillance des éléments redondants comme les capteurs, les actionneurs, ce qui rend impossible la détection des défauts provenant des éléments non redondants. La deuxième approche dite redondance analytique, utilise un modèle mathématique du système et les mesures réelles disponibles pour développer des algorithmes de détection et d'isolation des défauts. Les travaux de cette thèse se situent dans le cadre du diagnostic à base de modèles. Généralement, l'étude du diagnostic d'un défaut nécessite une phase de génération suivie d'une étape d'évaluation des résidus. Dans ce contexte, on rappelle quelques notions.

Definition 27. *Un défaut est une anomalie ou une déviation non souhaitée d'au moins une caractéristique d'un système de son état de fonctionnement normal.*

Definition 28. *On désigne par résidus les changements ou les divergences entre le comportement réel du système et celui prévu par le modèle.*

Procédure de diagnostic

Le diagnostic permet de détecter, d'isoler et d'identifier les défaillances d'un processus physique. La détection détermine si un défaut s'est produit ou non. L'idée de base consiste à générer un vecteur résidu, défini comme la différence entre le signal de sortie mesuré et estimé. En raison de présence de bruit et des incertitudes, le vecteur résidu, soumis à la fois aux signaux de défauts et aux signaux de perturbations, est souvent non nul même dans les processus normaux. Le gain d'observateur peut être conçu en résolvant un problème d'optimisation multiobjectif (le vecteur résidu est sensible aux défauts et robuste contre les perturbations). Des travaux ont été développés pour la détection de défauts pour divers systèmes tels que les systèmes non linéaires Lipschitz [228], les systèmes non linéaires flous TS [229], et les systèmes à commutations [230]. La localisation d'un défauts consiste à déterminer son emplacement. L'idée consiste à concevoir soit un seul vecteur résidu sensible au défaut concerné, mais robuste aux autres défauts [231], soit à rendre chaque vecteur résidu sensible à tous les défauts sauf un et à résister aux erreurs de modélisation et aux perturbations [113]. La dernière étape, l'identification d'un défaut, sert à déterminer son type de faute, son évolution dans le temps et sa sévérité. L'idée de base des méthodes d'identification de défaut consiste à construire un système augmenté en introduisant le défaut en tant qu'état supplémentaire. Le vecteur d'état étendu est ensuite estimé. Les techniques d'observateurs telles que les observateurs de type proportionnel intégral (PI) [144], les observateur adaptatifs [143] et les observateurs par modes glissants [40] sont généralement utilisées pour l'estimation des fautes. Dans le cadre de cette thèse, on s'intéresse à la détection des défauts pour une classe de système linéaires à commutations.

Classification des défauts

Les défauts peuvent être classés en défauts de nature multiplicative ou de nature additive selon leurs effets sur les performances du système.

- Les défauts multiplicatifs correspondent aux modifications paramétriques du modèle représentant le système et ils induisent des changements sur la dynamique du système.
- Les défauts additifs sont modélisés sous forme de termes additifs dans le modèle. Ils affectent son état ou sa sortie. Cette modélisation est habituellement attribuée aux défauts de capteurs et d'actionneurs.

Les défauts peuvent être classifiés également selon le composant affecté. Ils peuvent affecter le procédé, les actionneurs ou bien les capteurs.

- Les défauts sur le système correspondent à une dégradation des composants du système lui-même. Ces défaillances sont dues alors à des modifications de la structure ou des paramètres du modèle.
- Les actionneurs sont définis comme étant la partie opérative du système qui convertit les signaux de commande issus du contrôleur. Ainsi les défauts actionneurs s'ajoutent aux commandes du système et ils se traduisent par une incohérence entre la commande des actionneurs et la réponse en leur sortie. Par conséquent l'actionneur devient incapable de commander le système.

- Les défauts capteurs donnent une image erronée de la grandeur physique à mesurer. Ainsi, ils se manifestent par un écart entre la valeur réelle de la grandeur et sa mesure.

Détection des défauts

La phase de détection des défauts consiste à indiquer la présence d'un défaut et donc à déterminer si un système est défaillant ou non. Elle comprend deux étapes: (i) la génération des résidus, (ii) l'évaluation des résidus. La première phase repose sur la comparaison du comportement du modèle du système à celui du système réel. En absence de défauts, le vecteur résidu est généralement nul alors qu'il s'écarte notablement de la valeur zéro lorsque le système présente un défaut. Dans la pratique, le résidu n'est jamais parfaitement nul même en fonctionnement non défaillant, ceci est dû à la présence des perturbations, des incertitudes du modèle et de bruits de mesure. Par conséquent, l'une des exigences les plus essentielles imposées aux algorithmes de génération des résidus est la robustesse contre les perturbations endogènes et exogènes. Différents critères ont été développés dans la littérature pour évaluer les effets des incertitudes sur les résidus tels que H_∞ et H_2 dans [116] et [117]. D'autres performances ont été reportées dans [118] pour étudier la sensibilité des vecteurs résidus aux défauts tels que H_- et H_∞ . Plus récemment, la détection des défauts a été formulée comme un problème d'optimisation à objectifs multiples en maximisant la sensibilité des défauts sur les vecteurs résidus et en minimisant les effets des perturbations H_2/H_2 , H_2/H_∞ , H_∞/H_∞ et H_-/H_∞ tel que dans [119] et [120]. La deuxième étape de la détection "l'évaluation des résidus" consiste à comparer la valeur d'un résidu r à un seuil prédéfini ε . Une alarme est déclenchée à chaque franchissement de ce seuil :

$$\begin{cases} r_k \leq \varepsilon & \text{Fault-free} \\ r_k > \varepsilon & \text{Faulty} \end{cases}$$

Dans la littérature, le seuil peut être constant, adaptatif ou variable dans le temps. Il convient de mentionner que la conception d'un seuil approprié reste une tâche difficile, en particulier pour les systèmes dynamiques sujets à des perturbations. Afin de limiter les fausses alarmes et les non détections dans un contexte à erreurs inconnues mais bornées, les méthodes d'évaluation de résidus basées sur des techniques d'ensemble ont connu un essor considérable pour différentes classes de systèmes. En effet, ces méthodes permettent de fournir des seuils dynamiques systématiques pour l'évaluation de résidus. Néanmoins, l'extension de ce type de méthodes pour les systèmes linéaires à commutations demeure peu traitée dans la littérature. Dans ce mémoire, la synthèse des approches de détection des défauts des systèmes à commutations est envisagée en utilisant les techniques ensemblistes, notamment les intervalles, les zonotopes et les ellipsoïdes.

Détection des défauts à base d'observateurs par intervalles

Afin d'assurer une détection de défauts robuste aux perturbations et au bruit de mesure, on se propose dans cette partie de considérer deux approches par intervalles pour un système linéaire à commutations défini par :

$$\begin{cases} x_{k+1} = A_q x_k + B_q u_k + D_q w_k \\ y_k = C x_k + D_v v_k + F f_k, \end{cases} \quad (\text{B.20})$$

avec $x \in \mathbb{R}^{n_x}$, $u \in \mathbb{R}^{n_u}$, $y \in \mathbb{R}^{n_y}$, $f \in \mathbb{R}^{n_f}$, $w \in \mathbb{R}^{n_w}$ et $v \in \mathbb{R}^{n_v}$ sont respectivement l'état, l'entrée, la sortie, le défaut capteur, les perturbations sur l'état et le bruit de mesure. Les matrices A_q , B_q , C , D_q , D_v et F sont supposées connues. La commutation entre les sous-systèmes est assurée par un signal de commutation $q \in \mathcal{I} = \overline{1, N}$, $N \in \mathbb{N}$.

Dans la suite, on considère l'ensemble de ces hypothèses.

Hypothèse 8. *Le bruit de mesure et les perturbations d'état sont supposés inconnus mais bornés et de bornes connues tel que :*

$$\underline{w} \leq w \leq \overline{w}, \quad \underline{v} \leq v \leq \overline{v}, \quad (\text{B.21})$$

avec $\underline{w}, \overline{w} \in \mathbb{R}^{n_w}$ et $\underline{v}, \overline{v} \in \mathbb{R}^{n_v}$.

Hypothèse 9. *L'état initial x_0 vérifie $\underline{x}_0 \leq x_0 \leq \overline{x}_0$ avec $\underline{x}_0, \overline{x}_0 \in \mathbb{R}_x^n$.*

Hypothèse 10. *Les paires $(A_q, C) \forall q = 1, \dots, N$ sont détectables.*

Hypothèse 11. *Il existe des gains $\overline{L}_q \in \mathbb{R}^{n_x \times n_y}$ et $\underline{L}_q \in \mathbb{R}^{n_x \times n_y}$ tel que les matrices $A_q - \overline{L}_q C$ et $A_q - \underline{L}_q C$ soient Metzler pour tout $q \in \mathcal{I}$.*

Observateurs par intervalles classique

La structure de l'observateur par intervalles est donnée par :

$$\left\{ \begin{array}{l} \overline{x}_{k+1} = A_q \overline{x}_k + B_q u_k + \overline{L}_q (y_k - C \overline{x}_k) + \overline{\Delta} \\ \underline{x}_{k+1} = A_q \underline{x}_k + B_q u_k + \underline{L}_q (y_k - C \underline{x}_k) + \underline{\Delta} \\ \overline{y}_k = C^+ \overline{x}_k - C^- \underline{x}_k + D_v^+ \overline{v} - D_v^- \underline{v} \\ \underline{y}_k = C^+ \underline{x}_k - C^- \overline{x}_k + D_v^+ \underline{v} - D_v^- \overline{v} \\ \overline{r}_k = \overline{y}_k - y_k \\ \underline{r}_k = \underline{y}_k - y_k \end{array} \right. \quad (\text{B.22})$$

avec $\overline{L}_q, \underline{L}_q \in \mathbb{R}^{n_x \times n_y}$ sont les gains d'observateurs. $\overline{\Delta}$ et $\underline{\Delta}$ sont donnés par :

$$\left\{ \begin{array}{l} \overline{\Delta} = D_q^+ \overline{w} - D_q^- \underline{w} + (\overline{L}_q D_v)^+ \overline{v} - (\overline{L}_q D_v)^- \underline{v}, \\ \underline{\Delta} = D_q^+ \underline{w} - D_q^- \overline{w} + (\underline{L}_q D_v)^+ \underline{v} - (\underline{L}_q D_v)^- \overline{v}. \end{array} \right.$$

En utilisant l'observateur par intervalles (B.22), l'objectif est de concevoir des gains \overline{L}_q et \underline{L}_q qui assurent à la fois la coopérativité, la stabilité des erreurs d'estimation et la minimization de la norme L_∞ de la fonction de transfert des perturbations et de bruit de mesure par rapport aux vecteurs résidus \overline{r}_k et \underline{r}_k . Dans la littérature, de nombreux travaux considèrent la performance H_∞ pour atténuer l'effet des incertitudes. Il convient de noter que le critère H_∞ concernent des signaux à énergie finie. Néanmoins, dans la pratique, certains signaux ne peuvent pas être considérés à énergie finie mais ont des amplitudes bornées. D'où l'intérêt de l'utilisation du critère de performance L_∞ qui introduit l'indice de performance crête à crête.

Les conditions de coopérativité, de stabilité et de robustesse vis-à-vis les perturbations sont exprimées en termes des LMIs en utilisant les fonctions de Lyapunov communes et multiples.

Observateurs par intervalles : structure TNL

L'observateur par intervalles classique fournit une détection robuste de défauts du système considéré. Dans certains cas, il est rarement possible de trouver des gains \bar{L}_q et \underline{L}_q tel que les matrices $A_q - \bar{L}_q C$ et $A_q - \underline{L}_q C$ soient non négatives. Dans cette partie, un nouvel observateur par intervalles est proposé pour réduire le conservatisme dû à la conception des gains d'observateur. La technique introduite permet de fournir plus de degré de liberté en introduisant des matrices de pondération \bar{T}_q , \underline{T}_q , \bar{N}_q et \underline{N}_q . La structure de l'observateur par intervalles basée sur une structure TNL est donnée par :

$$\left\{ \begin{array}{l} \bar{\xi}_{k+1} = \bar{T}_q A_q \bar{x}_k + \bar{T}_q B_q u_k + \bar{L}_q (y_k - C \bar{x}_k) + \bar{\Delta} \\ \bar{x}_k = \bar{\xi}_k + \bar{N}_q y_k \\ \underline{\xi}_{k+1} = \underline{T}_q A_q \underline{x}_k + \underline{T}_q B_q u_k + \underline{L}_q (y_k - C \underline{x}_k) + \underline{\Delta} \\ \underline{x}_k = \underline{\xi}_k + \underline{N}_q y_k \\ \bar{y}_k = C^+ \bar{x}_k - C^- \underline{x}_k + D_v^+ \bar{v} - D_v^- \underline{v} \\ \underline{y}_k = C^+ \underline{x}_k - C^- \bar{x}_k + D_v^+ \underline{v} - D_v^- \bar{v} \\ \bar{r}_k = \bar{y}_k - y_k \\ \underline{r}_k = \underline{y}_k - y_k \end{array} \right. \quad (\text{B.23})$$

avec $\bar{\xi}_k, \underline{\xi}_k \in \mathbb{R}^{n_x}$ sont des variables intermédiaires, $\bar{x}_k, \underline{x}_k \in \mathbb{R}^{n_x}$ sont respectivement les bornes supérieure et inférieure de l'état x_k . $\bar{\Delta}$ et $\underline{\Delta}$ sont donnés par :

$$\left\{ \begin{array}{l} \bar{\Delta} = (\bar{T}_q D_q)^+ \bar{w} - (\bar{T}_q D_q)^- \underline{w} + (\bar{L}_q D_v)^+ \bar{v} - (\bar{L}_q D_v)^- \underline{v} + (\bar{N}_q D_v)^+ \bar{v} - (\bar{N}_q D_v)^- \underline{v} \\ \underline{\Delta} = (\underline{T}_q D_q)^+ \underline{w} - (\underline{T}_q D_q)^- \bar{w} + (\underline{L}_q D_v)^+ \underline{v} - (\underline{L}_q D_v)^- \bar{v} + (\underline{N}_q D_v)^+ \underline{v} - (\underline{N}_q D_v)^- \bar{v} \end{array} \right.$$

Dans (B.23), $\bar{L}_q \in \mathbb{R}^{n_x \times n_y}$ et $\underline{L}_q \in \mathbb{R}^{n_x \times n_y}$ représentent les gains d'observateur. $\bar{T}_q \in \mathbb{R}^{n_x \times n_x}$, $\underline{T}_q \in \mathbb{R}^{n_x \times n_x}$, $\bar{N}_q \in \mathbb{R}^{n_x \times n_y}$ et $\underline{N}_q \in \mathbb{R}^{n_x \times n_y}$ sont des matrices constantes qui doivent être conçues pour satisfaire

$$\bar{T}_q + \bar{N}_q C = I_{n_x} \quad (\text{B.24})$$

$$\underline{T}_q + \underline{N}_q C = I_{n_x}. \quad (\text{B.25})$$

En se basant sur une forme augmentée de la dynamique des erreurs d'estimation supérieure et inférieure, des conditions de coopérativité, de stabilité et d'optimisation du critère L_∞ sont exprimées en termes des LMIs en utilisant les fonctions de Lyapunov communes et multiples.

Evaluation des résidus

L'évaluation de résidus indique la présence d'un défaut. Lorsqu'un défaut s'est produit, une déviation est détectée. Ceci est justifié par le fait que les sorties estimées ne sont plus compatibles avec les mesures, i.e :

$$y_k \notin [\underline{y}_k \quad \bar{y}_k] \quad (\text{B.26})$$

L'inclusion (B.26) implique :

$$\begin{aligned} 0 &\notin [\underline{y}_k \quad \bar{y}_k] - y_k \\ \Rightarrow 0 &\notin [\underline{y}_k - y_k \quad \bar{y}_k - y_k] \end{aligned}$$

$$\Rightarrow 0 \notin [\underline{r}_k \ \bar{r}_k] \quad (\text{B.27})$$

Par conséquent, le signal zéro est encadré par les bornes supérieure et inférieure du résidu quand le système est non défaillant. Toutefois, un défaut est détecté dans le cas contraire.

Résultats de simulation

Le système linéaire à commutations est affecté par un défaut capteur f_k représenté comme suit :

$$f_k = \begin{cases} 1 & 35 \leq k \leq 55 \\ 0 & \text{otherwise.} \end{cases}$$

Les résultats de simulation montrent l'efficacité de deux approches proposées pour la détection d'un défaut capteur (Fig. B.7). Cependant, les résultats de détection obtenus par l'observateur par intervalles basé sur la structure TNL est plus précise que ceux obtenus par l'observateur par intervalles classique. Le cas d'un défaut de faible amplitude est également

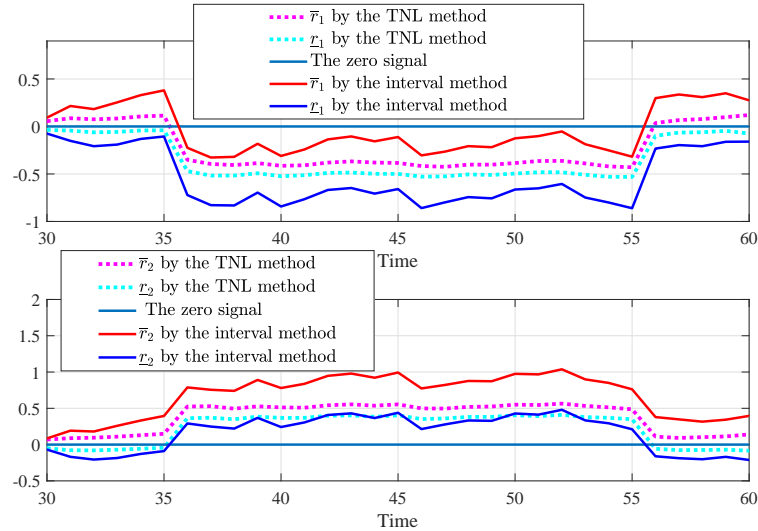


Figure B.7: Comparaison des performances de détection des défauts entre l'approche TNL et la méthode par intervalles classique.

considéré.

Les résultats de simulation montrent que le défaut est détecté en utilisant l'approche TNL et par conséquent $0 \notin [\underline{r}_k \ \bar{r}_k]$ alors que cette inclusion n'est plus vérifiée en considérant les observateurs par intervalles classiques (Fig. B.8). On peut en déduire que la combinaison des observateurs par intervalles TNL avec le critère de performance L_∞ permet une meilleure détection du défaut capteur.

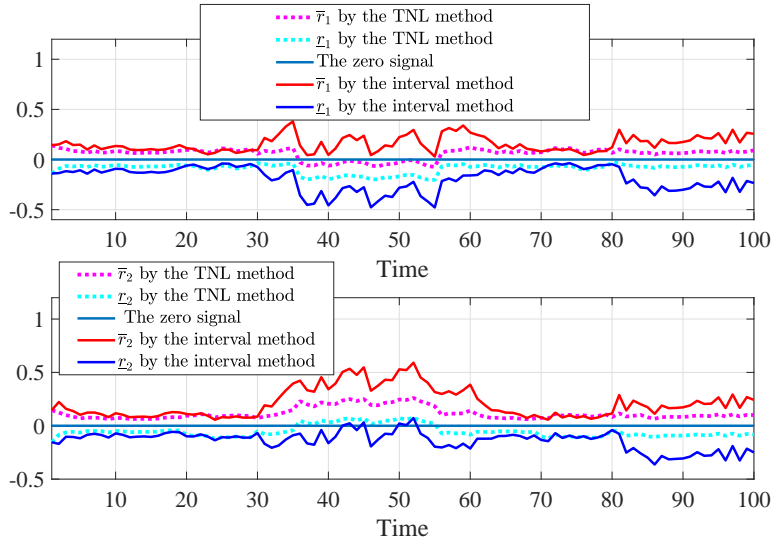


Figure B.8: Comparaison des performances de détection des défauts entre l'approche TNL et la méthode par intervalles classique (Défaut de faible amplitude).

Les résultats présentés ont fait l'objet de deux communications [195] et [196] dans les conférences internationales "European Control Conference" et "Mediterranean Conference on Control and Automation" et un article [194] dans la revue internationale "European Journal of Control".

Détection des défauts à base des techniques ensemblistes

Les méthodes par intervalles nécessitent la condition de coopérativité, qui peut être trop restrictive dans la pratique. Pour remédier à ce problème, les techniques ensemblistes sont introduites pour améliorer la précision de détection des défauts sans tenir compte de l'hypothèse de coopérativité.

Détection des défauts à base des techniques zonotopiques

Dans une première partie, on s'intéresse à la détection des défauts actionneurs, en considérant l'approche zonotopique, d'un système linéaire à commutations modélisé par :

$$\begin{cases} x_{k+1} &= A_q x_k + B_q u_k + D w_k + F_q f_k \\ y_k &= C x_k + D_v v_k, \end{cases} \quad (\text{B.28})$$

avec $x \in \mathbb{R}^{n_x}$, $y \in \mathbb{R}^{n_y}$, $u \in \mathbb{R}^{n_u}$, $f \in \mathbb{R}^{n_f}$, $w \in \mathbb{R}^{n_w}$ et $v \in \mathbb{R}^{n_v}$ représentent respectivement le vecteur d'état, l'entrée, la sortie, le défaut actionneur, les perturbations et le bruit de mesure. L'indice q représente le mode actif, $q \in \mathcal{I} = \overline{1, N}$, $N \in \mathbb{Z}_+$. Le signal de commutations est supposé connu.

Definition 29. Un zonotope d'ordre s noté \mathbf{Z} représente l'image affine d'un hypercube

$\mathbb{B}^s = [-1, 1]^s$ tel que :

$$\mathbf{Z} = \langle p, H \rangle = p + H\mathbb{B}^s = \{p + Hz, z \in \mathbb{B}^s\},$$

$p \in \mathbb{R}^n$ représente le centre de \mathbf{Z} et $H \in \mathbb{R}^{n \times s}$ est la matrice génératrice de \mathbf{Z} .

Hypothèse 12. L'état initial x_0 , le bruit de mesure v_k et les perturbations sur l'état w_k sont supposés inconnus mais bornés par des zonotopes tel que :

$$x_0 \in \langle p_0, H_0 \rangle, \quad w_k \in \langle 0, H_w \rangle, \quad v_k \in \langle 0, H_v \rangle, \quad (\text{B.29})$$

avec $H_0 = \text{diag}(\bar{x})$, $H_w = \text{diag}(\bar{w})$ et $H_v = \text{diag}(\bar{v})$.

L'observateur proposé pour (B.28) est donné par :

$$\begin{cases} \hat{x}_{k+1} = A_q \hat{x}_k + B_q u_k + L_q (y_k - C \hat{x}_k) \\ r_k = y_k - C \hat{x}_k, \end{cases} \quad (\text{B.30})$$

avec \hat{x}_k est l'estimation du vecteur d'état x_k et $L_q \in \mathbb{R}^{n_x \times n_y}$, $q \in \{1, \dots, N\}$, sont les gains de l'observateur.

L'objectif est de concevoir les gains L_q afin d'améliorer à la fois la sensibilité du défaut par rapport au résidu r_k , en considérant une nouvelle méthode de placement de pôle, et atténuer l'effet des perturbations en minimisent les performances H_∞ . L'idée est de diviser la dynamique d'erreur d'estimation en deux sous-systèmes où l'un est découplé de l'effet de f_k et l'autre est découplé de l'effet des perturbations.

En se basant sur cette méthodologie, des conditions de stabilité, de sensibilité du défaut et de robustesse sont exprimées en termes des LMIs en utilisant la fonction de Lyapunov commune.

Evaluation des résidus

En utilisant l'approche zonotopique, l'évaluation de résidus est basée sur un test d'appartenance du vecteur résidu r_k au zonotope \mathbf{R}_k . Le schéma de décision est alors obtenu comme suit :

$$\begin{cases} r_k \in \mathbf{R}_k & \text{Fault-free} \\ r_k \notin \mathbf{R}_k & \text{Faulty} \end{cases} \quad (\text{B.31})$$

La détermination du zonotope \mathbf{R}_k peut être résumée dans l'algorithme suivant :

Résultats de simulation

Une comparaison est faite entre l'approche de détection de défaut conçue et une autre sans considérer l'analyse de sensibilité et de robustesse. Un défaut actionneur f_k est représenté par :

$$f_k = \begin{cases} 0.002 & k \geq 20 \\ 0 & \text{otherwise} \end{cases}$$

Les résultats de simulation montrent que le défaut f_k peut être détecté à l'instant $k = 22$ ($r_k \notin R_k$) en utilisant l'approche conçue où à la fois la sensibilité au défaut et la robustesse aux incertitudes sont considérées (Fig. B.9). Cependant le défaut f_k peut difficilement

Algorithm 3 Evaluation des résidus : approche zonotopique

Input: u_k, y_k **Output:** r_k 1: **Initialization:**

$$x_0 \in \langle p_0, H_0 \rangle; \hat{x}_0 = p_0$$

$$w \in \mathbf{W} = \langle 0, H_w \rangle; v \in \mathbf{V} = \langle 0, H_v \rangle$$

2: **for** $k = 1$ to N **do**

3: $\hat{x}_{k+1} = (A_q - L_q C)\hat{x}_k + B_q u_k + L_q(y_k - C\hat{x}_k)$

4: $r_k = y_k - C\hat{x}_k$

5: $H_{k+1} = [(A_q - L_q C) \downarrow_l(H_k) \quad DH_w \quad -L_q D_v H_v]$

6: $R_k = [CH_k \quad D_v H_v]$

7: $\mathbf{R}_k = \langle 0, R_k \rangle$

8: On note par indice = 0 : aucun défaut détecté et indice = 1 : défaut détecté :

$$\text{indice} = \begin{cases} 0 & \text{si } r_k \in \mathbf{R}_k \\ 1 & \text{si } r_k \notin \mathbf{R}_k \end{cases}$$

9: **end for**

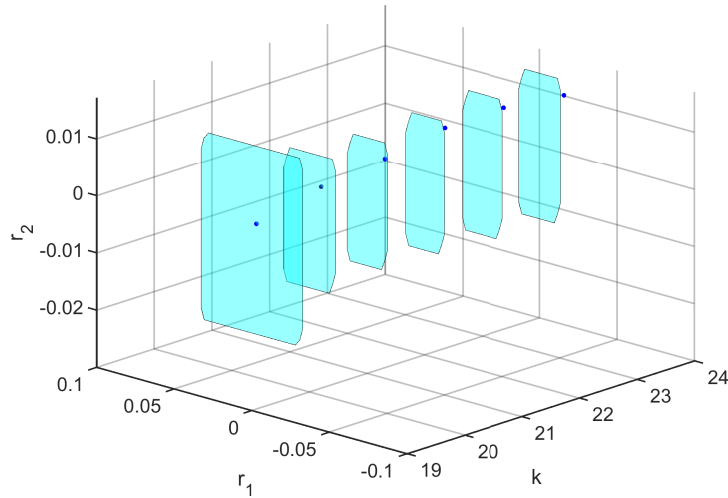


Figure B.9: Résultats de détection du défaut actionneur : Approche proposée avec optimisation

être détecté en utilisant la méthode sans optimisation (Fig. B.10). Ainsi, il convient de souligner que l'approche conçue permet d'assurer de meilleures performances de détection des défauts.

L'amélioration des résultats de détection des défauts est assurée en considérant des zonotopes de dimensions supérieures. Cela peut engendrer une complexité de calcul élevée. Les techniques ellipsoïdales peuvent être alors utilisées pour assurer un bon compromis entre la précision de détection et la complexité de calcul.

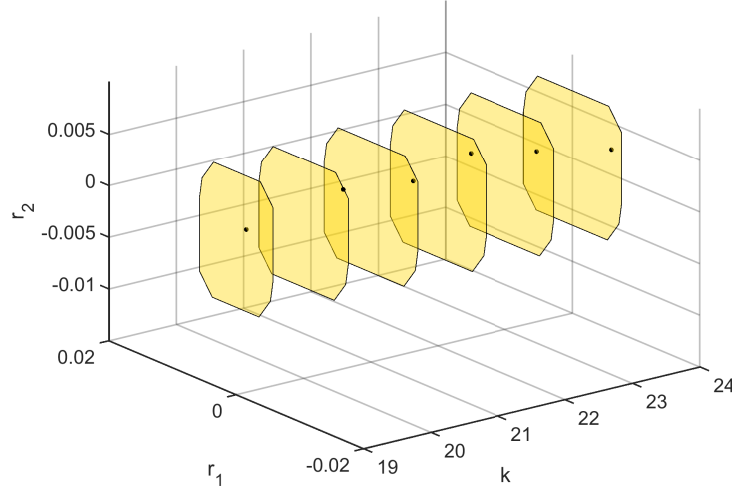


Figure B.10: Résultats de détection du défaut actionneur : Approche sans optimisation

Détection des défauts à base des techniques ellipsoïdales

Dans cette partie, on s'intéresse à la détection des défauts capteurs, en considérant l'approche ellipsoïdale, d'un système linéaire à commutations modélisé par :

$$\begin{cases} x_{k+1} = A_q x_k + B_q u_k + D_q w_k \\ y_k = C x_k + D_v v(k) + F f_k, \end{cases} \quad (\text{B.32})$$

avec $x \in \mathbb{R}^{n_x}$, $y \in \mathbb{R}^{n_y}$, $u \in \mathbb{R}^{n_u}$, $f \in \mathbb{R}^{n_f}$, $w \in \mathbb{R}^{n_w}$ et $v \in \mathbb{R}^{n_v}$ représentent respectivement le vecteur d'état, l'entrée, la sortie, le défaut capteur, les perturbations et le bruit de mesure. L'indice q représente le mode actif qui est supposé connu.

Definition 30. [206] Un ellipsoïde $\mathcal{E}(c, X) \subset \mathbb{R}^n$ est défini par :

$$\mathcal{E}(c, X) = \{x \in \mathbb{R}^n : (x - c)^T X^{-1} (x - c) \leq 1\}. \quad (\text{B.33})$$

Hypothèse 13. L'état initial x_0 , le bruit de mesure v_k et les perturbations sur l'état w_k sont supposés inconnus mais bornés par des ellipsoïdes tel que :

$$x_0 \in \mathcal{E}(c_0, X_0), w_k \in \mathcal{E}(0, W), v_k \in \mathcal{E}(0, V), \quad (\text{B.34})$$

avec $c_0 \in \mathbb{R}^{n_x}$ est un vecteur connu, $X_0 = \tilde{x}_0^2 I_{n_x}$, $W = \|w\|_\infty^2 I_{n_w}$ et $V = \|v\|_\infty^2 I_{n_v}$. $\|w\|_\infty$ et $\|v\|_\infty$, supposés connus, représentent respectivement la norme L_∞ de w et v . La constante \tilde{x}_0 est donnée par $\|x_0 - c_0\| \leq \tilde{x}_0$.

La structure de l'observateur proposé est donnée par :

$$\begin{cases} \hat{x}_{k+1} = T_q A_q \hat{x}_k + T_q B_q u_k + N_q y_{k+1} + L_q (y_k - C \hat{x}_k) \\ r_k = y_k - C \hat{x}_k, \end{cases} \quad (\text{B.35})$$

avec $\hat{x} \in \mathbb{R}^{n_x}$ représente l'estimation de x , r_k représente le vecteur résidu et $L_q \in \mathbb{R}^{n_x \times n_y}$ sont les gains d'observateur.

$T_q \in \mathbb{R}^{n_x \times n_x}$ et $N_q \in \mathbb{R}^{n_x \times n_y}$ sont des matrices constantes qui doivent être conçues pour satisfaire la relation suivante :

$$T_q + N_q C = I_{n_x}. \quad (\text{B.36})$$

La nouvelle structure d'observateur est proposée en se basant sur le critère de performance L_∞ pour atténuer les effets des incertitudes. Cette structure permet de fournir plus de degrés de liberté de conception en introduisant des matrices T_q et N_q .

Il convient de noter que si T_q et N_q sont choisis de telle sorte que $T_q = I_{n_x}$ et $N_q = 0$, l'observateur (B.35) est équivalent à un observateur de Luenberger.

En se basant sur cette méthodologie, des conditions de stabilité et de robustesse sont exprimées en termes des LMIs en utilisant les fonctions de Lyapunov multiples pour améliorer la détection du défaut capteur.

Evaluation des résidus

L'évaluation de résidus est basée sur un test d'appartenance du vecteur résidu r_k à l'ellipsoïde $\mathcal{E}(0, R_k)$. Le schéma de décision est donné par :

$$\begin{cases} r(k) \in \mathcal{E}(0, R_k) & \text{Fault-free} \\ r(k) \notin \mathcal{E}(0, R_k) & \text{Faulty} \end{cases} \quad (\text{B.37})$$

Plus de détails sur la détermination de l'ellipsoïde $\mathcal{E}(0, R_k)$ sont donnés dans le chapitre 5 de ce mémoire.

Résultats de simulation

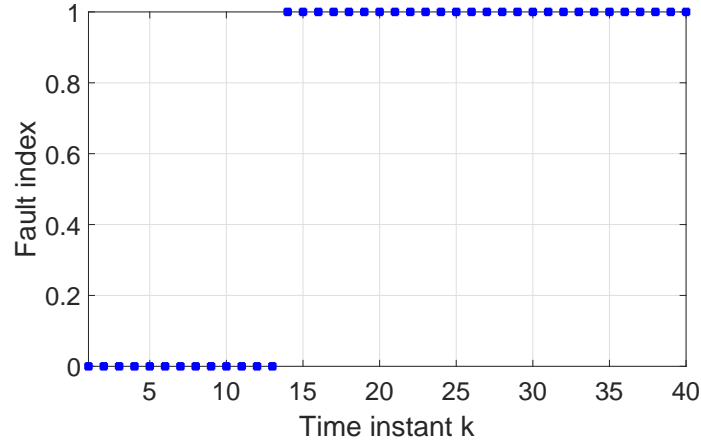
Afin de démontrer l'efficacité de la méthode de détection proposée, une comparaison est réalisée avec une approche qui combine la structure Luenberger et la performance L_∞ .

Un défaut capteur f_k est représenté par :

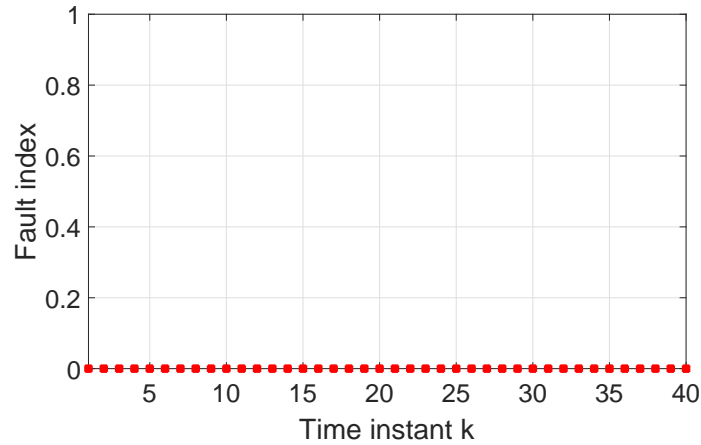
$$f_k = \begin{cases} 0.08 & k \geq 14 \\ 0 & \text{otherwise} \end{cases}$$

Les résultats de simulation montrent que le défaut f_k est détecté à l'instant $k = 14$ en utilisant la technique proposée alors qu'il n'est pas détecté en se basant sur l'observateur de Luenberger. Par conséquent, les résultats montrent la faisabilité et l'efficacité de la méthode conçue pour la détection du défaut capteur.

Les résultats présentés ont fait l'objet de deux communications [200] et [201] dans les conférences internationales "IFAC World Congress" et "Conference on Decision and Control".



(a) Résultats de détection du défaut capteur : Structure TNL



(b) Résultats de détection du défaut capteur : Structure Luenberger

Figure B.11: Comparaison entre les résultats de détection de l'observateur proposé et la structure de Luenberger.

Conclusion

Dans cette thèse, différentes méthodes de détection des défauts ont été développées pour des systèmes linéaires à commutations. Le principal enjeu consiste à apporter des solutions robustes à la détection des défauts en présence de différentes sources de perturbations supposées inconnues mais bornées. Afin de gérer ces perturbations, des méthodes ensemblistes ont été proposées.

La procédure de diagnostic nécessite à un certain moment l'estimation d'état du système en question. Dans une première partie, une méthode d'estimation par intervalles de l'état continu pour une classe de systèmes LPV à commutations est élaborée. Le principal avantage de l'approche proposée consiste à relaxer les conditions de coopérativité et de stabilité grâce à la forme polytopique des paramètres variants dans le temps et l'utilisation des fonctions de Lyapunov multiples. En outre, une méthode combinant la technique par modes glissants et l'approche par intervalles est développée puis appliquée à la détection du changement

d'état discret d'un système linéaire à commutations à entrée inconnue. La combinaison des deux techniques est l'une des principales avantages de la méthode proposée pour identifier le mode actif en temps fini en considérant la connaissance des bornes de l'entrée inconnue.

Les observateurs par intervalles sont également conçus pour la détection de défauts des systèmes linéaires à commutations. Une nouvelle structure de ces observateurs est développée pour offrir plus de degrés de liberté de conception en se basant sur la minimisation du critère L_∞ . Dans une dernière partie, deux méthodes ensemblistes basées sur des approches zonotopiques et ellipsoïdales sont proposées pour améliorer les résultats de détection sans tenir compte de l'hypothèse de coopérativité liée aux observateurs par intervalles. Des résultats de simulation, sur des exemples académiques, sont proposés pour valider les différentes approches proposées.

Les résultats obtenus ont permis de montrer que l'application de méthodes ensemblistes pour la diagnostic de défauts des systèmes linéaires à commutations sujets à des perturbations inconnues mais bornées est avantageuse. En effet, elle permet à la fois de fournir un moyen systématique d'évaluation de résidus et d'améliorer la précision des résultats de détection des défauts. Le choix de l'ensemble pour représenter l'état et les perturbations dépend principalement de la complexité de calcul et la précision de détection.

Bibliography

- [1] Cécile Durieu, E Walter, and Boris Polyak, “Multi-input multi-output ellipsoidal state bounding,” *Journal of optimization theory and applications*, vol. 111, no. 2, pp. 273–303, 2001.
- [2] Laurentiu Hetel, *Robust stability and control of switched linear systems*, Ph.D. thesis, TU Eindhoven, 2007.
- [3] Christophe Combastel, “A state bounding observer based on zonotopes,” in *2003 European Control Conference (ECC)*. IEEE, 2003, pp. 2589–2594.
- [4] A Levis, “Challenges to control: A collective view—report of the workshop held at the university of santa clara on september 18-19, 1986,” *IEEE Transactions on Automatic Control*, vol. 32, no. 4, pp. 275–285, 1987.
- [5] Panos Antsaklis, Wolf Kohn, Anil Nerode, and Shankar Sastry, *Hybrid systems II*, vol. 999, Springer Science & Business Media, 1995.
- [6] Daniel Liberzon, *Switching in systems and control*, Springer Science & Business Media, 2003.
- [7] Hai Lin and Panos J Antsaklis, “Stability and stabilizability of switched linear systems: a survey of recent results,” *IEEE Transactions on Automatic control*, vol. 54, no. 2, pp. 308–322, 2009.
- [8] Arjan J Van Der Schaft and Johannes Maria Schumacher, *An introduction to hybrid dynamical systems*, vol. 251, Springer London, 2000.
- [9] Rathinasamy Sakthivel, Maya Joby, Peng Shi, and K Mathiyalagan, “Robust reliable sampled-data control for switched systems with application to flight control,” *International Journal of Systems Science*, vol. 47, no. 15, pp. 3518–3528, 2016.
- [10] Hangli Ren, Guangdeng Zong, and Tieshan Li, “Event-triggered finite-time control for networked switched linear systems with asynchronous switching,” *IEEE Transactions on Systems, Man, and Cybernetics: Systems*, vol. 48, no. 11, pp. 1874–1884, 2018.
- [11] Xavier Allamigeon, Stéphane Gaubert, Nikolas Stott, Éric Goubault, and Sylvie Putot, “A scalable algebraic method to infer quadratic invariants of switched systems,” *ACM Transactions on Embedded Computing Systems (TECS)*, vol. 15, no. 4, pp. 1–20, 2016.

- [12] Rodrigo Cardim, Marcelo CM Teixeira, Edvaldo Assuncao, and Marcio Roberto Covacic, "Variable-structure control design of switched systems with an application to a dc–dc power converter," *IEEE Transactions on Industrial Electronics*, vol. 56, no. 9, pp. 3505–3513, 2009.
- [13] Di Wu, Xi-Ming Sun, Yun-Bo Zhao, and Wei Wang, "Stability analysis of nonlinear switched networked control systems with periodical packet dropouts," *Circuits, Systems, and Signal Processing*, vol. 32, no. 4, pp. 1931–1947, 2013.
- [14] Sara Ifqir, Dalil Ichalal, Naima Ait Oufroukh, and Said Mammar, "Robust interval observer for switched systems with unknown inputs: Application to vehicle dynamics estimation," *European Journal of Control*, vol. 44, pp. 3–14, 2018.
- [15] P. J. Antsaklis, "Special issue on hybrid systems: theory and applications a brief introduction to the theory and applications of hybrid systems," in *Proceedings of the IEEE*, 2000, vol. 88, pp. 879–887.
- [16] Raymond A DeCarlo, Michael S Branicky, Stefan Pettersson, and Bengt Lennartson, "Perspectives and results on the stability and stabilizability of hybrid systems," *Proceedings of the IEEE*, vol. 88, no. 7, pp. 1069–1082, 2000.
- [17] Robert Shorten, Fabian Wirth, Oliver Mason, Kai Wulff, and Christopher King, "Stability criteria for switched and hybrid systems," *SIAM review*, vol. 49, no. 4, pp. 545–592, 2007.
- [18] Robert Shorten, Kumpati S Narendra, and Oliver Mason, "A result on common quadratic lyapunov functions," *IEEE Transactions on automatic control*, vol. 48, no. 1, pp. 110–113, 2003.
- [19] Daniel Liberzon and A Stephen Morse, "Basic problems in stability and design of switched systems," *IEEE control systems magazine*, vol. 19, no. 5, pp. 59–70, 1999.
- [20] João P Hespanha, "Stabilization through hybrid control," *encyclopedia of life support systems (EOLSS)*, 2004.
- [21] Jamal Daafouz, Pierre Riedinger, and Claude Iung, "Stability analysis and control synthesis for switched systems: a switched lyapunov function approach," *IEEE transactions on automatic control*, vol. 47, no. 11, pp. 1883–1887, 2002.
- [22] Laurentiu Hetel, Jamal Daafouz, and Claude Iung, "Stabilization of arbitrary switched linear systems with unknown time-varying delays," *IEEE Transactions on Automatic Control*, vol. 51, no. 10, pp. 1668–1674, 2006.
- [23] Michael S Branicky, "Multiple lyapunov functions and other analysis tools for switched and hybrid systems," *IEEE Transactions on automatic control*, vol. 43, no. 4, pp. 475–482, 1998.
- [24] Hassan K Khalil and Jessy W Grizzle, *Nonlinear systems*, vol. 3, Prentice hall Upper Saddle River, NJ, 2002.

- [25] Daniel Liberzon, *Switching in systems and control*, Springer Science & Business Media, 2012.
- [26] Bo Hu, Guisheng Zhai, and Anthony N Michel, “Common quadratic lyapunov-like functions with associated switching regions for two unstable second-order lti systems,” *International Journal of Control*, vol. 75, no. 14, pp. 1127–1135, 2002.
- [27] Joao P Hespanha and A Stephen Morse, “Stability of switched systems with average dwell-time,” in *Proceedings of the 38th IEEE Conference on Decision and Control*. IEEE, 1999, pp. 2655–2660.
- [28] Hui Ye, Anthony N Michel, and Ling Hou, “Stability theory for hybrid dynamical systems,” *IEEE transactions on automatic control*, vol. 43, no. 4, pp. 461–474, 1998.
- [29] Eduardo D Sontag and Yuan Wang, “On characterizations of the input-to-state stability property,” *Systems and Control letters*, vol. 24, no. 5, pp. 351–360, 1995.
- [30] Stephen Boyd, Laurent El Ghaoui, Eric Feron, and Venkataramanan Balakrishnan, *Linear matrix inequalities in system and control theory*, vol. 15, Siam, 1994.
- [31] Matthias A Müller and Daniel Liberzon, “Input/output-to-state stability and state-norm estimators for switched nonlinear systems,” *Automatica*, vol. 48, no. 9, pp. 2029–2039, 2012.
- [32] Thomas Meurer, Knut Graichen, and Ernst-Dieter Gilles, *Control and observer design for nonlinear finite and infinite dimensional systems*, vol. 322, Springer Science & Business Media, 2005.
- [33] Gildas Besançon, *Nonlinear observers and applications*, vol. 363, Springer, 2007.
- [34] Yunkai Wu, Bin Jiang, and Ningyun Lu, “A descriptor system approach for estimation of incipient faults with application to high-speed railway traction devices,” *IEEE Transactions on Systems, Man, and Cybernetics: Systems*, 2017.
- [35] David G Luenberger, “Observing the state of a linear system,” *IEEE transactions on military electronics*, vol. 8, no. 2, pp. 74–80, 1964.
- [36] Rudolph Emil Kalman, “A new approach to linear filtering and prediction problems,” 1960.
- [37] Jie Chen, Ron J Patton, and Hong-Yue Zhang, “Design of unknown input observers and robust fault detection filters,” *International Journal of control*, vol. 63, no. 1, pp. 85–105, 1996.
- [38] Farzad Esfandiari and Hassan K Khalil, “Output feedback stabilization of fully linearizable systems,” *International Journal of control*, vol. 56, no. 5, pp. 1007–1037, 1992.
- [39] Reza Mohajerpoor, Hamid Abdi, and Saeid Nahavandi, “A new algorithm to design minimal multi-functional observers for linear systems,” *Asian Journal of Control*, vol. 18, no. 3, pp. 842–857, 2016.

- [40] Halim Alwi and Christopher Edwards, “Robust fault reconstruction for linear parameter varying systems using sliding mode observers,” *International Journal of Robust and Nonlinear Control*, vol. 24, no. 14, pp. 1947–1968, 2014.
- [41] Tarek Raïssi, Denis Efimov, and Ali Zolghadri, “Interval state estimation for a class of nonlinear systems,” *IEEE Transactions on Automatic Control*, vol. 57, no. 1, pp. 260–265, 2012.
- [42] Xiaohang Li, Fanglai Zhu, and Jian Zhang, “State estimation and simultaneous unknown input and measurement noise reconstruction based on adaptive H_∞ observer,” *International Journal of Control, Automation and Systems*, vol. 14, no. 3, pp. 647–654, 2016.
- [43] Huai-Ning Wu, Zhi-Yong Liu, and Lei Guo, “Robust L_∞ -gain fuzzy disturbance observer-based control design with adaptive bounding for a hypersonic vehicle,” *IEEE Transactions on Fuzzy Systems*, vol. 22, no. 6, pp. 1401–1412, 2013.
- [44] Zhendong Sun, S.S. Ge, and T.H. Lee, “Controllability and reachability criteria for switched linear systems,” *Automatica*, vol. 38, no. 5, pp. 775 – 786, 2002.
- [45] Mohamed Babaali and George J Pappas, “Observability of switched linear systems in continuous time,” in *International Workshop on Hybrid Systems: Computation and Control*. Springer, 2005, pp. 103–117.
- [46] Aneel Tanwani, Hyungbo Shim, and Daniel Liberzon, “Observability for switched linear systems: characterization and observer design,” *IEEE Transactions on Automatic Control*, vol. 58, no. 4, pp. 891–904, 2012.
- [47] Scott C Johnson, “Observability and observer design for switched linear systems,” 2016.
- [48] Michel Fliess, Cédric Join, and Wilfrid Perruquetti, “Real-time estimation for switched linear systems,” in *2008 47th IEEE Conference on Decision and Control*. IEEE, 2008, pp. 941–946.
- [49] Hongwei Lou and Pengna Si, “The distinguishability of linear control systems,” *Nonlinear Analysis: Hybrid Systems*, vol. 3, no. 1, pp. 21–38, 2009.
- [50] Hongwei Lou and Rong Yang, “Conditions for distinguishability and observability of switched linear systems,” *Nonlinear Analysis: Hybrid Systems*, vol. 5, no. 3, pp. 427–445, 2011.
- [51] Cüneyt M Özveren, Alan S Willsky, et al., “Observability of discrete event dynamic systems,” 1989.
- [52] Alessandro D’Innocenzo, Maria Domenica Di Benedetto, and Stefano Di Gennaro, “Observability of hybrid automata by abstraction,” in *International Workshop on Hybrid Systems: Computation and Control*. Springer, 2006, pp. 169–183.
- [53] Maria D Di Benedetto, Stefano Di Gennaro, and Alessandro D’Innocenzo, “Discrete state observability of hybrid systems,” *International Journal of Robust and Nonlinear Control: IFAC-Affiliated Journal*, vol. 19, no. 14, pp. 1564–1580, 2009.

- [54] Weitian Chen and S Mehrdad, "Observer design for linear switched control systems," in *Proceedings of the American Control Conference*. IEEE, 2004, vol. 6, pp. 5796–5801.
- [55] Abderazik Birouche, Jamal Daafouz, and Claude Iung, "Observer design for a class of discrete time piecewise-linear systems," in *Analysis and Design of Hybrid Systems 2006*, pp. 12–17. Elsevier, 2006.
- [56] Francisco J Bejarano and Leonid Fridman, "State exact reconstruction for switched linear systems via a super-twisting algorithm," *International Journal of Systems Science*, vol. 42, no. 5, pp. 717–724, 2011.
- [57] SM Hernandez and Rafael A García, "An observer for switched lipschitz continuous systems," *International Journal of Control*, vol. 87, no. 1, pp. 207–222, 2014.
- [58] Francisco Javier Bejarano and Alessandro Pisano, "Switched observers for switched linear systems with unknown inputs," *IEEE Transactions on Automatic Control*, vol. 56, no. 3, pp. 681–686, 2010.
- [59] Junqi Yang, Yantao Chen, Fanglai Zhu, and Fuzhong Wang, "Simultaneous state and output disturbance estimations for a class of switched linear systems with unknown inputs," *International Journal of Systems Science*, vol. 48, no. 1, pp. 22–33, 2017.
- [60] Haifa Ethabet, Tarek Raïssi, Messaoud Amairi, and Mohamed Aoun, "Interval observers design for continuous-time linear switched systems," *IFAC-PapersOnLine*, vol. 50, no. 1, pp. 6259–6264, 2017.
- [61] H Ethabet, T Raïssi, M Amairi, C Combastel, and M Aoun, "Interval observer design for continuous-time switched systems under known switching and unknown inputs," *International Journal of Control*, vol. 93, no. 5, pp. 1088–1101, 2020.
- [62] X. Wang, G. Zong, and H. Sun, "Asynchronous finite-time dynamic output feedback control for switched time-delay systems with non-linear disturbances," *IET Control Theory A.*, vol. 10, no. 10, pp. 1142–1150, 2016.
- [63] Xudong Zhao, Hao Liu, Junfeng Zhang, and Hongyi Li, "Multiple-mode observer design for a class of switched linear systems," *IEEE Transactions on Automation Science and Engineering*, vol. 12, no. 1, pp. 272–280, 2015.
- [64] Weiming Xiang, Jian Xiao, and Muhammad Naveed Iqbal, "Robust observer design for nonlinear uncertain switched systems under asynchronous switching," *Nonlinear Analysis: Hybrid Systems*, vol. 6, pp. 754–773, 2012.
- [65] Nicola Orani, Alessandro Pisano, Mauro Franceschelli, Alessandro Giua, and Elio Usai, "Robust reconstruction of the discrete state for a class of nonlinear uncertain switched systems," *Nonlinear Analysis: Hybrid Systems*, vol. 5, pp. 220–232, 05 2011.
- [66] Jorge Davila, Alessandro Pisano, and Elio Usai, "Continuous and discrete state reconstruction for nonlinear switched systems via high-order sliding-mode observers," *International Journal of Systems Science*, vol. 42, no. 5, pp. 725–735, 2011.

- [67] Jeremy Van Gorp, Michael Defoort, Kalyana C. Veluvolu, and Mohamed Djemai, “Hybrid sliding mode observer for switched linear systems with unknown inputs,” *J. Franklin Inst.*, vol. 351, no. 7, pp. 3987–4008, 2014.
- [68] Héctor Rios, Diego Mincarelli, Denis Efimov, Wilfrid Perruquetti, and Jorge Davila, “Continuous and discrete state estimation for switched LPV systems using parameter identification,” *Automatica*, vol. 62, pp. 139–147, 2015.
- [69] Luc Jaulin, “Nonlinear bounded-error state estimation of continuous-time systems,” *Automatica*, vol. 38, no. 6, pp. 1079–1082, 2002.
- [70] Tarek Raïssi, Nacim Ramdani, and Yves Candau, “Set membership state and parameter estimation for systems described by nonlinear differential equations,” *Automatica*, vol. 40, no. 10, pp. 1771–1777, 2004.
- [71] Nedialko Stoyanov Nedialkov, *Computing rigorous bounds on the solution of an initial value problem for an ordinary differential equation.*, University of Toronto, 2000.
- [72] Jean-Luc Gouzé, Alain Rapaport, and Mohamed Zakaria Hadj-Sadok, “Interval observers for uncertain biological systems,” *Ecological modelling*, vol. 133, no. 1-2, pp. 45–56, 2000.
- [73] Olivier Bernard and Jean-Luc Gouzé, “Closed loop observers bundle for uncertain biotechnological models,” *Journal of process control*, vol. 14, no. 7, pp. 765–774, 2004.
- [74] Marcelo Moisan, Olivier Bernard, and Jean-Luc Gouzé, “Near optimal interval observers bundle for uncertain bioreactors,” in *2007 European Control Conference (ECC)*. IEEE, 2007, pp. 5115–5122.
- [75] Denis Efimov, Wilfrid Perruquetti, Tarek Raïssi, and Ali Zolghadri, “Interval observers for time-varying discrete-time systems,” *IEEE Transactions on Automatic Control*, vol. 58, no. 12, pp. 3218–3224, 2013.
- [76] Jeremy Van Gorp, Michael Defoort, Mohamed Djemai, and Kalyana Chakravarthy Veluvolu, “Fault detection based on higher-order sliding mode observer for a class of switched linear systems,” *IET Control Theory & Applications*, vol. 9, no. 15, pp. 2249–2256, 2015.
- [77] Guang-Xin Zhong and Guang-Hong Yang, “Fault detection for discrete-time switched systems in finite-frequency domain,” *Circuits, Systems, and Signal Processing*, vol. 34, no. 4, pp. 1305–1324, 2015.
- [78] Stanislav Chebotarev, Denis Efimov, Tarek Raïssi, and Ali Zolghadri, “Interval observers for continuous-time LPV systems with l_1/l_2 performance,” *Automatica*, vol. 58, pp. 82–89, 2015.
- [79] Denis Efimov, Leonid Fridman, Tarek Raïssi, Ali Zolghadri, and Ramatou Seydou, “Interval estimation for LPV systems applying high order sliding mode techniques,” *Automatica*, vol. 48, no. 9, pp. 2365–2371, 2012.

- [80] Chun Hung Mustapha Ait Rami, Cheng and Cesar De Prada, “Tight robust interval observers: an lp approach,” in *2008 47th IEEE Conference on Decision and Control*. IEEE, 2008, pp. 2967–2972.
- [81] Lorenzo Farina and Sergio Rinaldi, *Positive linear systems: theory and applications*, vol. 50, John Wiley & Sons, 2011.
- [82] Frédéric Mazenc, Thach Ngoc Dinh, and Silviu Iulian Niculescu, “Interval observers for discrete-time systems,” *International Journal of Robust and Nonlinear Control*, vol. 24, no. 17, pp. 2867–2890, 2014.
- [83] Denis Efimov and Tarek Raïssi, “Design of interval observers for uncertain dynamical systems,” *Automation and Remote Control*, vol. 77, no. 2, pp. 191–225, 2016.
- [84] Frédéric Mazenc and Olivier Bernard, “Interval observers for linear time-invariant systems with disturbances,” *Automatica*, vol. 47, no. 1, pp. 140–147, 2011.
- [85] Denis Efimov, Wilfrid Perruquetti, Tarek Raïssi, and Ali Zolghadri, “On interval observer design for time-invariant discrete-time systems,” in *2013 European Control Conference (ECC)*. IEEE, 2013, pp. 2651–2656.
- [86] Elinirina I Robinson, Julien Marzat, and Tarek Raïssi, “Interval observer design for unknown input estimation of linear time-invariant discrete-time systems,” *IFAC-PapersOnLine*, vol. 50, no. 1, pp. 4021–4026, 2017.
- [87] Wentao Tang, Zhenhua Wang, Ye Wang, Tarek Raïssi, and Yi Shen, “Interval estimation methods for discrete-time linear time-invariant systems,” *IEEE Transactions on Automatic Control*, vol. 64, no. 11, pp. 4717–4724, 2019.
- [88] Frédéric Mazenc and Olivier Bernard, “Asymptotically stable interval observers for planar systems with complex poles,” *IEEE Transactions on Automatic Control*, vol. 55, no. 2, pp. 523–527, 2009.
- [89] Filippo Cacace, Alfredo Germani, and Costanzo Manes, “A new approach to design interval observers for linear systems,” *IEEE Transactions on Automatic control*, vol. 60, no. 6, pp. 1665–1670, 2014.
- [90] Christophe Combastel and Sid-Ahmed Raka, “A stable interval observer for lti systems with no multiple poles,” *IFAC Proceedings Volumes*, vol. 44, no. 1, pp. 14335–14341, 2011.
- [91] Denis Efimov, Raïssi Tarek, Stanislav Chebotarev, and Ali Zolghadri, “On set-membership observer design for a class of periodical time-varying systems,” in *2012 IEEE 51st IEEE Conference on Decision and Control (CDC)*. IEEE, 2012, pp. 6767–6772.
- [92] Rihab El Houda Thabet, Tarek Raïssi, Christophe Combastel, Denis Efimov, and Ali Zolghadri, “An effective method to interval observer design for time-varying systems,” *Automatica*, vol. 50, no. 10, pp. 2677–2684, 2014.

- [93] J Zhu and CD Johnson, “Unified canonical forms for linear time-varying dynamical systems under d-similarity transformations. i,” in *[1989] Proceedings. The Twenty-First Southeastern Symposium on System Theory*. IEEE, 1989, pp. 74–81.
- [94] Denis Efimov, Tarek Raïssi, Stanislav Chebotarev, and Ali Zolghadri, “Interval state observer for nonlinear time varying systems,” *Automatica*, vol. 49, no. 1, pp. 200–205, 2013.
- [95] Awais Khan, Wei Xie, Langwen Zhang, et al., “Interval state estimation for linear time-varying (ltv) discrete-time systems subject to component faults and uncertainties,” *Archives of Control Sciences*, vol. 29, 2019.
- [96] Tarek Raïssi, Denis Efimov, and Ali Zolghadri, “Interval state estimation for a class of nonlinear systems,” *IEEE Transactions on Automatic Control*, vol. 57, no. 1, pp. 260–265, 2011.
- [97] Thach Ngoc Dinh, Frédéric Mazenc, and Silviu-Iulian Niculescu, “Interval observer composed of observers for nonlinear systems,” in *2014 European control conference (ECC)*. IEEE, 2014, pp. 660–665.
- [98] Denis Efimov, Tarek Raïssi, and Ali Zolghadri, “Control of nonlinear and LPV systems: interval observer-based framework,” *IEEE Transactions on Automatic Control*, vol. 58, no. 3, pp. 773–778, 2013.
- [99] Lawton Hubert Lee, “Identification and robust control of linear parameter-varying systems,” *PhD Thesis*, 1997, University of California, Berkeley.
- [100] Andrés Marcos and Gary J Balas, “Development of linear-parameter-varying models for aircraft,” *Journal of Guidance, Control, and Dynamics*, vol. 27, no. 2, pp. 218–228, 2004.
- [101] WP Maurice H Heemels, Jamal Daafouz, and Gilles Millerioux, “Observer-based control of discrete-time LPV systems with uncertain parameters,” *IEEE Transactions on Automatic Control*, vol. 55, no. 9, pp. 2130–2135, 2010.
- [102] Denis Efimov, Tarek Raïssi, Wilfrid Perruquetti, and Ali Zolghadri, “Design of interval observers for estimation and stabilization of discrete-time LPV systems,” *IMA Journal of Mathematical Control and Information*, vol. 33, no. 4, pp. 1051–1066, 2016.
- [103] Rihab Lamouchi, Tarek Raïssi, Messaoud Amairi, and Mohamed Aoun, “Interval observer framework for fault-tolerant control of linear parameter-varying systems,” *International Journal of Control*, vol. 91, no. 3, pp. 524–533, 2018.
- [104] Tarek Raïssi, Gaétan Videau, and Ali Zolghadri, “Interval observer design for consistency checks of nonlinear continuous-time systems,” *Automatica*, vol. 46, no. 3, pp. 518–527, 2010.
- [105] Gaétan Videau, *Méthodes garanties pour l’estimation d’état et le contrôle de cohérence des systèmes non linéaires à temps continu.*, Ph.D. thesis, 2009.

- [106] Stefan Krebs, Martin Pfeifer, Sebastian Fugel, Jörg Weigold, and Sören Hohmann, “Interval observer for LPV systems based on time-variant transformations,” in *2016 IEEE 55th Conference on Decision and Control (CDC)*. IEEE, 2016, pp. 4090–4096.
- [107] Zhongwei He and Wei Xie, “Interval state observer for nonlinear switched systems with average dwell time,” in *34th Chinese Control Conference (CCC)*, 2015, pp. 2285–2288.
- [108] Shenghui Guo and Fanglai Zhu, “Interval observer design for discrete-time switched system,” *IFAC-PapersOnLine*, vol. 50, no. 1, pp. 5073–5078, 2017.
- [109] Djahid Rabehi, Denis Efimov, and Jean-Pierre Richard, “Interval estimation for linear switched system,” *IFAC-PapersOnLine*, vol. 50, no. 1, pp. 6265–6270, 2017.
- [110] Haifa Ethabet, Djahid Rabehi, Denis Efimov, and Tarek Raïssi, “Interval estimation for continuous-time switched linear systems,” *Automatica*, vol. 90, pp. 230–238, 2018.
- [111] Thach Ngoc Dinh, Ghassen Marouani, Tarek Raïssi, Zhenhua Wang, and Hassani Messaoud, “Optimal interval observers for discrete-time linear switched systems,” *International Journal of Control*, pp. 1–9, 2019.
- [112] Alaa Daher, *Default diagnosis and prognosis for a preventive and predictive maintenance. Application to a distillation column*, Ph.D. thesis, 2018.
- [113] Paul M Frank, “Fault diagnosis in dynamic systems using analytical and knowledge-based redundancy: A survey and some new results,” *automatica*, vol. 26, no. 3, pp. 459–474, 1990.
- [114] Rolf Isermann, “Model-based fault-detection and diagnosis—status and applications,” *Annual Reviews in control*, vol. 29, no. 1, pp. 71–85, 2005.
- [115] Rolf Isermann, *Fault-diagnosis systems: an introduction from fault detection to fault tolerance*, Springer Science & Business Media, 2006.
- [116] Zehui Mao, Bin Jiang, and Peng Shi, “ H_∞ fault detection filter design for networked control systems modelled by discrete markovian jump systems,” *IET control theory & applications*, vol. 1, no. 5, pp. 1336–1343, 2007.
- [117] Ligang Wu, Xiuming Yao, and Wei Xing Zheng, “Generalized h_2 fault detection for two-dimensional markovian jump systems,” *Automatica*, vol. 48, no. 8, pp. 1741–1750, 2012.
- [118] Jian Liu, Jian Liang Wang, and Guang-Hong Yang, “An lmi approach to minimum sensitivity analysis with application to fault detection,” *Automatica*, vol. 41, no. 11, pp. 1995–2004, 2005.
- [119] Ahmad Farhat and Damien Koenig, “ H_- / H_∞ fault detection observer for switched systems,” in *53rd IEEE Conference on Decision and Control*. IEEE, 2014, pp. 6554–6559.
- [120] Ding Zhai, An-Yang Lu, Jing-Hao Li, and Qing-Ling Zhang, “Simultaneous fault detection and control for switched linear systems with mode-dependent average dwell-time,” *Applied Mathematics and computation*, vol. 273, pp. 767–792, 2016.

- [121] Zhi-Hui Zhang and Guang-Hong Yang, "Fault detection for discrete-time LPV systems using interval observers," *International Journal of Systems Science*, vol. 48, no. 14, pp. 2921–2935, 2017.
- [122] Ye Wang, Meng Zhou, Vicenç Puig, Gabriela Cembrano, and Zhenhua Wang, "Zonotopic fault detection observer with h- performance," in *2017 36th Chinese Control Conference (CCC)*. IEEE, 2017, pp. 7230–7235.
- [123] Jitao Li, Zhenhua Wang, Yi Shen, and Ye Wang, "Zonotopic fault detection observer design for takagi–sugeno fuzzy systems," *International Journal of Systems Science*, vol. 49, no. 15, pp. 3216–3230, 2018.
- [124] Haifa Ethabet, Tarek Raïssi, Messaoud Amairi, and Mohamed Aoun, "Set-membership fault detection for continuous-time switched linear systems," in *2019 International Conference on Advanced Systems and Emergent Technologies (IC_ASET)*. IEEE, 2019, pp. 406–411.
- [125] Janos Gertler, *Fault detection and diagnosis in engineering systems*, CRC press, 1998.
- [126] Ron J Patton, "Robust model-based fault diagnosis: the state of the art," *IFAC Proceedings Volumes*, vol. 27, no. 5, pp. 1–24, 1994.
- [127] Yakov Ben-Haim, "An algorithm for failure location in a complex network," *Nuclear Science and Engineering*, vol. 75, no. 2, pp. 191–199, 1980.
- [128] J Chen, "Observers," in *European Control Conference 1995: Volume 1*. European Control Association, 1995, vol. 1, p. 348.
- [129] Richard Vernon Beard, *Failure accomodation in linear systems through self-reorganization.*, Ph.D. thesis, Massachusetts Institute of Technology, 1971.
- [130] JJ Gertler and R Monajemy, "Generating directional residuals with dynamic parity equations," *IFAC Proceedings Volumes*, vol. 26, no. 2, pp. 507–512, 1993.
- [131] Binfan Liu and Jennie Si, "Fault isolation filter design for linear time-invariant systems," *IEEE Transactions on Automatic Control*, vol. 42, no. 5, pp. 704–707, 1997.
- [132] J-Y Keller, "Fault isolation filter design for linear stochastic systems," *Automatica*, vol. 35, no. 10, pp. 1701–1706, 1999.
- [133] T-G Park and K-S Lee, "Process fault isolation for linear systems with unknown inputs," *IEEE Proceedings-Control Theory and Applications*, vol. 151, no. 6, pp. 720–726, 2004.
- [134] Habib Hamdi, Mickael Rodrigues, Chokri Mechmeche, Didier Theilliol, and N BenHadj Braiek, "Fault detection and isolation in linear parameter-varying descriptor systems via proportional integral observer," *International journal of adaptive control and signal processing*, vol. 26, no. 3, pp. 224–240, 2012.
- [135] Abdelkader Akhenak, Mohammed Chadli, José Ragot, and Didier Maquin, "Fault detection and isolation using sliding mode observer for uncertain takagi-sugeno fuzzy

- model,” in *2008 16th Mediterranean Conference on Control and automation*. IEEE, 2008, pp. 286–291.
- [136] Muhammad Taskeen Raza, Abdul Qayyum Khan, Ghulam Mustafa, and Muhammad Abid, “Design of fault detection and isolation filter for switched control systems under asynchronous switching,” *IEEE Transactions on Control Systems Technology*, vol. 24, no. 1, pp. 13–23, 2015.
- [137] Xiaodong Zhang, Marios M Polycarpou, and Thomas Parisini, “A robust detection and isolation scheme for abrupt and incipient faults in nonlinear systems,” *IEEE transactions on automatic control*, vol. 47, no. 4, pp. 576–593, 2002.
- [138] Xiaodong Zhang, Liang Tang, and Jonathan Decastro, “Robust fault diagnosis of aircraft engines: A nonlinear adaptive estimation-based approach,” *IEEE Transactions on Control Systems Technology*, vol. 21, no. 3, pp. 861–868, 2012.
- [139] Fabrizio Caccavale, Alessandro Marino, Giuseppe Muscio, and Francesco Pierri, “Discrete-time framework for fault diagnosis in robotic manipulators,” *IEEE Transactions on Control Systems Technology*, vol. 21, no. 5, pp. 1858–1873, 2012.
- [140] Khalaf Salloum Gaeid and Hew Wooi Ping, “Induction motor fault detection and isolation through unknown input observer,” *Scientific Research and Essays*, vol. 5, no. 20, pp. 3152–3159, 2010.
- [141] Ke Zhang, Bin Jiang, Vincent Cocquempot, and Huaguang Zhang, “A framework of robust fault estimation observer design for continuous-time/discrete-time systems,” *Optimal control applications and methods*, vol. 34, no. 4, pp. 442–457, 2013.
- [142] Zhiwei Gao, Steven X Ding, and Y Ma, “Robust fault estimation approach and its application in vehicle lateral dynamic systems,” *Optimal Control Applications and Methods*, vol. 28, no. 3, pp. 143–156, 2007.
- [143] Qinghua Zhang and Gildas Besancon, “An adaptive observer for sensor fault estimation in a class of uniformly observable non-linear systems,” *International Journal of Modelling, Identification and Control*, vol. 4, no. 1, pp. 37–43, 2008.
- [144] Zhiwei Gao, Xiaoyan Shi, and Steven X Ding, “Fuzzy state/disturbance observer design for t–s fuzzy systems with application to sensor fault estimation,” *IEEE Transactions on Systems, Man, and Cybernetics, Part B (Cybernetics)*, vol. 38, no. 3, pp. 875–880, 2008.
- [145] Wenhan Zhang, Zhenhua Wang, Tarek Raïssi, Ye Wang, and Yi Shen, “A state augmentation approach to interval fault estimation for descriptor systems,” *European Journal of Control*, vol. 51, pp. 19–29, 2020.
- [146] Mickaël Rodrigues, *Diagnostic et commande active tolérante aux défauts appliqués aux systèmes décrits par des multi-modèles linéaires*, Ph.D. thesis, 2005.
- [147] Rolf Isermann, Ralf Schwarz, and Stefan Stolzl, “Fault-tolerant drive-by-wire systems,” *IEEE Control Systems Magazine*, vol. 22, no. 5, pp. 64–81, 2002.

- [148] J Gertler, "Residual generation in model-based fault-diagnosis," *Control-theory and advanced technology*, vol. 9, no. 1, pp. 259–285, 1993.
- [149] R Isermann, "On the applicability of model-based fault detection for technical processes," *Control Engineering Practice*, vol. 2, no. 3, pp. 439–450, 1994.
- [150] Jie Chen, *Robust residual generation for model-based fault diagnosis of dynamic systems.*, Ph.D. thesis, University of York, 1995.
- [151] Venkat Venkatasubramanian, Raghunathan Rengaswamy, Kewen Yin, and Surya N Kavuri, "A review of process fault detection and diagnosis: Part i: Quantitative model-based methods," *Computers & chemical engineering*, vol. 27, no. 3, pp. 293–311, 2003.
- [152] Ron J Patton and Jie Chen, "Review of parity space approaches to fault diagnosis for aerospace systems," *Journal of Guidance, Control, and Dynamics*, vol. 17, no. 2, pp. 278–285, 1994.
- [153] Schwarte Anselm and Rolf Isermann, "Neural network applications for model based fault detection with parity equations," *IFAC Proceedings Volumes*, vol. 35, no. 1, pp. 205–210, 2002.
- [154] Janos Gertler and Marcel Staroswiecki, "Structured fault diagnosis in mildly nonlinear systems: parity space and input-output formulations," *IFAC Proceedings Volumes*, vol. 35, no. 1, pp. 341–346, 2002.
- [155] Vincent Cocquempot, Touria El Mezyani, and Marcel Staroswiecki, "Fault detection and isolation for hybrid systems using structured parity residuals," in *2004 5th Asian Control Conference (IEEE Cat. No. 04EX904)*. IEEE, 2004, vol. 2, pp. 1204–1212.
- [156] Taiyi Sun, Donghua Zhou, Yanzheng Zhu, and Michael V Basin, "Stability, l_2 -gain analysis, and parity space-based fault detection for discrete-time switched systems under dwell-time switching," *IEEE Transactions on Systems, Man, and Cybernetics: Systems*, 2018.
- [157] Ali Abdo, Steven X Ding, Jedsada Saijai, and Waseem Damlakhi, "Fault detection for switched systems based on a deterministic method," in *2012 IEEE 51st IEEE Conference on Decision and Control (CDC)*. IEEE, 2012, pp. 568–573.
- [158] Cocquempot Vincent Staroswiecki Marcel, Cassar Jean-Philippe, "Generation of optimal structured residuals in the parity space," *IFAC Proceedings Volumes*, vol. 26, no. 2, pp. 535–542, 1993.
- [159] Paul M Frank, "On-line fault detection in uncertain nonlinear systems using diagnostic observers: a survey," *International journal of systems science*, vol. 25, no. 12, pp. 2129–2154, 1994.
- [160] Steven X Ding, *Model-based fault diagnosis techniques: design schemes, algorithms, and tools*, Springer Science & Business Media, 2008.

- [161] Rolf Isermann, "Fault diagnosis of machines via parameter estimation and knowledge processing: tutorial paper," *Automatica*, vol. 29, no. 4, pp. 815–835, 1993.
- [162] Tao Jiang, Khashayar Khorasani, and Siamak Tafazoli, "Parameter estimation-based fault detection, isolation and recovery for nonlinear satellite models," *IEEE Transactions on control systems technology*, vol. 16, no. 4, pp. 799–808, 2008.
- [163] Smail Bachir, Slim Tnani, J-C Trigeassou, and Gérard Champenois, "Diagnosis by parameter estimation of stator and rotor faults occurring in induction machines," *IEEE Transactions on Industrial Electronics*, vol. 53, no. 3, pp. 963–973, 2006.
- [164] PM Frank and L Keller, "Sensitivity discriminating observer design for instrument failure detection," *IEEE Transactions on Aerospace and Electronic Systems*, , no. 4, pp. 460–467, 1980.
- [165] Yang Tian, Ke Zhang, Bin Jiang, and Xing-Gang Yan, "Interval observer and unknown input observer-based sensor fault estimation for high-speed railway traction motor," *Journal of the Franklin Institute*, vol. 357, no. 2, pp. 1137–1154, 2020.
- [166] Masoud Pourasghar, Vicenç Puig, and Carlos Ocampo-Martinez, "Characterisation of interval-observer fault detection and isolation properties using the set-invariance approach," *Journal of the Franklin Institute*, vol. 357, no. 3, pp. 1853–1886, 2020.
- [167] Héctor Rios, Denis Efimov, Jorge Davila, Tarek Raïssi, Leonid Fridman, and Ali Zolghadri, "Non-minimum phase switched systems: Hosm-based fault detection and fault identification via volterra integral equation," *International Journal of Adaptive Control and Signal Processing*, vol. 28, no. 12, pp. 1372–1397, 2014.
- [168] Jian Li and Guang-Hong Yang, "Simultaneous fault detection and control for switched systems with actuator faults," *International Journal of Systems Science*, vol. 47, no. 10, pp. 2411–2427, 2016.
- [169] D.E.C. Belkhiat, N. Messai, and N. Manamanni, "Design of a robust fault detection based observer for linear switched systems with external disturbances," *Nonlinear Analysis: Hybrid Systems*, vol. 5, no. 2, pp. 206–219, 2011.
- [170] Jinxing Lin, Shumin Fei, Zhifeng Gao, and Jie Ding, "Fault detection for discrete-time switched singular time-delay systems: an average dwell time approach," *International Journal of Adaptive Control and Signal Processing*, vol. 27, no. 7, pp. 582–609, 2013.
- [171] Wenhan Zhang, Zhenhua Wang, Tarek Raïssi, and Yi Shen, "Ellipsoid-based interval estimation for takagi-sugeno fuzzy systems," *Control and Decision Conference*, 2019.
- [172] Geoffrey C Shephard, "Combinatorial properties of associated zonotopes," *Canadian Journal of Mathematics*, vol. 26, no. 2, pp. 302–321, 1974.
- [173] Teodoro Alamo, José Manuel Bravo, and Eduardo F Camacho, "Guaranteed state estimation by zonotopes," *Automatica*, vol. 41, no. 6, pp. 1035–1043, 2005.
- [174] Vu Tuan Hieu Le, Cristina Stoica, Teodoro Alamo, Eduardo F Camacho, and Didier Dumur, *Zonotopes: From guaranteed state-estimation to control*, John Wiley & Sons, 2013.

- [175] Christophe Combastel, “Zonotopes and kalman observers: Gain optimality under distinct uncertainty paradigms and robust convergence,” *Automatica*, vol. 55, pp. 265–273, 2015.
- [176] Ye Wang, Zhenhua Wang, Vicenç Puig, and Gabriela Cembrano, “Zonotopic set-membership state estimation for discrete-time descriptor LPV systems,” *IEEE Transactions on Automatic Control*, vol. 64, no. 5, pp. 2092–2099, 2018.
- [177] Jitao Li, Zhenhua Wang, Yi Shen, and Mickael Rodrigues, “Zonotopic fault detection observer for linear parameter-varying descriptor systems,” *International Journal of Robust and Nonlinear Control*, vol. 29, no. 11, pp. 3426–3445, 2019.
- [178] Wentao Tang, Zhenhua Wang, and Yi Shen, “Interval estimation for discrete-time linear systems: A two-step method,” *Systems & Control Letters*, vol. 123, pp. 69–74, 2019.
- [179] Vu Tuan Hieu Le, Cristina Stoica, Teodoro Alamo, Eduardo F Camacho, and Didier Dumur, “Zonotopic guaranteed state estimation for uncertain systems,” *Automatica*, vol. 49, no. 11, pp. 3418–3424, 2013.
- [180] Boris T Polyak, Sergey A Nazin, CéCile Durieu, and Eric Walter, “Ellipsoidal parameter or state estimation under model uncertainty,” *Automatica*, vol. 40, no. 7, pp. 1171–1179, 2004.
- [181] S Ben Chabane, C Stoica Maniu, Teodoro Alamo, Eduardo F Camacho, and Didier Dumur, “Improved set-membership estimation approach based on zonotopes and ellipsoids,” in *2014 European Control Conference (ECC)*. IEEE, 2014, pp. 993–998.
- [182] Boris T Polyak, Sergey A Nazin, CéCile Durieu, and Eric Walter, “Ellipsoidal estimation under model uncertainty,” *IFAC Proceedings Volumes*, vol. 35, no. 1, pp. 25–30, 2002.
- [183] Chaima Zammali, Jeremy Van Gorp, Xubin Ping, and Tarek Raïssi, “Interval estimation for discrete-time LPV switched systems,” in *2019 IEEE 58th Conference on Decision and Control (CDC)*. IEEE, 2019, pp. 2479–2484.
- [184] Chaima Zammali, Jeremy Van Gorp, and Tarek Raïssi, “Interval estimation for continuous-time LPV switched systems,” *International Journal of Control*, pp. 1–12, 2020 (to appear).
- [185] Chaima Zammali, Jérémy Van Gorp, and Tarek Raïssi, “On interval observer design for continuous-time LPV switched systems,” *Acta Cybernetica*, vol. 24, no. 3, pp. 539–555, 2020.
- [186] Sara Ifqir, N Ait-Oufroukh, Dalil Ichalal, and Saïd Mammar, “Synchronous interval observer design for switched lpv systems using multiple quadratic iss-lyapunov functions,” in *25th Mediterranean Conference on Control and Automation (MED)*. IEEE, 2017, pp. 388–393.

- [187] Laurentiu Hetel, Jamal Daafouz, and Claude Iung, “Robust stability analysis and control design for switched uncertain polytopic systems,” *IFAC Proceedings Volumes*, vol. 39, no. 9, pp. 166–171, 2006.
- [188] Yan Wang, David M Bevly, and Rajesh Rajamani, “Interval observer design for LPV systems with parametric uncertainty,” *Automatica*, vol. 60, pp. 79–85, 2015.
- [189] Kaiqun Zhu, Yan Song, Derui Ding, Guoliang Wei, and Hongjian Liu, “Robust mpc under event-triggered mechanism and round-robin protocol: An average dwell-time approach,” *Information Sciences*, vol. 457, pp. 126–140, 2018.
- [190] Chaima Zammali, Jeremy Van Gorp, Xubin Ping, and Tarek Raïssi, “Switching signal estimation based on interval observer for a class of switched linear systems,” in *2019 IEEE 58th Conference on Decision and Control (CDC)*. IEEE, 2019, pp. 2497–2502.
- [191] Xiao-Jian Li and Guang-Hong Yang, “Fault detection for t-s fuzzy systems with unknown membership functions,” *IEEE Transactions on Fuzzy Systems*, vol. 22, no. 1, pp. 139–152, 2013.
- [192] Marco Tulio Angulo, Jaime A Moreno, and Leonid Fridman, “Robust exact uniformly convergent arbitrary order differentiator,” *Automatica*, vol. 49, no. 8, pp. 2489–2495, 2013.
- [193] Emmanuel Chambon, Laurent Burlion, and Pierre Apkarian, “Overview of linear time-invariant interval observer design: towards a non-smooth optimisation-based approach,” *IET Control Theory & Applications*, vol. 10, no. 11, pp. 1258–1268, 2016.
- [194] Chaima Zammali, Jérémy Van Gorp, Zhenhua Wang, and Tarek Raïssi, “Sensor fault detection for switched systems using interval observer with L_∞ performance,” *European Journal of Control*, 2020(to appear).
- [195] Chaima Zammali, Jérémy Van Gorp, and Tarek Raïssi, “Interval observers based fault detection for switched systems with L_∞ performances,” in *European Control Conference (ECC 20)*, 2020 (to appear).
- [196] Chaima Zammali, Jérémy Van Gorp, and Tarek Raïssi, “Robust fault detection for switched systems based on interval observers,” in *28th Mediterranean Conference on Control and Automation (MED)*, 2020(to appear).
- [197] Zhenhua Wang, Mickael Rodrigues, Didier Theilliol, and Yi Shen, “Actuator fault estimation observer design for discrete-time linear parameter-varying descriptor systems,” *International Journal of Adaptive Control and Signal Processing*, vol. 29, no. 2, pp. 242–258, 2015.
- [198] Samuel Fiorini, Serge Massar, Sebastian Pokutta, Hans Raj Tiwary, and Ronald De Wolf, “Exponential lower bounds for polytopes in combinatorial optimization,” *Journal of the ACM (JACM)*, vol. 62, no. 2, pp. 1–23, 2015.
- [199] Joseph K Scott, Davide M Raimondo, Giuseppe Roberto Marseglia, and Richard D Braatz, “Constrained zonotopes: A new tool for set-based estimation and fault detection,” *Automatica*, vol. 69, pp. 126–136, 2016.

- [200] Chaima Zammali, Zhenhua Wang, Jérémy Van Gorp, and Tarek Raïssi, “Fault detection for switched systems based on pole assignment and zonotopic residual evaluation,” in *21st IFAC World Congress*, 2020(to appear).
- [201] Chaima Zammali, Jérémy Van Gorp, Zhenhua Wang, Xubin Ping, and Tarek Raïssi, “Ellipsoid-based sensor fault detection for discrete-time switched systems,” in *59th IEEE Conference on Decision and Control*, 2020(to appear).
- [202] Christophe Combastel, “A state bounding observer for uncertain non-linear continuous-time systems based on zonotopes,” in *Proceedings of the 44th IEEE Conference on Decision and Control*. IEEE, 2005, pp. 7228–7234.
- [203] Mohammed Chadli, Ali Abdo, and Steven X Ding, “ H_∞ fault detection filter design for discrete-time takagi–sugeno fuzzy system,” *Automatica*, vol. 49, no. 7, pp. 1996–2005, 2013.
- [204] Meng Zhou, Zhenhua Wang, Yi Shen, and Mouquan Shen, “ H_∞ fault detection observer design in finite-frequency domain for lipschitz non-linear systems,” *IET Control Theory & Applications*, vol. 11, no. 14, pp. 2361–2369, 2017.
- [205] Li Tang and Jun Zhao, “Switched threshold-based fault detection for switched non-linear systems with its application to chua’s circuit system,” *IEEE Transactions on Circuits and Systems I: Regular Papers*, vol. 66, no. 2, pp. 733–741, 2018.
- [206] Yushuang Liu, Yan Zhao, and Falin Wu, “Ellipsoidal state-bounding-based set-membership estimation for linear system with unknown-but-bounded disturbances,” *IET Control Theory & Applications*, vol. 10, no. 4, pp. 431–442, 2016.
- [207] Benjamin Noack, Vesa Klumpp, and Uwe D Hanebeck, “State estimation with sets of densities considering stochastic and systematic errors,” in *2009 12th International Conference on Information Fusion*. IEEE, 2009, pp. 1751–1758.
- [208] Weixin Han, Zhenhua Wang, Yi Shen, and Juntong Qi, “ L_∞ observer for uncertain linear systems,” *Asian Journal of Control*, vol. 21, no. 1, pp. 632–638, 2019.
- [209] Thach Ngoc Dinh, Frédéric Mazenc, Zhenhua Wang, and Tarek Raïssi, “On fixed-time interval estimation of discrete-time nonlinear time-varying systems with disturbances,” in *The 2020 American Control Conference*, 2020.
- [210] Ali Zolghadri, “Advanced model-based fdir techniques for aerospace systems: Today challenges and opportunities,” *Progress in Aerospace Sciences*, vol. 53, pp. 18–29, 2012.
- [211] Damiano Rotondo, Rosa M Fernandez-Canti, Sebastian Tornil-Sin, Joaquim Blesa, and Vicenc Puig, “Robust fault diagnosis of proton exchange membrane fuel cells using a takagi-sugeno interval observer approach,” *International Journal of Hydrogen Energy*, vol. 41, no. 4, pp. 2875–2886, 2016.
- [212] Ali Zolghadri, Hervé Leberre, P Goupil, Anca Gheorghe, Jérôme Cieslak, and Rémy Dayre, “Parametric approach to fault detection in aircraft control surfaces,” *Journal of Aircraft*, pp. 846–855, 2016.

- [213] Xianchun Ding and Paul M Frank, "Fault detection via factorization approach," *Systems & control letters*, vol. 14, no. 5, pp. 431–436, 1990.
- [214] Kangkang Zhang, Bin Jiang, Xing-Gang Yan, Jun Shen, and Zehui Mao, "Interval sliding mode observer based incipient fault detection with application to a high-speed railway traction device," in *2016 IEEE International Symposium on Robotics and Intelligent Sensors (IRIS)*. IEEE, 2016, pp. 157–162.
- [215] Pavan Kumar Kankar, Satish C Sharma, and Suraj Prakash Harsha, "Fault diagnosis of rolling element bearing using cyclic autocorrelation and wavelet transform," *Neurocomputing*, vol. 110, pp. 9–17, 2013.
- [216] Rolf Isermann and Peter Balle, "Trends in the application of model-based fault detection and diagnosis of technical processes," *Control engineering practice*, vol. 5, no. 5, pp. 709–719, 1997.
- [217] SX Ding, PM Frank, and EL Ding, "An approach to the detection of multiplicative faults in uncertain dynamic systems," in *Proceedings of the 41st IEEE Conference on Decision and Control, 2002*. IEEE, 2002, vol. 4, pp. 4371–4376.
- [218] Sing Kiong Nguang, Ping Zhang, and Steven X Ding, "Parity relation based fault estimation for nonlinear systems: An lmi approach," *International Journal of Automation and Computing*, vol. 4, no. 2, pp. 164–168, 2007.
- [219] Hendrik M Odendaal and Thomas Jones, "Actuator fault detection and isolation: An optimised parity space approach," *Control Engineering Practice*, vol. 26, pp. 222–232, 2014.
- [220] Woohyun Hwang and Kunsoo Huh, "Fault detection and estimation for electromechanical brake systems using parity space approach," *Journal of Dynamic Systems, Measurement, and Control*, vol. 137, no. 1, pp. 014504, 2015.
- [221] H Wang and S Daley, "Actuator fault diagnosis: an adaptive observer-based technique," *IEEE transactions on Automatic Control*, vol. 41, no. 7, pp. 1073–1078, 1996.
- [222] Dongsheng Du, Shengyuan Xu, and Vincent Cocquempot, "Fault detection for nonlinear discrete-time switched systems with persistent dwell time," *IEEE Transactions on Fuzzy Systems*, vol. 26, no. 4, pp. 2466–2474, 2018.
- [223] Dalil Ichalal, Benoît Marx, José Ragot, and Didier Maquin, "Fault detection, isolation and estimation for takagi–sugeno nonlinear systems," *Journal of the Franklin Institute*, vol. 351, no. 7, pp. 3651–3676, 2014.
- [224] Héctor Ríos, Denis Efimov, Jorge Davila, Tarek Raissi, Leonid Fridman, and Ali Zolghadri, "State estimation and fault detection for linear switched systems with unstable internal dynamics," *IFAC Proceedings Volumes*, vol. 45, no. 20, pp. 522–527, 2012.
- [225] Dongsheng Du, Bin Jiang, and Peng Shi, "Fault detection for discrete-time switched systems with intermittent measurements," *International Journal of Control*, vol. 85, no. 1, pp. 78–87, 2012.

-
- [226] Simon Hecker and Andras Varga, “Generalized lft-based representation of parametric uncertain models,” *European Journal of Control*, vol. 10, no. 4, pp. 326–337, 2004.
- [227] Tarek Raïssi, Nacim Ramdani, and Yves Candau, “Bounded error moving horizon state estimator for non-linear continuous-time systems: application to a bioprocess system,” *Journal of Process control*, vol. 15, no. 5, pp. 537–545, 2005.
- [228] Qing Zhao Amr Pertew, Horacio J. Marquez, “Lmi based sensor fault diagnosis for nonlinear lipschitz systems,” *Automatica*, vol. 43, no. 8, pp. 1464 – 1469, 2007.
- [229] Dengfeng Zhang, Hong Wang, Baochun Lu, and Zhiquan Wang, “Lmi-based fault detection fuzzy observer design with multiple performance constraints for a class of non-linear systems: comparative study,” *International Journal of Innovative Computing, Information and Control*, vol. 8, no. 1, pp. 633–645, 2012.
- [230] Dong Wang, Peng Shi, and Wei Wang, “Robust fault detection for continuous-time switched delay systems: an linear matrix inequality approach,” *IET control theory & applications*, vol. 4, no. 1, pp. 100–108, 2010.
- [231] Janos J Gertler, “Survey of model-based failure detection and isolation in complex plants,” *IEEE Control systems magazine*, vol. 8, no. 6, pp. 3–11, 1988.

Résumé : Cette thèse s'intéresse à l'estimation d'état et à la détection de défauts de systèmes linéaires à commutations. De nouvelles approches d'estimation par intervalles sont développées pour des systèmes linéaires à commutations à paramètres variants en temps continu et en temps discret en supposant que le signal de commutations est connu. Les conditions de conception sont formulées en termes d'inégalités matricielles linéaires. Une autre approche qui consiste à proposer une nouvelle logique d'estimation du signal de commutations d'un système linéaire à commutations à entrée inconnue est introduite en combinant la technique par modes glissants et l'approche par intervalles. Le problème d'estimation d'état constitue une des étapes fondamentales pour traiter le problème de détection de défauts. Par conséquent, des solutions robustes de détection sont mises en oeuvre en présence des perturbations et du bruit de mesure en utilisant la théorie des ensembles. Tout d'abord, une approche de détection de défaut est proposée en se basant sur des observateurs par intervalles de différentes structures (une structure classique et une structure TNL) avec des performances L_∞ . Ensuite, une nouvelle méthode de détection des défauts est conçue en utilisant des techniques zonotopiques et ellipsoïdales. Ces outils permettent de fournir des seuils dynamiques pour l'évaluation du résidu et d'améliorer la précision des résultats de détection de défauts sans tenir compte de l'hypothèse de coopérativité. Les méthodes développées dans cette thèse sont illustrées par des exemples académiques et les résultats obtenus montrent leur efficacité.

Mots clés : Systèmes à commutations, Observateurs par intervalles, La théorie de Lyapunov, La performance L_∞ , Analyse zonotopique, Analyse ellipsoïdale.

Abstract : This thesis deals with state estimation and fault detection for a class of switched linear systems. New interval observers are investigated for continuous-time and discrete-time linear parameter varying switched systems, with a known switching signal and measured polytopic parameters. The design conditions are formulated in terms of linear matrix inequalities, and include the cases of arbitrary and dwell-time switching. In addition, a new switching signal observer, combining sliding mode and interval techniques, is developed for linear switched systems with unknown input. State estimation remains one of the fundamental steps to deal with fault detection. Hence, robust fault detection solutions are performed for linear switched systems subject to state perturbations and measurement noise using set-membership theory. First, a fault detection approach is proposed based on interval observers of different structures (a conventional one and a TNL structure) with L_∞ performances. Moreover, a new fault detection method is designed using zonotopic and ellipsoidal estimation tools, which can provide a systematic and effective way to improve the accuracy of the residual boundaries without considering the cooperativity assumption. Based on optimization criteria, fault sensitivity and disturbance attenuation conditions are presented. The developed techniques in this thesis are illustrated using academic examples and the results show their effectiveness.

Keywords : Switched systems, Interval observers, Lyapunov theory, L_∞ performance, Zonotopic analysis, Ellipsoidal analysis.